Centre for Ore Deposit and Exploration Studies

Proterozoic sediment-hosted base metal deposits

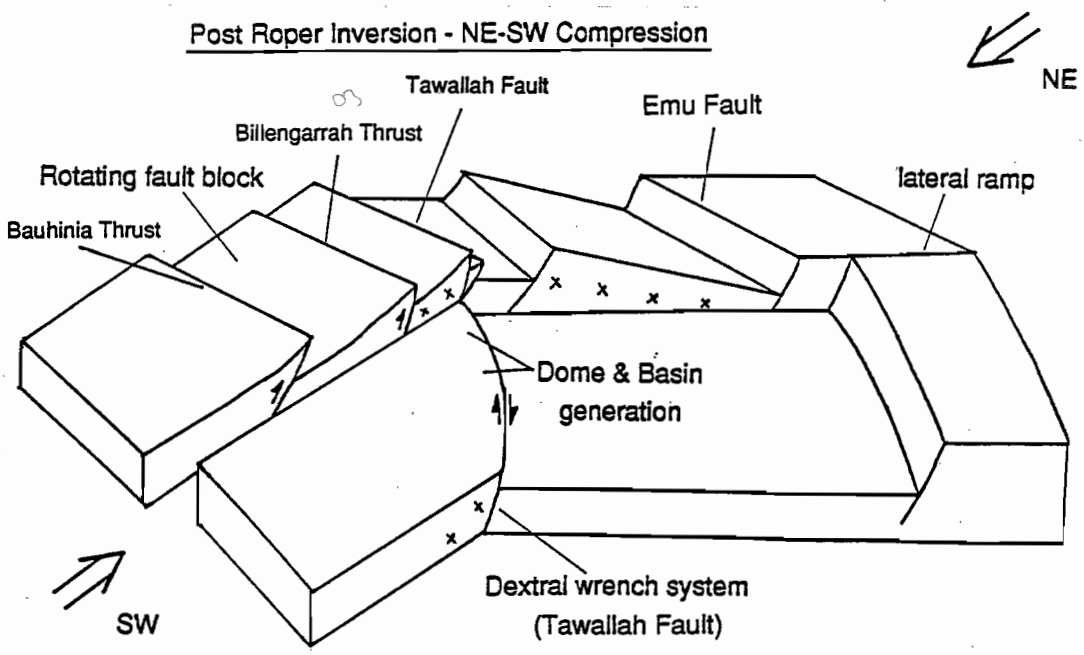

AMIRA/ARC Project P.384

Report No. 4

University of Tasmania
November 1993

Centre for Ore Deposit and Exploration Studies

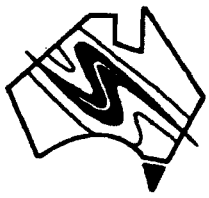

Proterozoic sediment-hosted base metal deposits

AMIRA/ARC Project P.384

Report No. 4

University of Tasmania
November 1993

Contents

Contents (cont.)

Introduction

PROJECT OBJECTIVES: P384

1. To determine the primary geological, geochemical and structural controls on the location and timing of base metal deposits in sedimentary basins.

2. To understand the chemical and hydrological evolution of metalliferous brines in selected Proterozoic sedimentary basins of Australia.

3. To develop basin metallogenic models and specific ore deposit models that may be used in the exploration for large-tonnage base-metal ore deposits.

RESEARCH FRAMEWORK

This research project involves a multi-disciplinary approach using regional geological, geophysical and structural studies, brine chemical modelling and geochemical and isotopic halo studies to provide a foundation on which to build a network of exploration criteria and ore deposit models for major sediment-hosted base metal deposits.

The project consists of three research modules as outlined below:

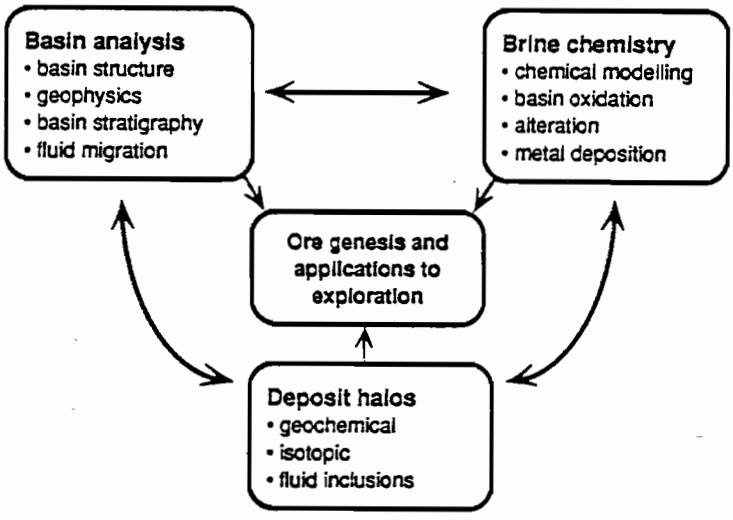

THIS REPORT

This is the fourth major report on the project and outlines results to date on the Basin Analysis and Brine Chemistry modules. A summary of research findings from the 1993 honours field programme is also provided. The structural and sedimentological evidence for early (mid- and late-Tawallah) inversion events in the McArthur Basin documented here has major implications for understanding fluid flow regimes during McArthur Group (HYC) times. Investigations into the origin(s) of alkali alteration, metal transport and ore depositional processes from sedimentary brines are also of significance in understanding regional-scale alteration and mineralisation features in the McArthur Basin.

The results presented here are derived primarily from the 1993 field season. The extensive field program mounted by the CODES research team could not have been achieved without the close cooperation and logistical support of the NTGS. In particular, we would like to acknowledge Paul Le Messurier, Barry Pietsch, Peter Haines, David (Rowdy) Rawlings and Brian Atkins.

Ross Large

Director
CODES

Summary of Research Findings

REGIONAL GEOPHYSICS - BASIN ARCHITECTURE 4: THE BAUHINIA SHELF

David Leaman

Interpretation of regional gravity and magnetic data in the Tanumbirini and Hodgson Downs regions, otherwise known as the Bauhinia Shelf with respect to the Batten Trough of the McArthur Basin, has shown that the region had a moderately stable history during Tawallah and McArthur Group times but has been very active subsequently. Proterozoic to Mesozoic deposition, including all units from the Roper Group to Cretaceous cover sequences, has been substantial but patchy.

The region possesses a largely granitic basement overlain by two massive volcanic sequences; the earlier one essentially felsic and the younger predominantly mafic. These gross associations have now been recognised across the entire McArthur Basin west of the Murphy Inlier and are inferred to continue SE beneath the inlier. Examination of structural relationships involving these associations suggests that each was controlled by primary basin faulting to yield asymmetric wedges of material but that considerable erosion occurred before and after each sequence. Each association can be defined magnetically and the older, less magnetic or more variable package is much more patchy. This may be a primary pattern or it may reflect extended erosion and uplift. The overlying mafics-dominated association is much more consistent in thickness but it, too, is variable - much more variable than on the facing Wearyan Shelf - although the maximum estimated thicknesses are comparable. There is every possibility that this sequence formed a large, continental sheet of flood basalts. Thickness variations are related to primary basin forms or subsequent local uplift and erosion.

These volcanic sequences have been tentatively linked to the Leichhardt-Argylla and Haslingden Group packages of the Isa Inlier in previous reports.

Substantial uplift and erosion has occurred prior to deposition of the Roper Group since these rocks may be inferred to directly overlie the mafic association in many parts of the region at depths up to 6 km. Either the Tawallah and McArthur Groups were never deposited in these zones or the units have been eroded. Either circumstance implies continuing tectonism across the Bauhinia Shelf but of different style to that within the Batten Trough or Wearyan Shelf regions.

Regional NW, NE and E-W trend systems are evident in the raw data and explained upon analysis to reflect proportions of the volcanic associations and the balance between cover and basement patterns. Major structures can be traced into the Batten Trough zone and some can be extended to the Murphy Inlier across the Wallhallow region. Depositional and erosional controls on the felsic suites is different north and south of the Hodgson Downs-Tanumbirini sheet boundary but the controlling structure seems only to have limited deposition or later uplift in terms of the mafic suites. Is this a compressional axis complementary to the Murphy and Urapunga zones?

No mineralisation is known in this region due to thickness and extent of cover sequences and none is yet known within the cover sequences themselves. The results, however, are of value in that they allow, when assembled in a basin-wide view, a comprehensive assessment of the shear couples acting throughout the early history of the McArthur Basin. A dextral wrench system acting NW-SE could generate the NE-trending extensional basins and the sub E-W compressional axes implied by all lower associations.

THE STRUCTURAL SETTING OF THE TAWALLAH GROUP, SOUTHERN McARTHUR BASIN, NORTHERN TERRITORY: IMPLICATIONS FOR AN EARLY TECTONIC EVENT

Jamie Rogers

Detailed structural mapping and fault sense determination in the Tawallah Group and lower McArthur Group of the Batten, Scrutton and southern Tawallah Ranges has recognised at least three distinct compressional tectonic events; a NE-SW compression (Post-Roper Inversion), a NW-SE compression and an early E-W compression (Mid-Tawallah Inversion). A four stage tectonic model is proposed for the study area invoking a complex structural history of large scale block faulting and high level, brittle deformation for the southern McArthur Basin.

PROGRESS REPORT - SEDIMENTOLOGY AND VOLCANOLOGY OF THE SOUTHERN McARTHUR BASIN

Stuart Bull

Detailed sedimentological and palaeocurrent data have been collected from the Masterton Sandstone at twelve localities in and around the Batten Trough. Two main facies associations have been identified, a conglomeratic basal sequence which is not always present and is very variable in thickness, overlain by a widespread fine- to medium-grained sandstone succession. These are provisionally interpreted as coarse-grained alluvial fan deposits developed on a deeply dissected palaeosurface, and associated finer-grained, high-energy braidplain or braided fluvial deposits respectively. These uniformly high-energy clasitc deposits are thought to have accumulated in fan or apron systems, and they interfinger with lower-energy/more distal fluvial and lacustrine or shallow marine deposits at some localities.

Provisional observations on the provenance of the basal conglomerates suggests that, in the Scrutton, Batten and Tawallah Range areas at least, they are derived from the lower Tawallah Group sandstone-dominated units, the Yiyinti and Sly Creek Sandstones. These units form the cores of each range, and the clear implication is that these Tawallah Group cores were lithified and subsequently uplifted by a major basin inversion event prior to the onset of McArthur Group sedimentation. This previously unrecognised syn- or post-Tawallah tectonic event has important implications for the development of southern McArthur basin, in that it indicates that the system could represent multiple generations of rift-phase/sag-phase couplets. In addition, an important implication for ore genesis models is that the proposed syn- or post-Tawallah basin inversion provides the potential for the existence of gravitationally driven, basin-wide meteoric fluid flow systems during the deposition of the mineralized McArthur Group.

The upper volcanic units of the Tawallah Group have been examined in the Mallapunyah Dome and Scrutton Ranges areas. The lower unit, the Settlement Creek Volcanics, consits dominantly of massive, medium-grained mafic material at both localities, and mafic peperitc textures have been described in the Gold Creek Volcanics in the Scrutton Ranges. A provisional depositional model has been proposed in which the bulk of the volcanic units represent mafic sills. Those of the Settlement Creek Volcanics were emplaced as largely coherent bodies at the base of the Wollogorang Formation, and those of the Gold Creek Volcanics breached this unit and intruded into unconsolidated sediments at a higher stratigraphic level. The whole sequence was later cut by rhyolite dykes. One of the main implications of this model for the analysis of southern McArthur Basin system, is that if both volcanic units are largely intrusive in character, then their distribution will be independent of the topographic control exerted in subaerial basaltic terrains. Care therefore needs to be taken when using these units as regional stratigraphic markers.

THE HISTORIES OF SOME FAULTS IN THE SOUTHERN McARTHUR BASIN: EVIDENCE FOR AN END-TAWALLAH UPLIFT AND A PRELIMINARY ANALYSIS OF STRESSES RELATED TO POST-McARTHUR AND POST-ROPER COMPRESSIONS

Richard Keele

Structural work has focussed on the northern part of the Southern McArthur Basin in the Tawallah and Costello Ranges. A combination of field work, interpretation of existing geological maps and drawing up cross-sections, has produced evidence for an end-Tawallah tectonic event that involved uplift and erosion of the underlying Tawallah Group rocks prior to the deposition of the Masterton Sandstones. A reconstruction of the geology at the time indicates that there was (1) a series of eastward facing tilt blocks (e.g. Four Archers-Hermit Fault block & Rosie-Emu Fault

block, and (2) a hanging block or dome which has exposed the Tawallah Group down as far as the Sly Creek Sandstone (Warrapirrmantila Dome). This may be explained by extension of the lithosphere during simple shear normal faulting in the lithosphere after a model proposed by Wernicke. This tectonic event at the end of the Tawallah may have been the driving force for uplift: in this scenario the Tawallah Group would be pre-rift, the Nyanantu syn-rift and the Masterton the post-rift sequence.

ALKALI ALTERATION IN THE MCARTHUR GROUP WITH PARTICULAR REFERENCE TO VOLCANICLASTIC MATERIALS: A PROGRESS REPORT

Garry Davidson

This is a progress report on a study of the behaviour of alkali elements in the saline-alkaline McArthur Group, with special reference to base metal mineralisation. The bulk of this report is a review of previous work on this topic. Feldspar-dominated alkali replacement of glassy volcaniclastic rocks can occur during low temperature saline diagenesis, or can characterise the passage of higher temperature saline fluids; the latter fluids can also be associated with Pb-Zn-Ag deposits in sedimentary basins. There is a clear need to discriminate the similar metasomatic products of these diverse processes.

A review of McArthur Basin data indicates (1) K-feldspar is an intimate part of the HYC ore assemblage; (2) albite forms the outermost alteration shell at HYC within tuff, surrounding an albite+K-feldspar zone; (3) tuff in regional BCF west of HYC consists of K-feldspar, whereas tuff in the Glyde sub-basin is dominated by albite. Oxygen isotope geochemistry separates Glyde sub-basin from HYC sub-basin volcaniclastics with similar Pb+Zn contents. Further work on the oxygen isotope interpretation is required, but the method has potential as an ore halo tool. Core samples of high-K tuff from west of HYC have been obtained and are presently being geochemically analysed.

TRANSPORT AND DEPOSITION OF BASE METALS FROM HIGH TEMPERATURE (250°C) AND LOW TEMPERATURE (150°C) SEDIMENTARY BRINES

David Cooke

Numerical simulations of transport and depositional processes for high temperature (250°C) moderate salinity (10 eq. wt. % NaCl) sedimentary brines have revealed that significant base metal transport can occur in acidic oxidised, alkaline oxidised, and acidic reduced brines. Moderate salinity alkaline, reduced brines are not capable of carrying sufficient quantities of base metals to be important in sediment-hosted base metal deposit formation.

Hematitic sandstones provide excellent aquifers for oxidised metalliferous brines. In contrast, significant alteration to potassic and/or propylitic assemblages will occur when brines interact with mafic volcanics. High temperature mineralised brines can migrate significant distances along faults without dumping their base metal load, provided the fluids do not interact significantly with the surrounding wallrocks. Cooling and/or boiling of these metal-rich fluids during cross-stratal transport will produce barren quartz veins.

In the trap environment, mixing of metalliferous brines with anoxic seawater is an excellent mechanism for producing Zn-Pb-rich massive sulfide mineralisation. Mixing of the same brines with oxidised seawater produces siliceous Cu-Ag-rich exhalites. Interaction of reduced, acidic brines with pyritic dolomitic sediments results in the precipitation of simple Zn-Pb-rich sulfide mineralisation. More complex silicates are produced together with the base metal sulfides when the replacement process involves oxidised brines.

At 150°C, similar depositional products are predicted for aquifer and cross-stratal transport, and for depositional processes. However, 10 wt % brines are mostly incapable of carrying sufficient base metals to form economic base metal mineralisation, unless the fluid is oxidised and/or acidic enough. High $CO_{2\ (aq)}$ contents (1 wt %) in the initial brines stabilises siderite as a depositional product in several low-T simulations, suggesting that sedimentary brines must be sufficiently overpressured to retain high CO_2 levels in solution. Reasonable water depths (several hundred metres) would be required to maintain such pressures (you'd definitely get your feet wet).

SECTION A

Basin Analysis Module

REGIONAL GEOPHYSICS - BASIN ARCHITECTURE

4. The Bauhinia Shelf

David Leaman
Centre for Ore Deposit and Exploration Studies

SUMMARY

Interpretation of regional gravity and magnetic data in the Tanumbirini and Hodgson Downs regions, otherwise known as the Bauhinia Shelf with respect to the Batten Trough of the McArthur Basin, has shown that the region had a moderately stable history during Tawallah and McArthur Group times but has been very active subsequently. Proterozoic to Mesozoic deposition, including all units from the Roper Group to Cretaceous cover sequences, has been substantial but patchy.

The region possesses a largely granitic basement overlain by two massive volcanic sequences; the earlier one essentially felsic and the younger predominantly mafic. These gross associations have now been recognised across the entire McArthur Basin west of the Murphy Inlier and are inferred to continue SE beneath the inlier. Examination of structural relationships involving these associations suggests that each was controlled by primary basin faulting to yield asymmetric wedges of material but that considerable erosion occurred before and after each sequence. Each association can be defined magnetically and the older, less magnetic or more variable package is much more patchy. This may be a primary pattern or it may reflect extended erosion and uplift. The overlying mafics-dominated association is much more consistent in thickness but it, too, is variable - much more variable than on the facing Wearyan Shelf - although the maximum estimated thicknesses are comparable. There is every possibility that this sequence formed a large, continental sheet of flood basalts. Thickness variations are related to primary basin forms or subsequent local uplift and erosion.

These volcanic sequences have been tentatively linked to the Leichhardt-Argylla and Haslingden Group packages of the Isa Inlier in previous reports.

Substantial uplift and erosion has occurred prior to deposition of the Roper Group since these rocks may be inferred to directly overlie the mafic association in many parts of the region at depths up to 6 km. Either the Tawallah and McArthur Groups were never deposited in these zones or the units have been eroded. Either circumstance implies continuing tectonism across the Bauhinia Shelf but of different style to that within the Batten Trough or Wearyan Shelf regions.

Regional NW, NE and E-W trend systems are evident in the raw data and explained upon analysis to reflect proportions of the volcanic associations and the balance between cover and basement patterns. Major structures can be traced into the Batten Trough zone and some can be extended to the Murphy Inlier across the Wallhallow region. Depositional and erosional controls on the felsic suites is different north and south of the Hodgson Downs-Tanumbirini sheet boundary but the controlling structure seems only to have limited deposition or later uplift in terms of the mafic suites. Is this a compressional axis complementary to the Murphy and Urapunga zones?

No mineralisation is known in this region due to thickness and extent of cover sequences and none is yet known within the cover sequences themselves. The results, however, are of value in that they allow, when assembled in a basin-wide view, a comprehensive assessment of the shear couples acting throughout the early history of the McArthur Basin. A dextral wrench system acting NW-SE could generate the NE-trending extensional basins and the sub E-W compressional axes implied by all lower associations.

INTRODUCTION

This report outlines analysis of gravity and magnetic data within the Tanumbirini and Hodgson Downs 1:250 000 map sheets in the

Codes: AMIRA / ARC Project P.384 - Proterozoic sediment-hosted base metal deposits. November 1993

western McArthur Basin. Parts of the Urapunga and Beetaloo sheets have also been considered. The area is known as the Bauhinia Shelf (Plumb & Wellman, 1987).

Previous work reported for adjacent parts of the basin include:

1. The Batten Trough region (Leaman, 1992)
2. The Wallhallow region (Leaman, 1993a)
3. The Wearyan Shelf and Murphy Inlier (Leaman, 1993d)

The basic methodology for this analysis has been outlined by Leaman (1992) and clarified in Leaman (1993b, c).

The principal objectives of the interpretation have been to define general relationships within the basin and provide information which may constrain concepts of structural evolution, fluid motion and mineralisation. Achievement of these goals requires a coherent assessment of the entire basin. The present work completes the third stage of this process.

GEOLOGY

The geology of the region is shown in Figure 1 to be dominated by the relatively recent cover sequences. There is negligible exposure of any rocks older than the Roper Group and the only significant occurrences lie in the NE corner of the Hodgson Downs sheet. These rocks are also younger than the McArthur Group.

Drilling and seismic survey activity within the region has been very limited and no substantive supporting or independent information is available.

Any geophysical interpretation in such conditions is essentially blind and must be tied either to better known conditions or rigorously undertaken to limit possible ambiguities.

GEOPHYSICAL DATA

Only regional gravity and magnetic data have been reviewed. These are illustrated in Figures 2 and 3 (AGSO compilations). Every indication offered by such data is important in view of the limited control offered by geological mapping.

Regional magnetic data (Figure 2) picks out some large regional features and some strings of local, shallow elements. There are some marked E-W and NW-SE trends but there is no correlation with any aspect of established local geology other than limited responses near minor intrusions within the Roper Group.

The gravity data are very different (Figure 3). E-W elements are not obvious but at least one major NW-SE feature is apparent. The gravity field is generally neutral or slightly positive in the Hodgson Downs area but strongly negative to the south

The central sub NW-SE gradients are significant within each data set and there are suggestions, especially in the magnetics case, of superimposed shallow sources.

ROCK PROPERTIES

Since there are no significant exposures of any units which may be present between ultimate basement and Nathan/Mt Rigg or Roper Groups, and certainly no property determinations, some properties and characteristics have been assumed. The values used have been based on implications from previous work and reasonable ranges for presumed lithologies.

Previous work has shown that many of the basement granitoids are relatively non magnetic, especially when contrasted with overlying felsic assemblages or mafic volcanics and intrusives. Basement sedimentary assemblages, as exposed near the Murphy Inlier, are also non magnetic in these terms. There is no magnetic basement and no gross simplifying assumptions can be made about basement. It has been presumed to be essentially non magnetic.

Response analysis for surveys across the Scrutton Ranges and the Murphy Inlier has indicated that the felsic Scrutton and Cliffdale Volcanics possess much more significant magnetic properties and although these are variable values in excess of 0.001-0.002 cgs (~0.015 SI) are likely as a bulk estimate. It is possible that the variations disguise internal divisions within these units (especially the Cliffdale Volcanics) and more work is necessary . Any such distinction may prove of considerable value in ultimate correlations.

Similar assessments of the mafic volcanic members of the Tawallah Group, coupled with some direct susceptibility measurements (Keele, pers. comm.) show that properties are variable but at least of the same order. Some of these units have clearly been altered and the properties confirm this. Units such as the Peters Creek Volcanics are more magnetic and values in excess of 0.003 cgs (~ 0.04 SI) are likely.

Thick mafic volcanic sequences common in the Isa Inlier possess bulk contrasts with associated sedimentary successions of at least 0.005 (0.004-0.008) cgs (~0.07 SI).

Some members of the Tawallah and McArthur Groups are very slightly magnetised but the effect is insignificant in local and regional terms and at least

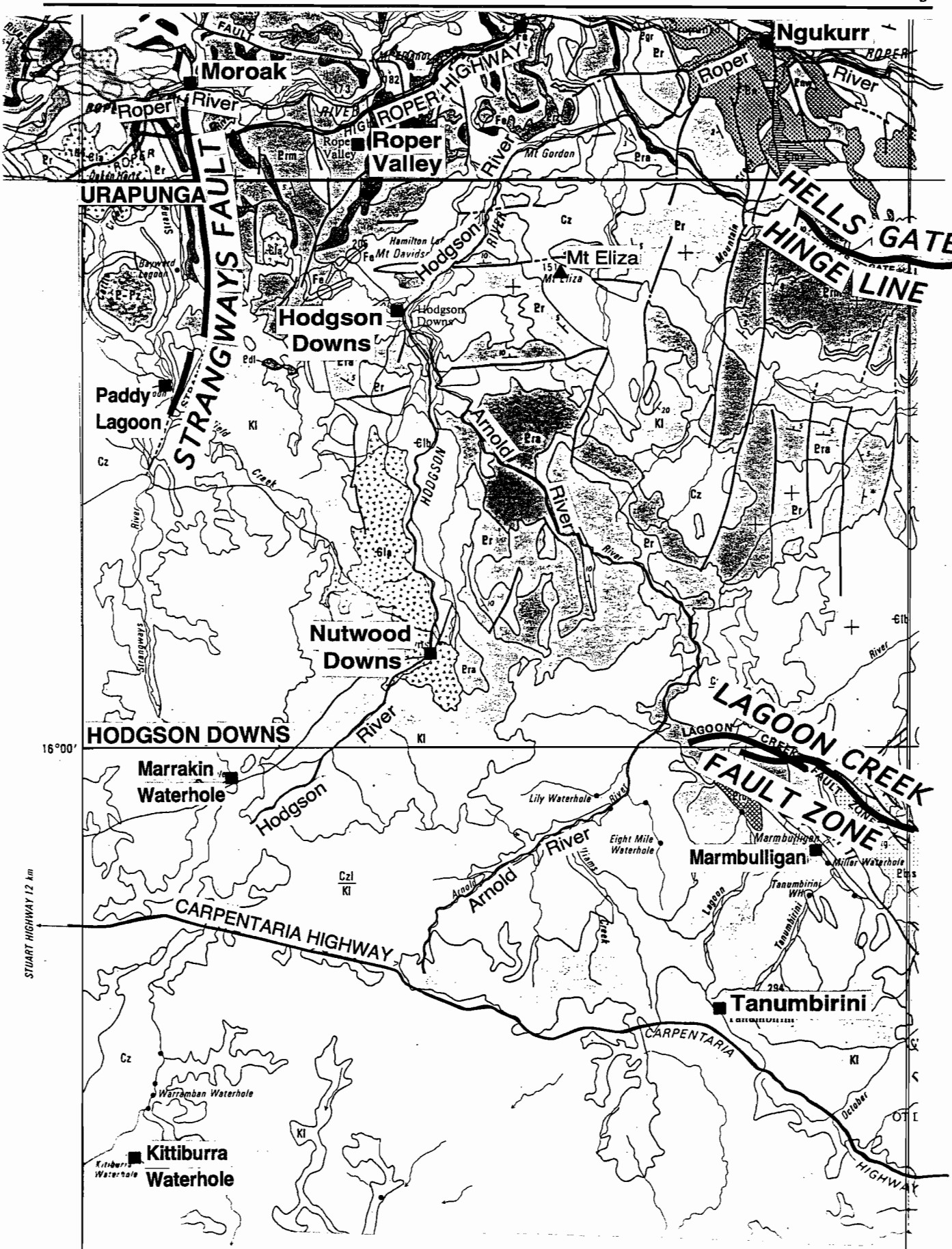

Figure 1. Geological base map after Plumb (1988) - Bauhinia Shelf.

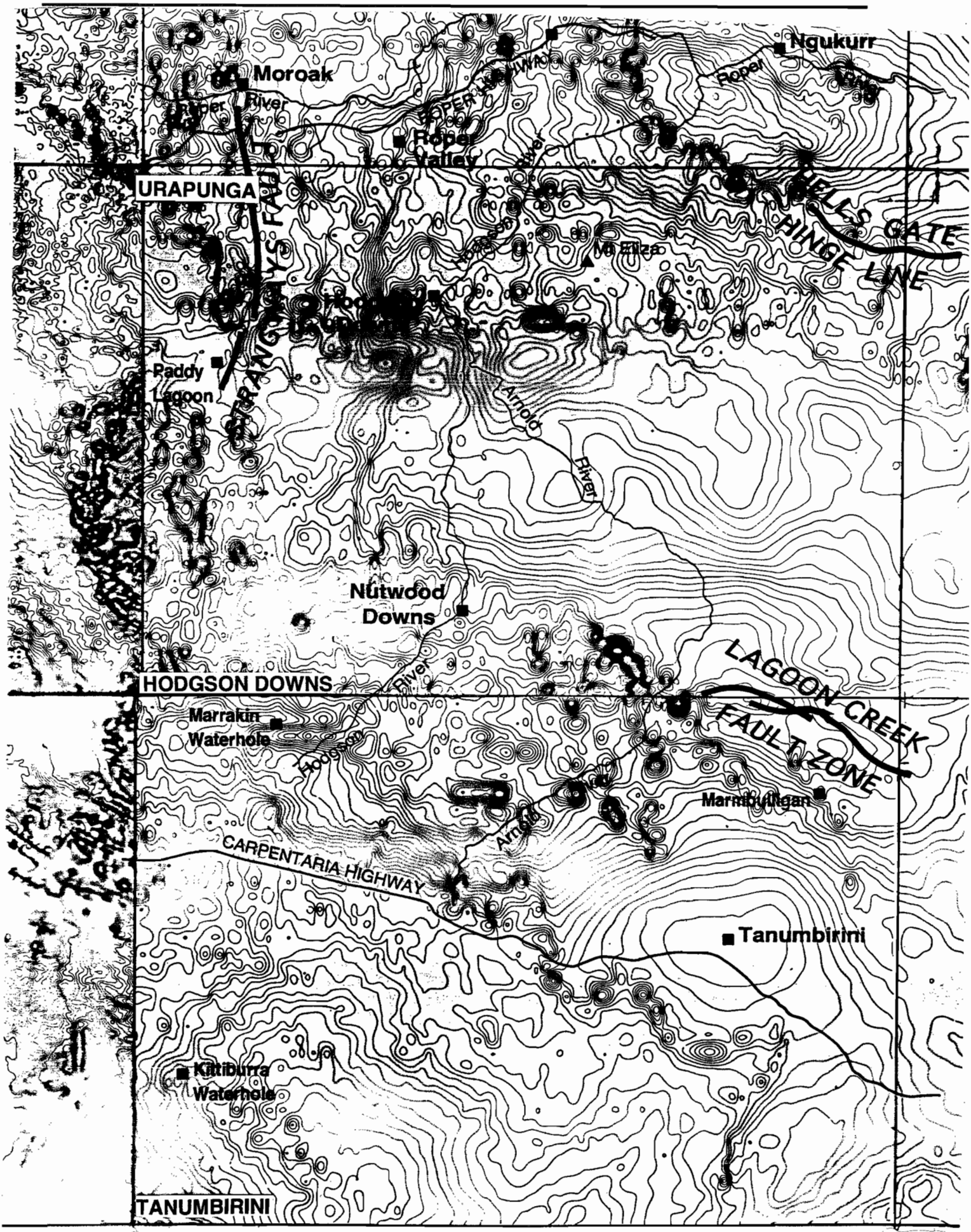

Figure 2. BMR regional compilation of magnetic field in Bauhinia Shelf region.

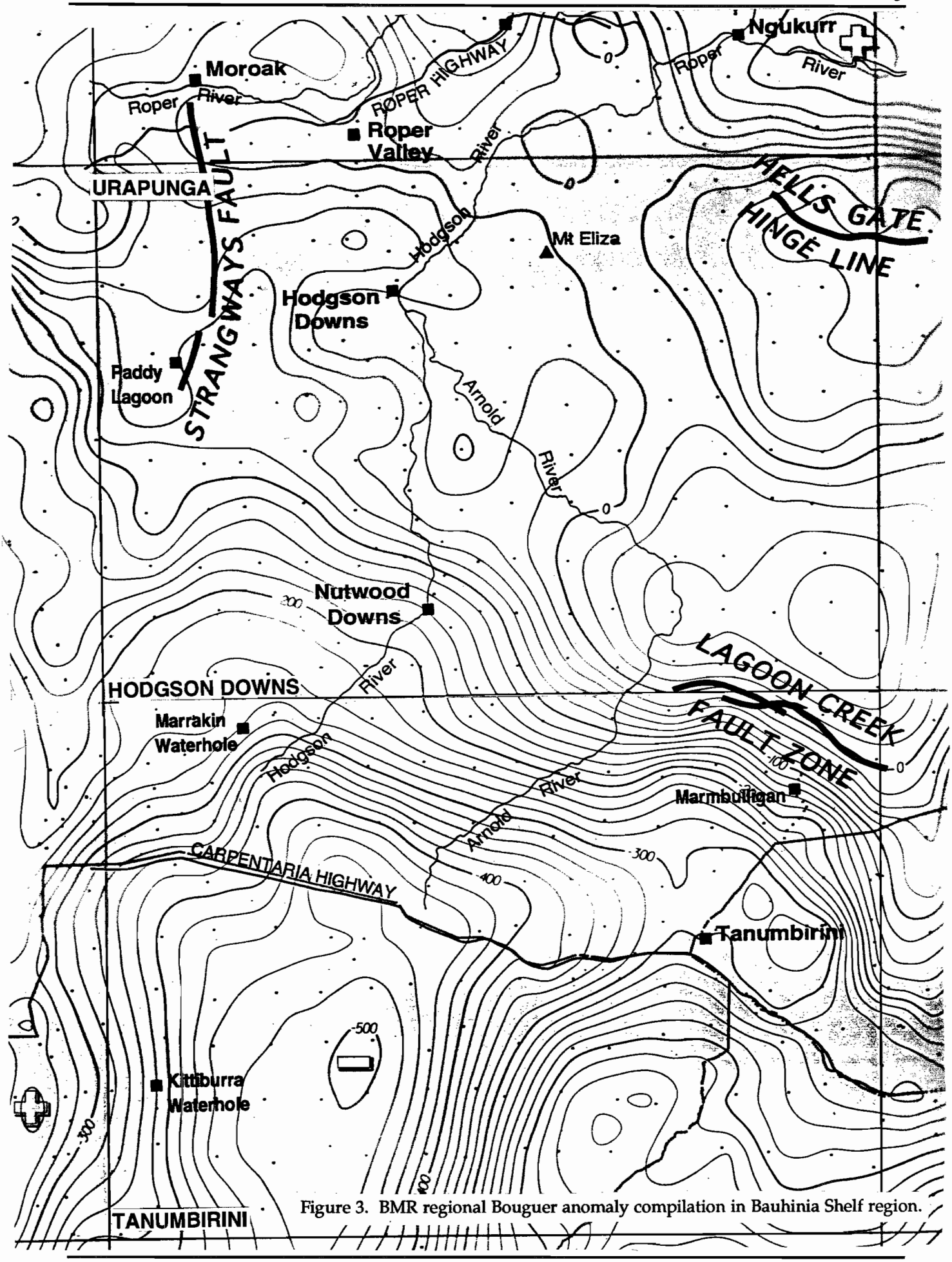

Figure 3. BMR regional Bouguer anomaly compilation in Bauhinia Shelf region.

two orders of magnitude less than observed results for both felsic and mafic rocks in the region.

Cover rocks are essentially non magnetic although some local young flows or intrusives may possess properties of the magnitude noted above. These units tend to be very thin, however, and do not contribute any substantial regional variations in the magnetic field.

Rock densities are not easily defined given the limited exposures in the basin and the paucity of sampling. Basement rocks may be considered to possess densities in excess of 2.74 t/cu m but their actual properties tend to be largely irrelevant due to the large volumes of associated granitoids. Direct inspection of contrast anomalies indicates that the granitoids have densities of the order of 2.64 t/cu m. Limits can be placed on this estimate. Densities of such rocks are unlikely to be less than 2.62 in any event and gradient assessments suggest that densities in excess of 2.66 are not realistic. The implied contrast with intruded sedimentary basement is about 0.12 t/cu m. This suggests that the basement contains large volumes of material with average densities of either 2.64 or 2.76 t/cu m. Leaman (1993d) indicated that at least part of the basement(?) may have densities of the order of 2.85 t/cu m and be non magnetic. Very few sedimentary or igneous lithologies can be suggested for such material but a number of metamorphic possibilities exist.

Previous interpretations have included large thicknesses of volcanic rocks and there can be no doubt of the existence of such accumulations given the magnetic evidence (Leaman, 1993b). But, given the scale implied and the likely densities some limits are imposed by the total gravity field responses. By comparing effects in those regions where cover is either present or absent, or there are clear structural variations it is possible to imply that the nominal felsic and mafic associations cannot be denser than 2.79 or 2.85 t/cu m respectively as bulk estimates. This implies that each package includes a moderate proportion of intercalated sediment. The density estimates obtained in this way are credible for the associations implied even if the values cannot be directly verified.

Sedimentary rocks of the Tawallah and McArthur Groups can be judged on their contrast with other materials, especially where closely sampled data constrain the anomalies, to have densities of about 2.71-2.75 t/cu m and 2.74 has been taken as a typical density. This is comparable with the results from similar cover sequences in the Isa Inlier. More detailed review in the HYC region of the Batten Trough suggests that the upper part of the McArthur Group is more massively dolomitic and denser (about 2.77-2.78 t/cu m).

Rocks such as the Roper Group are less dense and anomaly patterns indicate a bulk density of the order of 2.55-2.60 and 2.59 t/cu m has been used throughout this basin analysis. Lower densities have been employed for the Cambrian and Cretaceous cover sequences (2.5 max, and 2.35 t/cu m max respectively).

Values assessed in this way have been used throughout the interpretation. Many are unconfirmed but all are credible and reasonable and lead to no unexplained effect.

In summary, however, only two sequences are significantly magnetically; the felsic and mafic associations buried deep in the basin and which are only rarely exposed (felsics). Gravity analysis must, in contrast, consider the interactive effects of all sources. For this reason the magnetic data have been used to provide basic restraints on deep options, volcanic inferences and lateral variations and the gravity data have been applied to test feasibility and to derive information relevant to cover and basement variations.

INTERPRETATION

The interpretation has utilised the properties defined above in accordance with the interpretation criteria defined by Leaman (1993c) and the implications of previous work where wider ranges of exposures have produced convincing linkages between exposed materials and interpreted units.

Twenty five regional profiles across the Bauhinia Shelf have been assessed using 2D methods. These were oriented in a manner which allowed numerous intersection tests and also sample all aspects of the regional fields. 3D interactions and interference effects are inevitable but most such effects can be recognised and do not upset the interpretation in terms of gross relationships and source continuity.

Possible limits imposed on sensitivity and precision have been discussed by Leaman (1992, 1993d).

Model results for four typical profiles are shown in Figures 5 and 6. The location of these profiles is shown in Figure 4.

The models illustrate the variability of pre Roper Group geology. There are substantial thicknesses of mafic and felsic volcanics as described by Leaman (1993b). All modelling has used property values which are higher than determined for these rock associations based on near surface responses or measurements (see notes above). The susceptibility of the felsic and mafic sequences has been based on values of 0.003 and 0.005 cgs (0.045 and 0.065 SI) respectively. These are clearly extreme contrasts in terms of what is known in the McArthur Basin but

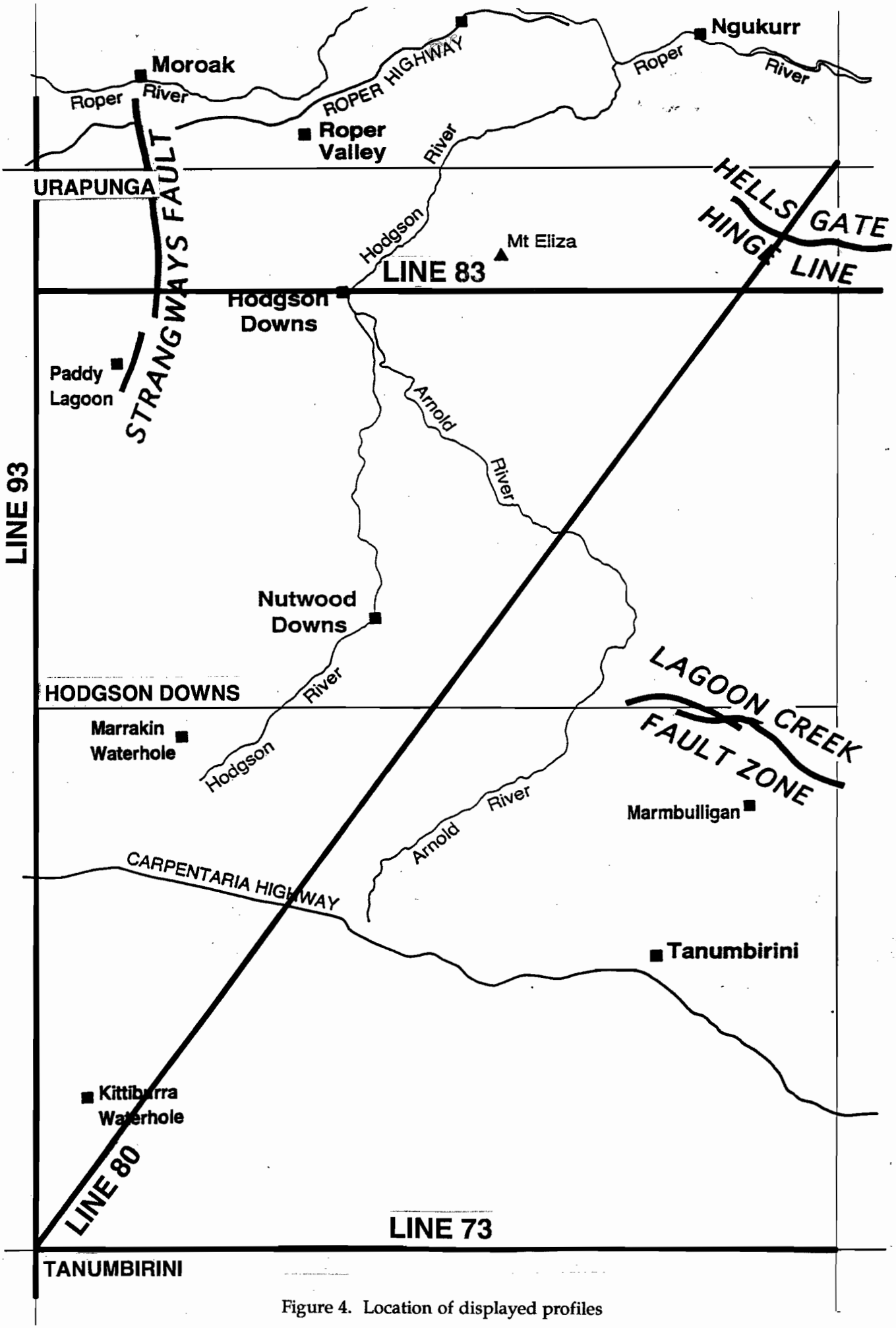

Figure 4. Location of displayed profiles

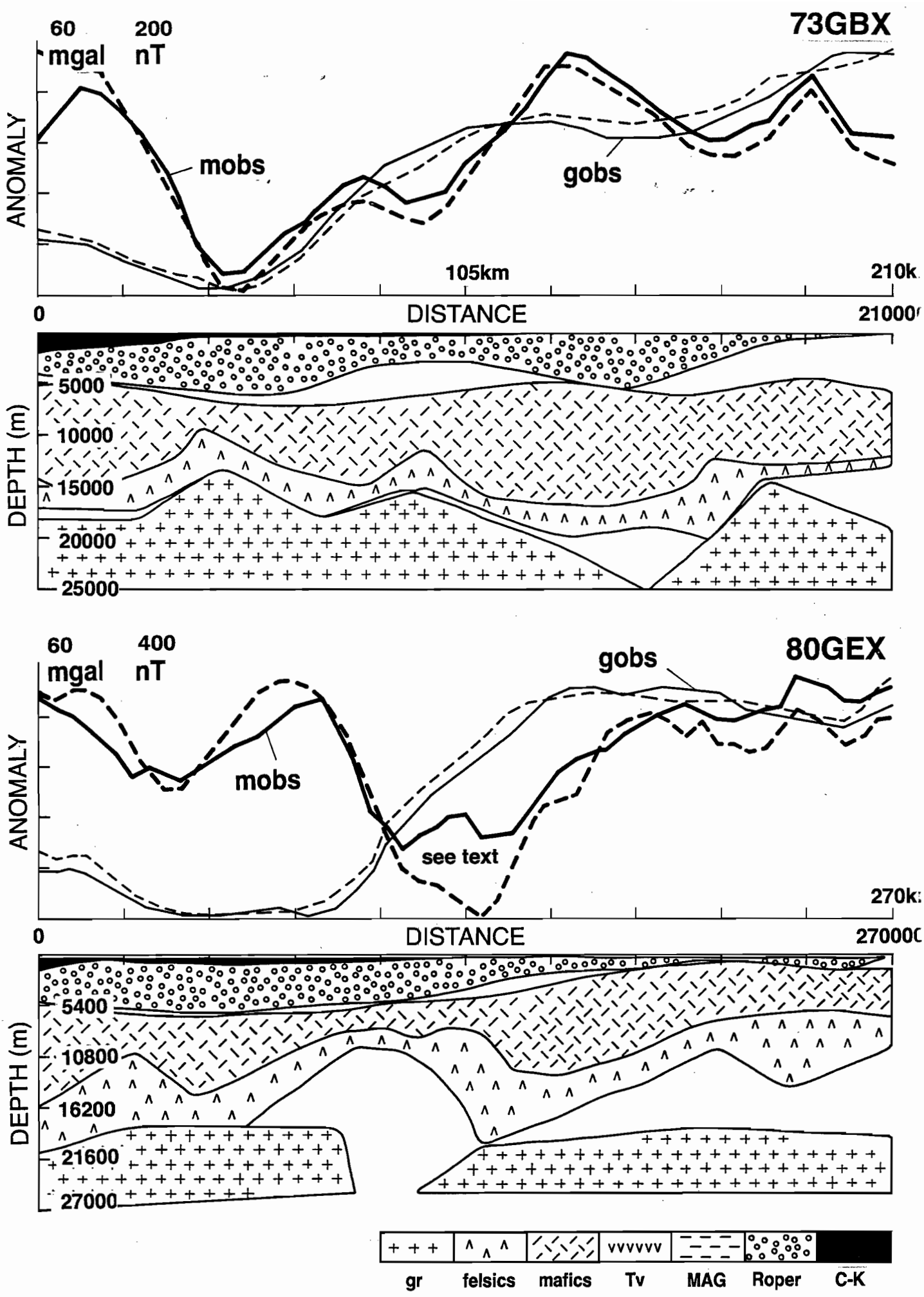

Figure 5. 2D gravity and magnetic models for profiles 73 and 80. gr = granite; felsics = felsic volcanic component; mafics = mafic volcanic component; Tv = Tawallah Volcanics; MAG = McArthur Group; C-K = Cambrian-Cretaceous.

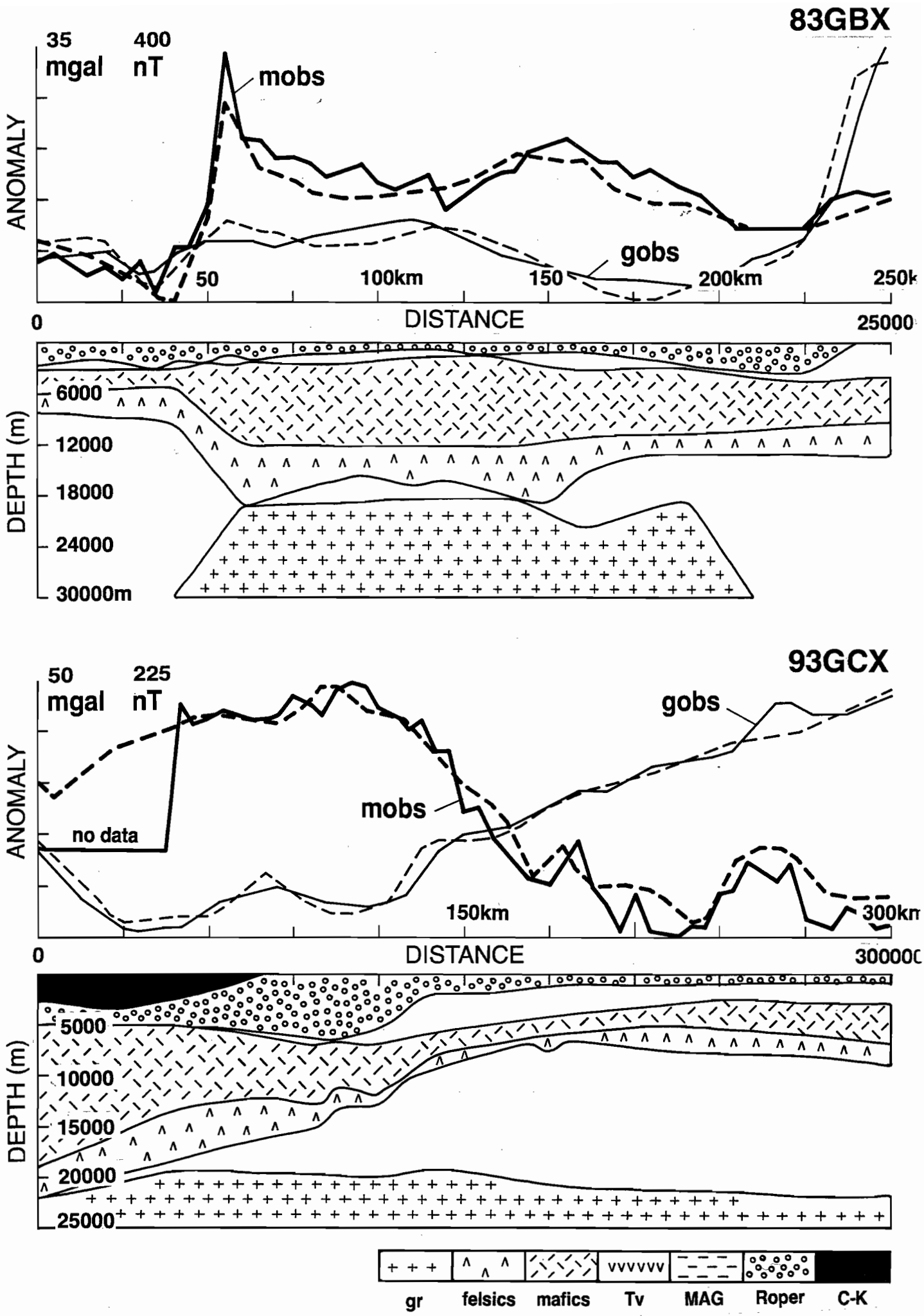

Figure 6. 2D gravity and magnetic models for profiles 83 and 93. gr = granite; felsics = felsic volcanic component; mafics = mafic volcanic component; Tv = Tawallah Volcanics; MAG = McArthur Group; C-K = Cambrian-Cretaceous.

are by no means atypical for the rock suites envisaged - if Isa Inlier comparisons are accepted. Use of such values does, however, mean that the interpretation may be considered to use virtual maximum contrasts and consequently recover minimum thicknesses. Given that the thicknesses implied even with such contrasts are large, any reduction would seem incredible. Not necessarily unbelievable or incorrect, simply incredible. Should the contrasts employed prove to have been inappropriate then the result would be to change implied thickness, or dips within the units but would not affect the overall implications of relationships or lateral variations.

In terms of this discussion it should be noted that the magnetic contrast of the mafic suite would appear to increase systematically to the north. The inferred contrast of 0.008 cgs may indicate more intense magnetisation or more mafic content in the package overall.

The profile interpretations provided are the result of combined analysis of both data sets.

Line 73 (Figure 5) displays quite smooth fields which require delicate balancing. The magnetic field is dominated by the thick mafic sequences and some large pinch structures which the gravity field is defined by the balance between Roper Group (and other cover) and the mafic sequence. Since basement granites are ubiquitous within the region these contribute in only a minor way to the gross pattern. The large negative anomaly in the western half of the Tanumbirini sheet is a function of cover, Roper Group and granite. The granite forms actual basement to the felsic association.

The role of the cover is illustrated for line 80 (Figure 5). This profile samples the major variations in the regional fields within the region. Asymmetric blocks of both volcanic piles are indicated and it is seen that these are overshadowed gravimetrically by the cover. Note that the granites of the basement are not significant contributors.

The magnetic profile presented is a median fit. It appears much worse than it actually is due to a number of subtle interactions - including some off line and 3D effects - which make for considerable instability in the resultant calculation. Variations of less than 500 m in the upper mafic sequence and less than 1000 m in its base (or small changes in dip) may lead to exchanges as great as the departures displayed, but in the opposite sense. The general form of the solution is satisfactorily defined within the stated limits and more work is not justified at this stage.

Line 83 (Figure 6) illustrates the character of the northern part of the Bauhinia Shelf in that part of the area where the gravity field is uniform and steplike. Note that the profile extends across the major positive step evident in the SE corner of the Urapunga Sheet (Figure 3) and which extends into the Mt Young area near the Hells Gate Hinge. This gradient marks the limit of significant Roper Group cover. Further west the Bouguer anomalies are a balance between mafic volcanics and basement type and either mafic deposition and preservation.

This profile also shows that at least one alignment of magnetic spike effects (Figure 2) is related to a major fault or thickness change in the volcanic piles. The mafic section is much more irregular in this part of the area and the felsics present substantial but variable accumulations.

Line 93 (Figure 6) lies at the western edge of the analysed region and shows that the piles thin northward and westward and begin to disappear. This clearly happens long before reaching Katherine. The cover sequences are substantial in the southern Tanumbirini zone.

All modelled profiles interlock consistently and isopachs have been extracted for both felsic and mafic piles. These isopach maps are presented as Figures 8 and 9. The implied relief on the roof of the basement granites is shown in Figure 7.

Figure 7 shows that the granite basement is of quite low relief overall with some large gaps. The basement style is comparable to that of the Wearyan Shelf, just deeper due to increases in Roper Group (and younger) cover sequences. The gaps may represent rending of a once contiguous granitic basement by NE-SW extension, or may a primary intrusion distribution.

There is no evidence of major disturbance or incremental uplift such as implied along the Batten Trough zone. The distribution and isopach variations within the felsic and mafic columns as interpreted suggests possible limits for the active Batten zone. It should be noted that the interpretation, with all its limitations, represents a view of relationships within the basin today, not as it might once have been at various stages in its evolution.

The felsic rocks are more disjointed and irregular in the SE quadrant of Hodgson Downs and the NE quadrant of Tanumbirini with a limit of change about midway along the common boundary. The mafics, however, suggest much more limited variations with the change restricted to the last sixth of the common boundary but with the projection of a structurally anomalous sub E-W feature extending far to the west near the sheet junction. It would appear that the active limits of the Batten zone lie near the eastern margins of the Hodgson Downs and Tanumbirini areas. These zone limits are indicated in Figure 10.

The piles of retained felsic rocks are localised and display NNE, NE and NW alignments with at least three E-W elements evident (absences or subsequent thinning). The felsic association is

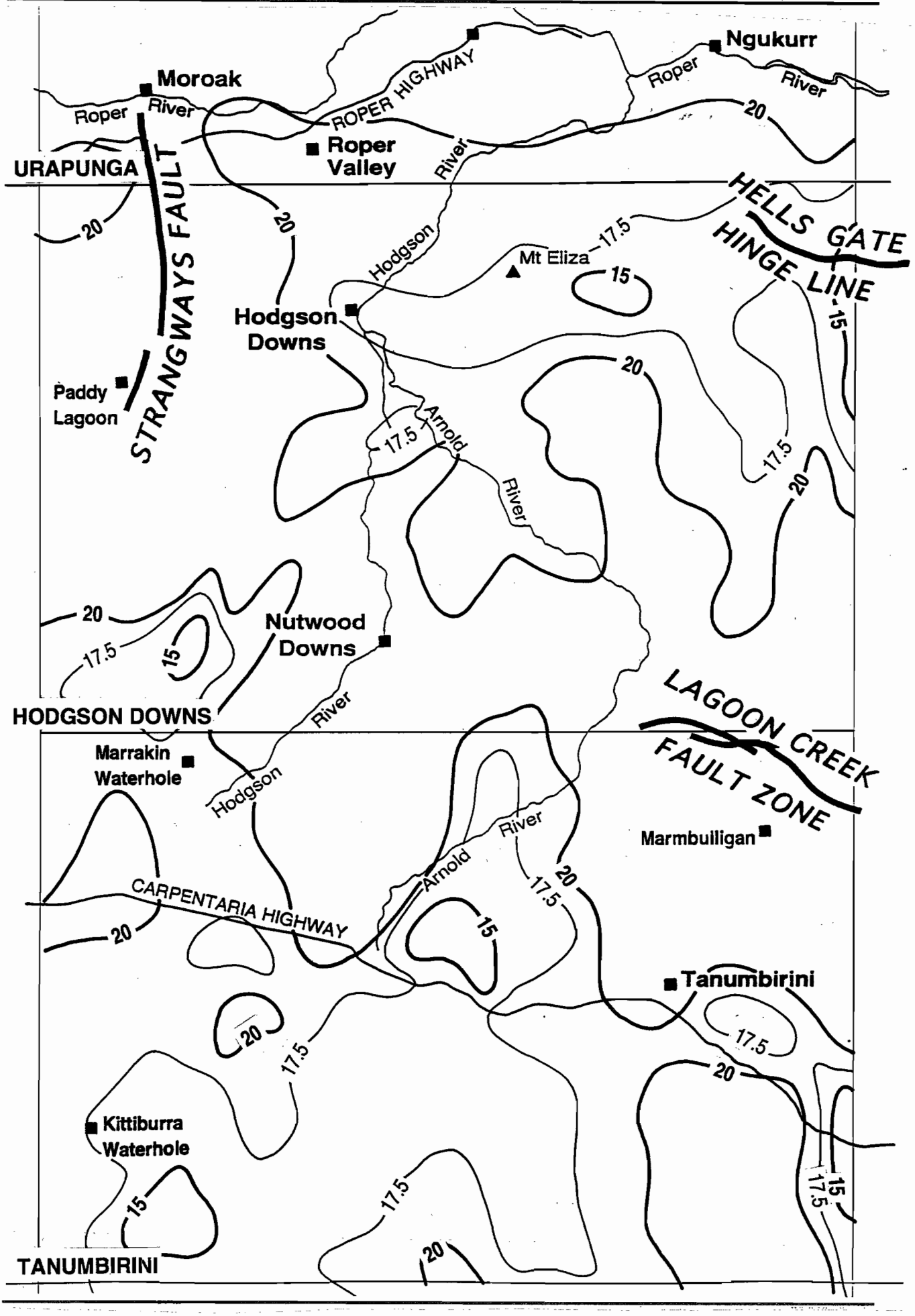

Figure 7. Distribution and form of the upper surface of the basement granitoids in the Bauhinia Shelf region.

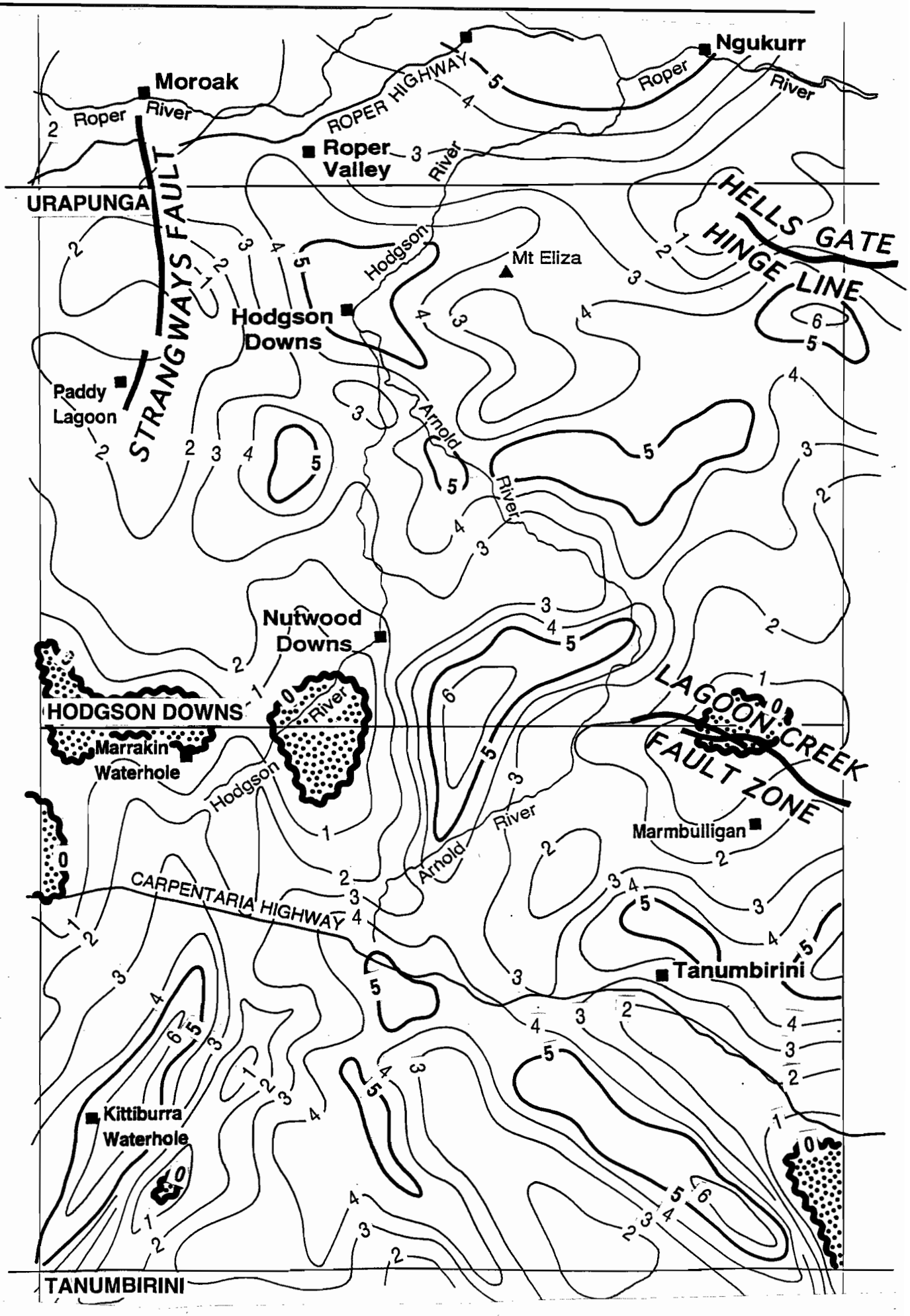

Figure 8. Thickness interpreted of lower felsic volcanic sequence, Bauhinia Shelf region.

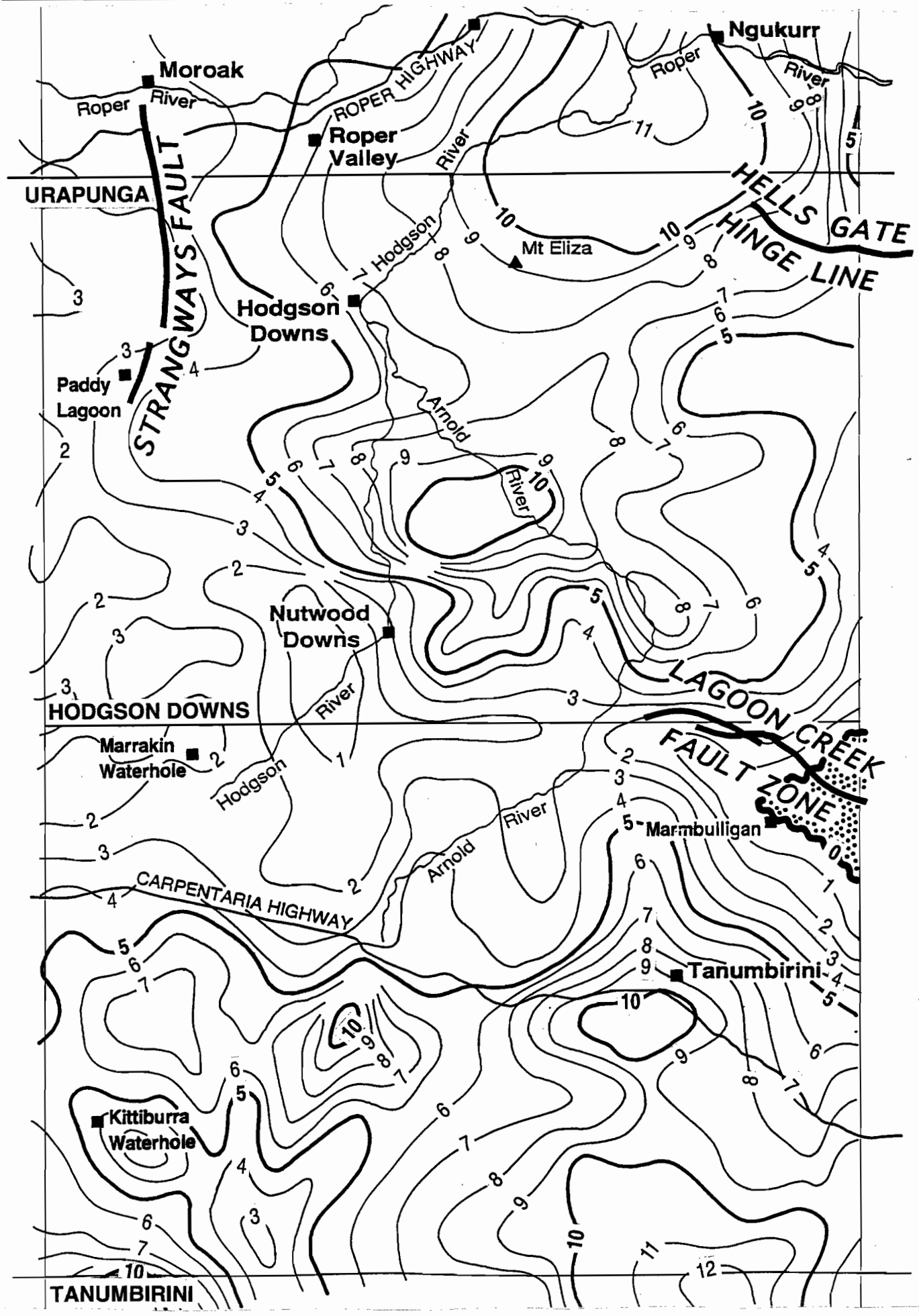

Figure 9. Thickness interpreted of main mafic volcanic sequence, Bauhinia Shelf region.

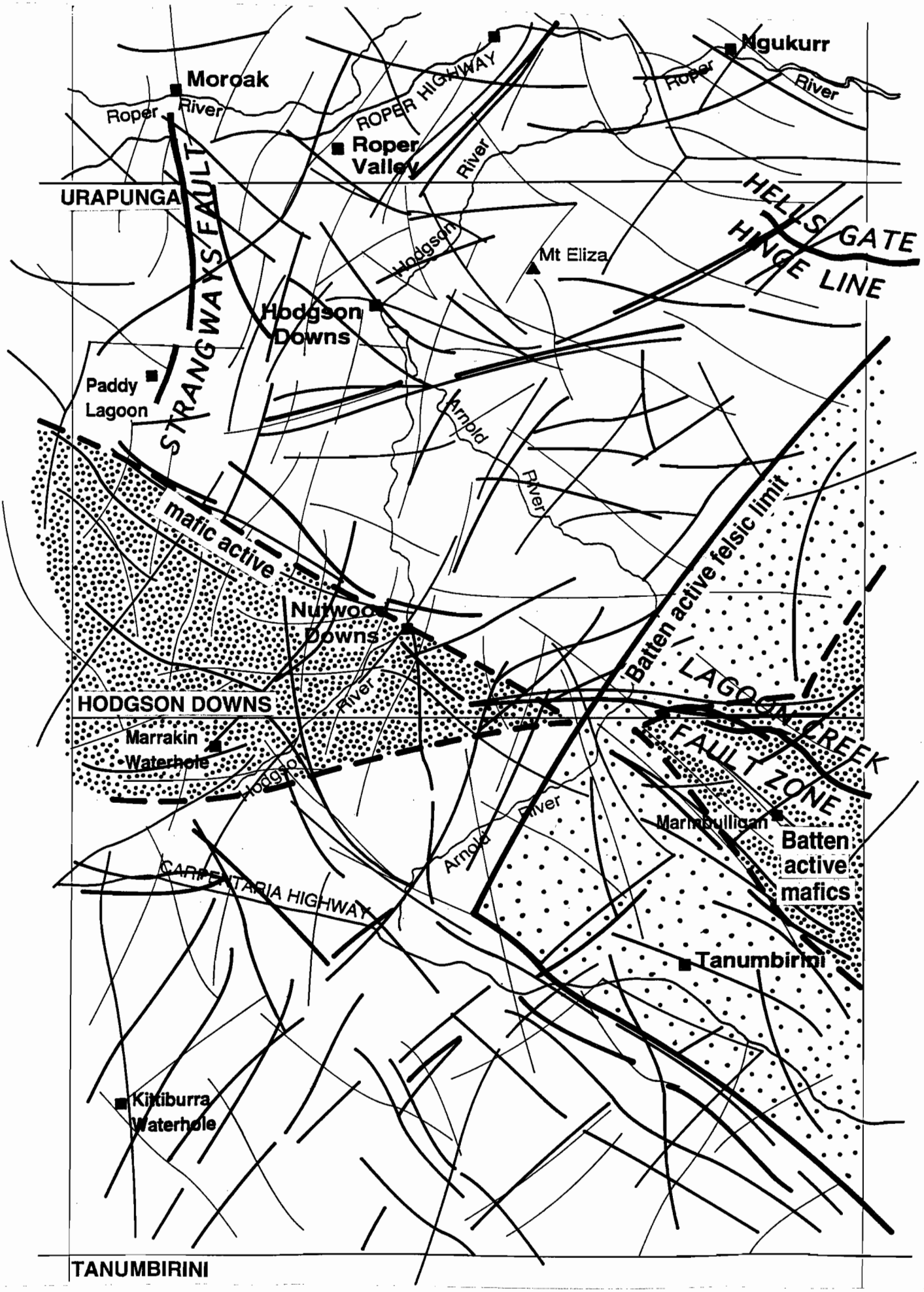

Figure 10. Trends inferred from observed fields and interpreted structures, Bauhinia Shelf region.

generally little more than 2 km thick but local accumulations of up to 7 km have been inferred. Alignments associated with the Lagoon Creek or Calvert Fault systems are not evident but a feature with similar trend is apparent in the southern part of the Tanumbirini sheet. It should also be noted that there is no correlation between the felsic occurrences and the main NW-SE gravity and magnetic gradients across the centre of the shelf. NNE-NE trends dominate.

This pattern is quite different to that displayed by the mafic column which gives the appearance of a large slab thinning westward but centrally uplifted (or perhaps partially onlapped during formation). The inference of differing contrasts north and south of this zone could be taken to support the implication that two piles onlapped a central rise with the northern pile containing more mafic volcanics. Clear correlations between the Lagoon Creek Fault system and the thickness of volcanic suites are evident.

Only two of these elements are mirrored in granite forms; the Urapunga E-W zone and the north-central Tanumbirini NNE-NW zone where granite is absent and the felsics are of high local relief.

This contrasts with the view suggested by the mafics.

No Urapunga E-W element is apparent in the mafic distribution and there is a marked reflection of the central NW-SE trend. There is a change of more than 5 km in the preserved thickness along this axis. The southernmost NW-SE trend, so obvious in the felsic distribution, is barely suggested in the mafic distribution.

The mafic volcanics of the Bauhinia Shelf are more segmented than on the Wearyan Shelf but the maximum thickness is similar (10 km +/- 1 km).

E-W trending features dominate the central part of the shelf and these can be traced directly into and across the Batten zone. It may also be noted that there is a slight rotation of the NE trend from NE-ENE to NNE-NE in passing from the Bauhinia Shelf eastward.

Trends (Figure 10) inferred from the data sets and the interpretation have been weighted in terms of likely rank and significance based on unit variations. A pronounced NE and NW grain has been recovered with some localised E-W elements superimposed.

It is now also possible to comment on some broader relationships within the McArthur Basin. A post Tawallah Group structural and depositional history has been attempted by Plumb et al (1990). The critical diagram was reproduced as Figure 7 in Leaman (1993e). This suggested that the eastern margin of the Batten Trough lay near the position of the Emu Fault. This is demonstrably false (see Leaman, 1993d); the Emu Fault is central to the trough. However, its intersection with major NE-trending structures may well have controlled mineralisation. This trend system and its relevance to deep structural and stratigraphic control has not been appreciated previously. In the absence of much surface stratigraphic control Plumb et al (1990) presumed some regularity of thickness for the Tawallah Group and indicated sub basin overlapping deposition for the McArthur Group and the Roper Group. While these styles have been supported by the architecture study there is much more to the basin sequence and a similar character must also be assigned to the Tawallah Group. The sections in this report illustrate the variability of the pre-Roper sequences and their virtual absence in the western part of the Bauhinia Shelf and Beetaloo sub basin areas. Major uplifts and periods of erosion are implied between the deep volcanic sequences and at each developmental stage thereafter, including developments related to the Roper Group. It may well be that the McArthur Group is restricted to the immediate vicinity of the Batten Trough as defined by this study - or in similar restricted regions, such as the South Nicholson Basin.

REFERENCES

Leaman, D.E., 1992. Regional geophysics -basin architecture #1. Report 1, Amira P384.

Leaman, D.E., 1993a. Batten Trough region, update and further analysis. Report 2, Amira P384.

Leaman, D.E., 1993b. Do volcanic piles really exist? Report 2, Amira P384.

Leaman, D.E., 1993c. Criteria for evaluation of potential field interpretations. Report 2, Amira P384.

Leaman, D.E., 1993d. Regional geophysics-basin architecture #3. Report 2, Amira P384.

Leaman, D.E., 1993e. Issues: basin correlations and overall architecture. Report 2, Amira P384.

Plumb, K.A., 1988. Geology of the McArthur Basin. 1: 1 000 000 map. BMR.

Plumb, K.A., & Wellman, 1987. McArthur Basin Northern Territory. Mapping of deep troughs using gravity and magnetic anomalies. BMR Journal Geology and Geophysics. 10, 243-252.

Plumb, K.A., Ahmad, M., Wygralak, A.S., 1990. Mid Proterozoic Basins of the North Australian Craton - Regional geology and Mineralisation. In Hughes, F.E. (ed.) Geology of the Mineral Deposits of Australia and New Guinea. Aust. I.M.M. 881-902.

The Structural Setting of the Tawallah Group, southern McArthur Basin, Northern Territory: implications for an early tectonic event.

Jamie Rogers
Centre for Ore Deposit and Exploration Studies

INTRODUCTION

This paper summarises the progress of a structural analysis conducted for areas of Tawallah Group exposure in the southern McArthur Basin, Northern Territory. Results of a regional stress analysis are presented and the style of deformation in the study area described. These results, together with a brief discussion of changes in Tawallah Group stratigraphy, are used to generate models describing the tectonic evolution of the study area.

Field report

This PhD. project forms part of AMIRA/ARC project 384. The study area is located some 50 km west of the McArthur River deposits and is bounded by the Tawallah Fault, the western margin of the Scrutton Ranges, the southern termination of the Batten Range and at the MOUNT YOUNG/BAUHINIA DOWNS 250 000 map sheet boundary (Fig. 1).

The 1992 field season comprised detailed mapping of the Batten Range. The 1993 season involved mapping of the Scrutton Range and parts of the southern Tawallah Ranges. Mapping was conducted at 1: 25 000 scale using colour air photographs and topographic maps and generally involved traverses through the stratigraphy and across structures. At each field locality, the sedimentary units and structural features were described and the sense of movement on faults determined. Representative samples of each sedimentary and volcanic unit were collected. The Scrutton Volcanics, Settlement Creek Volcanics, Gold Creek Volcanics and Tanumbirini Rhyolite were also sampled for geochemical analysis and hydraulic fault breccias from the Sly Creek Sandstone were sampled for fluid inclusion studies.

The aforementioned areas were chosen for detailed study because they contain some of the best exposure and most complete sections of the Tawallah Group. The Tawallah Group was targeted for two principle reasons: (1) it is dominated by thick, resistant sandstone units and is therefore well exposed; and (2) the Tawallah Group, being the oldest component of the southern McArthur Basin, should have recorded all of the structural history of the basin.

Previous structural modelling

The bulk of the available literature discussing the structural evolution of the McArthur Basin has been produced by the Australian Geological Survey Organisation (AGSO., formerly the BMR.), eg. Plumb (1979), Plumb *et al.* (1980), Jackson *et al.* (1987) and Plumb *et al.* (1990). The following is a brief summary of this literature with a discussion of their proposed structural models.

Plumb *et al.* (1980) suggests that deformation within the basin is defined by complex block faulting along the Batten and Urapunga Fault Zones which was controlled by pre-existing major faults. The Batten Fault Zone is the primary structural element of the southern McArthur Basin and constitutes a north-trending zone some 50 km wide.

The Batten Fault Zone contains two conjugate sets of faults; a NNW to N-trending set (eg. the Emu and Tawallah Faults) and a NE-trending set with the former displaying large vertical block movements (up to 7.5 km stratigraphic displacement) with a dextral component to them (Plumb *et al.*, 1990). Furthermore, major NW-trending faults (eg. the Mallapunyah, Calvert and Bulman Faults) show sinistral displacements and are interpreted as (reactivated ?) transfer faults (Plumb *et al.* , 1990). Plumb *et al.* (1990) conclude that the NE and NW-trending faults are a conjugate set that formed during a late, post depositional E-W compression event compatible with events in the Mount Isa

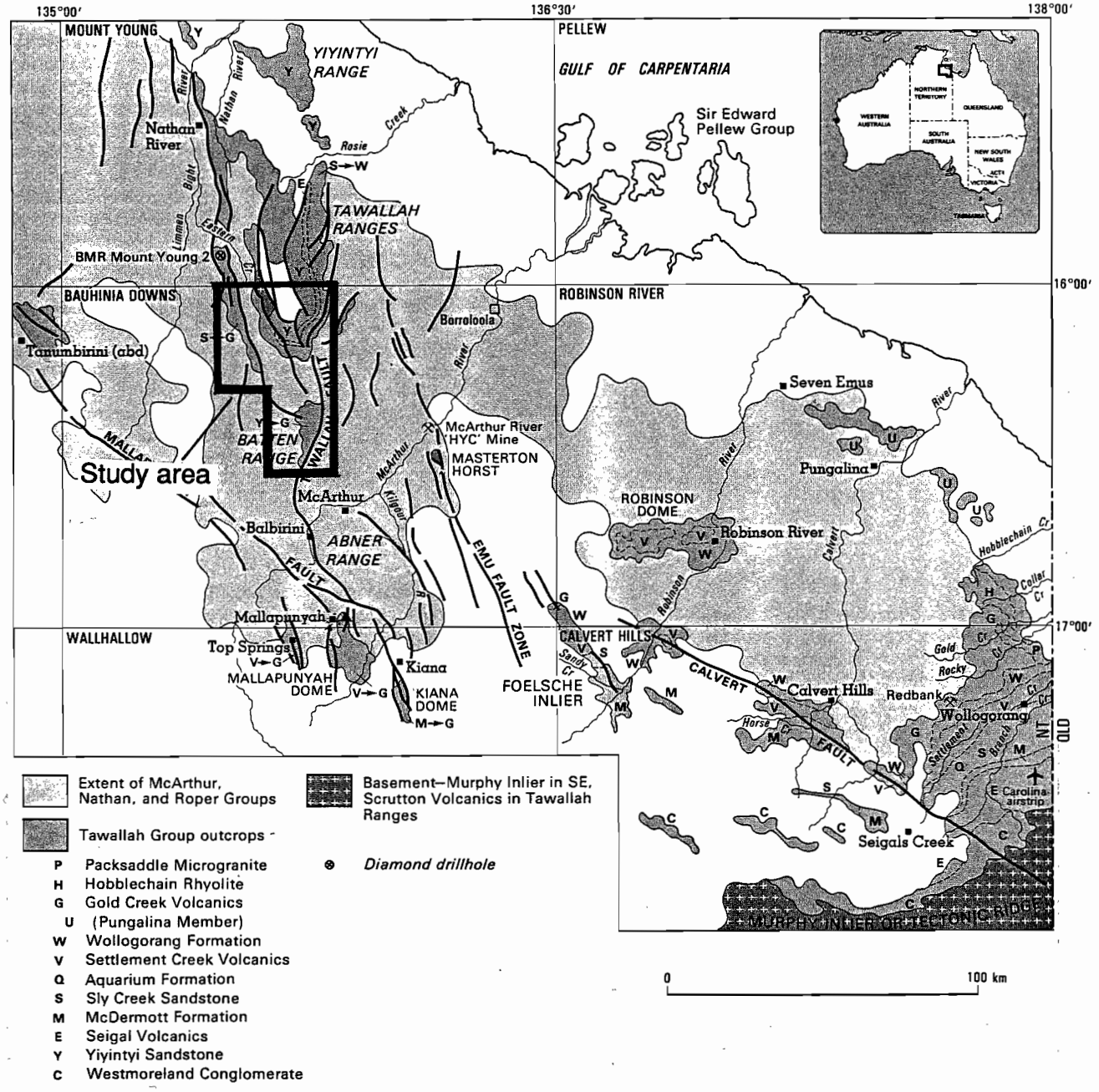

Figure 1. Location of study area (diagram from Jackson *et al.*, 1987).

region. This event essentially steepened and enhanced original extensional fault blocks.

The current tectonic model for the McArthur Basin is that the Batten Fault Zone represents a syndepositional graben or half graben where up to 12 km of sediments accumulated (the Batten Trough) (Plumb, 1980). Reversal of the original synrift tilt blocks (Plumb *et al.*, 1990) produced the present day horst where the basement (Scrutton Volcanics) and lower Tawallah Group rocks now crop out in the middle of the Batten Fault Zone along the Tawallah Ranges (Jackson *et al.*, 1987). Some features of this model are that:

- In the southern McArthur Basin, the Batten Trough was "*not evident as a half graben during deposition of the Tawallah Group*", as "*typical graben sediments (the Westmoreland Conglomerate) are present along the south eastern margin of the McArthur Basin and indicate early rifting.....with the orientation of the rift margin southwesterly - not northerly*" (Jackson *et al.*, 1987).

- In the southern McArthur Basin, subsidence of the Batten Trough is defined only by McArthur Group sedimentation whereas in the northern McArthur Basin, both the Tawallah Group and McArthur Group were subsided in the broadly symmetrical north trending Batten Trough (Jackson *et al.*, 1987).

- The strike-slip movement for many of the major faults has been interpreted as pre-McArthur Basin, as secondary fracture patterns are present in the basement (Ritarango beds, northern McArthur Basin, Plumb *et al.*, 1990). This has led to many of the known sub-basins, such as the Barney Creek sub-basin, being interpreted as strike-slip basins generated by major basement structures (Jackson *et al.*, 1987).

STRATIGRAPHY

The most up to date stratigraphy of the Tawallah Group is provided by Rawlings *et al.* (1993) and Pietsch *et al.* (1991). From a structural viewpoint it is important to note that the Tawallah Group can be divided into two parts. Plumb *et al.* (1980) has proposed two sub-units, a "lower succession" including the Westmoreland Conglomerate (Yiyintyi Sandstone equivalent), Seigal Volcanics and McDermott Formation which corresponds to the "Rifts and Marginal Basin" stage of the Mount Isa orogen and an "upper succession" which includes the Sly Creek Sandstone, Wollogorang Formation, Gold Creek Volcanics and Hobblechain Rhyolite. The upper succession corresponds to the "Marginal Subsidence and Transgression" stage of the Mount Isa orogen.

In the study area, this subdivision of the Tawallah Group has been modified according to the differing depositional environments, tectonic settings and structural histories recorded for each "succession". Furthermore, the Aquarium Formation in the BAUHINIA DOWNS region has been correlated with the McDermott Formation of the CALVERT HILLS region (Pietsch, Rawlings and Haines, pers. comm, 1993). The "lower succession" contains all units of the Tawallah Group up to and including the Aquarium Formation. The "upper succession" comprises the Wununmantyala Sandstone, Wollogorang Formation, Settlement Creek and Gold Creek Volcanics, Warramanna Sandstone, Tanumbirini Rhyolite and the Nyanantu Formation.

The lower sandstone units of the Tawallah Group (the Yiyintyi and Sly Creek/Rosie Creek sandstones) for the most part comprise intensely silicified, cross bedded and rippled shallow marine sandstones. These two sandstone units are separated by the Seigal Volcanics which have been interpreted as subaerial flood basalts (Plumb *et al.*, 1980). Above the Sly Creek Sandstone lies the Aquarium Formation, a unit of interbedded shale, sandstone and stromatolitic dolomite. As mentioned previously, this formation has been correlated with the McDermott Formation in the CALVERT HILLS region where the Sly Creek Sandstone is absent from the Tawallah Group stratigraphy.

The nature of the Tawallah Group sandstones change above the Aquarium Formation; they are less silicified and contain a higher proportion of coarser facies. Basal conglomerates are recognised locally for the Wununmantyala Sandstone, Warramanna Sandstone and also for the Masterton Sandstone, with the Warramanna Sandstone in the Scrutton Ranges containing thick sections of coarse, gritty interbeds. This may suggest a greater influence of fluvial depositional environments for the upper sandstones of the Tawallah Group. The volcanic members of the upper Tawallah Group are represented by a lower bimodal sequence of basalt cut by flow banded and autobrecciated rhyolite (the Settlement Creek Volcanics), an upper, more mafic sequence of coherent to peperitic basalt and volcanic sediments (the Gold Creek Volcanics) and a porphyritic quartz-feldspar rhyolite (the Tanumbirini Rhyolite). In the Scrutton Range, the Gold Creek Volcanics have been interpreted as shallow intrusive equivalents to the subvolcanic Settlement Creek Volcanics (Bull, 1993). The Settlement Creek Volcanics probably intruded as sills at the base of the Wollogorang Formation with part of the more mafic (less viscous) component intruding as high level sills into the unlithified and

water saturated sediments of the Wollogorang Formation to form the Gold Creek Volcanics (Bull, 1993). This suite of volcanic units in the upper Tawallah Group is very restricted laterally and regionally, may be confined only to small areas (eg. Scrutton Range, Mallapunyah and Kiana Domes).

STRUCTURE

Introduction

One of the most common misconceptions that is continually put forward in the literature is that the McArthur Basin is undeformed. While there is no mesoscopic pervasive fabric or fold development in the Tawallah Group, and essentially no metamorphism, there is abundant evidence for high level brittle deformation. The Tawallah Group in particular has seen at least three major compressional tectonic events which have caused brittle deformation (faulting, fracturing and brecciation), created local uplift and (in places) produced quite substantial crustal shortening.

Fault morphology

On the surface, fault zones in the Tawallah Group are expressed by one or more of the following features;

- resistant zones of silicification
- narrow cataclastic zones
- hydraulic brecciation

The size of the fault and (to a lesser extent) the type of fault control the surface expression of an individual structure. Large scale structures, such as the Tawallah Fault, have zones of silicification, cataclasite and brecciation up to 100m wide, whereas small scale structures may have silicification zones a few metres in width. The features associated with strike-slip faults seem to be concentrated into narrow zones (up to 100m for the Tawallah Fault), whereas low angle reverse structures are expressed over a much wider area (up to 500m for the Billengarrah Thrust). A possible explanation is that for low angle reverse faults, much of the applied strain is taken up by bedding plane slip and so cannot be concentrated into discreet zones, whereas strike slip faults cut obliquely and usually at a high angle to bedding.

Fault generations and geometries

One of the best kinematic indicators used for the determining the sense of movement on faults in brittle terrains are fault stria. These movement indicators are present on most fault surfaces in the study area, and their measurement has been the principle method used for determining fault sense in the field.

The stria measurements recorded in the field have been analysed using the computer program Etchecopar (Etchecopar *et al.*, 1981) which can identify different fault generations and their associated stress orientations from a given set of fault stria data.

The results of the analysis (Fig. 2) show that for each area analysed, there are up to three discrete fault generations, each corresponding to a particular stress field. These three fault sets have been generated during three distinct compressional events;

(1) NE-SW Compression

This is the major tectonic event to affect the McArthur Basin. The present-day structural geometry of the basin was generated during the NE-SW compression and the associated deformation post-dates all other structures and sedimentary deposition. For this reason, this event has been termed the "Post-Roper Inversion".

(2) NW-SE Compression

A second weaker event is recognised in the Tawallah Group that pre dates the Post-Roper Inversion, and may be responsible for the Tawallah Group/McArthur Group unconformity. A more detailed analysis of this event is provided by Keele (1993).

(3) E-W Compression

An early structural event separates the "lower succession" of the Tawallah Group from the "upper succession". Structures associated with this "Mid-Tawallah Inversion" are only recognised in the sandstones of the "lower succession. This event is discussed in more detail below.

Mid-Tawallah Inversion

A comparison of the fault patterns recorded in the "lower succession" of the Tawallah Group with those from the "upper succession" reveals a generation of faulting associated with E-W compression that is only expressed in the "lower succession" (the Yiyintyi and Sly Creek Sandstones). This clearly demonstrates that an early tectonic event has occurred in the Tawallah Group (the Mid-Tawallah Inversion).

Further evidence for this early event is the pervasive silicification of the sandstone units of the

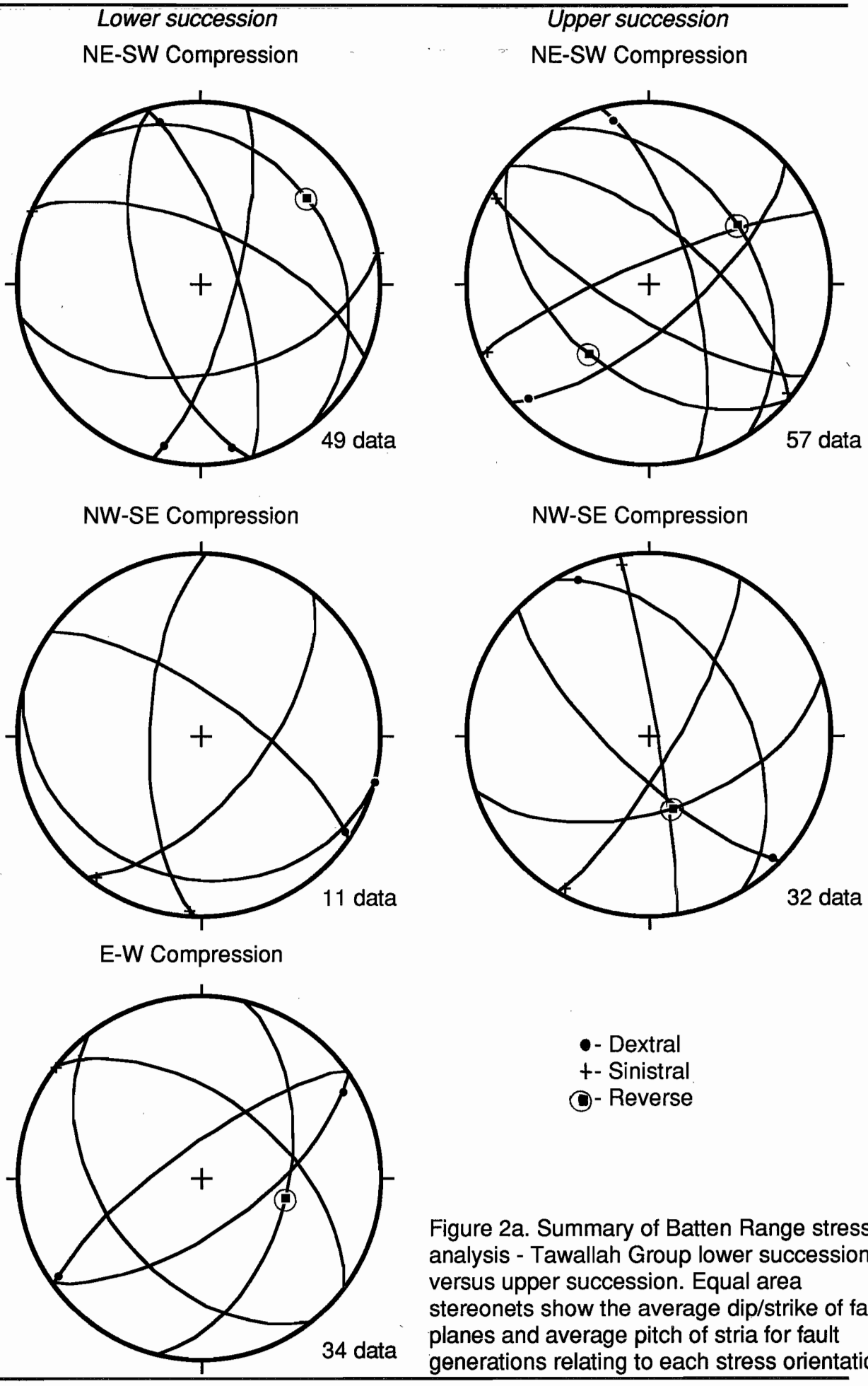

Figure 2a. Summary of Batten Range stress analysis - Tawallah Group lower succession versus upper succession. Equal area stereonets show the average dip/strike of fault planes and average pitch of stria for fault generations relating to each stress orientation.

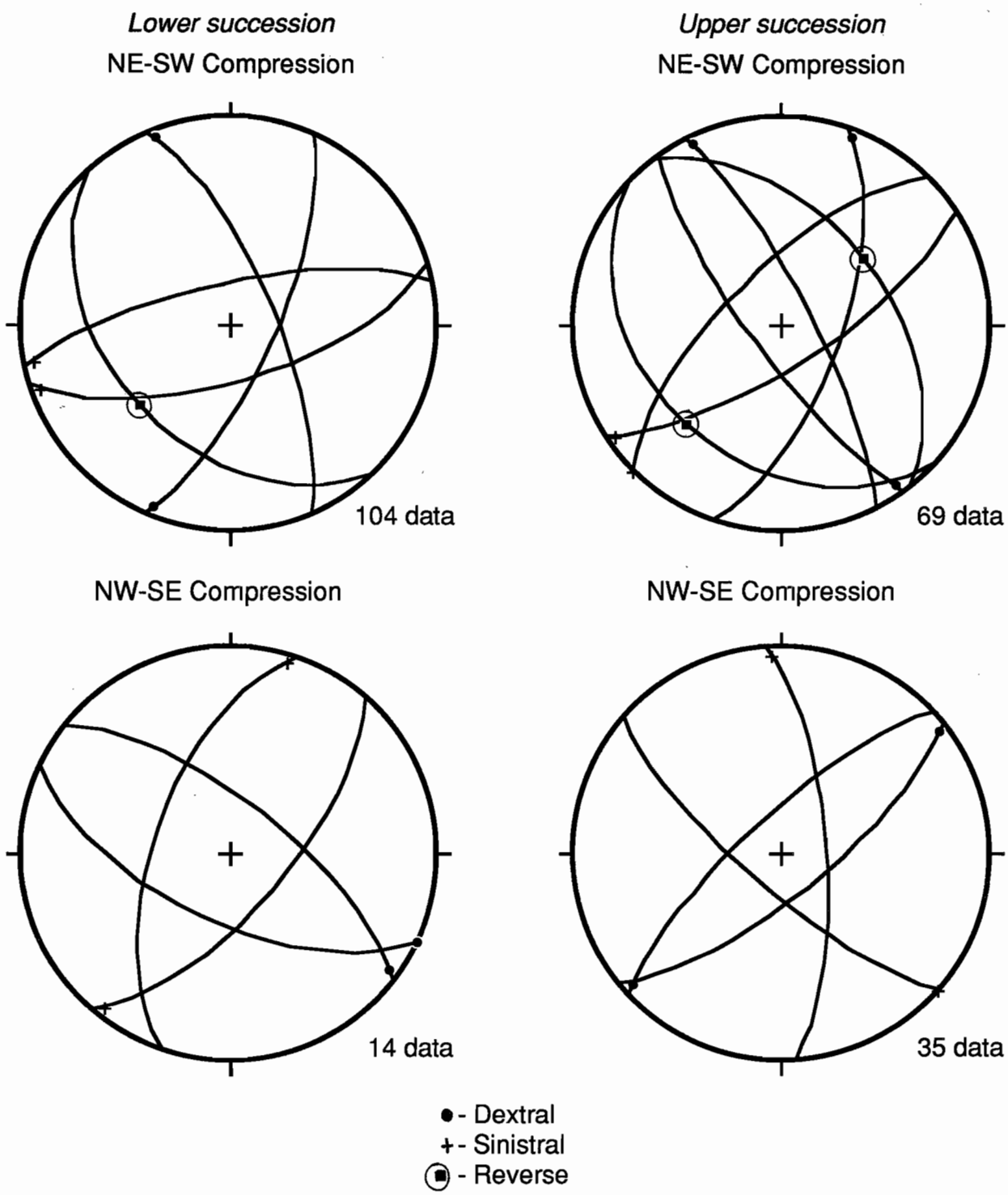

Figure 2b. Summary of Tawallah Range stress analysis - Tawallah Group lower succession versus upper succession. Equal area stereonets show the average dip/strike of fault planes and average pitch of stria for fault generations relating to each stress orientation.

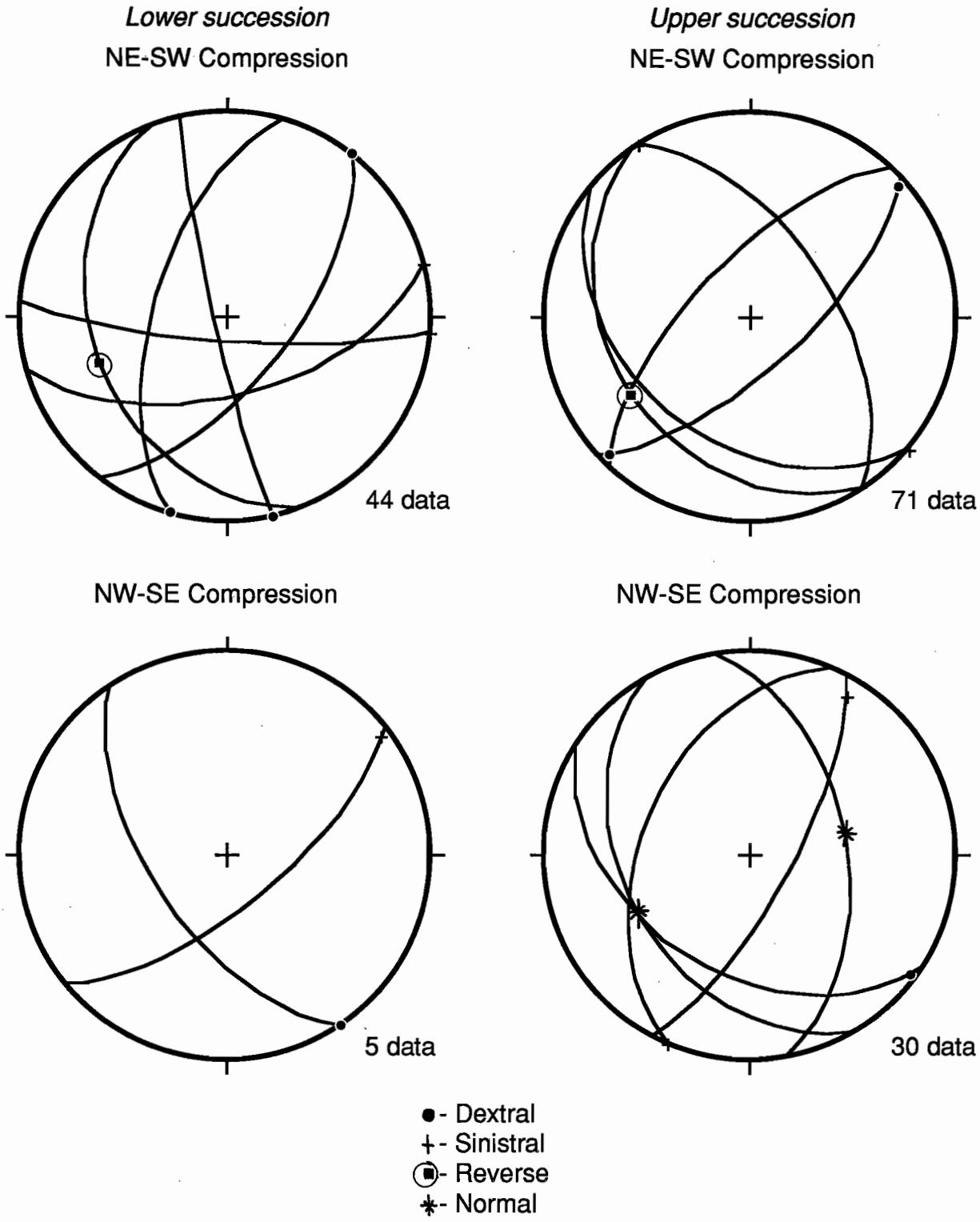

Figure 2c. Summary of Scrutton Range stress analysis - Tawallah Group lower succession versus upper succession. Equal area stereonets show the average dip/strike of fault planes and average pitch of stria for fault generations relating to each stress orientation.

"lower succession" compared to those of the "upper succession". The silicification is regionally extensive and is characteristic of the Yiyintyi and Sly Creek Sandstones within the study area.

Hydraulic fault brecciation is abundant in the "lower succession" sandstones compared to the "upper succession" and is believed to provide further evidence for the "mid-Tawallah Inversion. Dunn *et al.* (1973), conducted brittle fracture experiments on quartz arenites for varying porosities which show that for low porosities, rocks develop through-going shears at high differential stress (Fig. 3) and only after the generation of intense micro-fracturing. In the study area, the Yiyintyi and Sly Creek Sandstones were silicified, and hence their porosities reduced, during the Mid-Tawallah Inversion. Structures associated with later events produced intense fracturing and brecciation in the "lower succession" as they tried to propagate through the rigid lower sandstones. In the Batten Range, it is the second order structures of the Post-Roper Inversion that are associated with abundant hydraulic fault brecciation within the Sly Creek Sandstone.

TECTONIC MODELS

The present day structural geometry of the study area may be divided into three structural domains (Fig. 4a and b):

The southern domain is characterised by the effects of dextral wrench faulting. The Tawallah Fault is the major through-going dextral wrench and the post-Roper structures in the Batten Range form the classic pattern for second order structures in a dextral system (Fig. 2a.). This dextral wrench geometry was generated during the Post-Roper Inversion.

The northwestern domain is characterised by repetition of stratigraphy across large scale low angle Post-Roper Inversion reverse faults; the Bauhinia Thrust, the Billengarrah Thrust and the Tawallah Fault. An important feature of this domain is that upper units of the Tawallah Group are thrust up onto basement (Scrutton Volcanics) along the Billengarrah Thrust (Fig 4b). The magnetics for the region (Fig. 4a) clearly shows that the volcanic units of the Tawallah Group have been brought close to the surface by this thrusting, which is bounded in the south by a linear feature interpreted as a transform fault or lateral ramp.

The northeastern domain is comprised of a block of Tawallah Group which differs from the other fault blocks in that the sequence dips and youngs to the east. This domain has been targeted for field work in the 1994 season.

Tectonic evolution of the study area

A four stage model is proposed for the tectonic evolution of the study area based on the aforementioned structural analysis and on the sedimentological and palaeogeographical studies of Bull (1993). The evolution of the region during Tawallah Group times can be divided into four temporally distinct stages (Fig. 5).

Stage I - Extension (E-W ?)

Initial basin formation is envisaged as a half graben, with the Emu Fault forming the eastern margin to the early extension (Fig. 5a.). This initial extensional phase sees the development of the NE trending transform structure with differential rotation of normal fault blocks on either side of the structure. The easterly younging direction and dip for the fault block north of the transform structure may have been developed during this rotation.

Stage II - Mid-Tawallah Inversion (E-W compression)

The second stage of basin evolution is the Mid-Tawallah Inversion (Fig. 5b) with E-W compression inverting the early normal structures to create early topography within the southern McArthur Basin. This event probably occurred after the deposition of the Aquarium Formation and was associated with the pervasive silicification of the Yiyintyi and Sly Creek Sandstones. The development of topography within the southern McArthur Basin has important implications for both sedimentological and basinal fluid flow studies, and is discussed by Bull (1993). The generation of a trailing imbricate fan north of the transform structure becomes important in the following stages of basin evolution.

Stage III - Extension (E-W?)

Further extension followed the Mid-Tawallah Inversion event (Fig. 5c) resulting in the deposition of more fluvial-influenced sandstones together with mafic and felsic sills and dykes to form the "upper succession" of the Tawallah group. Some of the fault blocks must have remained inverted, including the fault block west of the proto-Tawallah Fault (south) and the block east of the proto-Billengarrah Thrust.

Intervening events

NW-SE compression followed this extension event, possibly at the end of Tawallah Group deposition but certainly post-Umbalooga Sub-group (Keele, 1993). Other minor events, not large enough to be recorded in the study area, are represented by the:

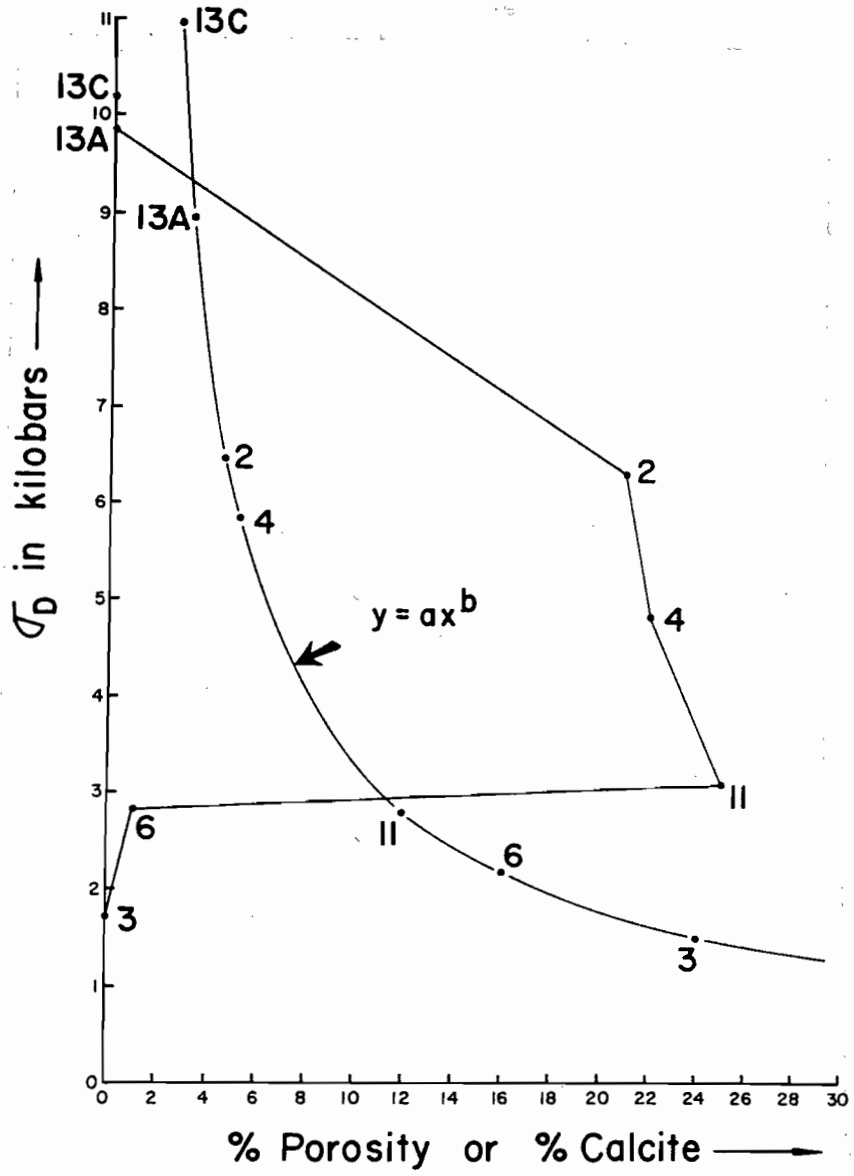

Figure 3. Graph of differential stress versus % porosity (smooth curve) and % calcite cement (irregular curve) for brittle fracture of quartz arenites (after Dunn *et al.*, 1973)

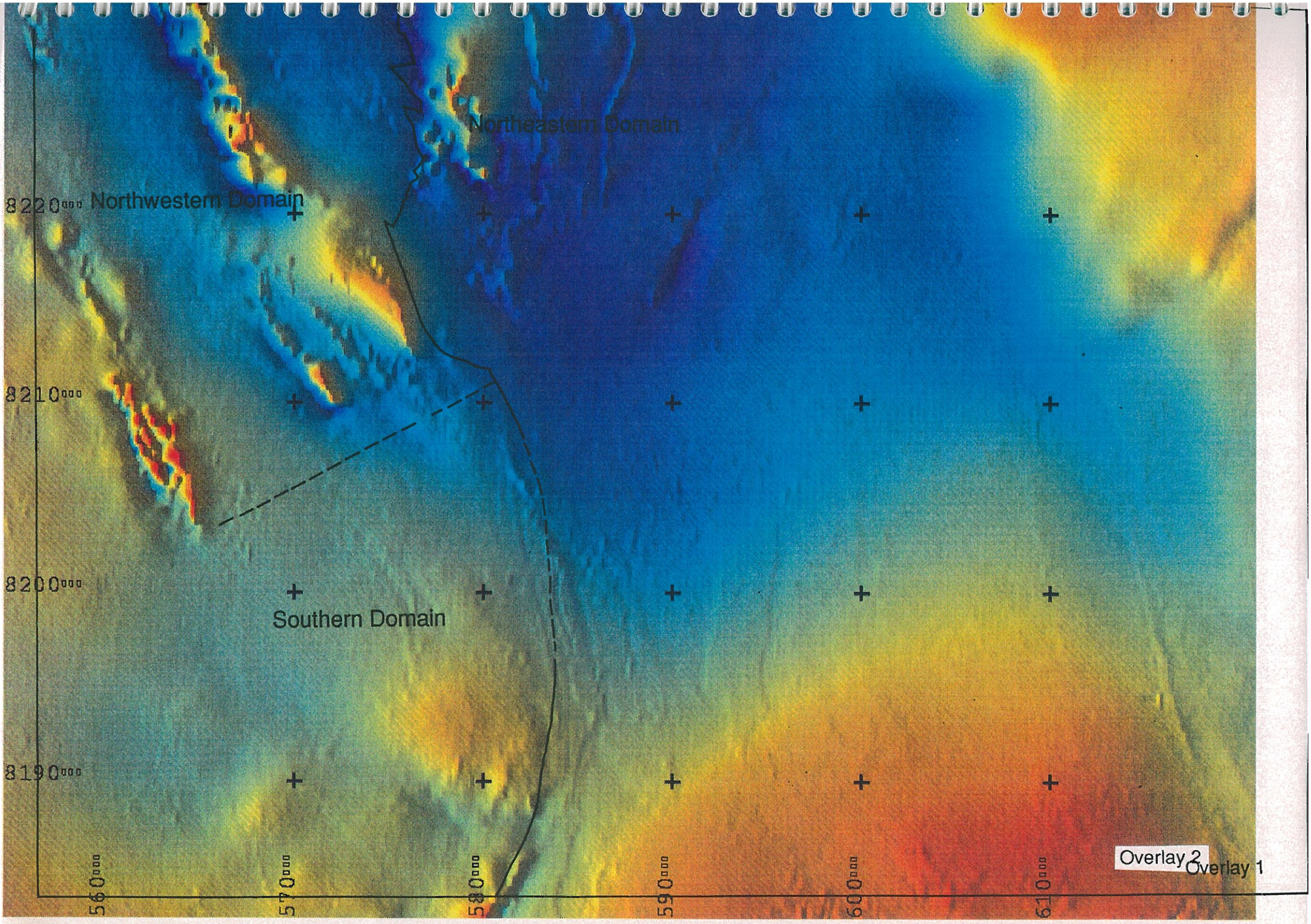
Northeastern Domain
Northwestern Domain
Southern Domain
8220000
8210000
8200000
8190000
560000
570000
580000
590000
600000
610000
Overlay 2
Overlay 1

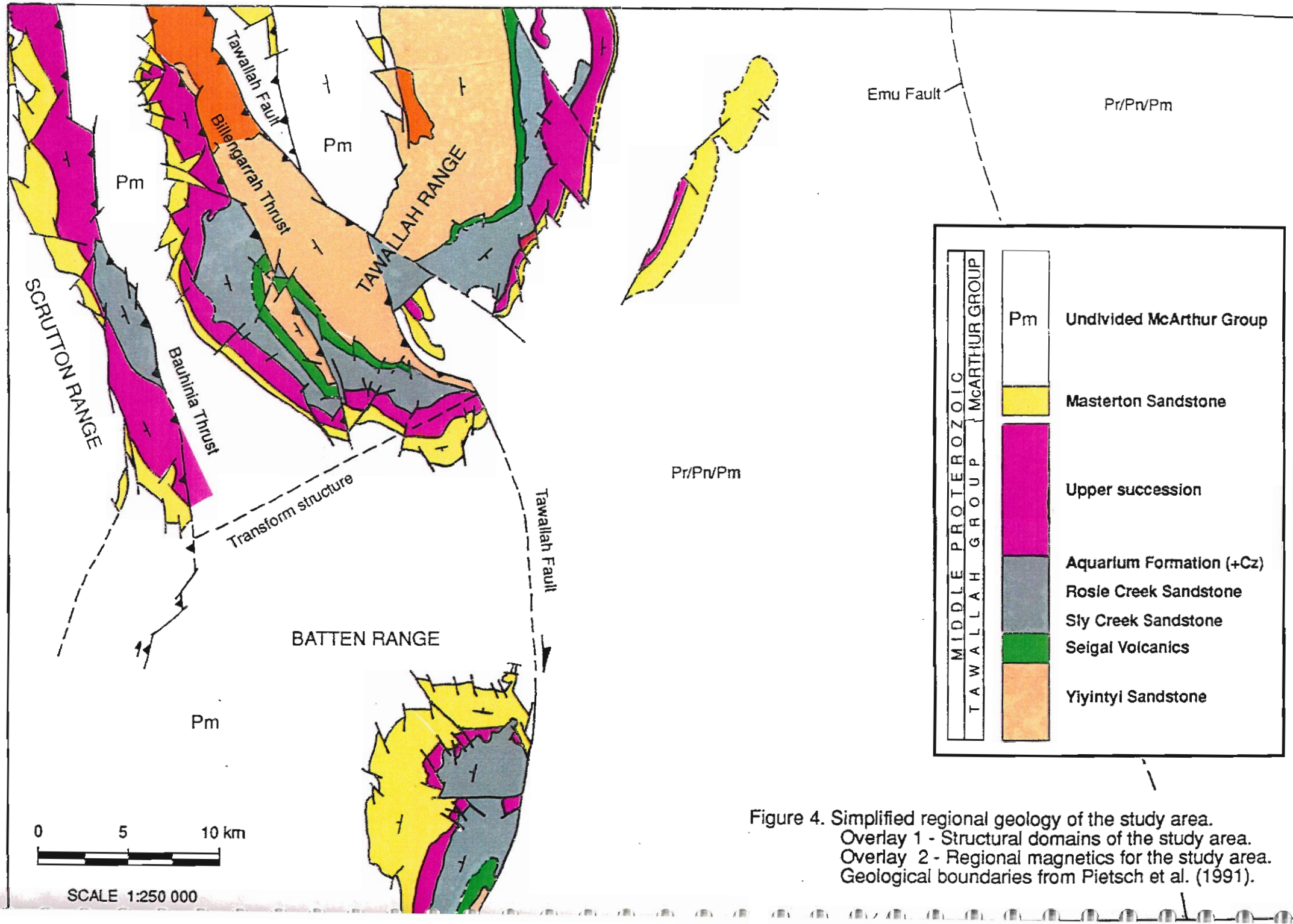

Figure 4. Simplified regional geology of the study area.
Overlay 1 - Structural domains of the study area.
Overlay 2 - Regional magnetics for the study area.
Geological boundaries from Pietsch et al. (1991).

- Umbolooga Sub-group/Batten Sub-group boundary
- McArthur Group/Nathan Group boundary
- Nathan Group/Roper Group boundary

Stage IV -Post-Roper Inversion (NE-SW compression)

The final stage of the tectonic basin evolution, following the deposition of the entire southern McArthur Basin sequence and which may therefore represent the final closing of the basin is the Post-Roper Inversion (Fig. 5d). The southern structural domain of the study area (Fig. 4a) was produced during reactivation of the Tawallah Fault as a dextral wrench system. In the northwestern structural domain (Fig 4a), low angle reverse faults were generated (in the case of the Billengarrah Thrust, thrusting upper Tawallah Group units onto the earlier inverted basement block). These two domains are separated by the NE-trending transform structure which acted as a southern lateral ramp to the thrust fault structures of the northwestern domain.

Features associated with the post-Roper structures are zones of silicification, cataclasite and hydraulic fault brecciation which are best developed in the sandstone units of the "lower succession".

CONCLUSIONS

The present-day structural geometry of the study area has been generated during a four stage basin evolution model. Based on a regional stress analysis (this study) and the palaeogeographical studies of Bull (1993), a subdivision of the Tawallah Group is proposed. The "lower succession" includes the Yiyintyi Sandstone, Seigal Volcanics, Sly Creek/Rosie Creek Sandstones and the Aquarium Formation. The "upper succession" comprises the Wununmantyala Sandstone, Settlement Creek and Gold Creek Volcanics, Wollogorang Formation, Warramanna Sandstone, Tanumbirini Rhyolite and the Nyanantyu Formation.

The "lower succession" was deposited into an (E-W ?) extensional basin envisaged as a north-trending half graben.

The results of the stress analysis suggest that an early E-W compressional event (the Mid-Tawallah Inversion) occurred at the "lower succession"/"upper succession" boundary. Evidence for the Mid-Tawallah Inversion are:

- The presence of a fault generation in the "lower succession" which is absent in the "upper succession".
- The pervasive silicification of the "lower succession" sandstones compared to those of the "upper succession"
- Abundant hydraulic fault brecciation in the "lower succession" sandstones compared to the "upper succession".
- The palaeogeographical studies of Bull (1993).

The Mid-Tawallah Inversion was followed by a period of (E-W ?) extension with both structural and sedimentological evidence suggesting that the fault block east of the proto-Billengarrah Thrust and the block west of the proto-Tawallah Fault (south) remained inverted during this period. Deposition of the "upper succession" occurred during this extensional phase.

A NW-SE compression followed the extensional phase, possibly at the Tawallah Group/McArthur Group boundary.

The final and largest structural event to affect the study area was the Post-Roper Inversion which post-dates McArthur Basin sedimentation

The present day structural geometry of the study area is divided into three structural domains: (1) a southern domain characterised by Post-Roper Inversion dextral wrench faulting on the Tawallah Fault; (2) a northwestern domain characterised by repetition of stratigraphy across low angle Post-Roper Inversion reverse faults (the Bauhinia Thrust, Billengarrah Thrust and Tawallah Fault) which are bounded in the south by a NE-trending lateral ramp; (3) a northeastern domain comprised of an easterly dipping and younging sequence of Tawallah Group which may represent an early rotated normal fault block.

Further studies

1993

- Balanced cross sections for the southern and northwestern domains.
- Fluid inclusion studies of fault breccias from the Sly Creek Sandstone.
- Isotopic and fluid inclusion study of the Berjaya Prospect.

Figure 5a. 1: Initial Basin Formation - Extensional Half Graben
- E-W Extension

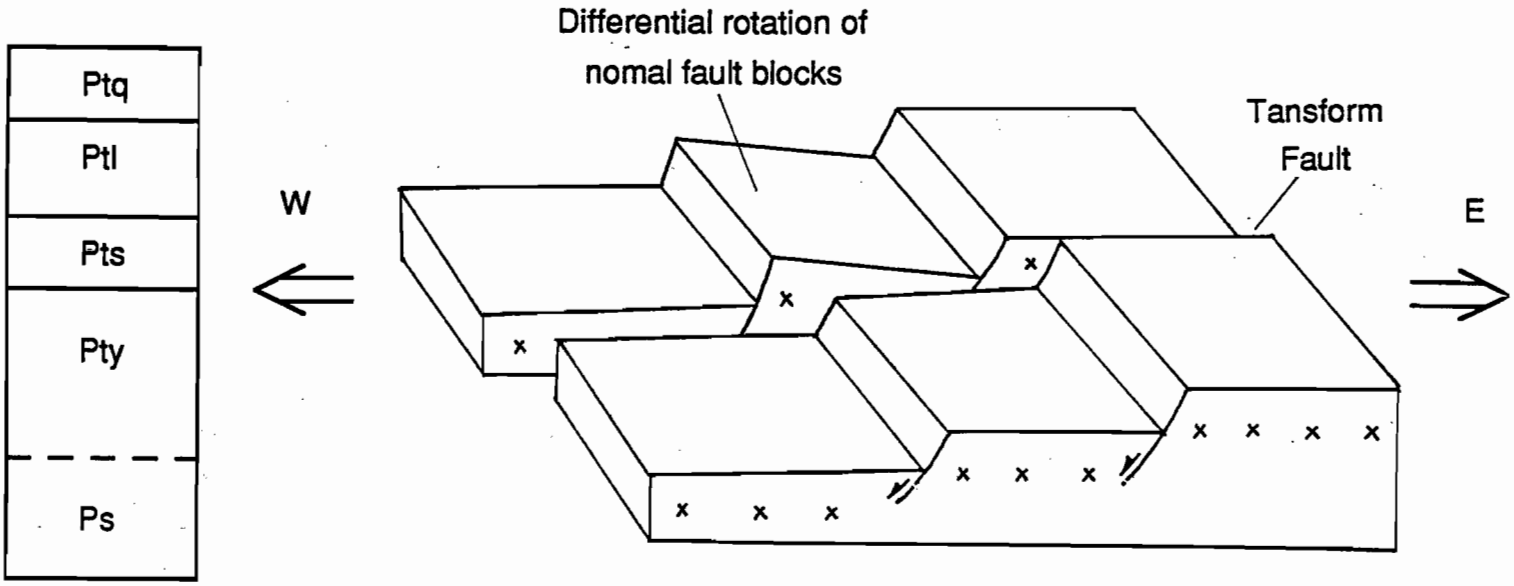

Figure 5b. 2: Mid-Tawallah Inversion - E-W Compression

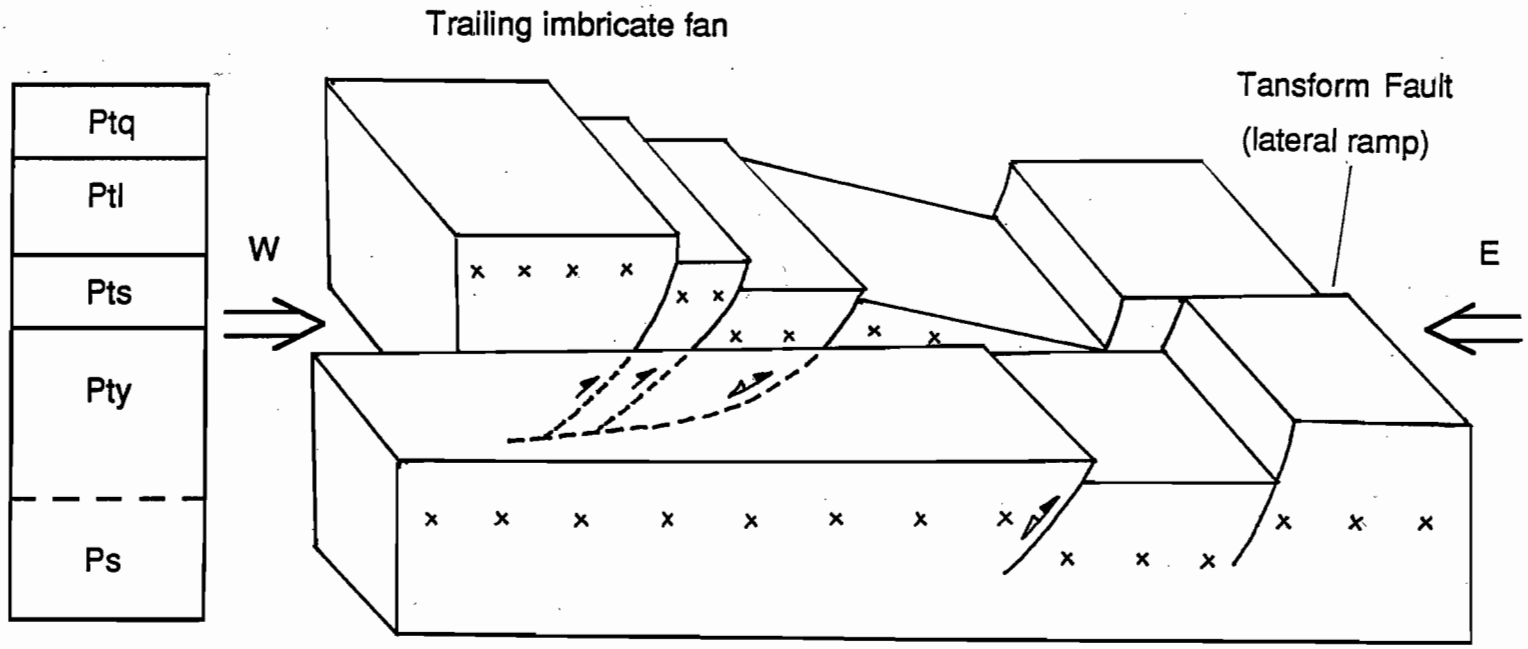

Figure 5c.

3: Upper Tawallah Extension - E-W Extension ?

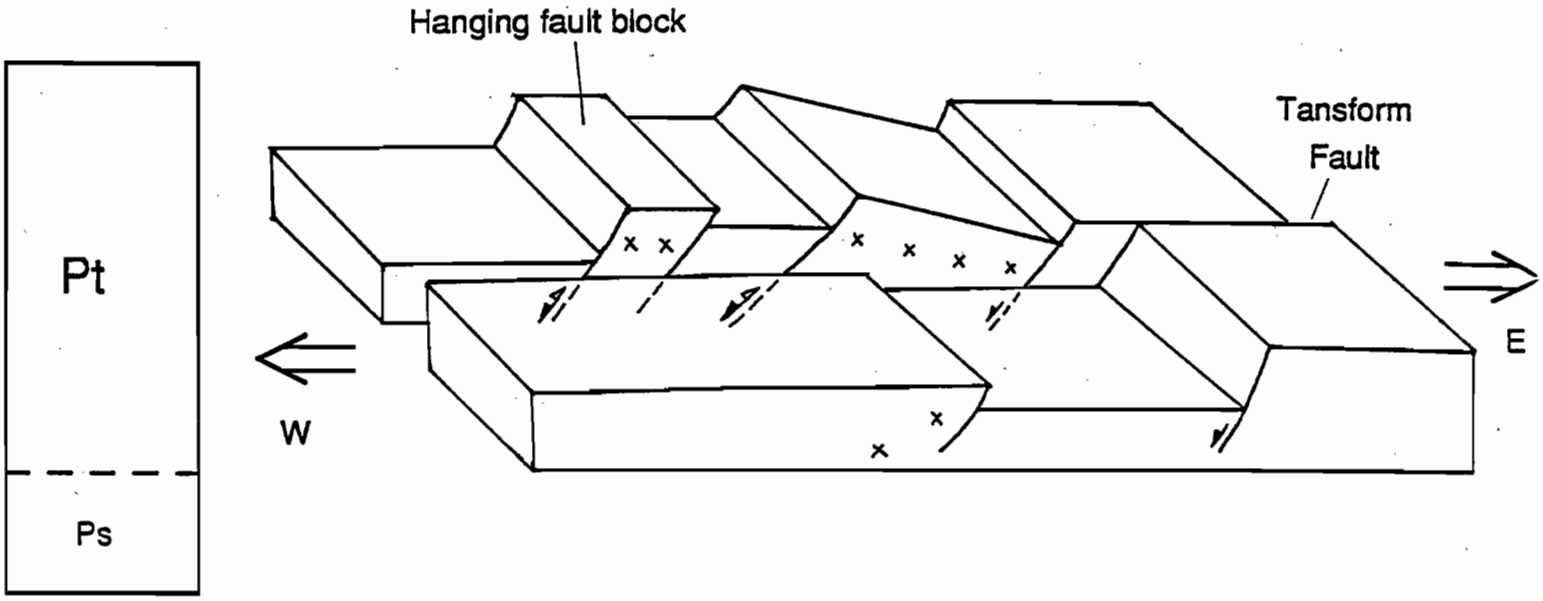

- Tawallah Gp./McArthur Gp. Event (NW-SE Compression)
- Nathan Gp./Roper Gp. Event

Figure 5d.

4: Post Roper Inversion - NE-SW Compression

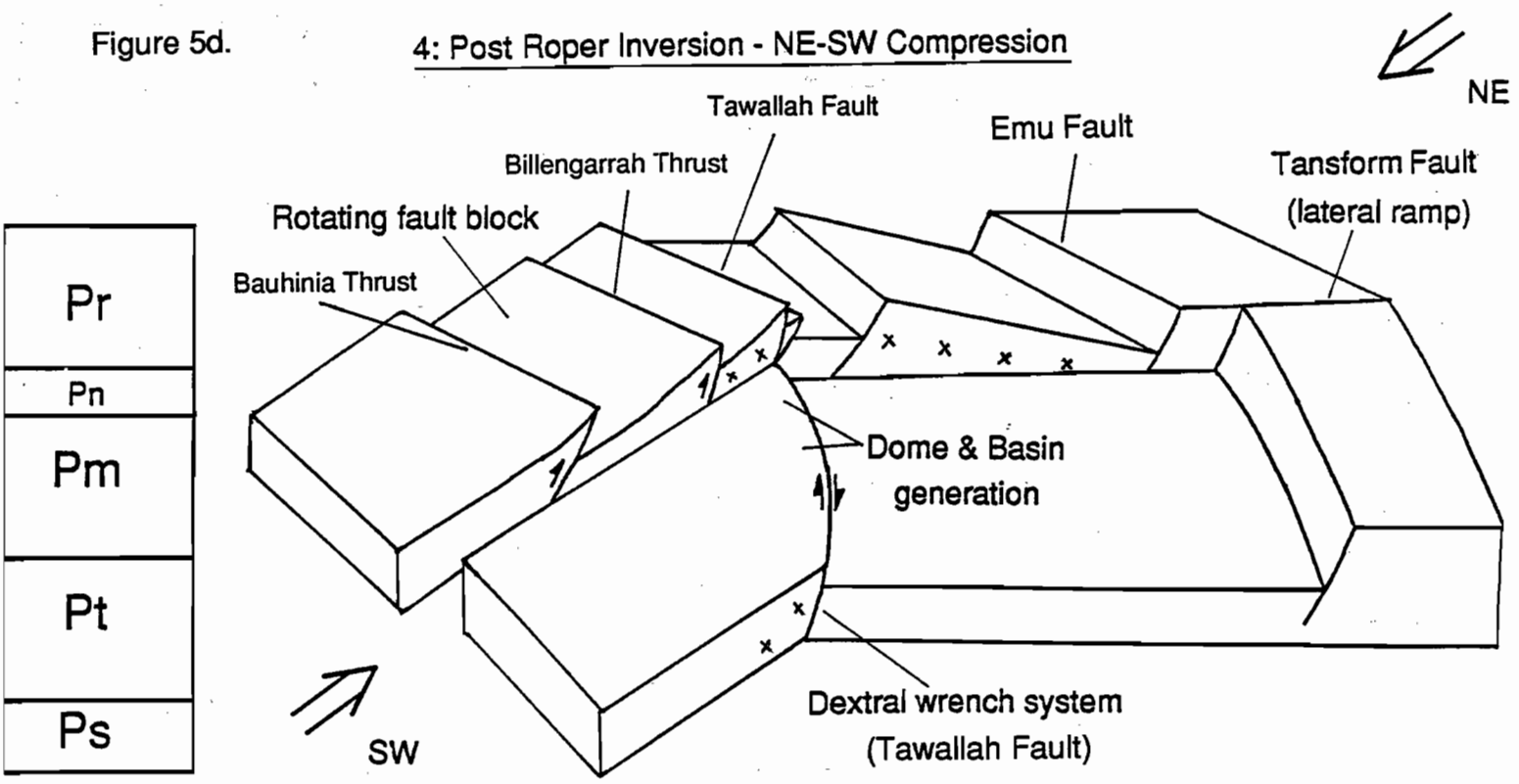

- Trace element and rare earth geochemistry of the Scrutton Volcanics, Settlement Creek Volcanics, Gold Creek Volcanics and Tanumbirini Rhyolite.

1994

- Field work with S. Bull in the northeastern domain.

REFERENCES

Bull, S., 1993. Progress report - sedimentology and volcanology of the southern McArthur Basin, *AMIRA/ARC project P384 rep.* 4 (unpublished).

Dunn D.E., LaFountain L.J. and Jackson R.E., 1973. Porosity dependence and mechanism of brittle fracture in sandstones, *J. Geophys. Res.*, 78/14: 2403-2417.

Etchecopar A., Vasseur G. and Daigniers M., 1981. An inverse problem in microtectonics for the determination of stress tensors from fault striation analysis, *J. Stuct. Geol.*, 3: 51-65.

Jackson M.J., Muir M.D. and Plumb K.A., 1987. Geology of the southern McArthur Basin, Northern Territory, *Bur. Miner. Resour. Geol. Geophys. Aust. Bull.* 220.

Keele R.A., 1993. The histories of some faults in the southern McArthur Basin: evidence for an end-Tawallah uplift and a preliminary analysis of stress related to post-McArthur and post-Roper compressions, *AMIRA/ARC project 384 rep.* 4 (unpublished).

Pietsch B.A., Rawlings D.J., Creaser P.M., Kruse P.D., Ahmed M., Ferenczi P.A. and Findhammer T.L.R., 1991. Bauhinia Downs SE53-3 - 1: 250 000 geological map series explanatory notes, *N.T. Geol Surv.*

Plumb K.A., 1979. Structure and tectonic style of the Precambrian shields and platforms of northern Australia, *Tectonophysics*, 58: 291-325.

Plumb K.A., Derrick G.M. and Wilson I.H., 1980. Precambrian geology of the McArthur River-Mount Isa region, northern Australia, in *The Geology and Geophysics of Northeastern Australia* (Eds R.A. Henderson and P.J. Stephenson), pp 71-88 (Geological Society of Australia, Queensland division: Brisbane).

Plumb K.A., Ahmad M. and Wygralak A.S., 1990. Mid-Proterozoic basins of the North Australian Craton - regional geology and mineralisation, in Geology of the Mineral Deposits of Australia and Papua New Guinea (Ed. F.E. Hughes), pp 881-902 (The Australasian Institute of Mining and Metallurgy: Melbourne).

Rawlings D.J., Madigan T.L., Pietsch B.A., Haines P.W. and Findhammer T.L.R., 1993. Tawallah Range 6066 - 1: 100 000 geological map series explanatory notes, *N.T. Geol Surv.*

Progress report - Sedimentology and volcanology of the Southern McArthur Basin

Stuart Bull
Centre for Ore Deposit and Exploration Studies

INTRODUCTION AND AIMS

The regional stratigraphy of the southern McArthur Basin has been relatively well defined by geological mapping of the Bauhinia Downs 250,000 sheet (Pietsch *et al.*, 1991a) and the Abner Range (Jackson *et al.*, 1984) and McArthur River Region (Pietsch *et al.*, 1991b) 100,000 scale sheets. However, very little analysis of this stratigraphy has been carried out in order to determine the sedimentological/structural development of the McArthur Basin system. At the beginning of this study it was proposed that the clastic units in the Tawallah and lower McArthur Groups should have the best potential to record the critical early phase of development of the southern McArthur Basin system. Within this framework, the field work carried out in the 1993 dry season had two main aims:

(1) To determine the sedimentological architecture of the southern McArthur Basin during the rifting event represented by the mineralized McArthur Group by examining the basal unit of the Group, the Masterton Sandstone. This ongoing study involves locating well-exposed sections through the Masterton Sandstone at a wide range of localities on the flanks of the Batten Trough (Fig. 1), where general sedimentological, and particularly palaeocurrent data can be collected. A progress report is presented below.

(2) To investigate the nature of the upper volcanic units of the Tawallah Group, focusing on the Settlement Creek and Gold Creek Volcanics. Some data, which will ultimately be incorporated into this study, has been collected from the Mallapunyah Dome area during mapping for the honours projects of John Wright and Serena Donovan whose study areas include exposures of Settlement Creek and Gold Creek Volcanics. The geochemical aspects of these studies in the Mallapunyah Dome region are being coordinated by Cooke et al. (1993). Additional field data has been collected by the author in the Mallapunyah Dome outside the honours field areas and also in the Scrutton Ranges. The provisional observations and conclusions of this work are presented below.

PROVISIONAL OBSERVATIONS AND INTERPRETATION OF THE MASTERTON SANDSTONE IN AND AROUND THE BATTEN TROUGH

Introduction

Many of the sedimentological features of the Masterton Sandstone were first documented by Jackson *et al.*, (1987) who examined outcrops of the unit over a wide area of the southern McArthur Basin during field mapping for the Abner Range 1:100,000 geological sheet. In the current study to date, sections through the Masterton Sandstone have been examined at five localities in the Mallapunyah/Kiana Domes area (Fig. 2) and two localities in the Scrutton Ranges, three localities in the southern Tawallah Ranges and two localities in the Batten Ranges (Fig. 3). Detailed sedimentological logs and palaeocurrent measurements from at least the basal parts of the sections were measured for all of the Mallapunyah/Kiana Domes localities (Fig. 4), and facies logs and palaeocurrent measurements were taken at all of the other localities. Analysis of the sedimentary logs allows a provisional interpretation of the depositional environment for the Masterton Sandstone. In combination with interpretation of the palaeocurrent data from the different localities, this yields significant information on the early

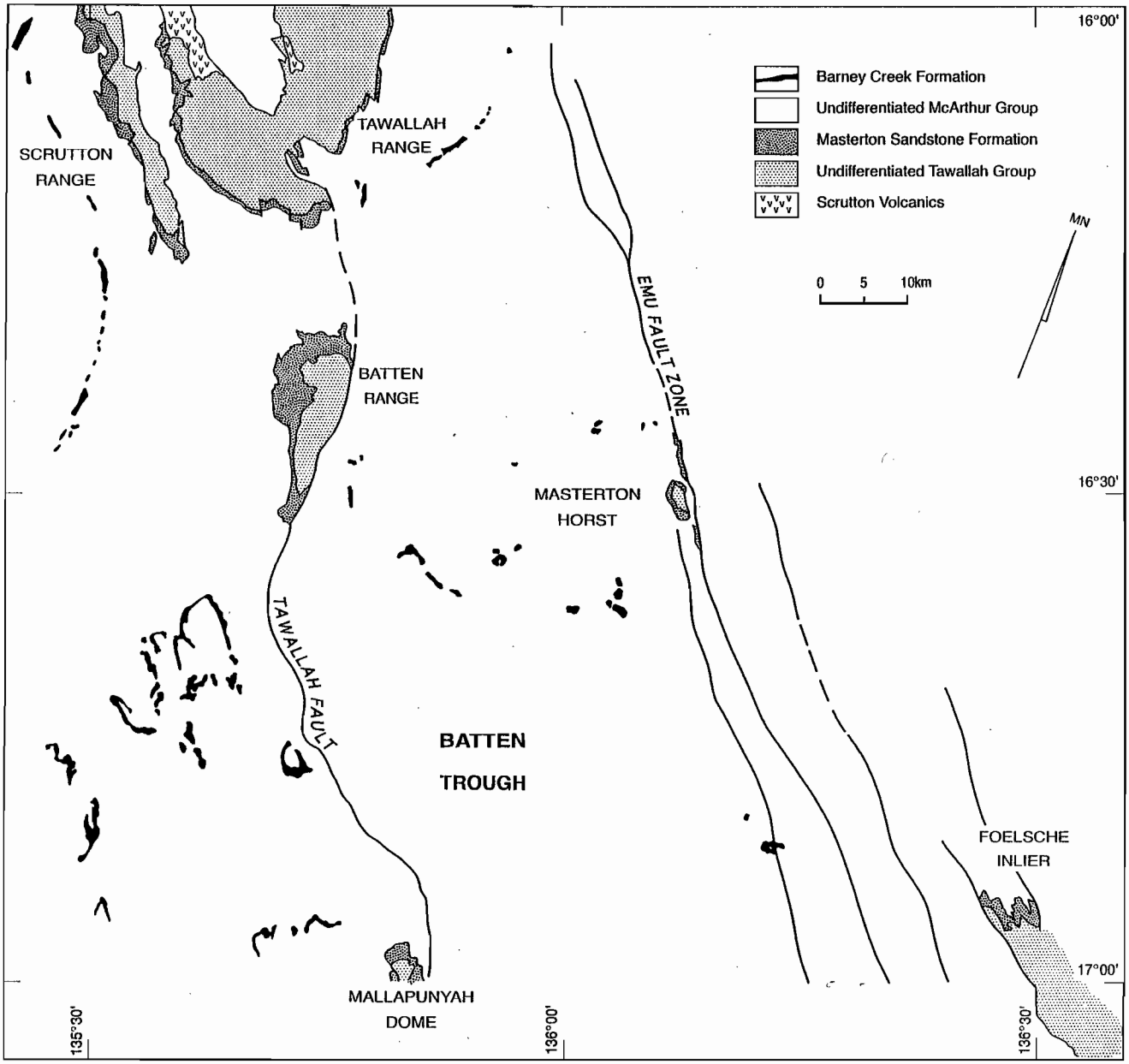

Figure 1. Distribution of the Tawallah Group, Masterton Sandstone and Barney Creek Formation in the southern McArthur Basin (after Pietsch *et al.*, 1991a).

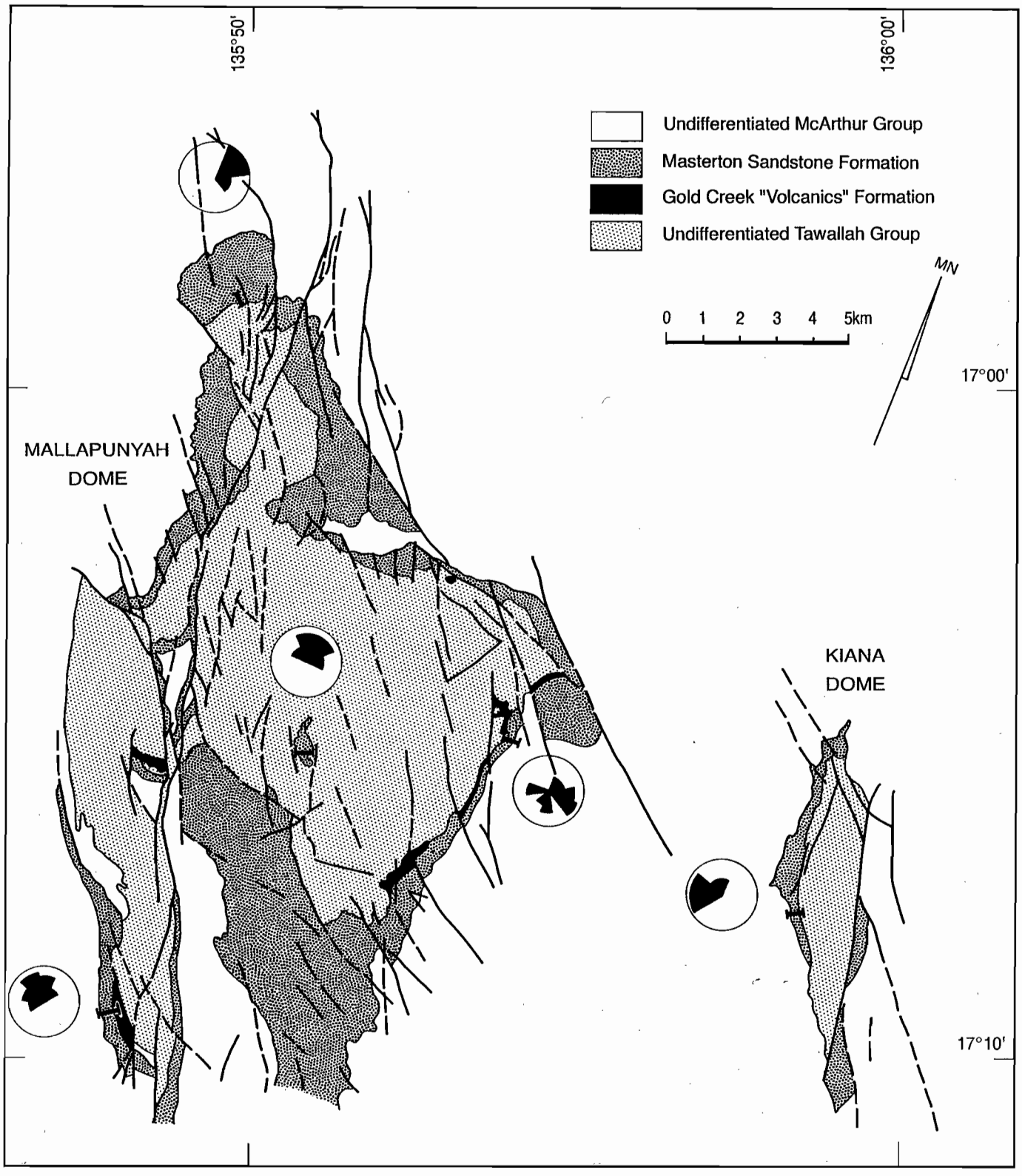

Figure 2. Location of Masterton Sandstone sections in the Mallapunyah/Kiana Domes area (geology after Jackson *et al.*, 1984). Rose diagrams are palaeocurrent data from each locality.

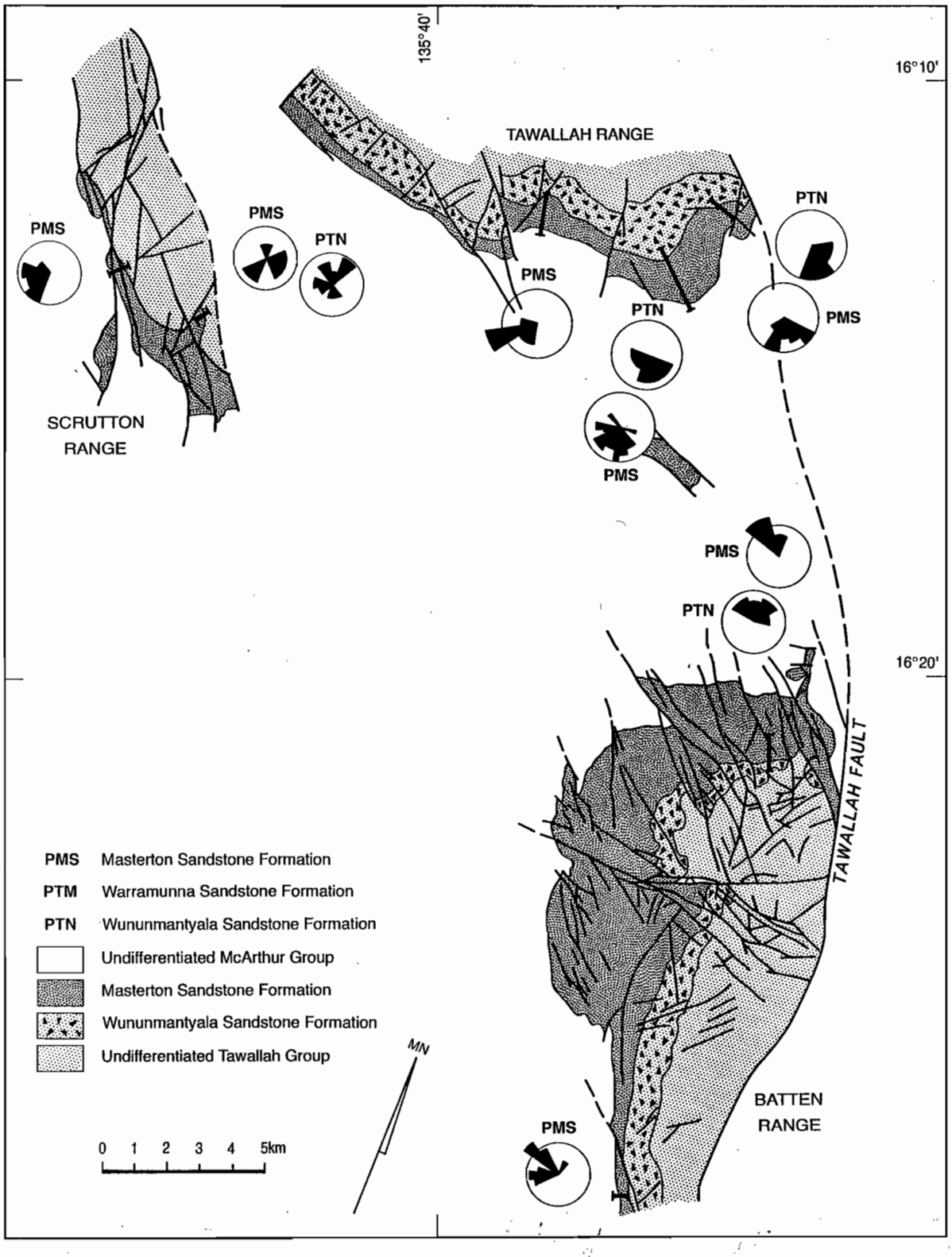

Figure 3. Location of Masterton Sandstone sections in the Scrutton, Batten and southern Tawallah Ranges (geology after Pietsch *et al.*, 1991b). Rose diagrams are palaeocurrent data from each locality, Ptn from the Wununmantyala Sandstone and Pms from the Masterton Sandstone.

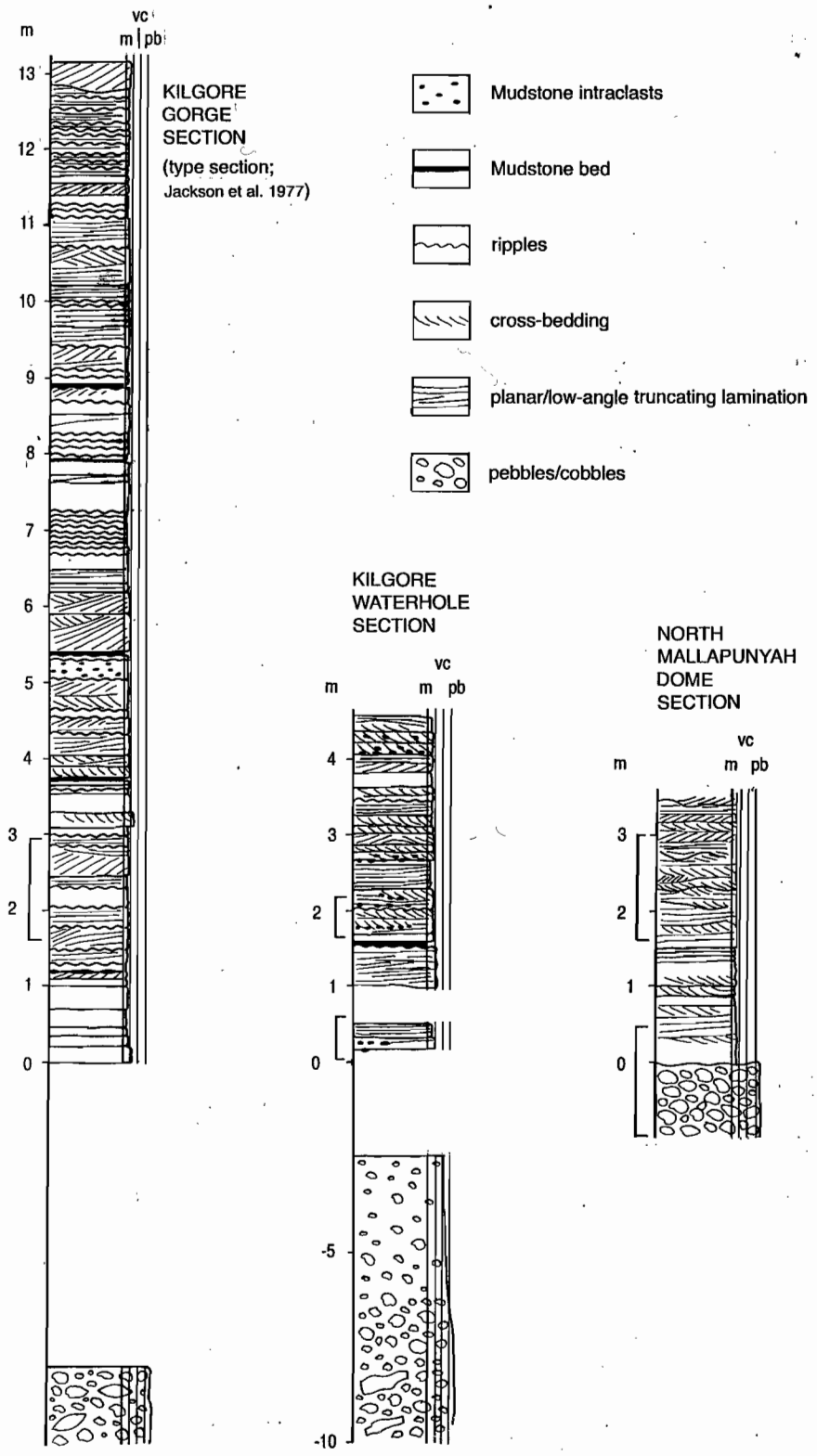

Figure 4. Detailed sedimentological sections measured through the Masterton Sandstone at three localities in the Mallapunyah/Kiana Domes area.

development of the southern McArthur Basin depositional system.

Description

In the Mallapunyah/Kiana Domes area the Masterton Sandstone consists of one major ridge-forming sandstone (Fig. 5a) which flanks the Tawallah Group units forming the core of the dome (Fig. 2). This unit varies in thickness from 50 to 150 m, however, there is some evidence that the thicker occurrences, for example the section at Kilgour Waterhole, are due to repetition of the sandstone sequence by reverse faulting.

The ridge-forming Masterton Sandstone in this area is typified by the type section defined by Jackson *et al.*, (1987) in Archies Creek (Fig. 4; Kilgour Gorge Section), where the unit is dominantly comprised of bedded, variably hematitic, fine- to medium-grained quartz sandstone. Bedding is on a scale of 5 to 60 cm in thickness and is tabular overall, although broad shallow channel features are occasionally present. Sedimentary structures are dominated by abundant, crudely- to well-defined, planar to low-angle truncating lamination with scattered trough and less commonly planar cross-bed sets with amplitudes ranging from 10 to 60 cm (Fig. 5b). Pavements of symmetrical to slightly assymetrical, straight crested and less commonly lunate ripples with wavelengths of < 5 cm are locally abundant (Fig. 5c). Less common features are hematitic mudstone drapes which generally occur on ripple pavements and may have well-developed polygonal mudcracks (Fig. 5d). Evaporitic features such as halite casts (Fig. 5e) and lensoidal hematitic spots presumed to be after gypsum also occur, particularly towards the top of the unit which is conformable with, and gradational into, the overlying Mallapunyah Formation.

To the north of the Mallapunyah/Kiana Domes area in the Scrutton, Batten and Tawallah Ranges the Masterton Sandstone can be markedly thicker and has a more complex facies stratigraphy (Fig. 3). In the northern Batten and southern Tawallah Ranges the Masterton Sandstone can reach a thickness in excess of 500 m, and in the southern Tawallah Range at least, the unit consists of up to four well-defined ridge-forming sandstones. There is no evidence of structural repetition, and the sandstone ridges are separated by a recessive fine-grained facies association.

The lowermost Masterton Sandstone ridge commonly has basal conglomerate with associated pebbly sandstone and gravel deposits which range in thickness from a few metres to at least 30 m. The conglomerate units are massive, clast-supported, pebble- to cobble-sized, closed framework deposits which have a sandstone matrix (Fig. 5f). Imbricate horizons are developed locally. Clasts consist of quartzite, hematitic quartzite and hematitic fine-grained sandstone, and similar deposits at the base of the Masterton Sandstone in the Scrutton Ranges adjacent to the Tanumbirini Rhyolite contain rhyolite clasts.

Above the basal coarse-grained facies where present, the ridge-forming sandstones themselves are dominated by laminated and cross-bedded, fine- to medium-grained sandstone deposits similar to those in the type section to the south. However, an additional thick-bedded facies is locally present in which the beds are up to 2 m thick and are associated with cross-bed sets with amplitudes of up to 1 m.

The recessive, fine-grained facies association which separates the sandstone ridges in the southern Tawallah Ranges consists of thin-bedded/flaggy, fine-grained sandstone and mudstone deposits (Fig. 5g). These have interbedded 20 to 40 cm thick sandstone beds which are commonly cross-bedded and closely resemble the facies which comprise the bulk of the ridge-forming sandstones suggesting a genetic relationship between the two facies associations.

In the southern Tawallah Range the contact with the overlying Mallapunyah Formation is conformable and gradational and is marked by hematitic spots after gypsum in the uppermost sandstones which are identical to those described from the type section. In the western Batten range this contact is also conformable and gradational, and intervals of bedded and cross-bedded hematitic sandstones which closely resemble those of the Masterton Sandstone occur sporadically in at least the basal few hundred metres of the Mallapunyah Formation.

Discussion/Interpretation

Depositional environment

Taken overall, the Masterton Sandstone in the southern McArthur Basin as observed so far can be considered in terms of two broad facies elements:

(1) A coarse-grained basal unit which is subject to marked thickness changes where present.

(2) A fine- to medium-grained upper unit which is always present and is typified by the type section in Archies Creek at the Mallapunyah Dome. This unit becomes more evaporitic and dolomitic at the top and is gradational to the overlying Mallapunyah Formation.

Previous workers have interpreted the coarse-grained basal facies as alluvial fan or braided river deposits developed on a highly dissected palaeosurface (Jackson *et al.*, 1987; Pietsch *et al.*, 1991a) and the author concurs with this interpretation. However, the overlying fine- to medium-grained sandstone facies has been interpreted to represent a very shallow, wave-dominated littoral environment (Jackson *et al.*, 1987). Although this interpretation is consistent with the rippled sandstone and mudstone deposits, the bulk of this facies is comprised of planar and low-angle truncating lamination associated with small- to medium- and in some cases relatively large-scale cross-bed sets (Fig. 5b). Such sedimentary structures are indicative of a relatively high-energy hydraulic regime, and the lack of structures conventionally associated with wave-associated reworking (eg. swash stratification diagnostic of beach face or hummocky cross-stratification diagnostic of deeper water storm-wave reworking; eg. Leckie and Walker, 1982) suggests that this is not a wave-dominated shoreline succession.

It is also significant that in the Batten and Tawallah Ranges where well-developed basal conglomerate and associated coarse-grained deposits are present, the general palaeoflow directions, as indicated by measurements of cross-bed foresets, are consistent throughout the sections. This indicates a strong genetic relationship between the coarse-grained basal alluvial deposits and the overlying fine- to medium-grained sandstones. The latter are, therefore, considered to have been deposited in a braided fluvial or braidplain depositional system which was intimately associated, and interfingered with, the underlying coarser-grained alluvial deposits.

In this model, the rippled sandstone and minor associated mudstone deposits, if they do represent littoral marine conditions, would indicate that the alluvial fan/braidplain system was fan-deltaic in character (ie. it fed directly into an adjacent marine environment). Alternatively these deposits could represent ephemeral lakes and pools developed on a relatively low-relief braidplain. More substantial and longer-lived bodies of standing water could account for the recessive, thin-bedded/flaggy, fine-grained sandstone and mudstone facies which separates the ridge-forming sandstones in the southern Tawallah and Batten Ranges (Fig. 5g).

Palaeocurrent study - evidence of basin inversion

The rationale behind the palaeocurrent part of the Masterton Sandstone study is based on the interpretation outlined above that the depositional system appears to have strong alluvial/proximal and high-energy fluvial characteristics. Palaeoflow within this depositional system should, therefore, record areas of uplift (?structural) and in doing so provide a palaeogeographic framework providing insight into the tectonic development of the southern McArthur Basin at earliest McArthur Group time.

Figure 3 summarises the palaeocurrent data from the Batten Tawallah and Scrutton Ranges. With the exception of the easternmost Scrutton Range section (which is adjacent to large sinistral strike-slip structure; J. Rogers pers. comm.), palaeoflow recorded from the Masterton Sandstone in all sections (labelled Pms) is away from the Tawallah Group units which form the core of each of the ranges. This suggests that these Tawallah Group cores were uplifted prior to the deposition of the Masterton Sandstone. In addition, the basal conglomerates of the Masterton Sandstone where present, consist almost entirely of quartzite clasts identical to lithologies typical of the lowermost sandstones of the Tawallah Group, the Yiyintyi and Sly Creek Sandstones. Additional evidence that these clasts are of relatively local derivation is provided by the intermixed rhyolite clasts adjacent to the Tanumbirini Rhyolite in the Scrutton Ranges. The occurrence of these locally-derived quartzite conglomerates indicates that in addition to being uplifted, the lower Tawallah sandstone units were also silicified prior to the deposition of the Masterton Sandstone. The clear implication is that a compressional tectonic (ie. basin inversion) event occurred prior to the development of the McArthur Group depositional system. Structural evidence of this event has been documented by Rogers (1993).

Timing of basin inversion

At this stage of the study the exact timing of this Tawallah Group basin inversion event is unclear. The simplest explanation would be that it occurred between the deposition of the Tawallah and McArthur Groups and is, therefore, responsible for the regional sub-McArthur Group unconformity. This interpretation appears valid in the Mallapunyah/Kiana Domes area where palaeoflow directions within the Masterton Sandstone, although less clear than the patterns from the north, still indicate general palaeoflow away from the Tawallah Group core of the dome (Fig. 2).

In this area, a unit which is locally present at the base of the Masterton Sandstone is mapped as the Gold Creek Volcanics on the Abner Range Region 1:100,000 scale geological map (Fig. 2). Where this unit has currently been observed, it consists entirely of massive heterolithic mass-flow breccias. In field exposures and hand-specimens at least, there is no clear suggestion that these deposits are volcanic in

Figure 5. (a) Typical ridge-forming Masterton Sandstone on the southern side of Archies Creek at the southeastern margin of the Mallapunyah Dome. This locality is the type section of the unit (Jackson *et al.*, 1987), and the measured section shown in Figure 4 was measured downdip to the left of the cliff in the picture. (b) Typical high-energy tractional facies association of the Masterton Sandstone from the basal part of the type section in Archies Creek in the Mallapunyah Dome area. Sedimentary structures are dominated by planar and low-angle truncating lamination developed in fine- to medium-grained sandstone, with scattered well-defined trough cross-bed sets. (c) Straight/bifurcating crested ripple pavement from the Masterton Sandstone type section in Archies Creek. (d) Thin haematitic mudstone drape on a ripple pavement from the Masterton Sandstone type section in Archies Creek. The well-developed polygonal mudcracks are indicative of subaerial exposure. (e) Halite casts from the upper part of the Masterton Sandstone in S. Donovan's honours field area. (f) Clast-supported quartzite conglomerate from the western Batten Range section (Fig. 3), which is typical of the coarse-grained basal facies often present in the Masterton Sandstone in the Scrutton, Batten and Tawallah Ranges. (g) Thinly-bedded/flaggy sandstone and mudstone facies which is generally recessive, and separates ridge-forming conglomerate and sandstone units of the Masterton Sandstone in the southern Tawallah Ranges. (h) Typical exposure of the Wununmantyala Sandstone in southern Tawallah Ranges showing the general similarity of sedimentary facies to those typical of the Masterton Sandstone.

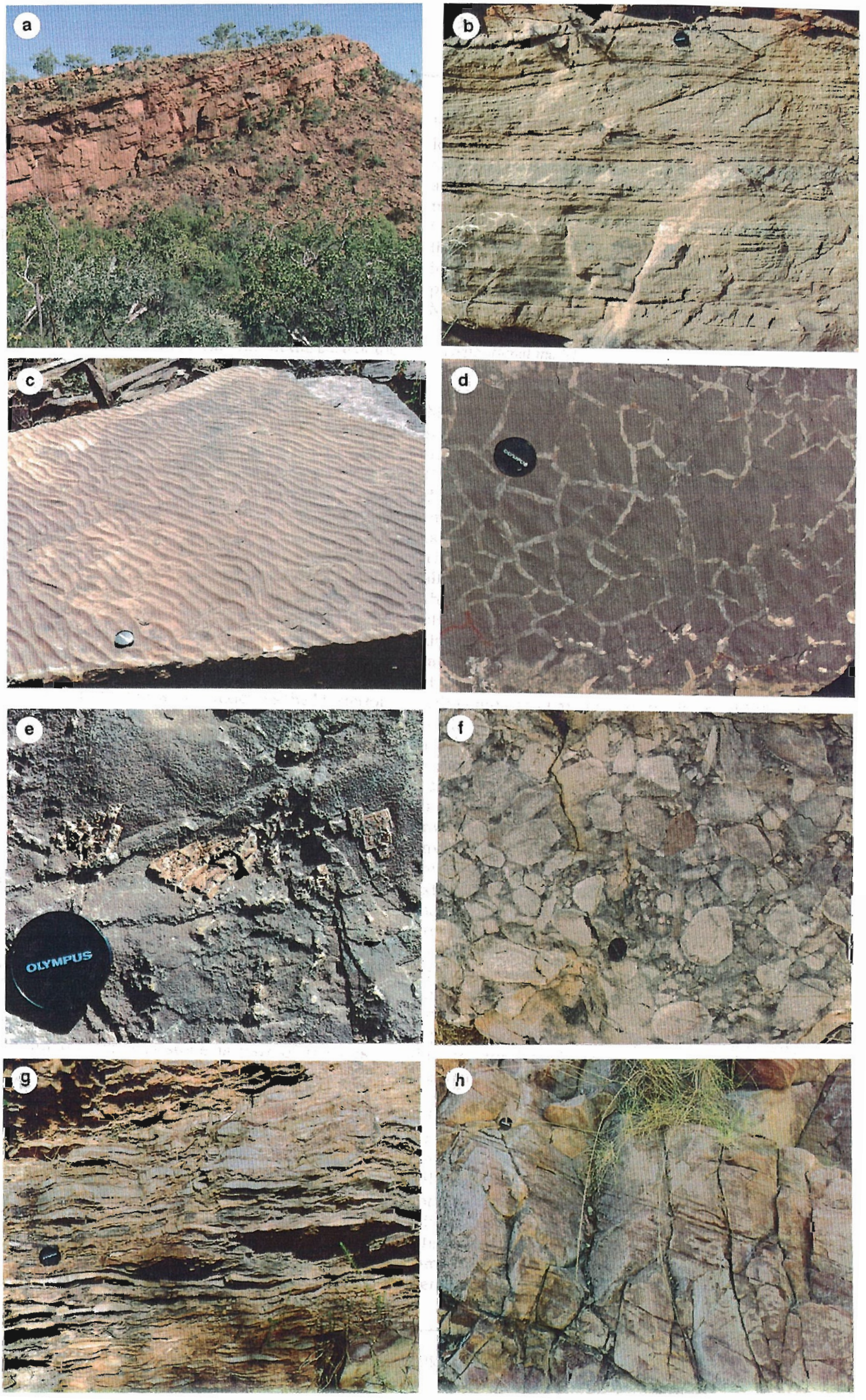
a
b
c
d
e
OLYMPUS
f
g
h

Blank

origin. They could equally be interpreted as epiclastic debris-flow deposits sourced from a proximal topographic high. The breccia deposits contain Settlement Creek Volcanics clasts and distinctive dolomite nodules which are characteristic of the base of the Wollogorang Formation (Pietsch *et al.*, 1991a). This indicates that if these deposits do represent epiclastic debris-flows then the Wollogorang Formation was lithified, and both the Settlement Creek Volcanics and the Wollogorang Formation were uplifted, prior to the emplacement of these breccia units at the base of the Masterton Sandstone. The breccia deposits could, therefore, have more affinity with the Masterton Sandstone than with the Tawallah Group. If this interpretation is correct, then the Wollogorang Formation is the uppermost unit of the Tawallah Group in the Mallapunyah/Kiana Domes area, and the basin inversion event in the Tawallah Group does in fact separate the Tawallah and McArthur Groups in this area.

The timing of the Tawallah Group compressional tectonic event is complicated by observations in the Batten and Tawallah Ranges. In these areas the Wollogorang Formation is absent and, with the exception of restricted recessive volcanic units in the Batten Ranges interpreted as Settlement Creek Volcanics (Pietsch *et al.*, 1991a), the uppermost Tawallah Group unit which underlies the Masterton Sandstone is the Wununmantyala Sandstone. This unit comprises a very similar facies association to the Masterton Sandstone itself (Fig. 5h) and there is no discernible structural unconformity between the two units such that, in places where a basal Masterton Sandstone conglomerate facies is lacking, it is very difficult to decide where the boundary between the two units lies. In addition, the few palaeocurrent measurements which were taken from the Wununmantyala Sandstone in the middle and eastern Tawallah Range sections and in the northern Batten Range section (Fig. 3; annotated Ptn) indicate a similar palaeoflow direction to that within the Masterton Sandstone.

Taken in isolation, the overall suggestion in the Batten and southern Tawallah Ranges is that the Wununmantyala Sandstone is part of the post-inversion clastic apron which is shedding from an uplifted core of lower Tawallah Group units. In marked contrast to the situation at Mallapunyah Dome, this interpretation would time the Tawallah Group inversion event as having occurred pre-Wununmantyala Sandstone (and therefore pre-Wollogorang Formation) in middle Tawallah Group time. Another factor which suggests this interpretation is that the lower Tawallah sandstone units which form the core of the Scrutton, Batten and Tawallah Ranges, the Yiyintyi and Sly Creek Sandstones, are markedly different from the Wununmantyala and Masterton Sandstones. The lower Tawallah units appear more silicified in outcrop, hand specimen and when observed on aerial photos and have clearly been subjected to a much greater degree of structural disruption Rogers (1993). These observations would be consistent with the Yiyintyi and Sly Creek Sandstones having been involved in a mid-Tawallah basin inversion event prior to the deposition of the Wununmantyala and Masterton Sandstones.

Depositional model

The model for the development of the southern McArthur Basin outlined above is summarised in a series of schematic block diagrams (Fig. 6) which use as a base the structural interpretation of Rogers (1993). Figure 6a and 6b show a model for the deposition of the Tawallah Group prior to the proposed Tawallah basin inversion. Figure 6a portrays the lower Tawallah clastic units, the Yiyintyi and Sly Creek Sandstones, accumulating as alluvial/high-energy fluvial or braidplain systems shed from the footwall scarps of successive tilt blocks. This model is very speculative, because although the lower Tawallah clastic units are clearly sandstone-dominated deposits, the high-degree of structural disruption makes detailed sedimentological analysis difficult. In addition, the Seigal Volcanics which also occur at this level have not yet been observed in the field. Another area of uncertainty arises from the proposal that the Tawallah Group currently exposed in the Batten and Tawallah Ranges is a result of structural inversion. Since the structural mechanism of basin inversion involves the reactivation of structures initiated as normal faults during the pre-existing extensional phase (Williams *et al.*, 1989), it follows that the Tawallah Group currently exposed in the ranges is relatively proximal to these reactivated structures. During deposition of the Tawallah Group, when these faults were of normal configuration, it is reasonable to assume that they would have been one of the major controls on deposition as is shown in Figure 6a. As a result of this structural configuration, nothing is known of the more distal equivalents of the lower Tawallah clastics which is reflected by the areas marked with ?s in Figure 6a.

Figure 6b portrays the accumulation of Aquarium Formation as a widespread carbonate blanket following the progressive levelling of the relief imparted by the initial tilt blocks. Taken in isolation, this basal part of the Tawallah Group can be interpreted as a rift-phase/sag-phase couplet commonly proposed for rifting models in the literature (eg. Dewey, 1982).

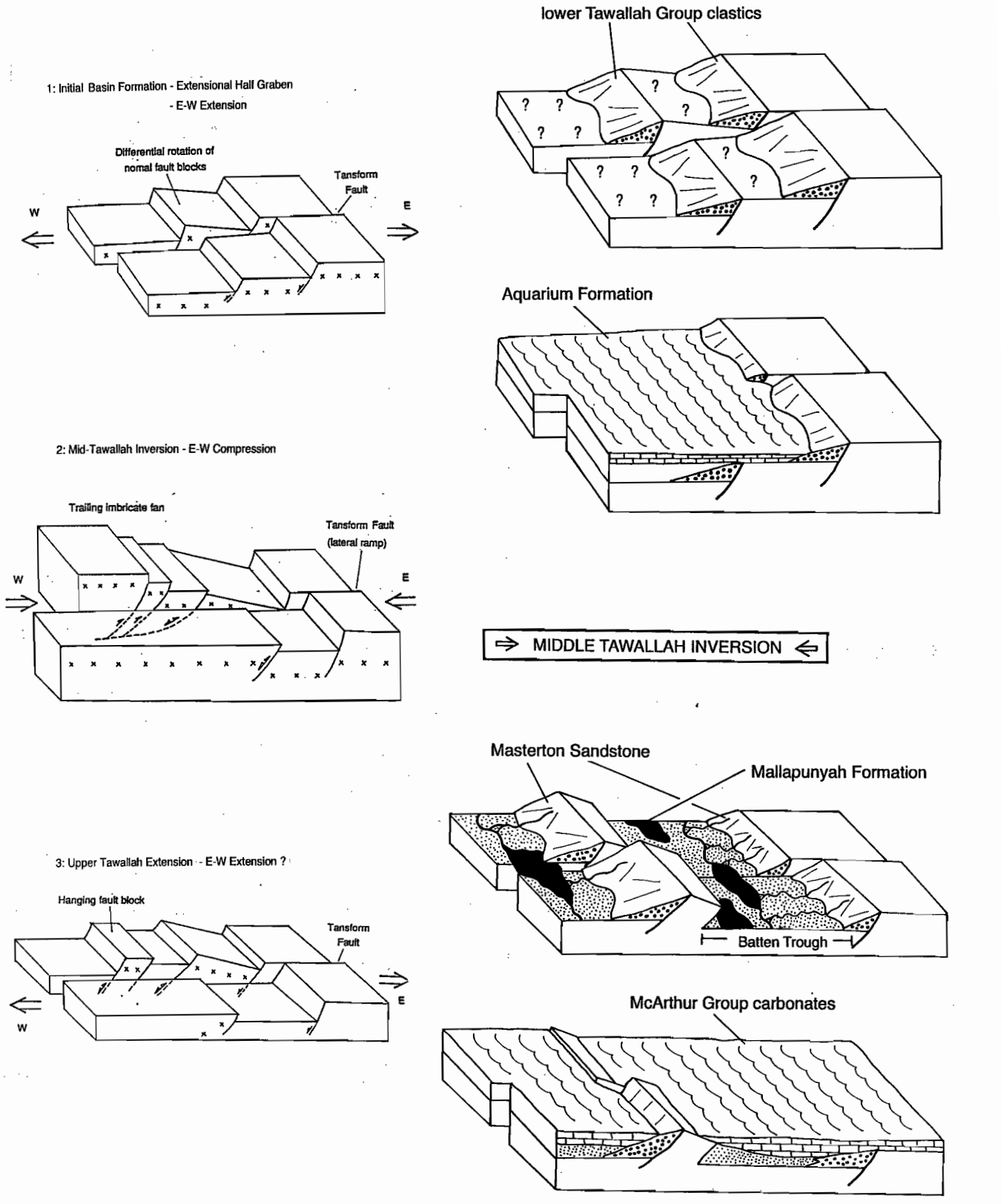

Figure 6. Schematic model for the development of the southern McArthur Basin. (a) Shows the lower Tawallah clastic units, the Yiyinti and Sly Creek Sandstones, accumulating as alluvial/high-energy fluvial or braidplain systems shed from the footwall scarps of successive tilt blocks. (b) Shows the subsequent accumulation of Aquarium Formation as a widespread carbonate blanket following the progressive levelling of the relief imparted by the initial tilt blocks. (c) Shows the Masterton Sandstone accumulating as clastic wedges of alluvial/proximal fluvial or braidplain deposits shed from Tawallah Group blocks uplifted by the syn- post-Tawallah basin inversion. These clastic wedges interfinger with, and are overlain by, the more distal/less energetic fluvial and lacustrine deposits of the Mallapunyah Formation. (d) Shows the accumulation of the carbonate-dominated bulk of the McArthur Group following suppression of the relief generated by the Tawallah basin inversion and resultant inundation of the southern McArthur Basin.

Figure 6c and 6d show a model for the depositional development of the southern McArthur Basin after the Tawallah basin inversion. Figure 6c shows the clastic wedges of alluvial/proximal fluvial or braidplain deposits of the Masterton Sandstone shedding from uplifted Tawallah Group blocks on either side of the Batten Trough. These clastic aprons interfinger with (see below), and are overlain by, the more distal/less energetic fluvial and lacustrine deposits of the Mallapunyah Formation. Figure 6d shows a situation similar to that proposed during the deposition of the Aquarium Formation, where suppression of relief has led to the inundation of the southern McArthur Basin during which time the carbonate-dominated bulk of the McArthur Group accumulated.

Implications of the depositional model

In summary, a provisional sedimentological analysis of the Masterton Sandstone in the southern McArthur Basin indicates that a significant basin inversion event occurred during and/or after the deposition of the Tawallah Group. The exact timing of this event is uncertain at this stage of the study. A possible explanation for the apparent discrepancies in the timing of the Tawallah inversion event between the Mallapunyah Dome in the south and the Batten and Tawallah Ranges to the north, highlights a recurrent problem with a sedimentological analysis of the southern McArthur Basin depositional system. The traditional interpretation of many southern McArthur Basin stratigraphic units is that they have extensive, sheet-like geometries. This interpretation appears to be valid for carbonate-dominated units such as the Aquarium and Wollogorang Formations which clearly accumulated in shallow subaqueous environments during periods of very low regional relief (Fig. 6b and 6d). However, if the above interpretation of the Wununmantyala and Masterton Sandstone units as alluvial/high-energy fluvial or braidplain systems is correct, then these sandstone-dominated units could have much more restricted geometries.

The composition and distribution of high-energy clastic depositional systems is largely controlled by the topographic highs from which they are shed (in the case of the Masterton Sandstone cores of structurally uplifted Tawallah Group). Typical geometries for this type of depositional system are fans or aprons which have a wedge-shaped cross-section. In environments more distal from the topographic high, these clastic wedges could be expected to interfinger with lower-energy and hence finer-grained deposits (Fig. 6c). In the southern McArthur Basin as presently exposed, these more distal environments are covered by younger McArthur Group deposits within and outside the Batten Trough (Fig. 1). However, the significance of this model is that the clastic wedges which are currently exposed (eg. those which flank the Mallapunyah Dome and those in the Batten and Tawallah Ranges), although they may appear very similar in terms of sediment composition and facies, need not be connected in the subsurface. This would make it difficult, if not impossible, to make direct regional stratigraphic correlations between sandstone-dominated units in widely separated localities which are not closely associated with a regionally extensive carbonate units. In broad terms, this model provides a possible explanation for the apparent regional discrepancies in the timing of the Tawallah basin inversion event, however, more field work is needed on this aspect of the study.

The proposal that a mid- or post-Tawallah basin inversion event occurred during the deposition of the southern McArthur Basin system also has important implications for the development of ore deposit models for this system. Of primary importance is that structural uplift prior to deposition of the mineralized McArthur Group provides the potential for basin-wide gravitationally driven fluid flow. Studies of Mississippi Valley Type ore districts, primarily those of the mid-continental basins of north America, have led to various proposals for the mechanisms which drive fluid flow in sedimentary basins (eg. basin compaction, episodic basin de-watering or overpressuring etc.). Of these, topographically-induced, gravitationally driven meteoric fluid flow is by far the most efficient at producing basin-wide fluid transport over long time periods (eg. Bjorlykke, 1993; Garven *et al.* 1993). In the models developed from the mid-continental basins of north America, the topographic uplift which initiates gravitational fluid flow is generated by fold and thrust belt tectonics (Fig. 7). Although this may not be a good structural analogue for the southern McArthur Basin system, it is possible that similar, if smaller-scale, gravitationally driven fluid flow systems were generated by the uplift of aquifers during the Tawallah basin inversion event.

Conclusions

The provisional conclusions of the study of the Masterton Sandstone in and around the Batten Trough are:

(1) Facies analysis of the Masterton Sandstone indicates that it consists of a clastic wedge of alluvial/high-energy braidplain or braided

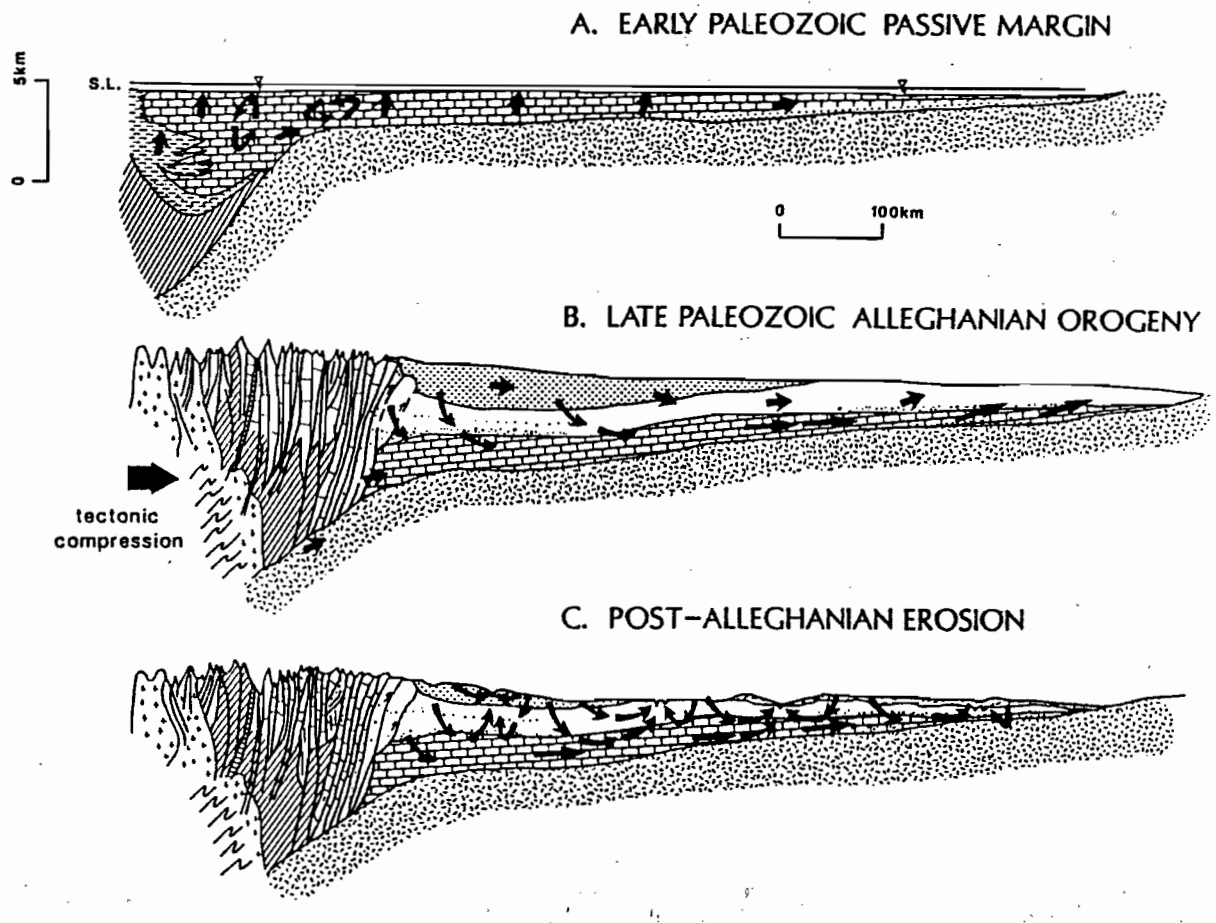

Figure 7. Evolution of flow systems associated with foreland basins (after Garven, 1993). (A) Fluid migration is driven by sediment compaction and density gradients during subsidence of rifted margin and platform. (B) Maximum uplift of Appalachian and Ouachita Mountains occurs in the Permian after the apex of the Alleghanian orogeny. Deep groundwater flow is driven by gravity across the Midcontinent through regional aquifers. Enormous MVT ore deposits are formed as brines of variable temperature and salinity discharge near basin margins. (C) Basin-wide migration of ore-forming brines wanes in the early Mesozoic because erosion reduces topographic drive and partitions regional flow systems.

fluvial deposits. These high-energy clastic deposits interfinger with lower-energy/more distal fluvial and lacustrine or shallow marine deposits in some areas.

(2) The Masterton Sandstone clastic wedge is shed from an uplifted core of Tawallah Group in the Scrutton, Batten and Tawallah Range areas, and possibly also in the Mallapunyah Dome area. This indicates that a major basin inversion event has occurred in the southern McArthur Basin prior to the onset of McArthur Group deposition.

(3) The proposal that a mid- to post-Tawallah basin inversion event occurred in the southern McArthur Basin provides the potential for the existence of gravitationally driven basin-wide fluid flow systems during the deposition of the mineralized McArthur Group.

Future Work

Future work to be carried out the Masterton Sandstone project includes:

(1) Petrological analysis of the samples collected this field season to determine the provenance of the Masterton Sandstone, with particular emphasis on the basal conglomerate facies.

(2) The main aim of the 1994 field season will be to examine sections of the Masterton Sandstone on the eastern side of the Tawallah Ranges (see also J. Rogers this report) and on the western side of the Batten Trough in the Masterton Horst and the Foelsche Inlier (Fig. 1). If successful, this work will provide a more comprehensive model for the development of the southern McArthur basin in late Tawallah/early McArthur Group time. A subsidiary aim is to collect more sedimentological and palaeocurrent data from the Wununmantyala Sandstone in order to clarify its relationship to the Masterton Sandstone in the Scrutton, Batten and Tawallah Ranges.

PROVISIONAL OBSERVATIONS AND INTERPRETATION OF THE SETTLEMENT AND GOLD CREEK VOLCANICS IN THE MALLAPUNYAH DOME AND SCRUTTON RANGE AREAS

Introduction

The palaeoenvironmental interpretation of the volcanic units of the Tawallah Group is an important factor in assessing the development of the southern McArthur Basin system. If these volcanic units represent extrusive activity, then the distribution of the mafic deposits will partly controlled by topography. In this case, the distribution of the volcanic units may provide considerable information regarding the palaeogeography of the developing Tawallah rift system. Alternatively, if these volcanic units are intrusive in nature, then their distribution has less palaeoenvironmental significance and they may be inappropriate for use as regional stratigraphic markers.

An investigation of the history and significance of the Mallapunyah Dome provides an example of the application of the interpretation of the Tawallah Group volcanic units. If the volcanics are extrusive in nature and have near-vent facies characteristics, then it is possible that the dome represents some form of volcanic edifice which was a topographic high during the deposition of the Tawallah Group. Alternatively, if the volcanic units are intrusive in nature then this interpretation is invalid and another origin must be proposed for the Mallapunyah Dome.

Description

The Settlement Creek Volcanics in both the Mallapunyah Dome and Scrutton Range areas are up to 100 m thick and are volumetrically dominated by massive to locally brecciated mafic rocks (Fig. 8a). In outcrop and hand-specimen this mafic material has a medium- and locally coarse- grained texture. Areas with an apparent fine-grained or glassy groundmass and/or scattered vesicles are rare. Both primary volcanic and secondary solution and vein breccias are present locally. The primary breccias are closed framework and often jigsaw-fit (Fig. 8b), and occur as irregular pods which appear to be best developed at or near the margins of the unit. The mafic material which comprises the bulk of the Settlement Creek Volcanics is cut by flow banded, aphanitic and locally autobrecciated rhyolite units (Fig. 8c). These are invariably thin and elongate in nature and often crosscut regional stratigraphy.

The Gold Creek Volcanics are markedly different in nature to the Settlement Creek Volcanics. Peperitic textures consisting of mafic blocks dispersed in a fluidised sediment matrix have been described from a 180 m thick sequence in the Scrutton Ranges (Pietsch *et al.*, 1991a; Rawlings, 1993; Fig. 8d). These deposits indicate that in this

Figure 8. (a) Typical massive and solution brecciated, medium-grained mafic Settlement Creek Volcanics in Archies Creek in the southern Mallapunyah Dome. (b) Jigsaw-fit and slightly rotated breccia in the Settlement Creek Volcanics approximately 100 m from the locality shown in Figure 7a. These deposits are interpreted as mechanical breccias which resulted from the disruption of a cooling unit margin during emplacement. (c) Flow banded and autobrecciated rhyolite unit from the Settlement Creek Volcanics in S. Donovan's honours field. This unit is approximately 1 m thick, clearly crosscuts the massive mafic units which comprise the bulk of Settlement Creek Volcanics and is interpreted as a dyke. (d) Mafic peperite from the Gold Creek Volcanics in the Scrutton Ranges. These deposits clearly indicate that the mafic magma was intrusive into unconsolidated sediment at this locality (Pietsch *et al.*, 1991; Rawlings, 1993). (e) Open-framework heterolithic breccia from beneath the Masterton Sandstone at Kilgour Waterhole. This unit has been mapped as Gold Creek Volcanics at a number of localities in the Mallapunyah Dome area.


a


b


c


d


e

Blank

area, the Gold Creek Volcanics consist of mafic sills/dykes intruded at relatively high levels into unconsolidated sediment. In contrast, the Gold Creek Volcanics in the Mallapunyah Dome area, as has currently been observed, consist of massive pebble/cobble/boulder breccia which contains distinctive Settlement Creek Volcanics and Wollogorang Formation clasts (Fig. 8e). Clasts are up to at least 50 cm in diameter, and are grossly normally graded overall, with some crude bedding-parallel layering enhanced by alignment of clasts towards the top of the unit. It is unclear in outcrop and hand specimen whether this breccia material has a volcanic origin, although Gold Creek Volcanics which are clearly volcanic and of a similar nature to the Settlement Creek Volcanics described above have been reported from the Mallapunyah Dome area (Donovan, 1993).

Discussion/Interpretation

Mode of emplacement

The intrusive parts of the Settlement Creek Volcanics have been interpreted as possible equivalents of the peperitic mafic rocks of the Gold Creek Volcanics in the Scrutton Ranges (Pietsch *et al.*, 1991a). The author concurs with this interpretation because the breccia textures observed in the two units, closed framework/jigsaw-fit in the Settlement Creek Volcanics and open framework clasts dispersed in a sediment matrix in the overlying Gold Creek Volcanics, are consistent with the emplacement of intrusive dykes/sills at progressively higher levels. In fact, the major question with respect to the Settlement Creek and Gold Creek Volcanics is whether or not there was any extrusive activity at all. Outcrops of the Settlement Creek Volcanics are sparsely vesicular in places, however, vesiculation is common in intrusive bodies emplaced at a relatively high-level (eg. Branney and Suthren, 1988). Other features which could be considered unequivocal evidence of extrusive volcanic activity such as erosional upper unit contacts or closely associated pyroclastic or volcaniclastic sediment deposits have not been observed to date.

Depositional model

In the absence of any clear evidence for extrusive volcanic activity, a schematic provisional model for the accumulation of the upper Tawallah Group spanning the Settlement Creek and Gold Creek Volcanics is presented in Figure 9. In summary, the Settlement Creek Volcanics are interpreted to have been emplaced as mafic sills which intruded the Tawallah Group along the base of the Wollogorang Formation. It is possible that they occur at this level because the fine-grained carbonate-dominated base of the Wollogorang Formation acted as a regional barrier which largely prevented further ascent of the mafic magma. The resultant sills are largely massive, but have local closed framework marginal breccias which are the result of mechanical disruption of a partly chilled margin during emplacement. Where the magma did breach the Wollogorang Formation the resultant deposits exhibit peperitic textures consistent with a higher-level of emplacement. The whole sequence was later cut by numerous relatively thin rhyolite dykes which crosscut regional stratigraphy. These rhyolite dykes do not appear to be directly associated with the emplacement of the Tanumbirini Rhyolite which caps the sequence in the Scrutton Ranges, because they are essentially aphanitic while the Tanumbirini Rhyolite is crystal-rich.

Implications of the depositional model

If the provisional model for the accumulation of the upper part of the Tawallah Group (Fig. 9) is correct, two main implications for the early development of the southern McArthur Basin exist. Firstly, if the Settlement Creek and Gold Creek Volcanics are in fact time equivalent units which are entirely intrusive in character, then the fact that the latter clearly intrude unconsolidated upper Tawallah Group sediments constrains this event to late Tawallah Group time. However, in spite of the fact that the Settlement Creek Volcanics appear to generally occur at the base of the Wollogorang Formation and the Gold Creek Volcanics above it, these units, if they are in fact intrusive, could also occur at lower stratigraphic levels. Considerable care therefore needs to be taken in using these upper volcanic units of the Tawallah Group as regional stratigraphic markers.

A second implication of the model concerns the nature and origin of the Mallapunyah Dome. The Masterton Sandstone study indicates that the dome was a topographic high by earliest McArthur Group time, and possibly earlier depending on the final interpretation of the breccias mapped as Gold Creek Volcanics which underlie the Masterton Sandstone in this area. However, if the Settlement Creek and Gold Creek Volcanics are intrusive in character then the Mallapunyah Dome cannot be considered as an extrusive volcanic edifice. Other possibilities for the origin of the dome are regional updoming of the sedimentary substrate during the emplacement of intrusive magmas in the subsurface, or structural uplift during the syn- or post-Tawallah Group basin inversion event indicated by the study of the Masterton Sandstone.

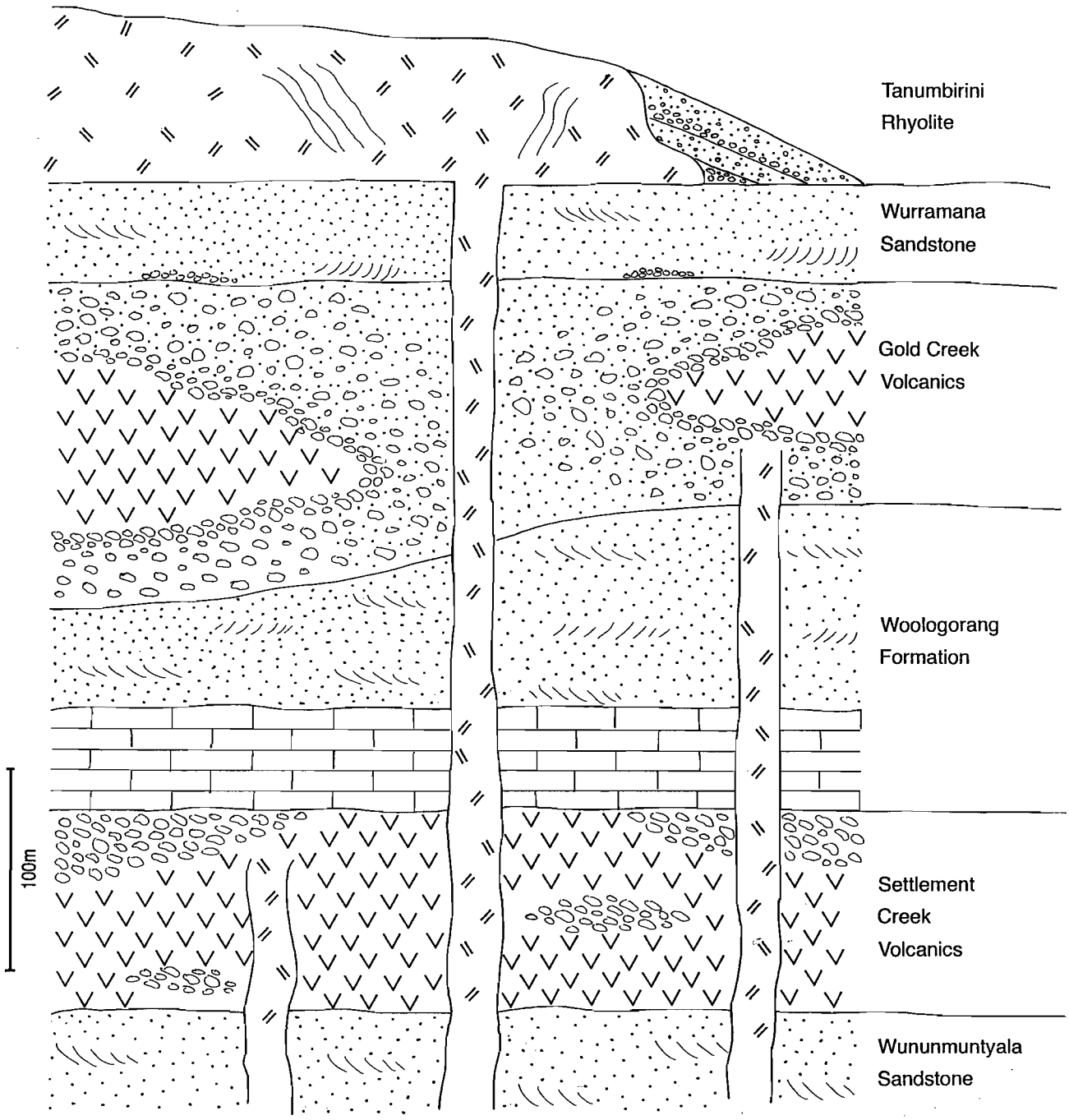

Figure 9. Schematic model for the accumulation of the upper part of the Tawallah Group in which the Settlement Creek and Gold Creek Volcanics represent mafic sills intruded at different stratigraphic levels. These mafic units are subsequently cut by rhyolite sills/dykes.

Conclusions

The provisional conclusions of the Settlement Creek and Gold Creek Volcanics study in the Mallapunyah Dome and Scrutton Ranges areas are:

(1) Both the Settlement Creek and Gold Creek Volcanics appear to be largely intrusive in character and, therefore, care needs to be taken when using these units as regional stratigraphic markers.

(2) The Mallapunyah Dome was not an extrusive volcanic edifice during the accumulation of the Tawallah Group.

Future Work

Future work to be carried out the upper Tawallah Group volcanics project includes:

(1) Petrological studies to determine whether microtextures validate the interpretation that the bulk of the Settlement Creek and Gold Creek Volcanic units are intrusive. The heterolithic breccia which comprises the bulk of the Gold Creek Volcanics in the Mallapunyah Dome will also be examined in an attempt to determine whether on not the unit has a volcanic origin.

(2) The main aim of the 1994 field season with respect to this study is to collect more descriptive data on the nature of the volcanic units with the emphasis, if possible, on detailed mapping of suitable key areas. Subsidiary aims are to examine the thin recessive volcanic units in the Batten Range in order to clarify the stratigraphic relationships in this area, and to examine the Seigal Volcanics in the Tawallah Ranges.

REFERENCES

Bjorlykke, K. 1993. Fluid flow in sedimentary basins. Sed. Geol., 86, p. 137-158

Branney, M. J. and Suthren, R. J. 1988. High-level peperitic sills in the English Lakes District: Distinction from block lavas, and implications for Borrowdale Volcanic Group stratigraphy. Geol. J., 23, p. 171-187.

Cooke, D.R., Bull, S.W. and Keele, R.A. 1993. Overview of 1993 honours research programme in the McArthur Basin. CODES: AMIRA/ARC Project P.384-, Proterozoic sediment-hosted base metal deposits, Rept. No. 4.

Dewey, J. F. 1982. Plate tectonics and the evidence of the British Isles. J. Geol. Soc. Lon., 139, p. 371-412.

Donovan, S. 1993. The geology of western Mallapunyah Dome. CODES: AMIRA/ARC Project P.384-Proterozoic sediment-hosted base metal deposits, Rept. No. 4.

Garven, G., Person, M. A. and Sverjensky, D. A. 1993. Genesis of stratabound ore deposits in the midcontinent basins of north America. 1. The role of regional groundwater flow. Am. J. Sci., 293, p. 497-568.

Jackson, M. D., Muir, M. D., Plumb, K. A., 1984. 1:100 000 scale Geology of the Abner Range region.

Jackson, M. D., Muir, M. D. and Plumb, K. A. 1987. Geology of the southern McArthur Basin, Northern Territory. B.M.R. Bull. 220.

Keele, R. A. 1993. The histories of some faults in the southern McArthur Basin: evidence for an end-Tawallah uplift and a preliminary analysis of the stresses related to post-McArthur and post-Roper compressions. CODES: AMIRA/ARC Project P.384-Proterozoic sediment-hosted base metal deposits, Rept. No. 4.

Leckie, D. A. and Walker, R. G. 1982. Storm- and tide-dominated shorelines in Cretaceous Moosebar-Lower Gates interval-outcrop equivalents of deep basin gas traps in western Canada. A.A.P.G. Bull., 66 (2), p. 138-157.

Pietsch, B. A., Rawlings, D. J., Creaser, P. M., Kruse, P. D., Ahmad, P., Ferenczi, P. A. and Findhammer, T. L. R. 1991a. Bauhinia Downs 1:250 000 geological map series. Northern Territory Geological Survey, Explanatory Notes SE53-3.

Pietsch, B. A., Wyche, S., Rawlings, D. J., Creaser, P. M. and Findhammer, T. L. R. 1991b. McArthur River Region, Northern Territory 1:250 000 geological map series. Northern Territory Geological Survey, Explanatory Notes SE53-3 (6065-6165).

Rawlings, D. J. 1993. Mafic peperite from the Gold Creek Volcanics in the Middle Proterozoic McArthur Basin, Northern Territory. Aust. J. of Earth Sci., 40, p. 109-113.

Rogers, 1993. The structural setting of the Tawallah Group, southern McArthur Basin, Northern Territory: implications for an early tectonic event. CODES: AMIRA/ARC Project P.384-Proterozoic sediment-hosted base metal deposits, Rept. No. 4.

Williams, G. D., Powell, C. M. and Cooper, M. A. 1989. Geometry and kinematics of inversion tectonics. in Geol. Soc. Spec. Publ. No. 44. Inversion Tectonics, Cooper M. A. and Williams, G. D. eds. p. 3-16.

THE HISTORIES OF SOME FAULTS IN THE SOUTHERN McARTHUR BASIN

Evidence for an end-Tawallah uplift and a preliminary analysis of stresses related to post-McArthur and post-Roper compressions

R.A. Keele
Centre for Ore Deposit and Exploration Studies

ABSTRACT

Faulting in the Four Archers region of the southern McArthur Basin was active during Tawallah times. The N- to NNE-trending Four Archers, Hermit, Lorella and Rosie Faults can all be shown to have uplifted the Tawallah Group by varying amounts prior to the deposition of the McArthur Group. The NW-SE trending Warrapirrmantila Dome, bounded by the Hermit and Lorella Faults, developed as a hanging block at the northern tip zone of the Tawallah Fault, exposing units down as far as the Sly Creek Sandstone on the pre-Masterton land surface. A reconstructed map of the geology prior to deposition of the Masterton Sandstone and a regional cross-section shows that the Rosie-Emu Fault block was tilted towards the east at a shallow angle (3-5 degrees): the result is that the Wununmantyala and Warramana Sandstones lie directly beneath the unconformity on the western and eastern edges of this block respectively. This can be explained by a phase of rifting at the end of the Tawallah, in which the Rosie Fault acted a normal fault with a west block down movement. In this scenario the Tawallah Group would be the pre-rift, the Nyanantu (Ptu) the syn-rift and the Masterton the post-rift sequence. The Wernicke model for extension of the lithosphere, involving normal simple shear along an eastward dipping fault at the base of the crust, can be used to suggest a possible cause for some of the features observed.

The history of the Lorella Fault records three main periods of activity. (1) Hematite-silica breccias and associated quartz veining in Sly Creek Sandstone which relate to an early episode of NW-trending block faulting which is absent in the overlying Masterton Sandstone: this relates to a period of (mid- to) late-Tawallah uplift on the west side of the fault, juxtaposing Aquarium Formation against Settlement Creek volcanics. (2) Colloform banded quartz veins - formed by the dilation of sets of conjugate fractures - overprint these breccias and early quartz veins, and are developed in both Sly and Masterton sandstone units: the stress field that controlled their orientation is consistent with late dextral wrench movements during the post-Roper inversion. (3) An east side up movement, also post-Roper in age, represents a final period of movement on the fault.

The stress inversion technique gives up to six palaeo-stress states for each of the areas studied. These states belong to five predominant stress fields: NW-SE extension (with minor NE-SW extension) and NW-SE, N-S, NE-SW & E-W compressions. The extensional stress regime found in both areas may pre-date the compression and belong to periods of crustal extension in Tawallah and McArthur Group times. The compressive stress regime in the Mallapunyah area varies systematically from N-S (wrench), through NE-SW (wrench & compression) to E-W (compression) in that order. Fold superimpositions at Kiana Dome, Coppermine Creek and the region west of the HYC deposit, also support a similar re-orientation of sigma 1 with time, from NNW (or N) through NE to E. Of the three latter fields, the first may belong to a post-Tawallah or post-McArthur inversion, whilst the last two belong to the post-Roper inversion. The reason for this apparent rotation of the stress field is not known

Codes: AMIRA / ARC Project P.384 - Proterozoic sediment-hosted base metal deposits. November 1993

INTRODUCTION

The southern McArthur Basin experienced early rifting along its southeastern margin where the basal Tawallah sandstones are seen to overlie Scrutton Volcanics (Jackson et al., 1987). Leaman (1992,1993) suggested that these basement volcanics actually consist of a series of half-graben structures, trending NE, NW and sub E-W, which were once filled with quantities of felsic and/or mafic volcanic rocks, some of which are equivalent to the Scruttons, but others of which represent a thick pile of mafics that lie deep within the Tawallah Group. The Batten Trough, a term coined by Plumb et al.(1980), refers to a N-S trending half-graben structure in which the Emu Fault, situated on the eastern side of the trough, played an important role in controlling deposition during McArthur Group times. Dextral wrench movements along northerly trending faults controlled sedimentation, volcanism and ultimately mineralisation, in a series of pull-apart basins developed during mid-McArthur Group times (Plumb and Wellman, 1987; Davidson & Dashlooty, 1993). At the closing stages of the basin these structures, and others (e.g Tawallah Fault) became the site of major reverse movements which uplifted the central part of the Batten Trough giving the southern McArthur basin its present form (Plumb et al., 1990). Geophysical evidence for two inversion events during Tawallah times has been provided by Leaman (1992).

The aim of this study is to test the validity of some of these ideas, especially in relation to the history and evolution of the early McArthur basin. Since the basement is extremely poorly exposed, scope for examining the earliest structures proposed by Leaman, with the exception of the Cliffdale Volcanics on the Murphy Tectonic Ridge, is limited. Therefore, this study has focussed on a number of fault structures along the western side of the Batten Fault Zone, e.g the Four Archers, Lorella, Rosie Faults in the Tawallah Ranges and the Mallapunyah Fault and Kiana Dome in the south. In these areas the Tawallah Group, as well as the Tawallah-McArthur Group boundary, are exposed (Plumb & Paine,1964; Smith et al.,1964; Pietsch et al., 1991; Rawlings et al.,1993). Faults thought to be particularly active during the early basin history were examined, principally in the Tawallah and Costello Ranges, for example the syn-rift faults of Plumb et al. (1990) in the Tawallah Ranges.

This report is to be viewed in conjunction with a detailed study of the structures in the Batten, Scrutton and southern Tawallah Ranges by Rogers (1993, this volume). It should be borne in mind that not all the basin history will necessarily be recorded in any one locality and a complete structural and tectonic evolution of the southern McArthur Basin will only come from a synthesis of a number of detailed studies over the entire basin. The stress inversion method (Angelier, 1979; Etchecopar et al.,1981) which is now widely accepted, with certain provisos, as being the best tool available to estimate directions of principal stress during basin closure (compression), was used in this study.

Method

Fault striae, folds, bedding, cleavage and quartz veins were measured in the field, with particular attention being paid to the timing of movements on the faults. The kinematics of small-scale or higher order faults provided much of the data because the major structures were often not sufficiently silicified to preserve all past movements. Whilst this enabled a reasonable assessment of the palaeo-stress fields to be made, it could not allow the building up of a detailed kinematic history. This can only be achieved when the history of sedimentation and nature of the various inversions within the basin are known (Bull 1993, this volume). For TAWALLAH RANGE, the structural data gathered in the field was combined with the data from the maps — where considerable uplift and erosion has been recorded at the end of Tawallah times (Rawlings et al.,1993) — to produce a working synthesis which incorporates some of the important tectonic elements in the region. This was achieved by:

(1) drawing cross-sections in areas where uplift had been at a maximum, and

(2) producing a map which shows the geology as it might have been just prior to the Masterton Sandstone being laid down, as well as,

(3) integrating the field data with (1) & (2) to give a working synthesis.

A number of localities on MANTUNGULA, TAWALLAH & ABNER RANGE 1:100,000 sheets were visited during the 1992/93 field seasons. They were:

(1) A section through the Four Archers Fault at Butterfly Springs.

(2) The faulted southern edge of the Scrutton Inlier where it abuts against the Four Archers Fault, near to the Roper Bar road.

(3) An exposure affording 3-D cross-section, side elevation and plan views of the Lorella Fault at Lorella Springs.

(4) The Coppermine Creek gossan locality adjacent to the Roper Bar road.

(5) The Mallapunyah Fault where it meets the Tawallah Fault immediately south of the Mallapunyah Springs homestead.

(6) The Kiana Dome, immediately west of Old Kiana Station.

Two other localities were visited, e.g. the Murphy Inlier and the Tanunbirini inlier, but neither are reported here because the Murphy Ridge does not fit well with the data presented here, and the Tanunbirini inlier is considered too far removed from the main area of study to be of any significance at this stage.

Stress analysis using fault striae data was carried out on several areas, including the Four Archers Fault near the Scrutton Inlier, Coppermine Creek and the Mallapunyah Dome. The stress inversion programme of Etchecopar (1981) was used; this software package proved to be robust, relatively easy to use and quite suited to the needs of this particular study. The results were related to the rare overprinting relationships observed in the field; by making the distinction between stress states and stress fields (there being fewer of the latter) a stress history has been proposed for the northern and southern areas.

The main set of assumptions used in the Tawallah Range study (1-4 above) are: (1) the uplift occurred at the end of the Tawallah, (2) the upper Tawallah stratigraphy is layer cake and (3) there are no significant variations in thickness and extent of the units, and (4) the Masterton unconformity is a planar surface. None of these assumptions are strictly correct since Rogers (1993, this volume) has described a mid-Tawallah inversion in which significant uplift can be predicted and Bull (1993, this volume) presents evidence that the volcanics are intrusive, and not extrusive, thereby affecting their distribution and stratigraphic level; he also suggests that the deposition of the Masterton sandstone may have, in many areas, followed on directly from the Wununmantyala, by re-establishing an early fluviatile system. This implies that uplift continued throughout the upper Tawallah. However, since we have to start somewhere and the assumptions are likely to hold over small parts of the basin they will, as far as this report is concerned, remain correct until proven otherwise.

FOUR ARCHERS FAULT

The Four Archers Fault (FAF) is a northerly trending 1st order structure that can be traced along the entire eastern edge of the MANTUNGULA sheet (Fig.1; see back pocket). It continues north onto TOWNS where it becomes lost in the vicinity of the Urapunga Ridge. In the other direction the fault dies out at the southern end of the Costello Range where its movement is transferred away onto a series of northwesterly trending fault and fold structures which link up with the Limmen Fault to the west. It should be noted that the FAF at this point steps across (in a left-hand sense) approximately 2 km on to a series of NW-trending faults, one of which is host to the Eastern Creek Pb-Ba prospect. Further south again, the movement has been transferred onto a number of structures including the Tawallah Fault, the Billengarah Thrust and the Bauhinia Thrust (Rogers 1993, this volume).

In the southern half of MANTUNGULA, a bend marks the change to a distinct north-northeasterly trend in sympathy with the Lorella Fault some 14 km to the east (Fig.1; see back pocket). A broad E-W zone connects the deepest exposed stratigraphy in the fault block; in particular, the lowest stratigraphy within the Four Archers-Limmen Fault block (McArthur Group) joins up with the unroofed basement (Scrutton inlier) in the adjacent Four Archers-Lorella Fault block. This uplift is interpreted to be due to W-directed thrusting on the FAF and Limmen Faults (Fig. 2; see back pocket).

Cross-Section at Butterfly Springs

A cross-section at Butterfly Springs comprises (from E to W) three zones:

- a zone of steeply dipping Yiyinti Sandstone beds which is of an undetermined width,
- a 10-25 m wide zone of recessive fault rock, and
- a 1-200 m wide zone of jointed, faulted and veined Yiyinti sandstones beds which also have a steep dip (Fig. 3A).

Rotation of bedding on the eastern side of the fault suggests that this block had moved up relative to the other. Although this movement cannot be dated precisely, evidence from the Masterton unconformity nearby indicates that part of it must have been pre-McArthour Group in age. Much of the movement took place under reasonably ductile conditions by a process of layer slip along bedding, possibly as the result of a monoclinal flexure draped over a high-angle reverse fault in the

Figure 3: FOUR ARCHERS & COPPER MINE CREEK

A. The Four Archers Fault looking south. Vertically dipping beds of Yiyinti Sandstone (Pty) can be seen on the left hand side of the fault; the contact with the main fault surface, which shows up as a recessively weathered 15-25 m wide zone right of centre, is slightly transgressive, with the bedding coming into the fault zone at a slight angle that suggests by its sense of drag an east block up movement on the fault. The sandstones on the right hand side are considerably fractured, brecciated and veined; the bedding is just visible, dipping steeply to the left (east), but a prominent fault-related joint set dipping moderately to the right (west) can also be seen. These beds are presumed to be Pty as well. Locality: Butterfly Springs near Nathan River Station.

B. Dip-slip reverse quartz fibres from the Four Archers Fault, near the Scrutton Inlier. Note that the fibres are slightly bent indicating a dynamic and probably changing stress field during movement; the greenish colour is due to high concentrations of sericite mixed in with the quartz which is usually taken to be an indication of textural reworking with continuing movement on the fault surface. Locality: Scrutton Inlier near Nathan River Station.

C. Quartz fibres and grooves in shear fracture/micro-fault from the Four Archers Fault. The green colouration is due to sericite intimately intergrown with the quartz and the fact that the shear had been reactivated several times destroying much of the original fibres. Locality: Scrutton Inlier, near Nathan River Station.

D. E-W trending gentle fold in Amelia Dolomite, .The contrary vergence on the limbs of this fold, i.e. "Z" where it should "S", suggests that solution collapse or slumping occurred prior to this folding event. Locality: Coppermine Creek.

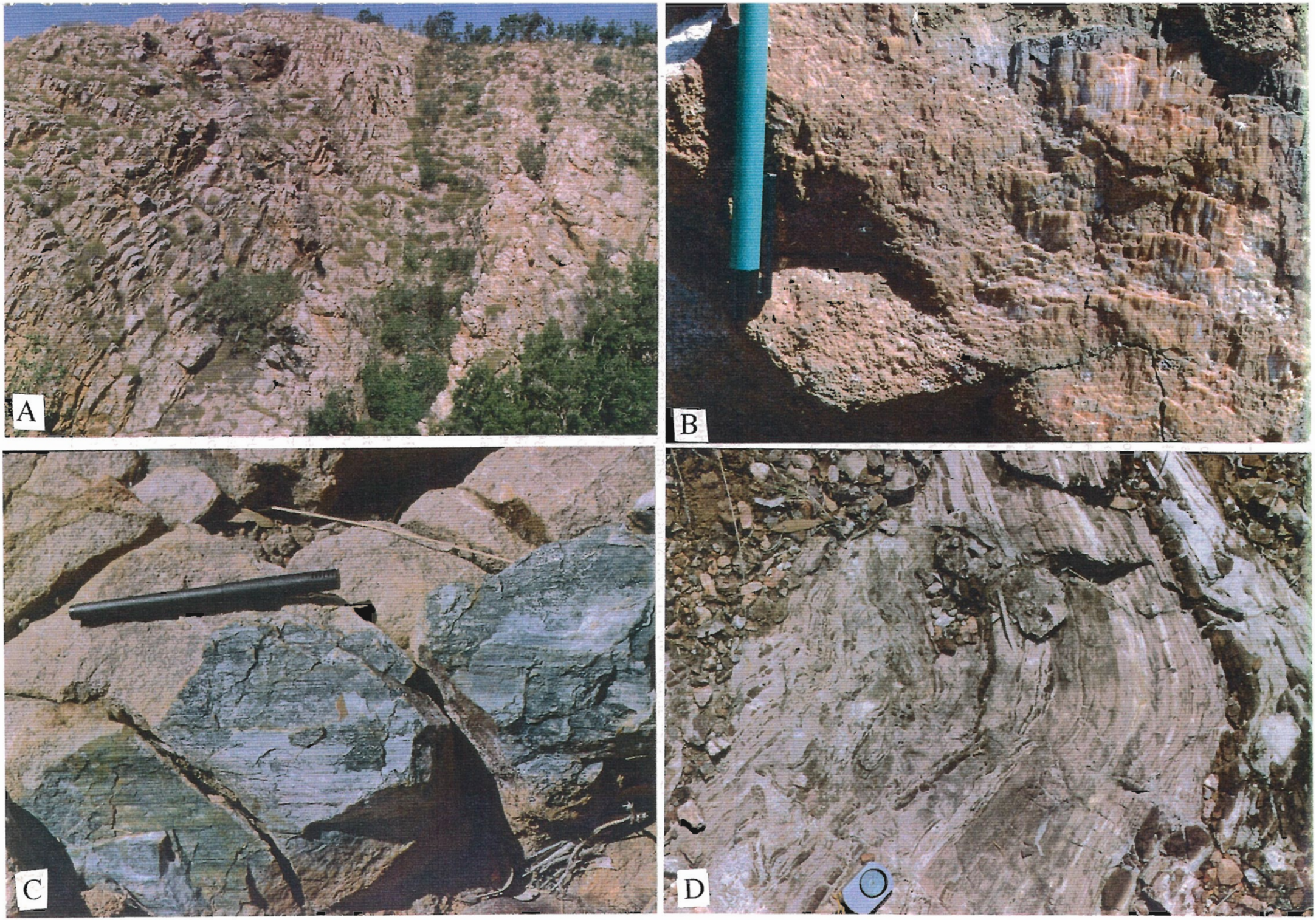
A
B
C
D

basement. The generally flat dipping Roper Group sandstones on the western side of the fault also indicate significant upthrow of the eastern block during the Post-Roper compression.

On the western side of the fault, the sandstones are more strongly deformed, with evidence of a pressure solution style of deformation. A number of sets of replaceive quartz veins, developed mostly parallel to the fault, show the effects of at least two deformations: a layer parallel and a layer perpendicular shortening. The bedding parallel deformations are manifest as contractional faults offsetting fault-parallel quartz veins; in particular, sets of low-angle conjugate quartz veins, including comb-textured extensional quartz veins, give a sigma 1 that acted parallel to bedding (i.e. N-S) and a sigma 3 that acted perpendicular to bedding (i.e. E-W). Stylolitic bedding surfaces indicate a shortening perpendicular to the bedding surface (i.e. E-W), a direction which can also be inferred from the presence of high-angle conjugate fractures.

Scrutton Inlier

The Scrutton inlier is 8 km long by 1 km wide and trends in a general northwesterly direction (Fig. 1). Its northern and southern contacts with the overlying Yiyinti Sandstone are generally conformable; however, the western contact against Roper sandstones is faulted. This NW-trending segment of the Four Archers Fault is well exposed where it is noted that the Hodgeson Sandstone Member is overturned, dipping to the NE. Since the Tawallah Group on the other side of the fault faces and dips NE, the fault here marks a change in younging direction. There are a number of gentle folds (plunging 13 degrees towards 120 degrees) in the Roper sediments immediately west of the fault.

Quartz veining and microstructure

A preliminary inspection of the veining associated with the Four Archers Fault at the edge of the Scrutton inlier, reveals the presence of at least two types of quartz veins. The first, and main, type comprises milky white quartz that forms sub-parallel, bifurcating, sheeted 2 mm - 2 cm wide vein sets; the quartz has completely replaced the matrix which usually consists of sub-rounded to sub-angular irregularly shaped quartz grains set in a fine grained sericitic matrix. The veins consist of 100% quartz and have diffuse boundaries indicating that they are replaceive and not dilational in origin.

A second generation of veins (up to 0.5 cm wide) related to a kinematically active phase of the Four Archers Fault, is characterised by fine grained quartz, sericite and ?hematite. These veins are dark grey to black in hand specimen, whilst in thin section the black mineral varies from being distinctly lath-like to fine grained and patchy. The vein margins are sharp and they offset the replaceive veins, but they are in turn offset by a later set of veins. The generally dynamic effects of this phase of movement are shown by the fact that a fabric caused by the weak alignment of sericite grains may just be discernable microscopically.

Quartz fibres

Examples of quartz fibres developed along fault surfaces during movement, show both the effects of a primary growth phase, as well as a later deformational and recrystallising event (Fig 3 B & C). Microscopically, this can be seen as a general elongation of quartz fibres which vary in length from 1-2 mm to 5-10 mm, depending on whether they are true grains or subgrains. The fibres have sutured boundaries indicating that grain boundary movement continued after their formation, probably in response to the directed stresses which were applied during and after movement. Extremely sharp boundaries consisting of microscopic hematite-quartz shears, may separate the normal undeformed sandstone rock — generally consisting of subrounded clastic grains set in a sericitic matrix — from the fibrous recrystallised quartz rock. In other examples, the superimposed deformations appear to dominate and an extremely sharp planar discontinuity, or shear, may separate secondary domains of interlocking mosaics of quartz grains and sub-grains, with patchy sericite devlopment, from a fine grained quartz sericite matrix in which the elongation of small quartz grains is parallel to the micro-shears.

LIMMEN FAULT

The Limmen Fault, situated halfway between the Four Archers Fault and the Mantungula Fault, shares some of the characteristics of its neighbours: for instance, it has the same northerly trend as the Four Archers Fault; it uplifts rocks from deeper levels in the basin and is probably, athough is hard to prove, a dextral wrench fault.

The Limmen (and Four Archers) Fault are interpreted to be high-angle reverse faults or thrusts. The limited amounts of dextral wrench movements available on the Mantungula-Willara wrench system (0.8 -1.2 km), which is clearly insufficient to account for the observed stratigraphic juxtapositions, requires thrusts which are interpreted to flatten off markedly at the base of the Yiyinti Sandstone (Fig. 2).

A number of long wavelength features control the highs and lows of stratigraphiy on the eastern sides

of the Four Archers and Limmen Faults. For example, the Scrutton inlier, the outcrops of Nathan Group and the lowest Tawallah rocks all lie at a regular spacing (11-13 km) along the eastern side of the Four Archers Fault. The amount of uplift along the Limmen Fault is also controlled, in part, by structures in the basement. For example, the broad E-W arching which brings Umbolooga Subgroup up against Roper Group opposite the Scrutton inlier, has a remake some 35 km to the north, where the Settlement Creek sits directly against the Roper and Nathan Groups. These sub E-W axes reflect the fundamental structural changes that occur in the basement on either side of the fault(s).Such periodic development reflects the fact that the most kinematically active parts of the reverse fault systems are controlled by deep structures within the basement such as: transfer zones related to early NW or NE extensions, thrusts associated with the mid-Tawallah inversion (Rogers,1993, this volume), and the grabens related to the deeply buried volcanic piles (Leaman, 1992).

Mantangula-Willara Wrench Fault

These faults form part of a northerly trending left-stepping dextral wrench system that can be traced for at least 70 km through MANTUNGULA and TOWNS (Fig. 1). This pattern of faulting is exclusively developed in the Roper sediments - i.e. the dissected domes of Plumb et al. (1980) - which attain a thickness of several kilometres in a depocentre centred on the Bauhinia Shelf west of the Batten Trough (Leaman, 1992). As the individual faults step to the left, they exhibit the classic anti-dilational jog structure whereby doubly plunging anticlines or synclines link two fault segments and their associated splays (Fig. 1). The southern end on the Mantungula Fault has one such dome connecting two splays; it also contains a 6 km long wrench fault that offsets a syncline-anticline pair by 850 -1000 m in a dextral sense. Further north the Mantungula and Willara Faults form a overlapping fault system in which an anticline is offset dextrally by a distance of 1.2 km, as measured by Prax and Prah sandstone units in the Lower Roper Group.

Other dextral wrench movements on N-S faults in this part of the Southern McArthur Basin range in magnitude from 250 m along splays off the Four Archers (e.g. the dolerite dykes in Yiyinti Sandstones) to the 2.5 km displacement of the Tawallah Fault by the Lorella Fault. An intermediate displacement of 850 m to 1.2 km occurs along the Mantungula-Willara Fault system which is, therefore, considered about average for this event.

Whether the wrench faulting was a late-stage reactivation of earlier structures during post-Roper compression, or whether it was part of an ongoing series of wrench movements during Tawallah and McArthur Group times, is not known. However, it is likely that the Limmen Fault, like the others, had experienced some dextral reactivation after the main uplift/thrusting event, but it must be stressed that the evidence for this is lacking due to a lack of suitable markers. This dextral wrenching is probably a late-stage reactivation at high crustal levels in an old fault system, a particularly common feature in wrench regimes (Harding,1974).

LORELLA FAULT

The Lorella Springs outcrop (568 820E; 8 261 650N) contains cross-section, side elevation and plan views of the fault (Fig. 4). The subvertically dipping fault trends north-northeasterly and juxtaposes Sly Creek sandstones (Ptl) on its eastern side against Masterton sandstone (Pms) on its western side (Fig. 5 A & B). Because of this, Lorella Springs is considered a good place to study a particular style of brecciation, veining and alteration which is typical of the quartz arenites in the Tawallah Group and then compare this directly with the same lithology in the McArthur Group.

Hematite-Silica Breccias

The earliest structures observed in the Lorella Fault are hematite-silica breccias. The breccias contain sub-angular clasts of pale pink to buff coloured silicified sandstone set in a red-brown silica-hematite and quartz matrix; they occur in both the Sly Creek and Masterton Sandstones, although they are considerably weaker in the latter (Fig. 5 C &F). Massive to weakly laminated quartz veins, up to 2-3 cm wide, subparallel the breccia zone margins and may be deformed by thin cross-cutting grey hematitic shears which trend sub E-W and show a consistent dextral sense of displacement (Fig. 5E). In the Sly Creek Sandstone the breccia zones trend NW, and rarely NE (see below); they form crudely planar anastomosing faults that developed across the whole width of the fault zone and have demonstrable offsets of bedding surfaces across them (Fig. 5D). In the Sly Creek Sandstone the NNE trending hematite-silica breccias are much less distinct than their NW trending counterparts and they appear to have controlled, in part, the position and trend of the later sheeted quartz veins. Unfortunately, no intersection of the two NW and NE trending breccia zones was observed in the field, thus their relative ages are unknown.

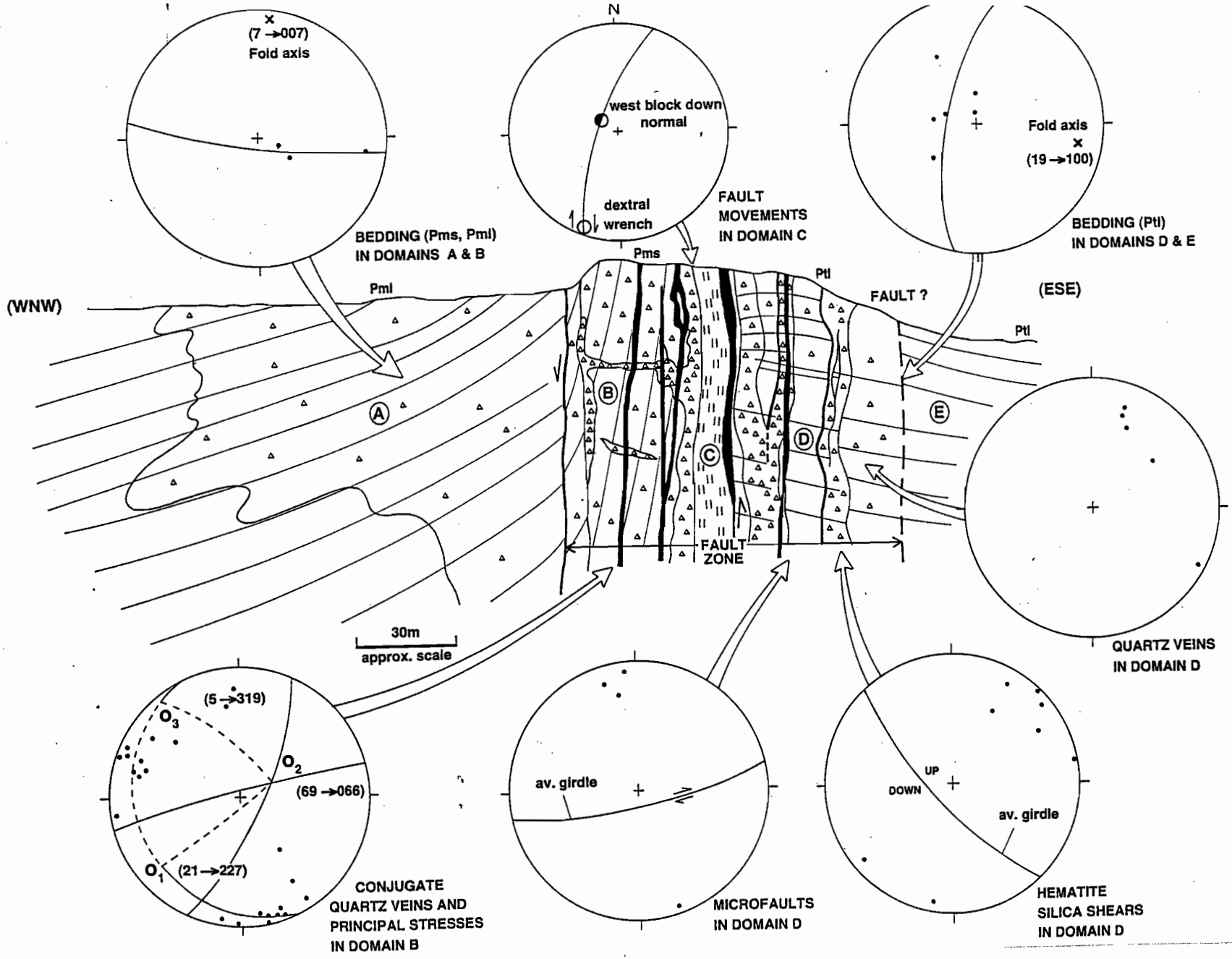

Fig. 4 Diagrammatic cross-section through the Lorella Fault at Lorella Springs. Domains A-E represent major sub-divisions across the fault. The principal stress directions in domain D have been calculated from the two sets of conjugate quartz veins; note similar, although not identical, orientation for post-Roper compression in [illegible] Dome (Fig. 11D). See text for further discussion.

Figure 5: LORELLA FAULT

A. The fault looking south showing domains B, C & D (refer to Fig. 4 for explanation). The main fault surface, some 2-3 m wide, separates Ptl (left) from Pms (right). The Masterton sandstone has a characteristic purply appearance due to hematite staining; this silicified rock which takes on the appearance of a stockwork, contains abundant quartz veining related to the post-Roper inversion. The Sly Creek Sandstone dips very flatly to the left (i.e. to the east) and the Masterton dips steeply to the right (west).

B. Sly Creek Sandstone with its strongly silicified counterpart is visible in this photograph (i.e. domain D & C contact) . Note that the transition between unsilicified and silicified sandstone is quite abrupt, with the bedding disappearing over the length of the pencil shown; this pencil rests on a joint surface which is a relict bedding plane. Locality: Lorella Springs.

C. Silica-hematite breccia in Sly Creek sandstone from the Lorella Fault (domain D). Note the sharp boundary to the main breccia zone, or shear, and the quartz vein that parallels it. The remainder of the sandstone has a network of hematite filled fractures, some of which post-date the shear, but the majority of which clearly pre-date the breccia zone as can be seen from the fractured silicified sandstone clasts. Locality: Lorella Springs.

D. An example of the silica-hematite breccia, or shear in the Sly Creek sandstone (lorella Fault, domain D). Note that the bedding is clearly displaced along these shears, although in this particular photograph it is not possible to put a sense of movement on this faulting. Locality: Lorella Springs.

E. A deformed quartz vein associated with the hematite-silica shears in Sly Creek sandstone from the Lorella Fault (domain D). The deformation is recorded in two distinct stages; firstly, a series of small-scale thrusts along the length of the quartz vein itself and secondly, as a single knife-sharp high strain dextral shear seen left of centre which truncates the earlier microfaults. Locality: Lorella Springs.

F. Several generations of quartz veins developed in Masterton Sandstone on the Lorella Fault (domain B). The earliest veins are irregular to planar quartz veins which are related to the silica-hematite brecciation event; these are cross-cut by two conjugate mutualy intersecting sets of quartz veins formed during the post-Roper compression (NE-SW). Although the thicker vein with minor open space fill textures is seen to cut the earlier hematitic quartz vein, elsewhere the opposite is true. Locality: Lorella Springs.

G. Silicified and hematised Masterton Sandstone with prominent stylolitic surface across which considerable amounts of material has been removed by pressure dissolution (domain B, Lorella Fault). Note that individual hematitic shears are sharply truncated on this surface and that it is impossible to correlate them across the stylolite. Locality: Lorella Springs.

H. Brecciated Mallapunyah Formation from the Lorella Fault (domain A). Relict beddin is recognisable in the pale silicified clasts, probably originally silstones or fine sandstones; the remaining dark red-brown areas are probabaly ferruginsed muddy layers. Note the extent of the hydraulic fracturing in the rock producing highly angular clasts which locally show limited coherence or fit. Locality: Lorella Springs.

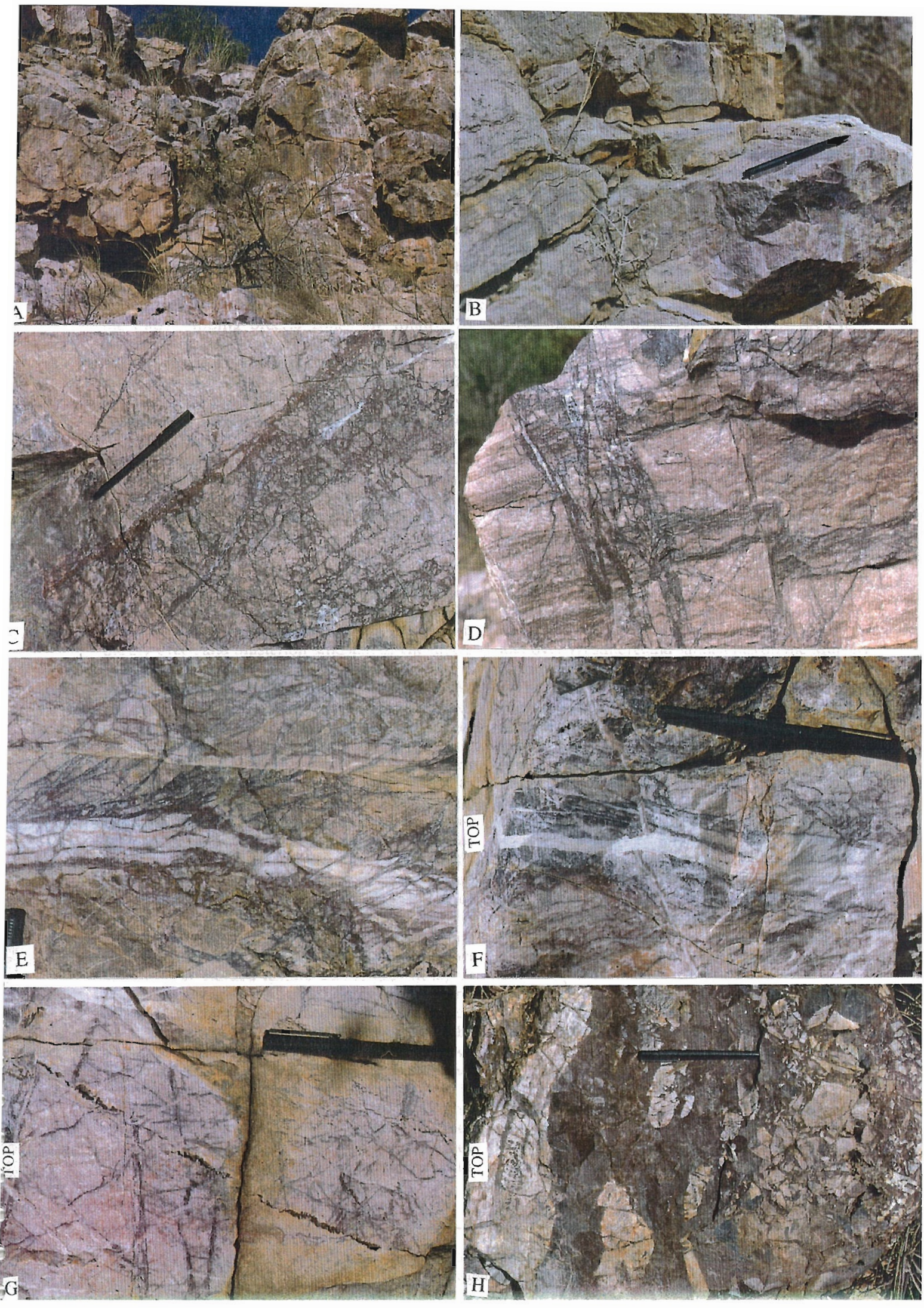
A
B
C
D
E
F
TOP
G
TOP
H
TOP

The volumetrically less important hematite-silica breccias in the Masterton Sandstone, however, are different in character to those in the Sly Creek. In the Masterton the silicified clasts are pink rather than buff to grey, they lack the strong sub-planar fabric of the other and are most intensely developed immediately adjacent to the main fault plane. Where the hematite-rich zones do approximate a planar geometry, which is not often, they may be sub-horizontal and offset the structures along pressure dissolved or stylolitic surfaces (Fig. 5G). If the flatly dipping breccia zones are rotated 70 degrees back to their original position (i.e. by taking out the dip of the Masterton), they have a similar orientation to the NNE trending breccia zones in the Sly Creek on the other side of the fault plane. However, as already stated, the relative ages of the two sets of breccia zones in the Sly Creek are not known; therefore, they need not necessarily belong to the same event. Unusually for the Mallapunyah Formation, it is strongly brecciated to within a distance of 1-200 m from the fault (Fig. 5H).

Quartz Veins

The quartz veins are of two generations. The first generation occurs in the Sly Creek Sandstone only, whereas the second generation is present in both the Sly Creek and Masterton sandstones. The first is considered Tawallah in age, whilst the second is post-McArthur in age; however, since the NE-SW compressive stress field, with which it is associated, is thought to represent the post-Roper event, it may well be post-Roper in age too.

The Tawallah veins may be up to several cms wide and have a weakly laminated structure due to thin partings of hematite within the veins. The quartz is massive, milky and otherwise textureless, displaying a microstructure which consists of myriads of secondary fluid inclusions along small-scale fracture. They are clearly fractured, faulted and weakly rotated giving lazy "z" senses of vergence (Fig. 5E).

The post-McArthur quartz veins are composite millimetric to centimetric sized veins with a distinct colloform or banded texture due to growth layers (Fig. 5F). They are white, pink or grey in colour and attain their best development in the Masterton Sandstones where they form a stockwork. The presence of mutually cross-cutting veins with two dominant directions (NNE & ENE) indicates that they formed as a conjugate pair in a stress field in which sigma 1 was directed NE-SW (Fig. 4). This same generation of veins occurs in the Sly Creek Sandstone on the eastern side of the fault, but they only form one set of the conjugate pair, namely the one that parallels the fault plane.

Kinematics and Stress Orientations

Three kinematically significant events are recorded along the fault. In the order in which they probably occurred, they are: block faulting on early hematite-silica breccia zones; strike-slip movements associated with a stress field that formed the late conjugate quartz veins; and E block up vertical movements related to the rotation of the Masterton sandstone beds. These movements are discussed in more detail below.

The main hematite breccia zones in the Sly Creek sandstone trend NW and dip steeply south; a south block down movement on these structures is indicated. These movements may account for the apparent W-block up movement that juxtaposes Aquarium Formation against Settlement Creek prior to the Masterton Sandstone (Fig. 8) The breccia zones are cut by a set of dextral shears which trend approximately E-W suggesting that the two stress fields that fit this scenario best are a NE-SW extension — giving S-dipping normal or block faults striking NW-SE, followed by a NW-SE compression giving dextral movement on the E-W shears. Such a direction for sigma 1 has been connected with a post-Tawallah uplift along the southeastern edge of the Wearyean Shelf, where SE-directed thrusts have pushed Cliffdale volcanics up and over Westmoreland sandstones on the Murphy tectonic inlier (Leaman,1993).

The late stockwork quartz veins which are present on both sides of the fault formed by dilation along a pair of conjugate shear fractures. The main group strikes NNE-SSW whilst the subsidiary group strikes ENE-WSW, giving the following orientations for the three principal stresses: sigma 1 plunges 2 degrees towards 227, sigma 3 5 degrees to 319 degrees and sigma 2, the intersection of the two vein sets, plunges 69 degrees towards 066 degrees (Fig. 4). These results accurately reflect the state of stress at a time the fault moved, probably during post-Roper times, because the criterion for brittle failure and conjugate fractures are satisfied, i.e. the fractures mutually intersect each other. Also this stress field is identical to that required for dextral strike-slip movement on the fault.

The dips of the McArthur Group sediments (including the Pms and Pml) on the hangingwall side of the fault lie along an E-W girdle which defines a rotation axis that plunges 7 degrees towards 007 (Fig. 4). The movement vector lies at the intersection of this girdle with the fault plane which, together with the drag of the beds up into the fault, gives a west-block-down sense of movement. From the stereonet in figure 4 it becomes apparent that the beds on either side of the fault have behaved differently during this event: whilst Pms and Pml beds have been dragged up

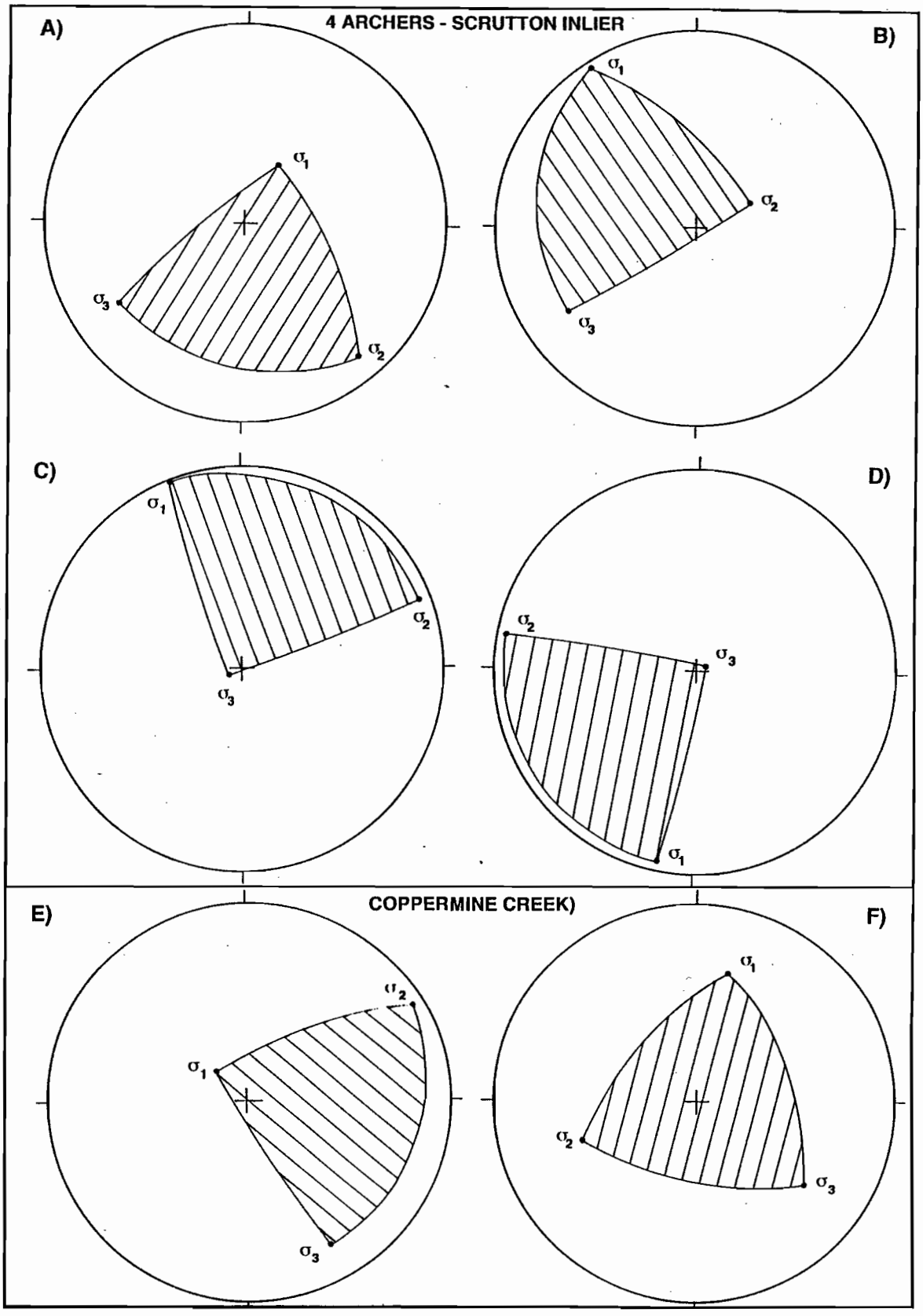

Fig. 6 Orientations of the three principal stresses for the northern area. (A - D) are from the Four Archers Fault, adjacent to the Scrutton Inlier, whilst (E) & (F) are from Coppermine Creek. Stereonet (A) represents a stress field for normal faulting along a direction parallel to the southern side of the Scrutton inlier; (B) is a variation of this theme in that sigma 3 had remained constant whilst sigma 1 and sigma 2 swapped positions. Stereonets (C) and (D) are very similar figures and probably represent two resolved stress directions for sigma 1 around a stable N-S direction of compression. Stereonet (E) represents a stress field that induced normal faulting along an ENE trend; (F) is N-S compressive stress field with both wrench and contractional characteristics (i.e sigma 2 is neither vertical nor horizontal). For further explanation, see text.

into the fault with a west-block-down or normal sense of movement, the bedding in Ptl on the eastern side of the fault, has been folded into a series of gentle folds whose axes plunge 19 degrees towards 101 degrees. The symmetry of this figure is interesting, because it can be seen that the two pi-pole girdles *intersect in a direction which is both in the fault plane and perpendicular to the recorded movement direction.* Thus whilst this vertical movement on the Lorella Fault cannot be timed precisely it is most likely related to the later strike-slip post-Roper event.

The NNE-SSW compressive stress field (sigma 1) required to produce E-W folding on the eastern side of the fault in the Sly Creek sandstones was directed *along* the fault; the different stress state in the Masterton and Mallapunyah Formations on the other side of the fault induced extension and caused considerable vertical movements with the hangingwall block moving down relative to the footwall block. This state represents a local reorientation of the regional stress field with the near vertically plunging sigma 1 (for vertical movements) changing places with sigma 2 (for wrench movements) at some stage in the post-McArthur & Roper compression. The relative timing of the two cannot be determined with absolute confidence but by analogy with faults of the same age to the west in the main Roper basin, where folding in the Roper beds pre-dates the dextral wrench movements along N-S faults (see below); this suggests that the vertical movements may have just pre-dated the wrench movements.

Summary

Small-scale structures in and around the Lorella Fault reveal differences in the orientation and intensity of development of hematite-silica breccias and quartz veining in the two sandstone units. An episode of faulting present in the lower sandstone unit is absent in the upper unit, supporting the existence of a significant pre-McArthur tectonic event, which involved both a NE-SW extension & NW-SE compression as well as west block up movement. However, the effects of a post-Roper compression is observed in both sandstone units in which a dextral strike slip movement and an east block up movement are inferred.

COPPERMINE CREEK

Two fold styles and orientations are present immediately south of the main E-trending fault; they occur in Amelia Dolomite which, because of its silt content, was more susceptible to ductile deformation adjacent to the fault; they are :

(1) Early open E-W folding with a weak axial plane fracture cleavage. The folds plunge gently to ESE (Fig. 3D).

(2) Later close to tight NW-trending folds with interlimb angles of 90 degrees with a stronger and better developed axial plane fracture cleavage.

The major fault at the prospect is the the Coppermine Creek Fault which strikes E-W and juxtaposes Pri on the north side against Pma on the south side (Fig. 1). Timing relationships (locality CM63) indicate that strike-slip sinistral movement overprints a normal movement; there is also a late dextral strike-slip movement that cuts obliquely across this sinistrally reactivated fault.

STRESS INVERSION METHOD

Four Archers-Scrutton Inlier

An analysis of 18 fault striae from two localities (Butterfly Springs and Scrutton Inlier) has produced four stress states during slip on the Four Archers Fault (Fig. 6 A-D). No timing relationships between these faults or their striae were observed in the field, consequently the following stress states are described in order of relative importance, and not age.

The most significant stress states from a regional point of view are NNW to NNE directed compressive stress regime where sigma 1 is horizontal and sigma 3 (Fig. C & D). These results may be due to a single N-S stress field, which resolved itself into two stress states, or it may be viewed as two separate and distinct stress fields. Another stress field, which includes two related stress states, is a NNW compression in wrench mode (i.e. sigma 2 was steeply plunging, Fig. 6B) and an extension with sigma 1 plunging moderately steep to the NE (Fig. 6A). It is interesting to note that these last two solutions, despite their relatively high stress ratios of 0.97 & 0.99 respectively, changed from oblique (wrench) faulting to normal faulting with only a very small change in the minimisation percent of the samples used in the calculation, namely from 80% to 75%. This indicates that they are really two different stress states within the one stress field. This is discussed further below.

It should be noted that the stress state in Fig. 6B, i.e. the NNW directed sigma 1 in wrench mode, accounts for compression directed along the length of the Four Archers Fault, especially where it parallels bedding (see above).

Coppermine Creek

An analysis of 26 fault striae from around the copper prospect yielded two reasonable stress states for slip along the Coppermine Creek Fault, both of which are to an extent oblique-slip (Fig. 6E & F). This is not to say that others might not be possible, because the field data suggests that this is the case. The best result involves a steeply plunging sigma 1 (73 towards 312) and sigma 3 which plunges flatly to the southeast (16 towards 151). This is an extensional stress field that favours the development of sub E-W normal faulting (Fig. 6E). The Coppermine Fault is one such fault that fits this stress field and accounts for the Roper Group now being faulted against McArthur Group.

The second stress state is mid-way between a wrench faulting (sigma 2 vertical) and a typical compression (sigma 3 vertical) (Fig. 6F). In fact, sigma 3 plunges 32 towards 128 which is parallel to the plunge of the sub E-W folds in the Amelia Dolomite (Fig. 3D), strongly suggesting that this stress field was responsible the earlier episode of folding observed in this locale. Such a stress field could account for the sinistral rectivation along the fault and possibly the dextral reactivation; however, the latter would be best explained by a principal stress that was oriented more northeasterly than this.

TAWALLAH UPLIFT

A series of 1:100,000 scale cross-sections covering the Tawallah sheet in the Southern McArthur Basin were drawn up to study the effects of uplift and rotation of beds during and at the end of the Tawallah. Cross-section A-A', trending ESE-WNW, is 65 km long and cuts the Hermit, Lorella and Rosie Faults, including the newly named Warrapirrmantila Dome, and terminates on the eastern side of the Emu Fault Zone. Section B-B' is a shorter NE-SW section at right angles to the main cross-section.

Geological Section line A-A' (Hermit Fault to Emu Fault)

The existence of a Tawallah event can be demonstrated from the number of Tawallah units missing below the Masterton Sandstone. At the western end of the section Pms rests on Wununmantyala Sandstone (Ptn) and it can be shown to do so over a wide area occupying the far northwestern corner and western side of the Tawallah Range sheet (Fig. 7). A rapid change occurs in the vicinity of the Hermit Fault where an erosional surface can be seen cutting deeply into the Tawallah Group reaching as far down as the Sly Creek Sandstone. The core of the Warrapirrmantila Dome is predominantly composed of this unit. On the northern end of the dome immediately east of the Hermit Fault, Masterton Sandstone sits directly on "thinned" Ptn; this contrasts with a much thicker Ptn on the western side of the fault. One possible explanation for this is that the Hermit Fault was a growth fault during Wununmantyala times and that the sandstone thickenned towards the fault. Another explanation is that this fault was active during the Tawallah tectonic event, lifting the eastern side more than the western side causing more stratigraphic stripping on the uplifted footwall block.

The Hermit fault has been shown as having a steep W-dip even though the fault was not actually visited in the field. This can be considered a reasonable interpretation because the rotation of the beds on either side of the fault supports a west-block-down movement. The bending up of the Tawallah Group sediments in the hangingwall of the fault is not reflected in the overlying Masterton sandstone which can be seen to pass almost uninterrupted through the fault.

The Lorella Fault also has an implied west-block-up movement at the end of the Tawallah times. Pms rests directly on Aquarium Formation (Ptq) west of the fault and on upper Wununmantyala Sandstone (Ptn) east of the fault, implying a maximum stratigraphic uplift of approximately 200-250 m. Thus whilst these two faults define an uplifted horst (called the Hermit-Lorella fault block), the lack of any evidence for rotated beds on the eastern side of the Lorella Fault, suggests that much of the uplift could be more apparent than real, or it could have been emphasised by later strike-slip movements. Nevertheless, the data indicates that between the two faults a broad arching of the Tawallah Group sediments took place during this phase of inversion and that the whole had been affected by a second gentle folding event which was due to a NE-SW directed compression. This event gave the dome its present shape, probably during post-Roper times.

The Rosie Fault shows many of the features already described for the Hermit Fault; i.e the bending up of the Tawallah Group sediments against the fault, particularly Ptq, Ptn & Ptnw, due to west-block-down movement. Pms beds also steepen towards the fault, but to a much lesser extent than the underlying Tawallah beds (such movement has already been documented on the Lorella Fault, see above). As a consequence of this much deeper stratigraphic levels have been exposed in this part of the sedimentary basin (e.g. the Yiyinti Sandstone). The Masterton Sandstone rests directly on Settlement Creek (Pte) volcanics and Wollogorang Formation (Pto1 + Pto2) east of the

Rosie Fault, implying an east-block-down movement. The steepening of the units Pts throught to Ptn east of the Yiyinti horst block also implies a significant amount of east-block-down movement on the Rosie Fault. However, the Rosie Fault clearly was the most active of the three faults and much of this activity may have been post-Roper in age. Unfortunately, it is not possible to say with certainty which movement had been the stronger because the Masterton Sandstone has been largely stripped away here. So whilst for the western end of the regional cross-section we can say with certainty that the Sly Creek Sandstone was eroding during the Tawallah event, making it a possible source rock for the Masterton Sandstone, we cannot say with certainty whether the Yiyinti sandstone was similarly exposed.

The 20 km section between the Rosie Fault and the Emu Fault comprises a faulted and broken up slab of Tawallah rocks that is tilted towards the east. Dips flatten off noticeably from 30-40 degrees in the west to almost horizontal in the east. Since the Masterton Sandstone is shown, from data projected up from the south, to lie over six units from the upper part of the Tawallah Group, with the oldest Wunnunmantyala Sandstone (Ptn) adjacent to the Rosie Fault and the youngest, the Warramana Sandstone (Ptm), adjacent to the Emu Fault, this tilting must have originated at the end of Tawallah times. Consequently normal faulting and associated block rotation was probably initiated on the Rosie Fault, and to a lesser extent the Lorella Fault, at about this time. It should be noticed that the crust has been pulled apart by 8 km between the western end of the cross-section and the Emu Fault, or 16% extension (it now measures 56 km). The predominance of normal or block faults, and the lack of folds of thrusts would generally support an extension of about this order.

The final part of the section from the Emu Fault zone to the end (56km - 66km) shows open folds and high angle reverse faults in McArthur Group sediments, suggesting that the fault zone had suffered compression as well as subsidence during part of its long history; however, since the Emu Fault is not the subject of this report, no further discussion is warranted.

Section line B-B' (Warrapirrmantila Dome)

A cross section across the Warrapirrmantila Dome reveals that there is a gentle anticline in the Masterton Sandstone due to post-McArthur NE-SW compression. On the south side of the dome the Tawallah Group is dragged up into a pre-McArthur aged arch, or fault-bound horst (Fig. 7). A simplified plan view of the dome shows that the interpreted trace of the tops of individual beds on the base of Pms is asymmetric with respect to the present dome. The symmetry can be partially restored if the Tawallah Group are tilted *towards the southwest*, implying that the block originally was tilted towards the northeast. The cross section (B-B') also reveals that the Masterton Sandstone is thicker on the southwestern side of the dome, suggesting that this feature, or the faulted SW edge of the dome, may have persisted through to McArthur Group times as a weak topographic high or a persistent hinge line favouring thicker sedimentation to the southwest.

Regional Tilting

The mapped positions of the tops of units in the Tawallah Group below the Masterton unconformity surface have been recorded on a plan (Fig. 8). These positions are known in space and therefore, given a reasonable estimate of the stratigraphic separation, it is possible to calculate the angle of tilt of the block prior to deposition of the Masterton. This has been done in two places: firstly, in the Lorella-Rosie Fault block and secondly, in the Rosie Fault block. In the former, a gentle and uniform tilt of 1 & 1/4 degree towards the NE has been calculated over a distance of 25 km between points X and X' (Fig. 8). Here the stratigraphic separation between the top of the Aquarium Formation and the top of the Wuraliwuntya Member is here assumed to be 400 m. The point to note is that the top of Ptn has been picked up twice and that the line joining the two points has a trend which is perpendicular to the edges of the fault block; thus the line X-X' which parallels the faults approximates to the true dip of the tilt block. The second example is about 15 km east of the Rosie Fault where a tilt angle of 3 & 1/4 degrees was measured between points Y and Y' which are set 5 km apart. The stratigraphic thickness between the top of Ptn and the top of Pto1 is assumed to be 285 m. The line joining equal stratigraphic levels on the unconformity surface cannot be drawn with the same degree of confidence as with the first example; nearby outcrops of the unconformity, however, constrain the trend to approximately NNW, indicating that the true angle would be about twice the apparent tilt angle of 5-6 degrees.

Faulting

The map shown as Figure 8 is a representation of the geology as it would have been immediately prior to the laying down of the Masterton Sandstone. It is therefore a snap shot in time during the evolution of the McArthur Basin; it shows which units were exposed, either sub-aequously or sub-aerially, at the end of Tawallah times. The most

striking feature about this map is the nature and variety of units exposed at the time and their relationships to the faults; the units range in age from the Sly Creek sandstone to the Wollogorang Formation, a total stratigraphic separation of 800-1000m. The following points emerge from this map:

1. The greatest amount of uplift, i.e. where the deepest parts of the Tawallah stratigraphy are exposed, occurs in the central, western and northwestern parts of the area. The least amount occurs in the southeast where Pto1, Pto2 and the Warramana Sandstone are preserved beneath the Masterton unconformity.

2. Maximum differential uplift is recorded across the Four Archers, Tawallah, Hermit and Lorella Faults, all of which are deduced to have been active during the Tawallah.

3. Maximum uplift occurred in two regions, one associated with the northern end of the Tawallah Fault and the other with the Four Archers Fault. In the first case, the Warrapirrmantila Dome is a ductile tip zone developed at the northern end of the Tawallah Fault which has exposed the Sly Creek Sandstone at its core. A subsidiary high some 10 km to the south exposed down as far as the Rosie Creek Sandstone. In the second case a large amount of uplift occurred at the northern end of the Four Archers Fault, where it swings into a northwesterly trend and disappears (or dies?) under recent cover.

4. A N-S trending ridge, or axis high, occurs west of and parallel to the Tawallah Fault. This ridge runs for 20 km and connects the high in the Warrapirrmantila Dome with the subsidiary uplift at the intersection with the Lorella Fault referred to above. It also may connect with a zone of secondary uplift at the southern end of the Lorella Fault, in which Ptnw is seen to be absent; this could indicate that this region was high enough at the time so as not to allow the Wuriliwuntya to deposit.

5. The Tawallah-Rosie Fault Block was tilted 1 & 1/4 degrees towards the north. For this number to have much meaning, it has to be assumed that the all the units were laid down in layer cake fashion and that none were missing or markedly thinned during this process. This may, in fact, not be a valid assumption (see point 4 above).

6. Masterton sits directly on Sly Creek Sandstone east of the Four Archers Fault at its northern end. The presence of a small pocket of Settlement Creek volcanics on the western side of the fault at this locality is extremely significant (see Mantungula 1:100,000 map sheet), because it means that the Masterton Sandstone, which is mapped as resting on Settlement Creek some12 km to the south within the Limmen-Four Archers Fault block, must rest on Settlement Creek or a stratigraphically higher unit. This indicates that the Four Archers Fault had been active during the Tawallah.

Summary

The Lorella and Hermit Faults were active during the Tawallah event. An uplifted horst situated between the Hermit and Lorella Faults caused considerable erosion of Tawallah Group sediments prior to the deposition of the Masterton Sandstone. Similar uplift and erosion occurred along the Rosie Fault. A series of fault blocks, e.g. the Hermit-Lorella, Lorella-Rosie and Rosie-Emu Fault blocks, were tilted towards the NE or E along a series of steeply dipping faults prior to McArthur times. The positions of stratigraphic time lines (or points) on the Masterton unconformity are different within each fault block, suggesting that they suffered different amounts of tilting and uplift.

MALLAPUNYAH AND KIANA DOMES (with a contribution from J. Rogers)

Mallapunyah Fault

Five separate localities along a three kilometre section of the Mallapunyah Fault were analysed in the northern part of the Mallapunyah Dome. The following data was obtained: fault striae, rare overprinting relationships and the stress fields inferred from the multitude of minor faults and shears. The data has been looked at from two points of view, firstly, as a study of the different styles of movement which are possible along a single fault plane (Mallapunyah Fault), and secondly, as a treatment of the local and regional stresses developed around the convergence of two first-order faults in the southern McArthur Basin (Tawallah and Mallapunyah Faults) (Fig. 9).

At the far northwestern end of the secton studied, close to the Mallapunyah Springs homestead (loc. 45/93), a prominent scarp of Masterton Sandstone sits against Mallapunyah Formation, the latter having been dropped down to the southwest by movement along the fault. The movement observed here is normal with a large dip-slip component on moderately to flatly SW-dipping fault surfaces (Fig. 10). Hematite staining and/or coatings on quartz arenite breccia fragments are relatively common

Fig. 7 Cross-sections A-A' (Hermit Fault to the Emu Fault) & B-B' across the Warrapirrmantila Dome. The data is from Rawlings et al.(1993) and Leaman, 1992).

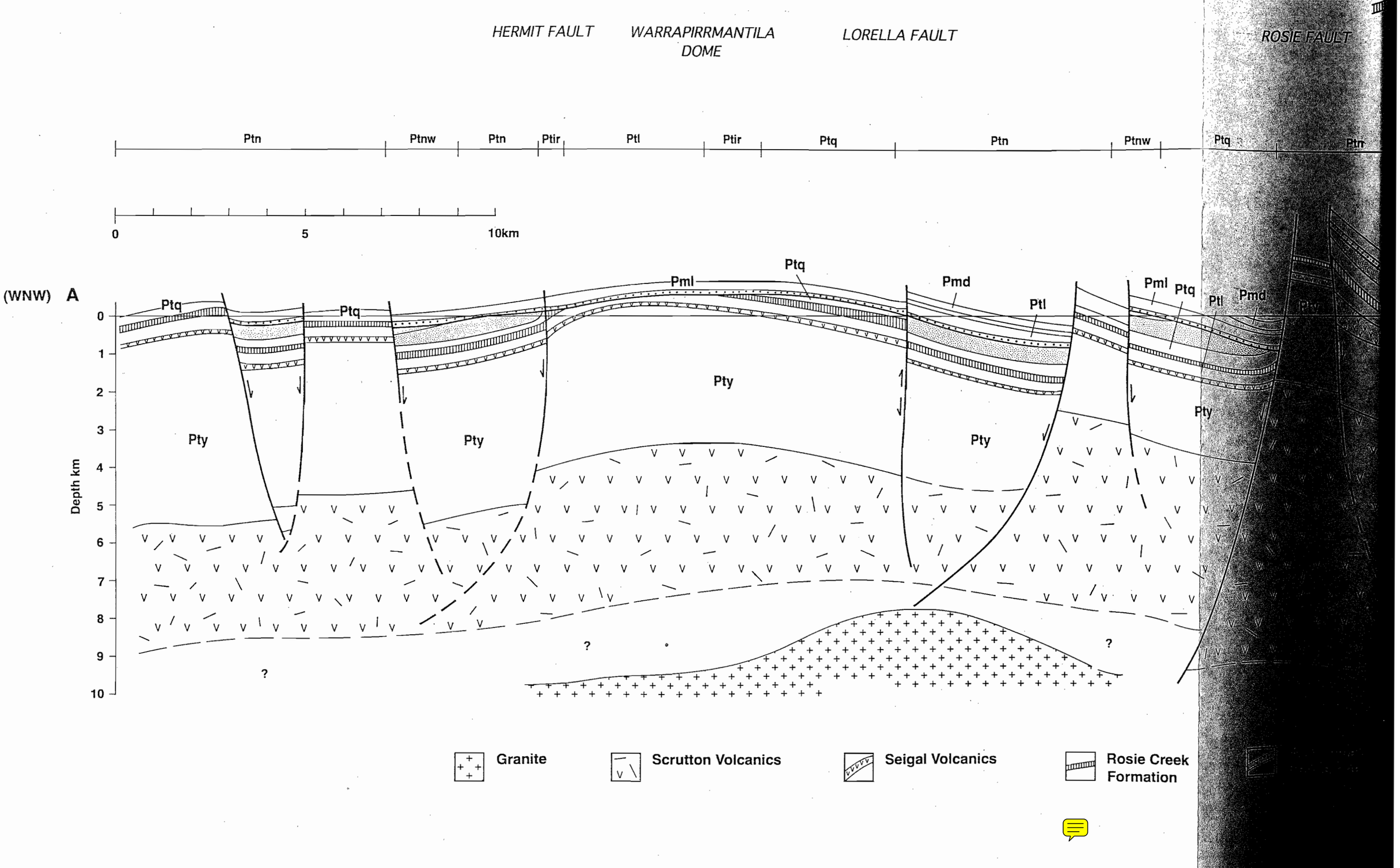

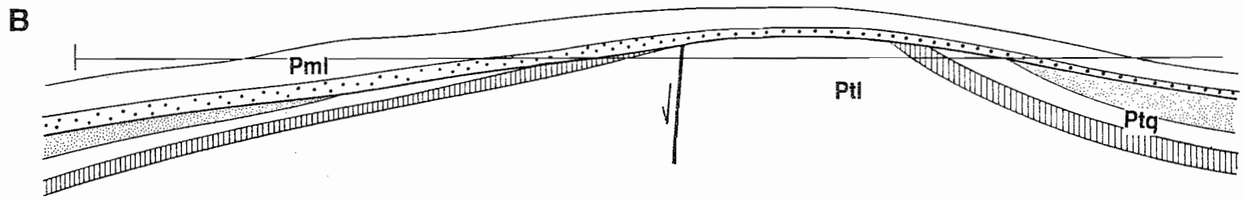

ROSIE FAULT

EMU FAULT ZONE

Ptq | Ptn | Ptnw | Pte | Pt01 | Pt02 | Ptm

Tawallah Units exposed on pre-Masterton surface

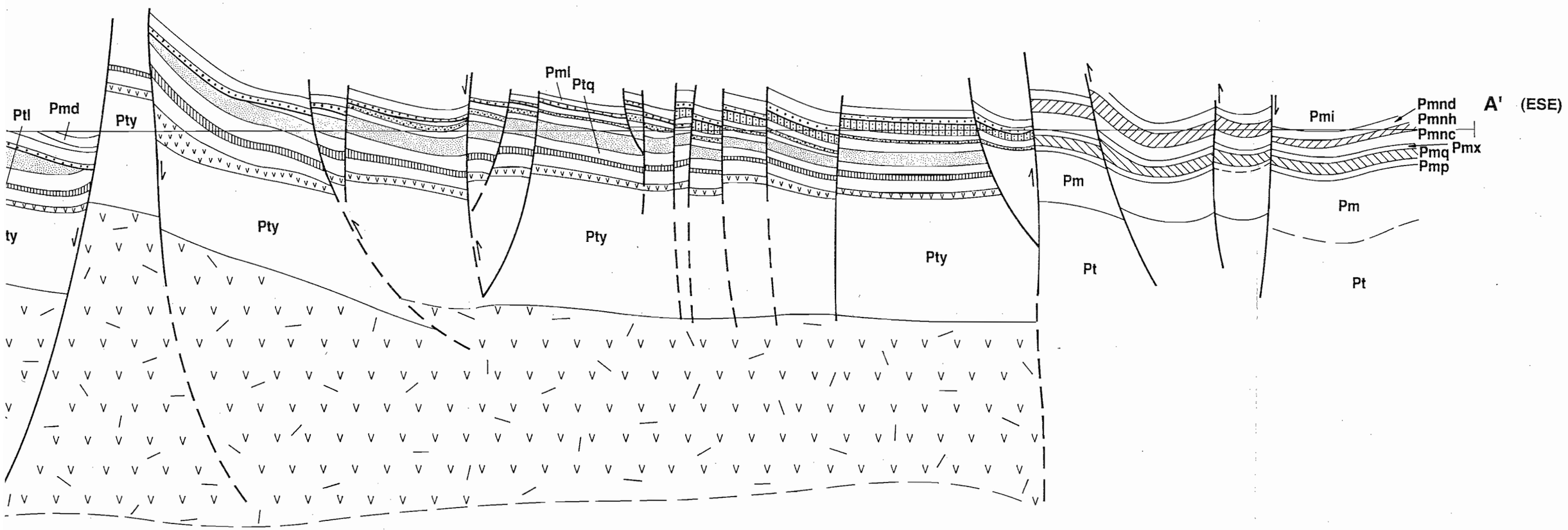

Wununmantyala Sandstone

Settlement Creek Volcanics

Warramana Sandstone

Barney Creek Formation

Hot Spring Member

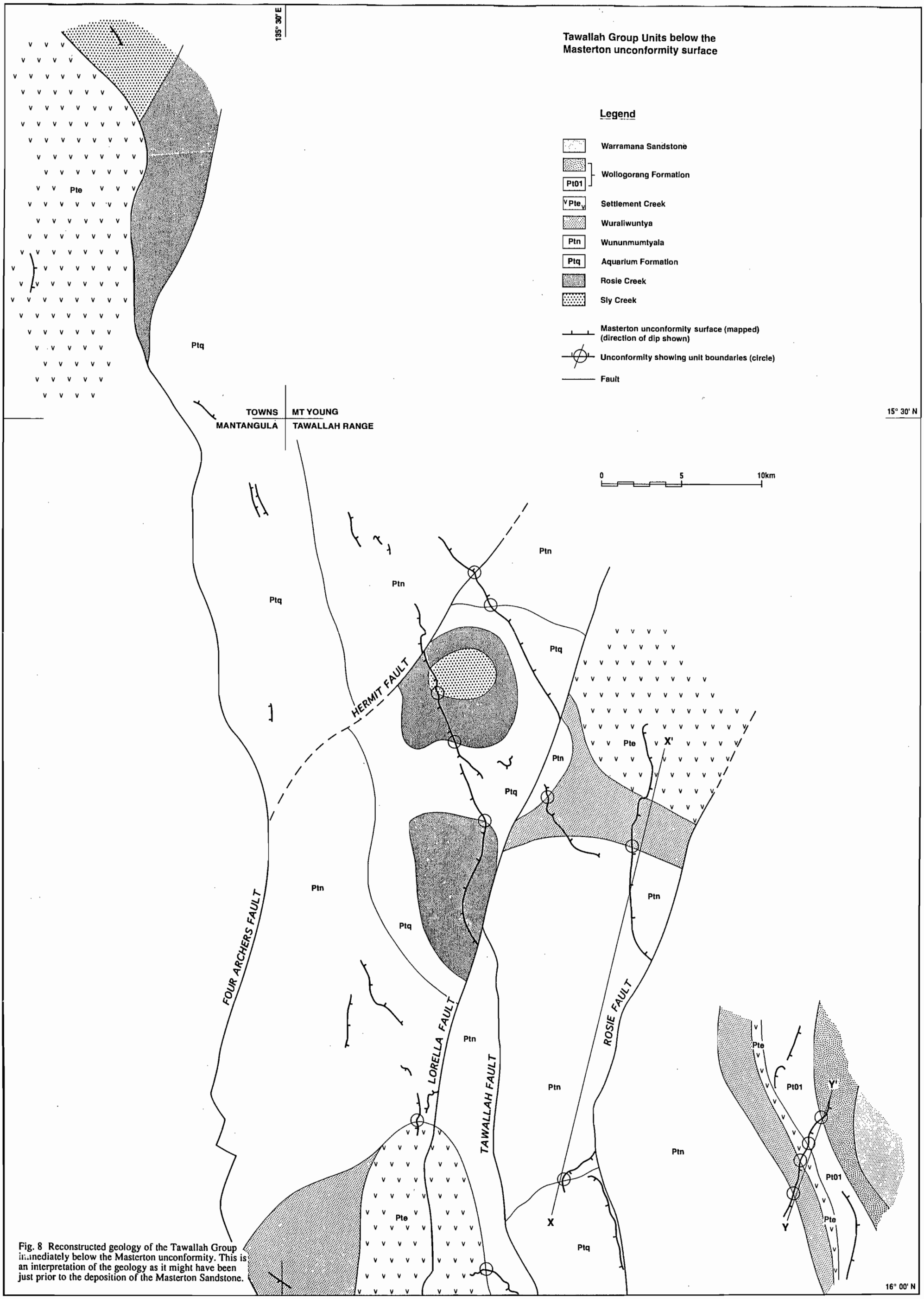

Fig. 8 Reconstructed geology of the Tawallah Group immediately below the Masterton unconformity. This is an interpretation of the geology as it might have been just prior to the deposition of the Masterton Sandstone.

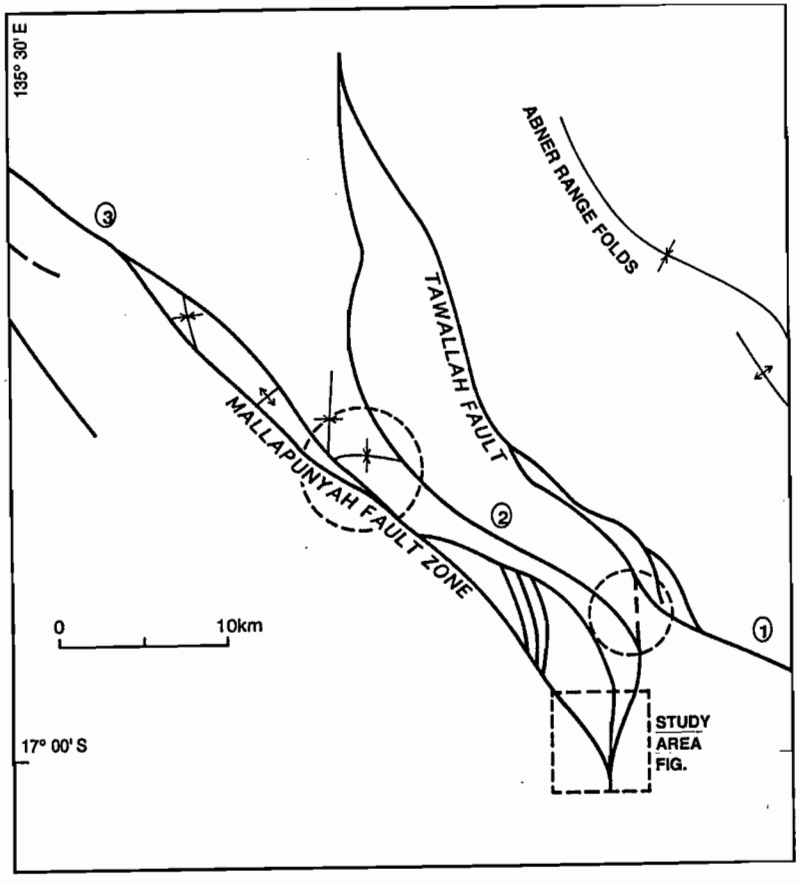

Fig. 9 Locality diagram for northern Mallapunyah Dome. The Mallapunyah Fault Zone comprises a series of left-stepping faults trending in a WNW direction (individual elements are numbered 1-3) . The two circles mark the positions of maximum overstep or overlap. The E-W and N-S trending folds in the circle at the centre of the diagram would support both sinsitral and dextral phases of strike-slip movement along the fault; the elongate fault slice along segment 3 indicates contraction took place along the length of the fault here. Abner Range folds indicate one of the Post-Roper compressions (NE-SW).

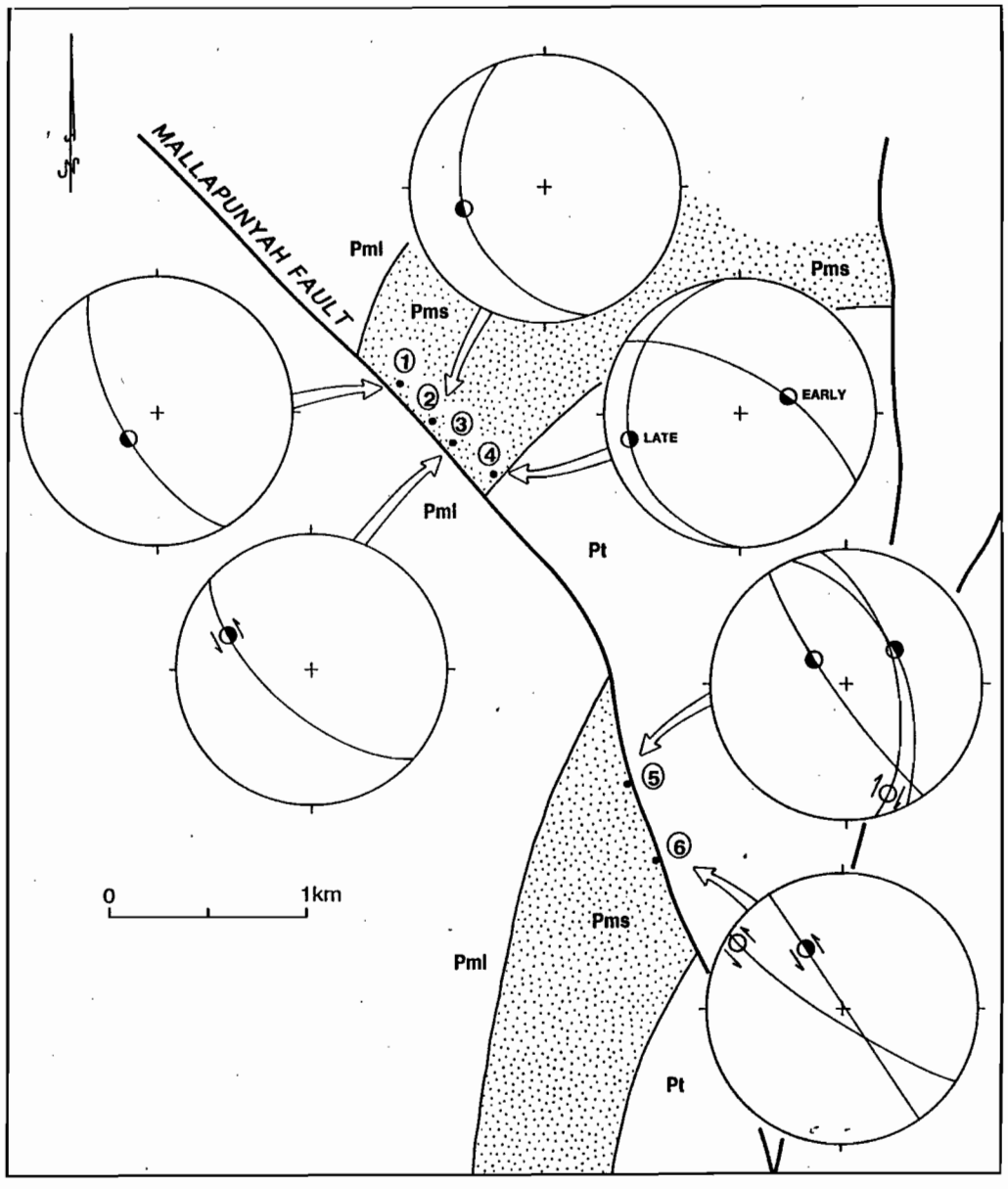

Fig. 10 The Mallapunyah Fault at Mallapunyah Springs. The fault plane was studied at six localities. Only those faults that parallel the main fault are shown - the principal exception being the N-trending thrust at loc. 6. A number of movements have been recorded (sinistral-reverse, dextral, reverse and normal); however, the order in which some of these movements could have taken place can be deduced from the relative timings of the different local stress fields (see Fig. 11). For further discussion, see text.

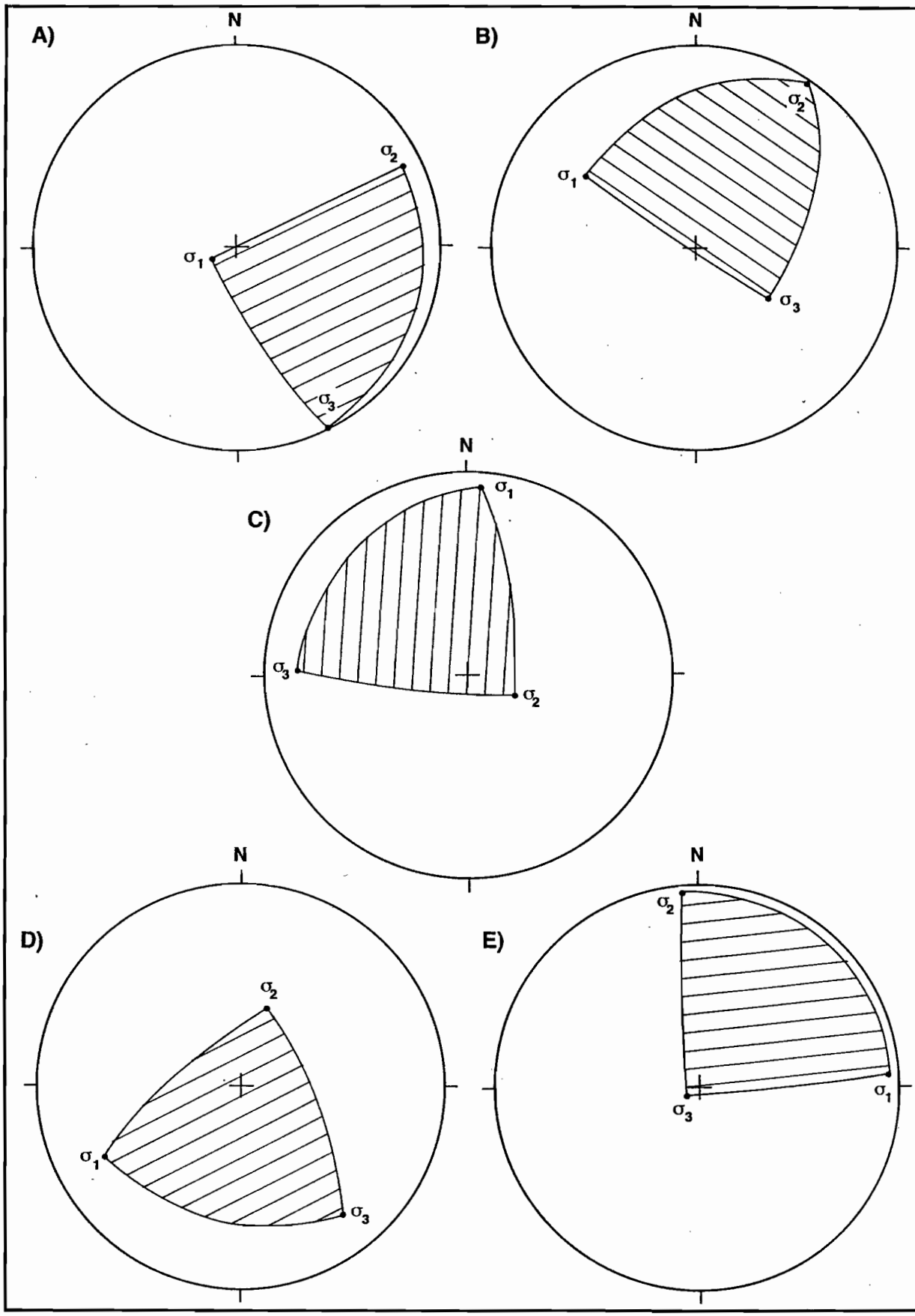

Fig. 11 Orientations of the three principal stresses for the northern Mallapunyah Dome, southern McArthur Basin. A & B represent an episode of normal faulting and a NW-SE compression that can be dated, at best, as post-Masterton Sandstone; C, D & E are N-S, NE-SW and E-W compression events the last two of which aredue to the post-Roper Group inversion. For further explanation, see text.

features in the fault zone at this locality; for example, a pale grey to greeny siliceous matrix, whose abundant quartz veins are clearly replaceive and not dilational in origin, is present in the fault zone here; locally, quartz crystal terminations are also to be seen in the open, drusy cavities that are present.

The SW-dipping minor fault surfaces along the remainder of this scarp have been activated as reverse faults, or small-scale thrusts, during a NE-SW to E-W compression event. Where timing relationships can be observed, the thrusts are themselves cut by ENE trending sinistral and dextral wrench faults and where thrusts cut each other (locs. 46-7/92), the SW-directed thrusts are earlier than the E-directed thrusts.

The southern fault scarp separates Masterton sandstone to the west from Wununmantyala Sandstone to the east, implying that the east block had moved up relative to the west block, or if only strike-slip movements had taken place, the east block had moved north. A detailed analysis of striations at two localities along this scarp (locs.10 & 23/92), whilst finding good evidence for movements along the main fault surface itself, as opposed to the secondary fault surfaces, only one out of a total of four movements can adequately explain the actual juxtaposition of stratigraphic units observed. This movement is east block up on a steeply W-dipping fault surface. The remaining movements are either dextral strike-slip or normal movements with east block down movement, neither of which can explain the observed juxtaposition of units; further, the one example of a sinistral movement has a significant oblique component to it which involves east block down movement, which again is not capable of providing the required offsets.

Folding

Folding is of two types: firstly, open to occasionally close folds developed in beds adjacent to the Mallapunyah Fault, and secondly, broad open folds which occur up to several hundreds of metres away from any particular fault surface. The first type is generally restricted to the fault itself and may involve all lithologies that happen to be caught up in the faulting process: an example of folding in potash altered flow banded rhyolites or sediments of the Wollogorang Formation shows minor thrusts breaking through a fold developed in the primary banding. In another example, a N-trending fracture cleavage is axial planar to minor parasitic folds in sandstone beds within a well defined slice of fault rock along the fault (so-called because the stratigraphic position of this unit is not able to be determined with any degree of confidence because of a lack of top and bottom stratigraphic reference beds).

The second type of folding trends E-W and is gentle in style. Folds of this type have been observed on the western slopes of the Masterton Sandstone ridge to the south and have also been mapped at the extreme southern termination of the Mallapunyah Fault (Wright, 1993).

Stress inversion technique

By selecting only those faults that appear to be related to a particular stress field it has been possible to find at least two, and possibly three, realistic stress fields from 5 stress states (Fig. 11). The fault striation data were first sorted into three groups based on a feel for the kind of stress states they might be related to (i.e. N-S, E-W compression etc.) and the programme (Etchecopar et al.,1981) was used to calculate stress tensors, as well as the orientations of the three principal stresses. The results proved that high levels of confidence could be attached to most of the stress states associated with these initial groups. The remaining fault data (i.e. those rejected during minimisation of the data at 65-70% during the three runs) were then collected together and run separately producing to produce a fourth stress state, which naturally had a lower level of confidence attached to it, but nevertheless, produced a realistic answer at 80% of the samples.

The results presented here demonstrate that at least five different stress states existed during basin subsidence and compression: a N-S compression associated with wrench faulting (Fig 11C), a NE-SW compression also associated with wrench faulting (Fig. 11D), and an E-W compressive stress regime associated with thrusts, whereby the tectonic escape or extension direction was vertical (Fig. 11E). Fourth and fifth stress states associated with extension (in which sigma 1 was steeply plunging) can also be shown to have existed (Fig. 11A & B).

Timing relationships observed in the field suggest that the three compressive stress states developed in a particular order: N-S, NE-SW and E-W. This implies, at least within this compression, that sigma 1 intermittently rotated in a clockwise sense from a northerly to an easterly direction, as the tectonic regime changed from wrench to compression. The normal faulting has not been dated with respect to any of the compressive stress regimes, therefore, in the following descriptions it is placed at the end, although this should not be seen as implying that this was actually the case.

N-S compression

The first of the known stress states was a sub-horizontal N-S compression with sigma 2 plunging

steeply (70/116) which is consistent with a wrench regime. This result was produced from 13 data out of a total of 18, and a stress ratio of 0.23 was obtained (Fig. 11C). The most obvious expression of such a stress field is to be found in the dextral wrench movements on the WNW trending Mallapunyah Fault.

NE-SW compression

The second known stress state was a NE-SW compression in which sigma 1 had a flat southwesterly plunge (25/242), whilst sigma 2 had a somewhat intermediate plunge value (57/019) which could be interpreted as being a wrench regime (Fig. 11D). The fault striae for localities 1,2 & 3, at the northwestern end of the Mallapunyah Fault (Fig. 10) which was studied in some detail but which was not part of the original data set (17 fault striae), were run separately and the results showed that it is not always possible to resolve sigma 2 & 3 on the stereonet whose points spread out evenly along a girdle; however, the position of sigma 1 in this case was the same, illustrating that the latter was stable but that the tectonic regime flipped from wrench to compression, and vice versa. This stress field had been responsible for the dextral strike slip offsets on the N-S trending Tawallah, and its associated faults, at the northern end of the Mallapunyah Dome.

E-W compression

This, the third known stress field, was by the far the most stable of the three. Sigma 1 (5/086), sigma 2(3/356) and sigma 3 (85/234) produced an almost perfectly symmetrical orthogonal distribution on the stereonet (Fig.11E). The stress ratio is 0.23. This compression results from the convergence of the Tawallah and Mallapunyah Faults with the result that the tectonic escape direction (i.e. sigma 3) was upwards. Detailed observations in the field have shown that there was an initial W-directed thrusting event which was superceded by a later E-directed thrusting.

Normal faulting

The fourth, but not necessarily final, stress state is an extensional stress regime in which sigma 1 is steeply (although not necessarily vertically) plunging. Two sets of data gave large plunge differences in sigma 1 (i.e. 36 & 80); however, in both cases, sigma 3 was oriented NW-SE and sigma 2 was oriented NE-SW (Fig. 11A & B). This solution fails to explain the normal fault movements observed on the NW-trending Mallapunyah Fault, but suggests instead that there should be normal faults trending in a NE, or an ENE direction which have not yet been observed. This illustrates one of the problems with this programme, namely, that at low population densities within multi-stress state situations, the results can be highly erratic whereby the orientations of stress diections can flip with minimal change to the input data. As a consequence, this data should be regarded with some caution; more work is required to resolve this particular problem.

Kiana Dome

The Kiana Dome, situated at the southern end of the McArthur Basin, is an inlier of Middle Proterozoic rocks surrounded by Cambrian limestones (Fig. 12). The exposed sequences range from the McDermott Formation at the base to the Tooganinnie Sandstone Formation at the top (Jackson et al., 1987). However, the recent decision by NTGS workers to map the McDermott Formation on the Abner Range sheet as being the equivalent of the Aquarium Formation in the McArthur River Region (Pietsch et al.,1993), the main sandstone unit which underlies the Settlement Creek Volcanics, originally mapped as the Sly Creek Sandstone, is in fact Wununmantyala Sandstone. This led Keele & Rogers (1992) to an incorrect preliminary interpretation (map in supplement to report No.1) that the Mallapunyah Formation was present in a down-faulted E-W block within the northern Mallapunyah Dome area; this outcrop, in fact, belongs the Wollogorang Formation and indicates that the structure here is much simpler than was originally thought and does not involve early E-W normal faulting.

Structural information was gathered from a traverse across the dome, and the existing geological maps. The following structures were observed on the ground: shallowly plunging folds in bedding, a weak rare axial plane cleavage, strike-slip wrench faulting, hematite-silica breccias, minor quartz veining and massive fractured & intensely potash-altered volcanics with minor coarse grained quartz. Limited time available for this traverse prevented the gathering of sufficient data for a statistical analysis of fault striae data; however, the stress orientations for each event have been estimated using a combination of fold, fault and vein data. In this way a qualitative picture of the stress fields during deformation has been built up.

Folding

A series of fold trends (NE-SW, NW-SE and N-S) can be identified in the area. The NW-SE set has a rare weak axial planar fracture cleavage associated with it. The earliest folding comprises a NE-trending anticline-syncline pair developed in the

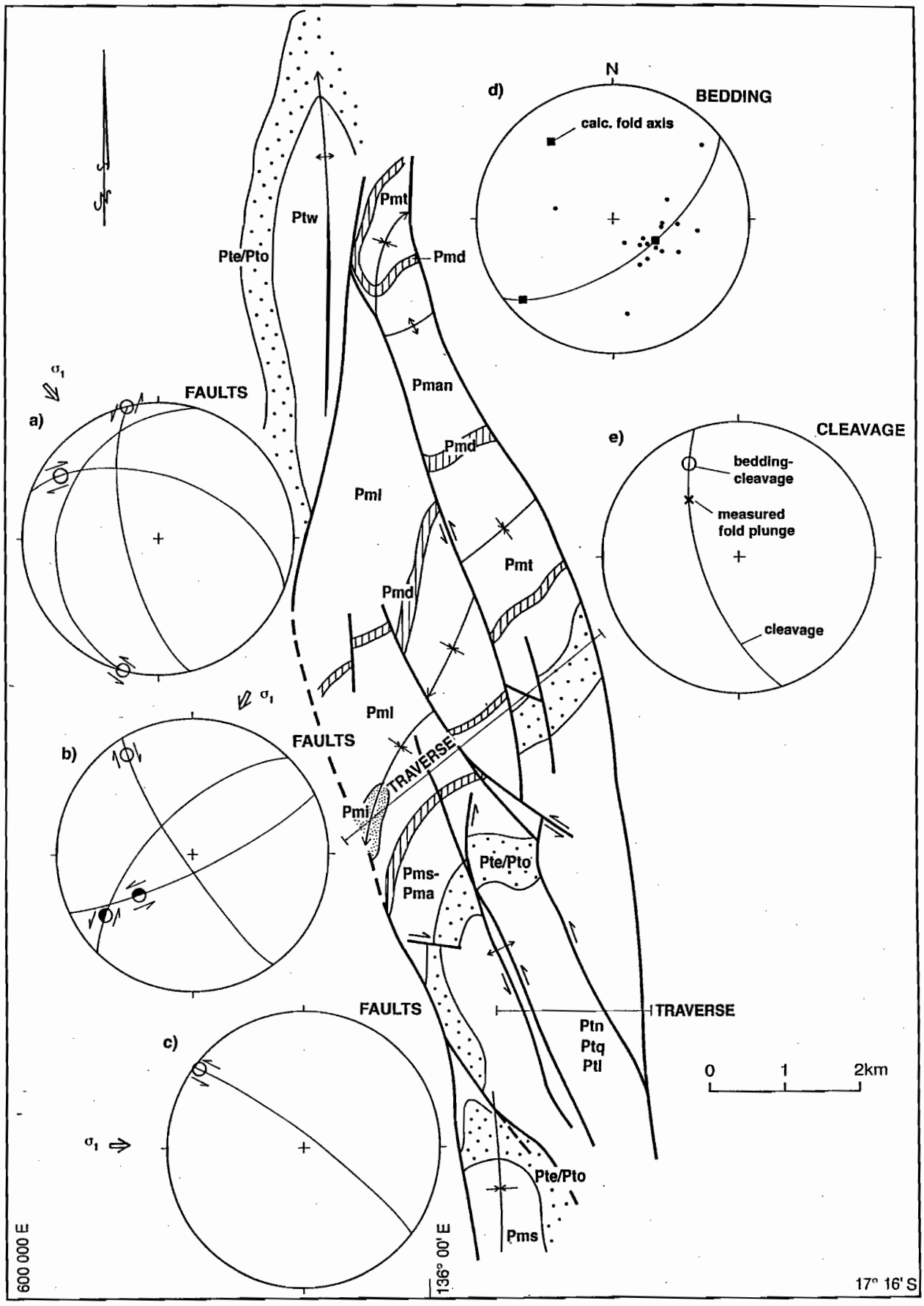

Fig. 12 Main structural elements of the Kiana Dome, southern McArthur Basin (from Jackson et al.,1987). The stereonets (a), (b) & (c) represent inferred principal stress directions based on overprinting relationships of macroscopic and mesoscopic structures (sigma 1 only shown). Faults are shown in relation to the stress fields suggested by the fold trends. Note the similarities of the orientation and timing of the stress fields here with those at the Mallapunyah Dome (Fig. 11). Stereonets (d) & (e) are plots of the poles to bedding, and cleavage-bedding intersection and fold plunges respectively.

McArthur Group sediments in the central and northern parts of the dome; these open folds have a half wavelength of approximately 3.5 km (Fig. 12). The second folding event which refolds this earlier fold set, consists of a single, shallow NW-plunging fold about 2 km across; it may have weak axial plane cleavage associated with it because small-scale folds in the purple to grey siltstones of the Wollogorang Formation have a fracture cleavage dipping moderately to steeply W, with a bedding-cleavage intersection that has a similar plunge to the pi-pole defined by bedding on the stereonet (Fig. 12). The third period of folding is represented by a single N-S trending anticline in the Tawallah Group at the north and south ends of the exposed dome; this fold is offset in a left-lateral sense along faults related to the E-W compression. Thus whilst there is no direct evidence for overprinting of the two earlier fold sets by this one, the main NW-SE folding is offset by faults related to an E-W compression.

Faulting

With one exception the measured faults all have strike-slip movements on them (Fig. 12). The lack of any measured thrusts is probably due to the small size of sample taken, given their general occurrence in the nearby Mallapunyah Dome and Freida Fault areas (J.Wright, 1993; S. Donovan,1993).

The main set of sinisitral strike-slip faults trend NNW-SSE through the inlier and are apparently related to, but slightly post-date, the main period of NW-trending post-Roper folding. A average displacement of1 km (range between 0.5 and1.5 km) is inferred on one such fault that can be traced for a distance of15 km through the inlier. This particular fault is offset in turn, by a WNW sinisitral strike-slip fault which has a smaller recorded movement of approximately 200-300 metres on it.

Quartz veins

In general the quartz vein data is too sparse to be of much use; however, a critical timing relationship was observed in one particular fault zone (loc.KD40/93), where a dominant set of NW-SE trending quartz veins is cut by a fracture direction with minor quartz veining that has an azimuth of 100 degrees. This indicates, assuming the veins are extensional in origin, that the sub E-W compression post-dated the principal NW-SE compression related to the large-scale folding.

Summary

Four distinct movements are recorded on the Mallapunyah Fault (dip-slip normal, dip-slip reverse, oblique sinistral/reverse, and dextral strike-slip) resulting from at least two stress fields. After an initial period of extension along NE-SW trending axes, the main period of crustal compression involved a stable, regional stress field with sigma 1 oriented NE-SW, which resolved itself into into two transient local stress fields directed N-S & E-W.

The Kiana Dome experienced three discrete deformation events: NW-SE, NE-SW and E-W crustal compressions in that order, each being accompanied by a phase of wrenching. The first compression was in part post-McArthur Group in age, and may have been timed at end-Umbolooga Sub-group times; the NE-SW compression was clearly related to the post-Roper inversion, whilst the E-W compression, the latest of the three, may have been a reactivation of earlier structures which had been active in the Tawallah (Rogers, this volume).

DISCUSSION AND CONCLUSIONS

Correlating deformation events

In the southern part of the basin, at least three discrete deformation events are correlatable over a distance of several tens of kms. Two of the stress states in the Mallapunyah Dome can be correlated with deformations in the Kiana Dome, some 35 km to the SE. The principal stresses vary from N-S, through to NE-SW to E-W in that order at Mallapunyah; a similar NW-SE, NE-SW and E-W sequence of stress re-orientations has been recorded at Kiana. It is concluded that both areas had suffered similar compressions in which sigma 1 had intermittently and progressively changed direction in a clockwise sense. The two latest stresses (NE-SW & E-W compression) are common to both areas and are therefore considered identical events. This sequence of early E-W open folds in the McArthur Group sediments transected by later NW-trending folds is present at Coppermine Creek and in the vicinity of the HYC deposit. In the latter a shallowly W-plunging gentle E-W fold some 15 kilometres across, defined principally by the Pnmh/Pmnc boundary, is over overprinted by smaller wavelength NW-SE trending folds which maintain a general "S" sense of vergence on both limbs of the larger fold.

In the Mallapunyah Dome, a change in orientation of the intermediate stress (sigma 2) from vertical to horizontal, between the N-S and E-W compression, signifies a local change from strike-slip to compression with time.This is consistent with dextral strike-slip movements on the Mallapunyah and Tawallah Faults and compression

developing in the area of convergence where they meet, especially along the latter (Wright, 1993). An intermediate stage, in which sigma 2 and sigma 3 are interchangeable, during NE-SW compression has been recognised. Therefore, all we can say with certainty of the NW-SE & N-S compressions in the southern region of the Mc Arthur Basin is that they are post-Emmarugga Dolomite in age, this being the age of the youngest unit involved in the folding at Kiana. By analogy with structures in the Abner Range and in the vicinity of the Four Archers Fault, the NE-SW and E-W compressions are post-Roper in age.

Inversion, block tilting or uplift?

The section line A-A', as drawn in Fig. 7, gives us an approximate 15% extension for the main part of the section up to the Emu Fault Zone (i.e. the original length of a typical unit in the Tawallah Group was 48 km whereas now it is 56 km) and begs the question: is this due to extension alone or is it due to a combination of extension and contraction? The fault structures on the section that can be construed as contractional are very few in number and quite limited in what they could have achieved in terms of overall shortening; indeed as has already been pointed out, the only significant contraction occurs within the Emu Fault Zone itself, where folding and high-angle reverse faults can be inferred (Fig.7). From this it is possible to conclude that the contraction noted by Rogers (1993,this volume) in the Scrutton and southern Tawallah Ranges, may be absent here or at least only have a minimum of expression. It is accepted that some of the faults could have been drawn with their dips the other way, which could have a dramatic effect on line lengths of units, thus affecting the overall shortening and/or extension ratio. However, the situation changes to the west along section C-C' (Fig. 2), where the Four Archers and Limmen Faults have been interpreted as thrust faults. The Limmen Fault is unusual because like the Lorella Fault to the east, it defines a broad antiformal structure with the regional dips being away from the fault; this may be due to the post-Roper E-W compression which not only accounts for the change in dip, but also accounts for the thrusting of Tawallah against Nathan and McArthur against Roper Groups, or it may be due to original block tilting. The extent to which this episode of thrusting is a reactivation of the mid-Tawallah thrusts will be the subject of further work.

The area east of the Lorella Fault has a distinct geometric pattern of its own, in that the units below the Masterton unconformity all have a consistent regional tilt. The Rosie-Lorella-Tawallah fault block is the more poorly constrained of the two tilt blocks, because there are only three known unit boundaries mapped below the unconformity surface (circles on fig. 8); if the western one is ignored (it does in fact lie close to a splay off the Lorella Fault) then a series of alternative boundaries could be drawn which have a more northerly, or north-northwesterly strike, similar to block to the east. The 1 & 1/4 degrees calculated as a tilt becomes in the order of 3-5 degrees, a more reasonable value in terms of block rotation due to extension. The (5 degree) eastward tilt of the Rosie-Emu fault block, however, would suggest that the Rosie Fault had acted as a listric normal fault during crustal extension and dipped to the west (see cross-section, fig. 7).

A model for this style of crustal extension is given in Fig.13 (after Wernicke, 1985), in which the Rosie Fault and others would lie at the limit of significant upper crustal extension, i.e. in the "discrepant zone", where tectonic subsidence is replaced by tectonic uplift as a result of normal simple shear of continental lithosphere (Wernicke, 1985). Much of the uplift recorded in the stratigraphic column would imply, according to this model, a thinned mantle under this region (just as the opposite, a thinned crust, implies tectonic subsidence) and a shallow east-dipping normal fault at the base of the crust. The tectonic and sedimentological implications are interesting because as Ingersoll (1988) states " tilt blocks/half grabens are common in the ancient record, but it is not clear how many of them represent primarily high-angle faulting, listric faulting or low-angle detachment faulting." However, what is certain is that coarse grained facies would be small in volume and form adjacent to footwall uplands, whilst fine grained facies would be more extensive and relate to hangingwall dip slopes (Leeder and Gawthorpe, 1987). This might imply that the Tawallah Group is the pre-rift sequence, the basal Masterton (or Nyanantu) the syn-rift fill and the Masterton the post-rift phase of sedimentation in a true rifting event (Bull, pers. comm. 1993).

The extent to which the Lorella Fault acted in concert with the Rosie Fault during this event is not known; the sequences along the Lorella Fault indicate E block down rather than up, suggesting that the Lorella-Rosie Fault block may in fact have behaved differently to its neighbour, i.e. uplift rather extension dominated here. If such a model were applicable then there would had have to have been an area to the west which at one time involved considerable amounts of crustal thinning (for the McArthur Basin that is) where both thermal and tectonic subsidence occurred together; such an area might lie under the present Roper basin to the west, or to the SW of the Kiana Ridge (Plumb et al., 1980). The Four Archers Fault could also be interpreted to be the western bounding fault on an eastward tilt

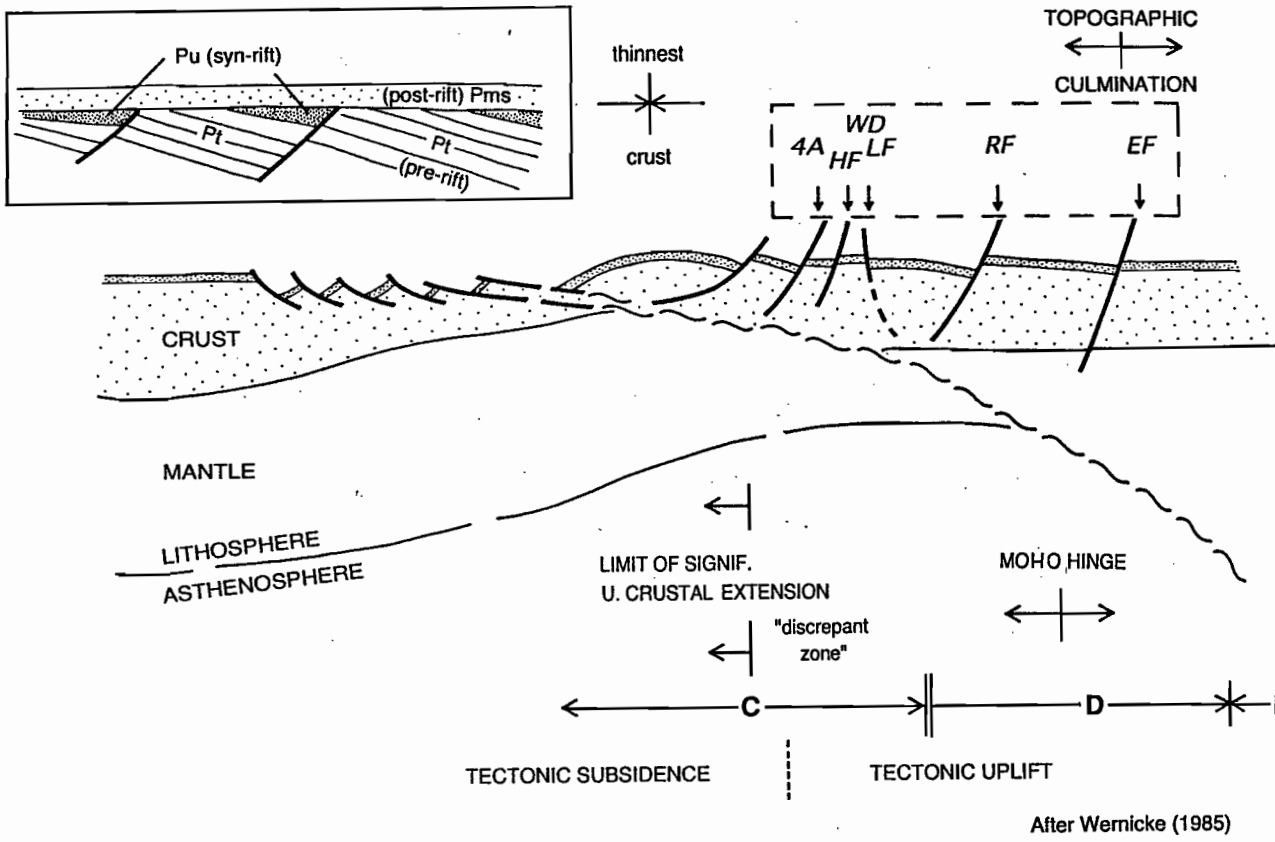

Fig. 13 A possible way in which the uniform-sense simple normal shear model of Wernicke (1985) might apply to lithosphere extension in the McArthur basin during Tawallah times. The part which is relevent here is the under the dashed rectangle where the amount of crustal extension is small. Note that the antithetic nature of the Lorella Fault implies there is probably a component of pure shear which is not present in the model. Significantly higher extensions implied by the model may occur under the covered SW part of the basin. A diagram showing possible rift-related sedimentation at end-Tawallah times is shown in the inset.(4A=Four Archers Fault, HF=Hermit Fault, WD=Warrapirrmantila Dome, LF=Lorella Fault, RF=Rosie Fault & EF=Emu Fault). (Pu=Nyanantu, Pms=Masterton & Pt=Tawallah Group).

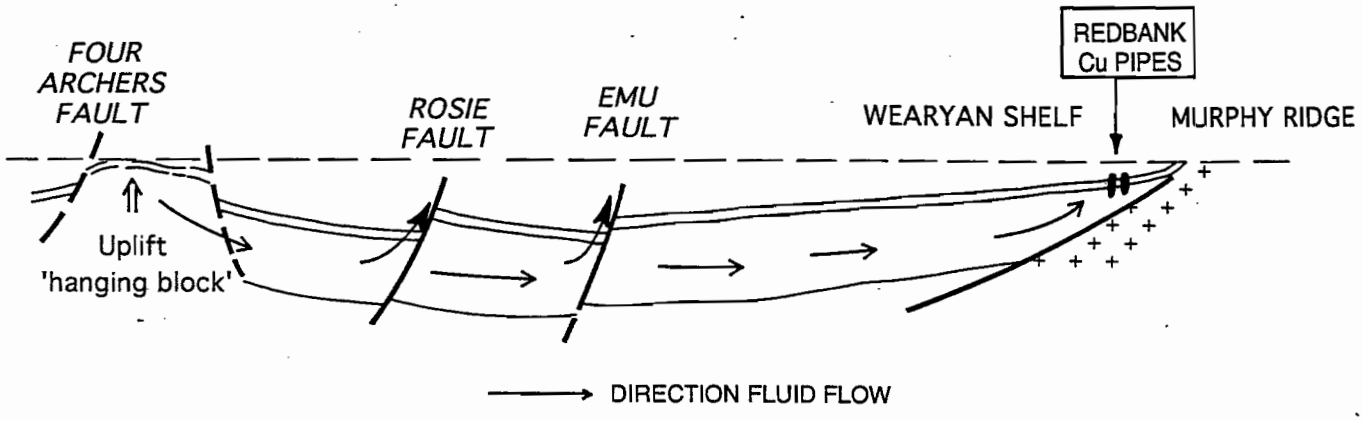

Fig. 14 A model for gravity-driven fluid flow (after Garven, 1985); such a pattern might have been established towards the end of the Tawallah. The fluids would be expected to flow eastwards away from the areas of uplift towards the edges of the basin. It is suggested that the fluids utilised the E-facing tilt block initially and then travelled along the very low gradients on the Wearyan platform, to be expelled near the Murphy Ridge. Depending on whether the Rosie and Emu Faults had been permeable or impermeable to fluid flow, these faults may have acted as short circuits for the fluids, in which case most, but not necessarily all, of the expelled fluids could have contributed to the Redbank Cu-pipes.

block (Fig. 8), although evidence for this, other than through uplift, is somewhat lacking. The cross-section in Fig. 2, unfortunately suggests that the normal faults would have dipped the other way, i.e. to the east.

(The section drawn in Fig.7 does not properly illustrate the angular difference between the Tawallah and McArthur Groups because of the low angle between them (< 6 degrees); this can only properly be done if the section has a vertical exaggeration, something that will be done in subsequent presentations.)

Fluid flow and Cu deposits

Recent contributions to the literature describe a continental setting for copper mineralisation in which rifting played a significant role in the localisation of deposits. In one paper, Jowett (1987) states that the rift setting itself is the primary control on the location of Kupferschiefer-style deposits. The Cu-rich volcanics from the early rift phase provided the source for the metals, whilst the numerous syn-basin faults provided the pathways, and the reduced beds — where the oxidised fluids encountered reducing conditions for the first time in the basin — were the sites of metal deposition which formed during early or late diagenesis. Jowett further emphasises the importance of a second rifting event which involved further high heat flow and structuration and provided the means of focussing the ore fluids. However, the author is not too specific about the exact nature of this process and whether the unconformity surface itself influenced the mineralising event.

In a second paper Mauk et.al. (1992) went one step further at White Pine, Michigan and postulated a two-stage mineralising process, in which the first stage is a classic sediment-hosted stratiform deposit formed during early diagenesis, and the second stage is a deposit controlled by regional deformation processes such as thrust faults and strike-slip faults. In this logical progression of ideas metallic deposits in sedimentary basins are being linked to basin inversion, or to the closing up of the initial rift.

Two points of interest arise out of the above discussion both of which may have relevence to this study. The first is that the presence of an unconformity surface within a basin, implying uplift and erosion between initial and subsequent rifting phases, may be a crucial element in generating and focussing basinal fluids. The second is that the fluids are generally forcefully expelled during the closing up stage of the basin (Mauk et al.,1992).

The gravity-driven fluid flow model in sedimentary basins, where the fluids are suggested to flow down a sloping water table that approximates a subdued version of the topography (Garven 1985), is relevent to the McArthur Basin. This study has shown that the greatest uplift prior to the McArthur Group times, for whatever reason, (uplift or inversion) occurred between the Four Archers and Lorella Faults. This implies that one of the directions of fluid flow would have been towards the east at end-Tawallah times, i.e. towards what is now the Batten Trough (see also Bull 1993, this volume). An eastward tilt of the Rosie-Emu Fault block implies that basinal fluids would have migrated along the gently E-dipping strata until they encountered "short circuit" fault structures such as the Rosie or Emu Faults which could have caused discharge of fluids onto the basin floor. Alternatively, they may have migrated much greater distances eastwards until they were able to travel upwards along the gently W-dipping basal Tawallah units on the Wearyan Shelf, discharging into the sediments and volcanics of the upper Tawallah, immediately below the Nyanantu unconformity, in the vicinity of the Murphy Inlier (e.g. Redbank Cu; Ahmad & Wygralak, 1989). A simple model for fluid flow is given in Fig. 14.

The mineralisation at Coppermine Creek occurs along a fault which was active during the post-Roper compression. Faulting accompanied a NW-trending folding event which has an axial plane fracture cleavage associated with it and is interpeted to represent the highest metamorphic grade, or deepest crustal levels, yet attained by any preceding stage of compression in the McArthur Basin. The fluids associated with this event, therefore, would have circulated much more deeply and more widely through a greater range of rock types, than any fluid thus far in the history of the basin. The prospect lies at the southwestern end of a NE-trending ridge axis of thick buried mafic volcanics (Leaman, 1992), suggesting that the Coppermine Creek Fault may, in part, be a high-level reactivation of a deeply buried half-graben structure associated with the volcanics. A similar conclusion may be made about the Eastern Creek Pb-Ba prospect which lies at the southeastern end of a WNW-trending ridge axis, only in this case the deeper structure is reflected in a fault that transfers movement off the Four Archers Fault and on to other faults in the region.

Palaeostress analysis (inversion method)

The stress inversion method (Angelier, 1979, Etchecopar et al., 1981, Armijo et al., 1982) by which the palaeostress tensors are estimated from the measurement of fault striae in the field, has been applied with some success in the southern McArthur Basin. Much of this is probably due to the

fact that the style of deformation is brittle and that the assumptions used in the method, namely that the faulted rock mass comprises rigid blocks that interact without friction, the faults are planar and infinite in extent, displacements on the faults are small and independant of each other, the stress field is homogeneous and that there was little rotation of individual blocks etc, are generally valid. However, situations where the technique may be invalid, such as where stress perturbations around adjacent fault systems interact (small fault splays off the ends of large faults) or where strike-slip faults step across (Pollard et al.,1993), can be counteracted to a certain extent by having a large data set and by the presence of faults with several orientations (Dupin et al., 1993). However, the limitations of the method require some discussion.

The faults in the Mallapunyah area would, on the face of it, appear to provide reasonable grounds for invalidating the method, because the study was conducted at the confluence of two 1st-order structures, the Mallapunyah and Tawallah Faults. Here, the stress interaction would be expected to have been significant; for example, the left-stepping nature of the MFZ is clearly present (Fig. 9) with a number of different fold trends being present along it (E-W, N-S, NE-SW & NNW-SSE); this suggests that the local stresses need not necessarily reflect the far field stress. However, the main reason for studying this area in the first place was the greater number of faults present, thus this fact alone may go part way to negating this effect by having a large data set (Dupin et al., 1993). Another reason to be confident of the results is that a similar stress history can be inferred from the macroscopic patterns of folding and faulting at the nearby Kiana Dome.

The five stress states inferred to be present at the northern Mallapunyah Dome probably resulted from three stress fields (Fig.11). The first stress state (A & B) represents extension, with the second of these two (B) possibly being a reactivation of earlier structures giving an oblique stress field (Bott, 1959). The second main stress field is strike-slip (C) which passes into another oblique-slip system. The final state is a compression (E).

As far as the number of stress states is concerned, it is as well to note that this study compares favourably with a detailed study at the Hoover Dam site, Colorado by Angelier (1989), in which he was able to reproduce 8 stress states from 2 different stress fields. Most of the differences involved stress flips, principally between sigma 2/sigma 3 and sigma 1/sigma 2, i.e. changes in tectonic style from compression to strike-slip and from extension to strike-slip. The northern area in the McArthur Basin, which includes the Four Archers Fault and Coppermine Creek, can be interpreted to have been under the influence of at least two, and possibly three, directed stress fields (Fig. 6). The first is an extension in which the principal direction of pull apart changes from NE-SW to NW-SE (A and F); a possible sigma 1/sigma 2 flip between E and F in which the extension direction remains constant but the structural regime changes from normal faulting to oblique-slip faulting. A second stress field is a NNW-SSE compression (C), in which sigma 2/sigma 3 flip to give a strike-slip tectonic regime (B). A possible third stress field may have existed if D is interpreted to represent a significant shift in the direction of sigma 1 during compression; however, an alternative interpretation, which has considerable merit, is that C & D represent two resolved stress systems which really belong to one long-lived N-S compression.

It is interesting to speculate that if the assumption regarding Andersonian conditions of faulting are accepted i.e. that one of the initial principal stress was close to vertical (Anderson,1951); and if it accepted that the oblique stress fields are due to modification of an existing (Andersonian) stress field by reactivation along pre-existing faults rather than by a gross rotation of the stress field (Bott,1959), then a definite stress history is suggested. The stress fields are grouped into an early E, A & F, which principally involved extension and later C, D & B, which involved compression. This sequence of events does not contradict any of the observed overprinting relationships at Coppermine Creek, i.e. that the E-W normal fault is overprinted by sinistral strike-slip movements; and it certainly allows for the fact that compression followed extension, a normal pre-requisite for an inverting basin.

Further work

Warapirrmana Dome (Tawallah Range sheet)

Detailed structural work in the vicinity of the Warapirrmana Dome would confirm when the Hermit and Tawallah Faults had been most active. Sedimentological studies should determine whether doming had been active during middle Tawallah times (i.e. Ptq, Ptn, Ptnw) or at end Tawallah times (i.e. Pms).

Further work is also required to determine whether the Aquarium Formation and Wununmantyala Sandstone (including the Wuriliwuntya Member) thicken towards the Hermit and Rosie Faults. Clearly the latter had been a normal fault throughout much of its history, but an important question is whether normal or reverse movements had occurred during Tawallah sedimentation. A cursory inspection of the 1:100 000

geological map suggests that the Wuriliwuntya Member (of the Wununmantyala Sandstone) thickens towards the Hermit and Rosie Faults; also at Lorella Springs the Wuriliwuntya Member is mapped as cutting out abruptly against a splay fault (P.Haynes, pers. comm., 1993). Detailed structural and sedimentological studies tied closely to the present regional cross-sections would help to elucidate this problem.

Murphy Tectonic Ridge

The results of the reconnaissance study on the Murphy inlier were not reported here; however, there are a number of reasons why the inlier is important to this project and that further work should be conducted in the region:

- The Cliffdale Volcanics provide the only extensive exposures of "basement" volcanics in the McArthur Basin.
- A granite mapped on the inlier has given a Tawallah age and a style of alteration that may be due to a K-rich fluid that circulated through the basin at this time.
- The Calvert Fault has Cu mineralisation associated with it.

My initial impression gained from studying the Calvert Fault is that it becomes less active rather than a more active towards the centre of the inlier. Such results would have to be carefully checked against the conclusions of Sweet et al. (1981) which are that the largest movement occur in the oldest rocks. It has been suggested by past workers (Plumb et al.,1990) that the tens of kilometres of sinistral wrenching along the WNW-trending Calvert, Bulman and Mallapunyah Faults, during the Early Proterozoic, controlled the initial rifting in the McArthur basin. It is, therefore, desirable to establish whether the Calvert Fault had been active at this time in order to test this hypothesis.

Northern McArthur Basin

Further studies in other parts of the basin may help to establish whether the crustal extension proposed for the northern and southern parts of the basin (Plumb et al., 1990) conforms to a simple shear model (Wernicke) or a pure shear model. Recent data that has become available in the northern part of the basin could be used to extend this study.

REFERENCES

Ahmad M & Wygralak A.S., 1989. Calvert Hills (SE53-8) 1:250 000 metallogenic map series, explanatory notes. Northern Territory Geological Survey, Darwin.

Anderson E. M. (1951). The dynamics of faulting, Oliver and Boyd, Edinburgh.

Angelier J. (1979). Determination of the mean principal directions of stress for a given fault population. *Tectonophys.*, 56, T17-T26.

Angelier J. (1989). From orientation to magnitudes in palaeo stress determination using fault slip data. *J. Struct. Geol.*. v. 11, pp37-50

Armijo R., Carey E. & Cisternal A. (1982). The inverse problem in microtectonics and the separation of tectonic phases. *Tectonophys.*, 82, pp145-160.

Bull S., 1993. Progress report - sedimentology and volcanology of the southern McArthur Basin. CODES: AMIRA/ARC Project P.384 — Proterozoic sediment-hosted base metal deposits, Rept. No. 4 (this report)

Bott M.H.P., (1959) The mechanics of oblique slip faulting. *Geol. Mag.* XCVI, No. 2, 109-117.

Davidson C.J. & Dashlooty S. (1993). The Glyde Sub-basin: a volcaniclastic-bearing pull-apart basin coeval with the McArthur River base metals deposit, Northern Territory. Aust. J. Earth Sci. (in press).

Donovan S. (1993). The geology of Western Mallapunyah Dome (this report).

Dupin, J. -M., Sassi W. & Angelier J. (1993). Homogeneous stress hypothesis and actual fault slip — a distinct element analysis. *J. Struct. Geol.*, v. 15, No. 8, pp1033-1043.

Etchecopar A., Vasseur G. & Daignieres M.(1981). An inverse problem in microtectonics for the determination of stress tensors from fault striation analysis. *J. Struct. Geol.* p 351-365.

Garven G. 1985. The role of regional fluid flow in the genesis of the Pine Point deposit, Western Canada sedimentary basin. *Econ. Geol.* v. 80, 307-324.

Harding T.P., 1974. Petroleum traps associated with wrench faults. *AAPG Bull 58*: 1290-1304

Ingersol R.V. (1988). Tectonics of sedimentary basins. *Geol. Soc. Am Bull.*, v.100 p1074-1719.

Jackson M.J., Muir M.D. & Plumb K.A. 1987. Geology of the southern McArthur Basin, Northern Territory. *Bulletin* 220. Bureau of Mineral Resources, Canberra.

Jowett E.C. 1986 Effects of Continental rifting on the location and genesis of stratiform copper-silver deposits, in Boyle R.W., Brown A.C., Jefferson C.W., Jowett E.C. & Kirkham R.V. eds., Sediment-hosted Stratiform Copper Deposits: Geological Assoc. Canada, Spec. Paper 36, p.53-66.

Jowett E.C., Rydzewski A. & Jowett R.J. 1987. The Kupfershiefer Cu-Ag ore deposits in Poland: a re-appraisal of the evidence of their origin and presentation of a new genetic model. *Can. J. Earth Sci.*, v. 24, 2016-2037

Keele R.A. & Rogers J. 1992 Structures in the Southern McArthur Basin. CODES:AMIRA/ARC Project

P.384 —Proterozoic sediment- hosted base metal deposits, pp 35-38.

Leaman D.E. 1992. Regional Geophysics — Basin Architecture 1. Batten Trough Region. CODES:AMIRA/ARC Project P.384 —Proterozoic sediment- hosted base metal deposits, Rept .No.1, pp1-34.

Leaman D.E. 1993. Regional Geophysics - Basin Architecture 2. The Batten Trough Region — Update and further analysis. CODES:AMIRA/ARC Project P.384 Proterozoic sediment-hosted base metal deposits, Rept. No. 2, pp1-15.

Leeder M.R. & Gawthorpe R.L. (1987). Sedimentary models for extensional tilt block/half graben basins. *Geol. Soc. Lond. Spec. Publ.* No. 28, p 139-152.

Mauk J.L., Kelly W.C., Van der Pluijm B.A. & Seasor R.W. 1992. Relations between deformation and sediment-hosted copper mineralisation: Evidence from the White Pine part of the Midcontinent rift system. *Geology*, v. 20, p 427-430.

Pietsch B.A., Wyche S., Rawlings D.J., Creaser, P.M. & Findhammer T.L.R., 1991 McArthur Region (6065-6165) 1:100 000 map series, explanatory notes. Northern Territory Geological Survey, Darwin.

Pietsch B.A., Rawlings D.J., Creaser P.M.,Kruse P.D., Ahmad M., Ferenczi P.A. & Findhammer T.L.R. (1991) Bauhinia Downs SE53-3. Explanatory notes, 1:250 000 Geological map series. Dept. of Mines & Energy, N.T.Geol. Surv., Darwin.

Plumb K.A., Ahmad M. &Wygralek A.S. (1990). Mid-Proterozoic Basins of North Australia Craton - Regional Geology and Mineralisation. In: *Geology of the Mineral Deposits of Australia and Papua-New Guinea* (Ed.F.E.Hughes), pp 881-902 (The Australian Institute of Mining and Metallurgy, Melb.).

Plumb K.A., Derrick G.M. & Wilson I.H. (1980). Precambrian geology of the McArthur River- Mnt. Isa region, northern Australia, in *The Geology and Geophysics of Northeastern Australia* (Eds. R.A. Henderson and P.J. Stephenson), pp 71-88 (Geological Soc. Aust., Qland Div: Brisbane)

Plumb K.A. & Paine A.G.L., (1964). Mount Young (SD 53-3), Explanatory Notes and Map. Bureau of Mineral Resources, Canberra.

Plumb K.A. & Wellman P. (1987). McArthur Basin, Northern Territory: mapping of deep troughs using gravity and magnetic anomalies. *BMR J. Aust. Geol. Geophys.* 10 243-251.

Pollard D.D., Saltzer S.D. & Rubin A.M. (1993). Stress inversion methods: are they based on faulty assumptions? *J. Struct. Geol.*, v. 15, No. 8, pp1045-1054.

Rawlings D.J., Madigan T.L., Pietsch B.A. ,P.W. Haines & Findhammer T.L.R. (1993) Tawallah Range 6066. 1:100 000 Geological Map Series, Explanatory notes. Dept. of Mines & Energy, Northern Territory Geological Survey, Darwin.

Rogers J. (1993). The structural setting of the Tawallah Group, southern McArthur Basin, Northern Territory: implications for an early tectonic event. CODES: AMIRA/ARC Project P.384 — Proterozoic sediment-hosted base metal deposits, Rept. No. 4. (this report)

Smith J.W., Roberts, H.G., Plumb K.A. & Webb A.W.,1964. Bauhinia Downs (SE 53-3) 1:250 000 geological map sheet and explanatory notes. Bureau of Mineral Resources, Canberra

Sweet I.P., Mock C.M., & Mitchell J.E. (1981). Seigal, Northern Territory; Hedleys Creek, Queensland. !:100,000 Geological map commentary. Dept. of Nat. Devel. & Energy, Bur. Min. Res., Geol. Geophys; Dept. Mines Energy, Queensland. Canbera.

Wernicke B. (1985). Uniform sense normal simple shear of the continental lithosphere. *Can. J. Earth Sci.*, 22, p108-125.

Wright J.V. (1993). The geology of the North Mallapunyah Dome region. CODES: AMIRA/ARC Project P.384 — Proterozoic sediment-hosted base metal deposits, Rept. No. 4 (this report).

APPENDIX

Structural data - Field name locality index

MD = MALLAPUNYAH DOME

TF = TAWALLAH FAULT, BATTEN RANGE

T = TANUNBIRINI

NR = NATHAN RIVER STATION AREA

CM = COPPERMINE CREEK

KD = KIANA DOME

FF = FRIEDA FAULT LOCALITY

MR = MURPHY RIDGE

LF = LORELLA SPRINGS)

Progress Report - GIS Compilation for the McArthur Basin

M.L. Duffett
Centre for Ore Deposit and Exploration Studies

Since the last meeting, work has been split evenly between this project and the acquisition and reduction of gravity data from the Lady Loretta Pb-Zn deposit. Delays in the GIS compilation have been caused mainly by difficulties in obtaining a digitised copy of the Bauhinia Downs 1:250 000 map. However, virtually all the planned GIS component databases (whole-rock geochemistry, mineral deposits, digital elevation models of major basement units, regional geophysics, geology) will be either in place or else undergoing processing into presentable and/or analysable form by December.

Digital acquisition of Bauhinia Downs 1:250 000 geology has been made possible with the cooperation of AGSO and the NTGS. The original map was scan-digitised into Intergraph and exported as seven different 'levels' into ArcInfo. Unfortunately the scanning process has only partly distinguished lines representing joints, bedding trends, geological boundaries etc., and thus these levels have little meaning as geological coverages. Each dash in dashed lines (of which there are many) has been scanned as a discrete arc, each of which must be individually attributed in order to enable separation into the appropriate coverage. These problems, together with the presence of ubiquitous spurious micro-arcs generated in the scanning process, will delay the production of a topologically coherent map to around the end of 1993.

Some coverages suggested in the original project proposal are now unlikely to be included in the final GIS compilation. These include airborne EM, stream sediment geochemistry, Pb isotopes, geochronology and drillholes. Their unsuitability in a GIS of this nature is due to such factors as inappropriate database size (both too large and too small), lack of regional extent and difficulty of access. Some of these, however, may be included as part of the attribute table for geology polygons.

AGSO whole-rock geochemical data from the McArthur Basin (extracted from ROCKCHEM) have been obtained as a dataset in Oracle. Methods of linking this database with the main GIS in ArcInfo are currently being investigated, however the utility of this dataset will not be fully realised until cleaning of the digital geological covers is complete.

Resolution of geophysical datasets is variable. While all of Bauhinia Downs has been covered by regional low-resolution gravity, magnetic and radiometric surveys, only the survey flown for the NTGS in 1989 provides higher resolution data (magnetic and radiometric) over a region of significant size (McArthur River Region 1:100 000 map). CODES already possesses a copy of this dataset, and it will be incorporated into the appropriate data compilations.

With the major datasets in place, the project will be ready to move into its second phase, namely co-registration and analysis of the various datasets. This work will occupy at least the first half of 1994, and a final report is planned for presentation in November 1994.

Codes: AMIRA / ARC Project P.384 - Proterozoic sediment-hosted base metal deposits. November 1993

SECTION B

1993 Honours Programme

Overview of 1993 honours research programme in the McArthur Basin

David Cooke, Stuart Bull and Richard Keele
Centre for Ore Deposit and Exploration Studies

In the 1993 field season, three honours mapping projects have been completed in the Cape Crawford - Mallapunyah Dome region (Fig. 1). Although partly constrained by logistical problems, each field area was selected for its relevance to research being carried out within one or more of the research modules in project 384.

Karen Mathews has been investigating the depositional and diagenetic environments of the McArthur and Nathan Groups in the Top Crossing area (Mathews, 1993) under the supervision of Stuart Bull and David Cooke. Regionally, the McArthur Group is generally poorly exposed and most of the field based research to date has focussed on the Tawallah Group. However, the McArthur and Nathan Groups are well exposed in the Top Crossing area, so this project has been designed as a pilot study for the Basin Analysis group's research into the McArthur Group.

John Wright is completing a structural and stratigraphic study of the upper Tawallah and Lower McArthur Groups in the North Mallapunyah dome region (Wright, 1993) under the supervision of Richard Keele and Stuart Bull. John's work extends and refines a pilot study of this area conducted for the Basin Analysis group by Keele and Rogers (1992) and Keele (1993). In particular, he has applied a domain analysis approach to the study of fault striae in his area and can demonstrate that a late E-W compression is related to a phase of movement on the southern continuation of the Tawallah Fault.

Serena Donovan's research is focussed on the geochemistry, volcanology and structure of the Upper Tawallah Group in the Western Mallapunyah Dome area (Donovan, 1993) under the supervision of David Cooke and Stuart Bull. Serena's geochemical work forms an integral part of the brine chemistry module's investigations into the origin of regional-scale potassic alteration in the Settlement Creek volcanics. Further analytical work is currently being conducted on Settlement Creek volcanic samples collected by D. Cooke from elsewhere in the Mallapunyah and Kiana Dome regions, and a final report on the origins and styles of alteration in the Settlement Creek volcanics will be provided at the next sponsors' meeting. Serena's stratigraphic and volcanological work falls under the umbrella of the more regional study of the upper Tawallah and lower McArthur Groups by Bull (1993) for the basin analysis group. Her structural investigations are part of the ongoing investigation into the structural setting of Mallapunyah Dome (Keele, 1993)

REFERENCES

Bull S., 1993. Progress report - sedimentology and volcanology of the southern McArthur Basin. CODES: AMIRA/ARC Project P.384 — Proterozoic sediment-hosted base metal deposits, Rept. No. 4 (this report)

Donovan S., 1993. The geology of Western Mallapunyah Dome. CODES: AMIRA/ARC Project P.384 — Proterozoic sediment-hosted base metal deposits, Rept. No. 4 (this report).

Keele R.A. & Rogers J. 1992 Structures in the Southern McArthur Basin. CODES:AMIRA/ARC Project P.384 — Proterozoic sediment- hosted base metal deposits. Rept. No. 1,, pp 35-38.

Keele R.A., 1993. The histories of some faults in the Southern McArthur Basin: Evidence for an end-Tawallah uplift and a preliminary analysis of stresses related to post-McArthur and post-Roper compressions. CODES: AMIRA/ARC Project P.384 — Proterozoic sediment-hosted base metal deposits, Rept. No. 4 (this report).

Mathews, K.A., 1993. The geology of the Top Crossing area, Cape Crawford, Northern Territory. CODES: AMIRA/ARC Project P.384 — Proterozoic sediment-hosted base metal deposits, Rept. No. 4 (this report).

Wright J.V., 1993. The geology of the North Mallapunyah Dome region. CODES: AMIRA/ARC Project P.384 — Proterozoic sediment-hosted base metal deposits, Rept. No. 4 (this report).

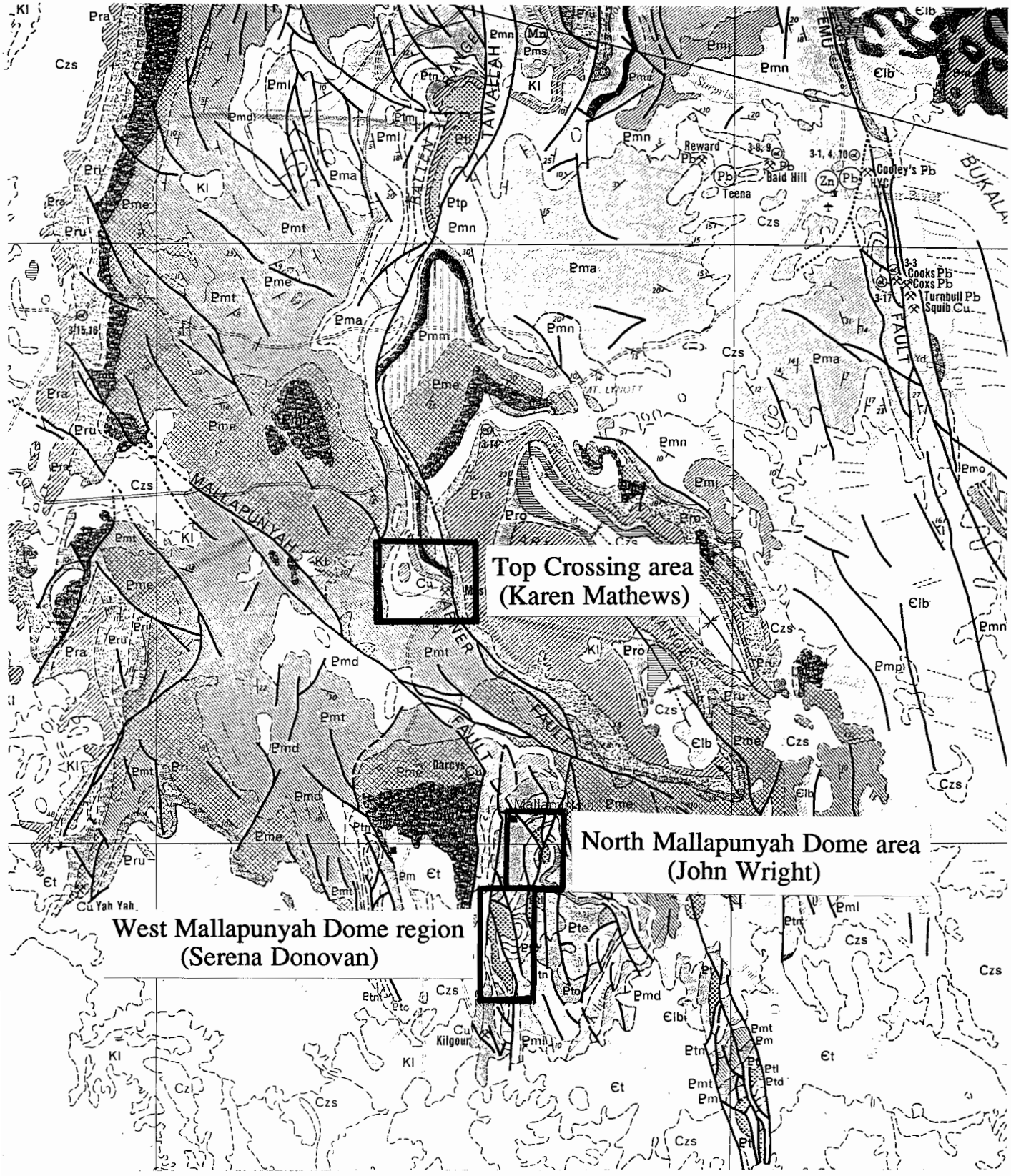

Figure 1. Locality map: 1993 honours field areas.

The geology of the Top Crossing area, Cape Crawford, Northern Territory

Karen Mathews
Centre for Ore Deposit and Exploration Studies

In the Top Crossing area of the McArthur Basin, the upper eleven units of the McArthur Group and the four units of the Nathan Group are exposed. On a regional scale, this thick succession of evaporitic and stromatolitic carbonates, siltstones and sandstones hosts several styles of mineralisation, ranging from large sediment-hosted Pb-Zn deposits (HYC) to vein-type and karst-filled breccia-type base metal occurrences. The Top Crossing area is significant because it is one of few areas where the Barney Creek Formation, which hosts Pb-Zn ores at HYC, crops out.

The McArthur and Nathan Group carbonates in the field area display a variety of sedimentary features, including abundant evaporitic pseudomorphs, stromatolite bioherms, tuffaceous(?) beds and intraclastic and solution collapse breccias. These features are consistent with a shallow water, evaporitic depositional environment. A generalised facies association section for the McArthur and Nathan Group stratigraphy in the study area has been constructed from detailed sedimentary sections measured in each unit. Interpretation of these different facies and their association has not yet been finalised.

In outcrop, the carbonates contain pseudomorphs of evaporitic minerals that provide evidence of hypersaline depositional conditions. Displacive evaporites indicate evaporation during early diagenesis. From these features it is clear that the depositional setting was a shallow water, restricted marine/meteoric environment. However, at this stage a depositional model has not been proposed.

Stable isotope data for carbonates from the McArthur and Nathan Groups are lighter than expected from marine diagenesis and $\delta^{18}O$ -7.5 to -11.5‰ PDB and $\delta^{13}C$ -1.5 to 1.5‰ PDB indicate a burial diagenetic environment. Trace element analyses indicate high concentrations in Fe (2024-7860 ppm) and Mn (0-989 ppm) and considerably lower Sr (0.7-48 ppm) and Na (13.5-224 ppm) concentrations in the carbonates. These results indicate a burial diagenetic environment, which has destroyed any original geochemical signatures during initial deposition. The high Fe and Mn concentrations also indicative of reduced fluids that could have possibly been meteoric in origin.

Cathodoluminescence work on some of the coarse-grained carbonates, interpretation of x-ray diffraction results on some of the tuffaceous(?) beds and a full facies interpretation are still being carried out. Due to this, a model for the depositional environment is yet to be finalised.

Codes: AMIRA / ARC Project P.384 - Proterozoic sediment-hosted base metal deposits. November 1993

The geology of the North Mallapunyah Dome region

John V. Wright
Centre for Ore Deposit and Exploration Studies

North Mallapunyah Dome is located in the southern portion of the Middle Proterozoic McArthur Basin. A 35km2 area has been mapped with particular emphasis on structural aspects of the region. Units of the upper Tawallah and lower McArthur Groups are exposed.

The oldest unit exposed in the area is the Wununmantyala Sandstone, a thin to thickly bedded, well rounded and generally well sorted fine to medium grained, pink to purple hematitic quartz arenite sequence of mainly sublittorial origin. The sequence is characterised by common mud clasts and symmetrical bifurcating and parallel ripples, and less common ooids. Close jointing often gives the outcrop a tessellated appearance. The Wuraliwuntya Member of the Wununmantyala Sandstone outcrops poorly and is composed of halite-bearing finely laminated silty dololutite and subordinate doloarenite beds.

The Settlement Creek Volcanics conformably(?) overlie the Wununmantyala Sandstone and are composed of massive and extensive vesicular basalt, andesite and dolerite with subordinate flow banded and autobrecciated aphanitic rhyolites, occasionally showing ropey surface textures. Shales and siltstones similar to those of the overlying Wollogorang Formation are intercalated with the volcanics and contact metamorphosed by them. They indicate periods of hiatus in volcanic activity.

The Wollogorang Formation is dominated by laminated fine-grain ferruginous purple and brown dololutite with common evaporite pseudomorphs and algal laminations. This unit is very poorly exposed and is often only indicated by the presence of surface deposits of calcrete and scattered float. Useful marker horizons are a dolomitic black shale facies with common ovoid bituminous nodules and a white to grey crystalline dolomite facies, which are generally better exposed than the rest of the formation.

Massive fine-grained basalts and dolerites of the Gold Creek Volcanics intrude and cover upper sections of the Wollogorang Formation. The volcanics are laterally restricted, variable and appear very episodic in nature. The dololutite sequence is intensely deformed while rip-up clasts and rafts are included in the volcanics. Late magmatic associated potassium metasomatism is pervasive in both volcanic formations and is especially intense in the Gold Creek Volcanics. Plagioclase is replaced by K-spar and sericite while ferromagnesium minerals are principally replaced by chlorite.

The Masterton Sandstone, the basal formation of the McArthur Group, overlies the Tawallah Group disconformably. This unit is composed predominantly of a monotonous sequence of white to buff coloured generally thickly bedded quartz arenite with abundant ripples and planar cross-beds. A basal clast-supported conglomerate is exposed in one locality. The pebble to cobble-sized sub-rounded quartz arenite clasts and gritty sandstone matrix are now intensely silicified.

The Masterton Sandstone grades upwardly into the Mallapunyah Formation with a distinctive sequence providing a good marker bed. A finely laminated dolomitic sandstone with common anhydrite moulds and ripples is overlain by a thin (10 to 30 cm) pale-green chert bed and thence by a chertified stromatolite bed and thinly bedded gritty sandstone.

The Mallapunyah Formation is characterised by mottled reddish-purple and green shales and siltstones with common ripples and occasional cauliflower chert nodules, halite casts or barite concretions. Sandstone interbeds occur regularly while stromatolite beds are rare.

A small-fault bounded block of Amelia Dolomite is the youngest McArthur Group unit in the area. The section is composed of interbedded buff to orange coloured dolarenite, cream silty dololutite, and purple shale with some beds containing abundant cauliflower chert nodules. Thin chertified

Codes: AMIRA / ARC Project P.384 - Proterozoic sediment-hosted base metal deposits. November 1993

stromatolitic horizons are regularly spaced over 3 metre intervals.

Two major faults of the McArthur Basin converge in the study area. The Mallapunyah Fault trends northwest, while a northerly trending fault dissecting the area is the southern continuation of the Tawallah Fault Zone. An early dextral movement of the Tawallah Fault and associated NE-trending normal faulting and NW-trending low-angle thrusting suggests a compressional event directed northeast-southwest. Sinistral movement of the Mallapunyah Fault may have also occurred. This event is evident in all units represented in the area and thus at least post-dates the deposition of the lower McArthur Group sequence. Some fault striae suggest an earlier east-west directed extensional event. However, no set of fault striae are confined to the pre-McArthur Group sequence. The present structure is dominated by a strong late (probably post-Roper in age) compressional event directed east-west. This event resulted in dextral movement of the Tawallah Fault, the development of NE-trending sinistral antithetic X shears about the Mallapunyah Fault, low angle north*f*south trending thrusts with a large proportion of movement taken-up on the bedding planes and possibly broad regional-scale open folding. There is no evidence of the essential reactivation of the locally steep southwest dipping Mallapunyah Fault during this phase.

Faults of all orientations are surrounded by zones of hematization and silicification, with the size of the fault determining the extent of alteration. The first order Tawallah and Mallapunyah Faults have 50 m wide hematitic breccia zones developed within adjacent sandstones. The breccias have a hematitic matrix and are generally clast supported. An outer zone of silicification usually extends no more than 20 m from the hematitic breccia, though it is significantly more developed in the Wununmantyala Sandstone than the Masterton Sandstone sequence, perhaps due to a more extensive joint pattern. In areas of extension associated with fault bending the breccia zones are highly silicified and up to 300 m wide. Second and third order faults have hematite alteration zones up to a few metres with little silicification. The lower sandstone beds of the Mallapunyah Formation are characterised regionally by a horizon of intense hematitic alteration. Large (up to 30 cm) hematite veins crosscutting the volcanic units and the Wollogorang Formation, and quartz veining in the Wununmantyala and Masterton Sandstone sequences, are associated with the early northwest-southeast directed tectonic event. These veins have been deformed and offset by the strong late east-west compressional event.

Work is continuing on the analysis of fault data to determine age relationships and establish the structural evolution of the study area and its relationship to the overall development of the McArthur Basin. More detailed petrographic work is being undertaken to better describe the lithologies and alteration features.

The Geology of Western Mallapunyah Dome

Serena Donovan
Centre for Ore Deposit and Exploration Studies

The Western Mallapunyah Dome area is located in the southern McArthur Basin, approximately 50 kilometres south of Cape Crawford on Mallapunyah Station. This study focuses on the stratigraphy, structure, petrology and alteration characteristics of the upper Tawallah Group and lower McArthur Group exposed in the area. Work completed at this stage includes:

- Detailed mapping of 32 km^2 at 1:12500 scale.
- Field and petrographic investigations of the upper Tawallah Group (Aquarium Formation, Wununmantyala Sandstone, Settlement Creek Volcanics, Wollogorang Formation and Gold Creek Volcanics), and lower McArthur Group (Masterton Sandstone, Mallapunyah Formation and Amelia Dolomite).

What had previously been mapped as the McDermott Formation and Sly Creek Sandstone were remapped as the Aquarium Formation and Wununmantyala Sandstone, based on lithological and stratigraphic relationships. The Settlement Creek Volcanics are seen as intrusive not extrusive as previously written. No evidence for extrusive volcanic activity was found at West Mallapunyah Dome, and field relationships between the bimodal "rhyolites" and "dolerites" (field terms) suggest that the dolerite intruded at the base of the Wollogorang Formation as a series of sills (Jackson *et al.* 1987) and this was in turn intruded by rhyolite dykes. The Gold Creek Volcanics (hyaloclastites, rhyolites and mafic intrusives) probably represent high level intrusive and extrusive equivalents of the Settlement Creek Volcanics (S. Bull pers. comm. 1993). The Masterton Sandstone was deposited unconformably above the Gold Creek Volcanics (Jackson *et al.* 1987), in a fluvial to shallow marine environment. A transition to shallow marine and evaporitic conditions at the top of the Masterton Sandstone allowed the onset of deposition of the Mallapunyah Formation and Amelia Dolomite.

X-ray diffraction analysis of samples from the Settlement Creek and Gold Creek Volcanics has shown definite groupings of "rhyolites" and "dolerites". Rhyolites (both Settlement Creek and Gold Creek Volcanics) are composed of 45-85% quartz, 15-30% K-feldspar, 2-15% hematite, with minor anatase, mica and kaolinite. Dolerites are composed of 10-35% quartz, 50-75% K-feldspar, 5-10% hematite, with minor anatase, mica and kaolinite. Pervasive potassic alteration has affected the rhyolites and dolerites of the Settlement Creek and Gold Creek Volcanics, accounting for the high levels of K-feldspar recorded by X-ray diffraction. Some samples have also suffered propylitic alteration, characterised by chlorite ± dolomite.

An oxygen isotope traverse has been conducted through the Settlement Creek Volcanics from the fault contact with the Masterton Sandstone at Dillingham's Fault, to a north trending fault one kilometre to the east. The purpose of this study is to determine if the potassic alteration in the volcanics is fault-related. The $\delta^{18}O$ value obtained from a quartz vein in the Masterton Sandstone at Dillingham's Fault was 20·6‰, consistent with meteoric water that has undergone significant evaporation i.e. basinal brines. The volcanics also record a basinal brine isotopic overprint, although the rocks have not undergone isotopic exchange with the fluids to the same extent as the quartz vein. The highest value recorded from the volcanics (19·7‰) was from an autobrecciated rhyolite, which would have been most permeable to the alteration fluids. The lowest value (16·4‰) is still significantly heavier than the values obtained for pristine igneous rocks (7-9‰) (Barnes, 1979), indicating that isotope exchange between the volcanics and basinal brines has occurred.

Relative $\delta^{18}O$ enrichment in the volcanics implies interaction with diagenetic fluids at low

Codes: AMIRA / ARC Project P.384 - Proterozoic sediment-hosted base metal deposits. November 1993

temperatures (Muehlenbachs, 1987). Formation waters in sedimentary basins contain a sizeable fraction of meteoric water, but they do not have $\delta^{18}O$ values that plot on the meteoric water line. Instead they trend towards higher isotopic values because warmer saline waters generated heavier isotopic values, especially during interaction with carbonates (Longstaffe, 1987). Thus saline fluids expelled from the compacting sediments permeated through and reacted with the volcanics.

The silicification and quartz veining in the Masterton Sandstone is clearly fault-related, and is thus most likely due to later basinal brines passing upwards along Dillingham's Fault.

Sulphur isotope analyses of an extensive, (over two kilometres long), apparently stratiform barite occurrence on the western margin of the field area yielded very heavy values (37·7, 42·3, 47·5 and 50·0‰). The heavy isotopic signatures indicate replacement of evaporites. It is likely that the barite has replaced gypsum from an evaporite bed in the Amelia Dolomite or upper Mallapunyah Formation, retaining the primary evaporitic signature. At Eastern Creek there is good evidence that at least some of the barite was originally gypsum (Muir *et al.* 1985). Lady Loretta barite has $\delta^{18}O$ values of around 40‰ (Gustafson and Williams, 1981) which is also interpreted to indicate replacement of evaporites. Further evidence for an evaporitic (gypsum) origin comes from the texture of the barite. Nodules of barite have internal aggregates of possible gypsum dissolution breccia, surrounded by a rim of swallow tail crystals with curved crystal faces. This is characteristic of gypsum when impurities such as NaCl are present. On top of the nodules there is invariably a zone of fibrous crystals (satin spar; Deer, Howie and Zussman, 1962). The barite source is likely to be seawater, the same as the barite occurrences found in botryoidal quartz nodules from the Mallapunyah Formation and Amelia Dolomite (Muir *et al.* 1985).

Work to be completed includes:

- Further analysis of the barite textures and the implications of these textures.
- A structural analysis to determine principle stresses on West Mallapunyah Dome and the history of fault movements.
- X-ray fluorescence and trace element analysis on the Settlement Creek Volcanics and the Gold Creek Volcanics to determine original lithologies and the chemical effects of hydrothermal alteration.
- A fluid inclusion study of quartz veins in the Settlement Creek Volcanics to determine the temperature constraints on the alteration fluids.
- An assessment of the mineral potential of the dome.

REFERENCES

Barnes, H. L. (1979). Geochemistry of Hydrothermal Ore Bodies. Wiley & Sons

Deer, W. A., Howie, R. A. & Zussman, J. (1962). Rock Forming Minerals. Vol. 5. Non Silicates. Longman.

Gustafson, L. B. & Williams, N. (1981). Sediment Hosted Stratiform Deposits of Copper, Lead and Zinc. Economic Geology 75th Anniversary Volume. 139-178.

Jackson, M. J., Muir, M. D. & Plumb, K. A. (1987). Geology of the Southern McArthur Basin, Northern Territory. BMR Bulletin 220. Aust. Govt. Publishing Service.

Longstaffe, F. J. (1987). Stable Isotope Studies of Diagenetic Processes, *in* Kyser, T. K. (ed.) (1987). Short Course in Stable Isotope Geochemistry of Low Temperature Fluids. Vol. 13. Mineralogical Society of Canada.

Muehlenbachs, S. K. (1987). Oxygen Isotope Exchange During Weathering and Low Temperature Alteration, *in* Kyser, T. K. (ed.) (1987). Short Course in Stable Isotope Geochemistry of Low Temperature Fluids. Vol.. 13. Mineralogical Society of Canada.

Muir, M. D., Donelly, T. H., Wilkins, R. W. T. & Armstrong, K. J. (1985). Stable Isotope, Petrological and Fluid Inclusion Studies of Minor Mineral Deposits From the McArthur Basin: Implications For the Genesis of Some Sediment-Hosted Base Metal Mineralisation From the Northern Territory. Australian Journal of Earth Sciences, 32. 239-260.

SECTION C

Brine Chemistry Module

Alkali alteration in the McArthur Group with particular reference to volcaniclastic materials: a progress report

Garry J. Davidson
Centre for Ore Deposit and Exploration Studies

SYNOPSIS

This is a progress report on a study of the behaviour of alkali elements in the saline-alkaline McArthur Group, with special reference to base metal mineralisation. The bulk of this report is a review of previous work on this topic. Feldspar-dominated alkali replacement of glassy volcaniclastic rocks can occur during low temperature saline diagenesis, or can characterise the passage of higher temperature saline fluids; the latter fluids can also be associated with Pb-Zn-Ag deposits in sedimentary basins. There is a clear need to discriminate the similar metasomatic products of these diverse processes. A review of McArthur Basin data indicates (1) K-feldspar is an intimate part of the HYC ore assemblage; (2) albite forms the outermost alteration shell at HYC within tuff, surrounding an albite+K-feldspar zone; (3) tuff in regional BCF west of HYC consists of K-feldspar, whereas tuff in the Glyde sub-basin is dominated by albite. Oxygen isotope geochemistry separates Glyde sub-basin from HYC sub-basin volcaniclastics with similar Pb+Zn contents. Further work on the oxygen isotope interpretation is required, but the method has potential as an ore halo tool. Core samples of high-K tuff from west of HYC have been obtained and are presently being geochemically analysed.

AIMS

Previous work by many authors has indicated that the fine-grained clastic and volcaniclastic rocks of the McArthur Group have unusual alkali element compositions for sediments, particularly in the vicinity of the McArthur River base metals deposit. This sub-project is aimed at:

(1) characterising these chemical compositions and their associated mineralogy, capitalising on previous work;

(2) determining the timing of the development of these compositions, particularly differentiating between synsedimentary, diagenetic, diagenetic-hydrothermal, and epigenetic-hydrothermal timings;

(3) determining the relationship between sediment geochemistry and base metal mineralisation in the McArthur Group, with a view to establishing mineralisation halo parameters for use in exploration; and

(4) determining the relevance of these chemical changes to models of fluid movement in the McArthur Group.

OVERVIEW OF THIS SUB-PROJECT

The relationship between alkali alteration and shale-hosted lead-zinc formation in saline basins is poorly understood. Concentrating on tuff beds, this sub-project is researching this relationship from a number of viewpoints, using the McArthur River deposit and its host basin. Tuffs are favourable rocks for such a study because (1) they originated as a chemically and mineralogically homogeneous medium; (2) they can be correlated broadly throughout the McArthur River ore environment, and (3) by virtue of their reactive glassy character, they reflect chemical change induced by post-depositional fluids very well.

Several benefits could come from this sub-project. Firstly, it is presently not possible to differentiate high temperature hydrothermal alteration from low temperature alkali alteration in saline basins, on the basis of mineralogy. This would be very useful to

Codes: AMIRA / ARC Project P.384 - Proterozoic sediment-hosted base metal deposits. November 1993

achieve in an exploration context, because shale-hosted Pb-Zn mineralisation is commonly associated with high temperature potassic alkali alteration. Secondly, there is no strong understanding of the conditions which control whether it is albitic or potassic feldspar alteration which dominates a particular saline hydrothermal system. Thirdly, changes in isotopic character of the alkali alteration away from an ore zone could be used in an exploration context as a direct ore-indicator. Fourthly, understanding the distribution of alteration should provide constraints on circulation models of basinal fluids.

ALKALI ALTERATION, METALS, AND SALINE BRINES: A REVIEW

General behaviour of alkali elements in saline volcaniclastic settings

Low temperature alkali metasomatism characterises many shallow evaporitic basins of the world, particularly those which at some time contained playa lake systems. It is a feature of some Proterozoic rifted basins of northern Australia, including the virtually undeformed McArthur Basin. Many studies have emphasised the geochemical and mineralogical changes observed in volcaniclastic debris in these environments (e.g., Sheppard & Gude, 1968; Deike & Jones, 1980; Stamatakis, 1989), but similar changes also occur in clastic lithologies (e.g., Moine et al. 1981, Beeson et al. 1989).

In evaporitic, felsic volcaniclastic-rich basins, concentric mineralogical zonation is observed from the basin margin to its centre, developed by reaction of increasingly concentrated alkaline solutions with volcanic glass, during diagenesis (e.g., Stamatakis, 1989). Most commonly this zonation changes basinward from a carbonate-rich zone, to a zone of zeolites (phillipsite, erionite, clinoptilolite; av. B content 267 ppm; Stamatakis, 1989), to a zone of sodic zeolite (analcite; av. B content of 356 ppm), to a central zone of boron-rich potassium feldspar (av. B content of 1703 ppm). The character of the zonation reflects the changing nature of the diagenetic fluid; for instance, highly alkaline fluids (pH~< 9) should produce sodium carbonate phases such as shortite, and suppress the stability of the zeolites clinoptilolite and heulandite (Boles & Surdam, 1979).

In addition to the chemical reactions which take place within a few metres of the sediment surface, volcaniclastic debris can continue to react with circulating basinal brines after burial, which can result in complex paragenetic sequences. Hay et al. (1988) have shown with K/Ar and Rb/Sr dating, that metasomatism can occur hundreds of millions of years after sedimentation, raising the possibility that observed mineralogies do not relate in any way to contemporary diagenesis. Hay et al. (1988) relate this metasomatism to the topographic and density-driven descent of potassic groundwater from overlying evaporitic environments (of much younger age) during epeirogenesis. In one instance, the fluid source region and the area of eventual sub-surface metasomatism were separated by ~400 km. Hay et al. (1988) have made radiometric dating a mandatory addition to any study of alkali alteration in sedimentary basins.

Alkali alteration also intimately accompanies the deposition of base metals in saline basins. For instance, as well as alkali alteration documented around HYC in the McArthur Basin (discussed in more detail below), massive K-feldspar also characterises tuffs at the Mt Isa, Dugald River (Australia) and Meggen (Germany) Pb-Zn deposits (Muir, 1983; Krebs, 1981), whereas albitic alteration is associated with the stratabound Pb-Cu-Ba Abra deposit in the Western Australian Bangemall Basin (Vogt & Stumpfl, 1987).

Alkali feldspar replacement in sedimentary basins is not confined to Pb-Zn-rich ore deposits. For instance, alkali alteration is pervasive around Cu-Au deposits in the Mount Isa Eastern Succession (Beardsmore 1988, Davidson et al. 1989, Adshead 1993). K-feldspar alteration is also commonly observed in the upper plate of detachment faults in the western United States, overprinted by Cu, Au and Ag-bearing veins. Here brines with 13 to 17 wt. % NaCl descended into the extending crust after accumulating in overlying evaporitic rift basins; early K-metasomatism apparently liberated metals, which were then incorporated into the mineralising basinal brines (Lindley & Chapin 1986, Roddy et al. 1988).

Previous work on alkali element behaviour within McArthur Group tuff

Some systematic analysis of alkali zonation in tuff has carried out for the Barney Creek Formation around the giant shale-hosted HYC Pb-Zn-Ag deposit (Logan 1979). Six correlatable volcaniclastic horizons were systematically examined using major element wholerock geochemistry, XRD-determined mineralogy, cathodoluminescence, and mineral chemistry. This study found that the tuffs at HYC presently consist of microcline, adularia, albite, quartz, pyrite, calcite, ferroan dolomite, chlorite, illite, kaolinite, and bitumen. These components are distinctly zoned with respect to the Cooley Dolomite and the Emu Fault Zone. There is a general progressive change from K-feldspar, to K-feldspar + albite, to albite away from the Cooley

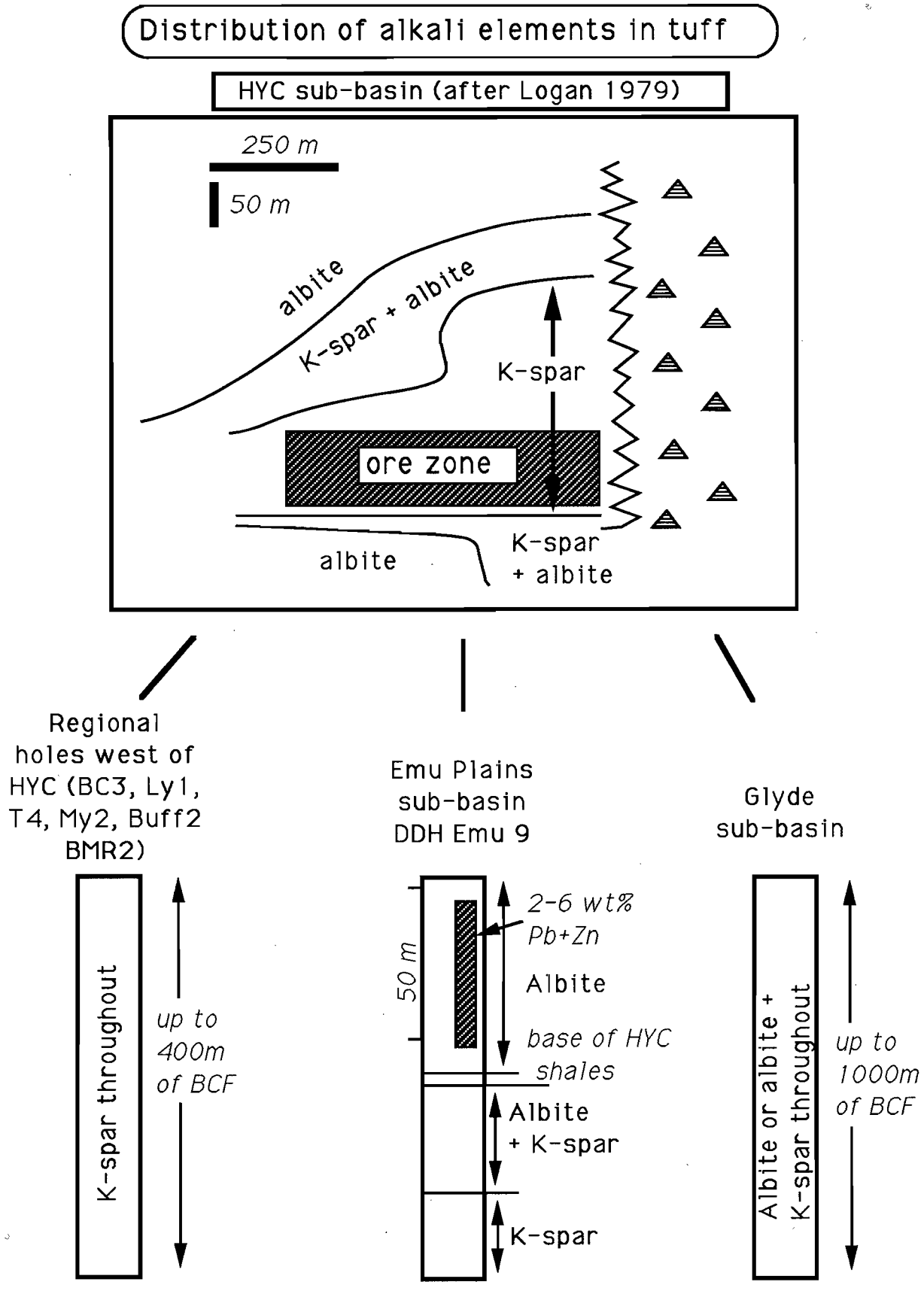

Figure 1. A summary of the distribution of alkali elements in volcaniclastic rocks, as deduced from open-file data (mainly from Logan, 1979).

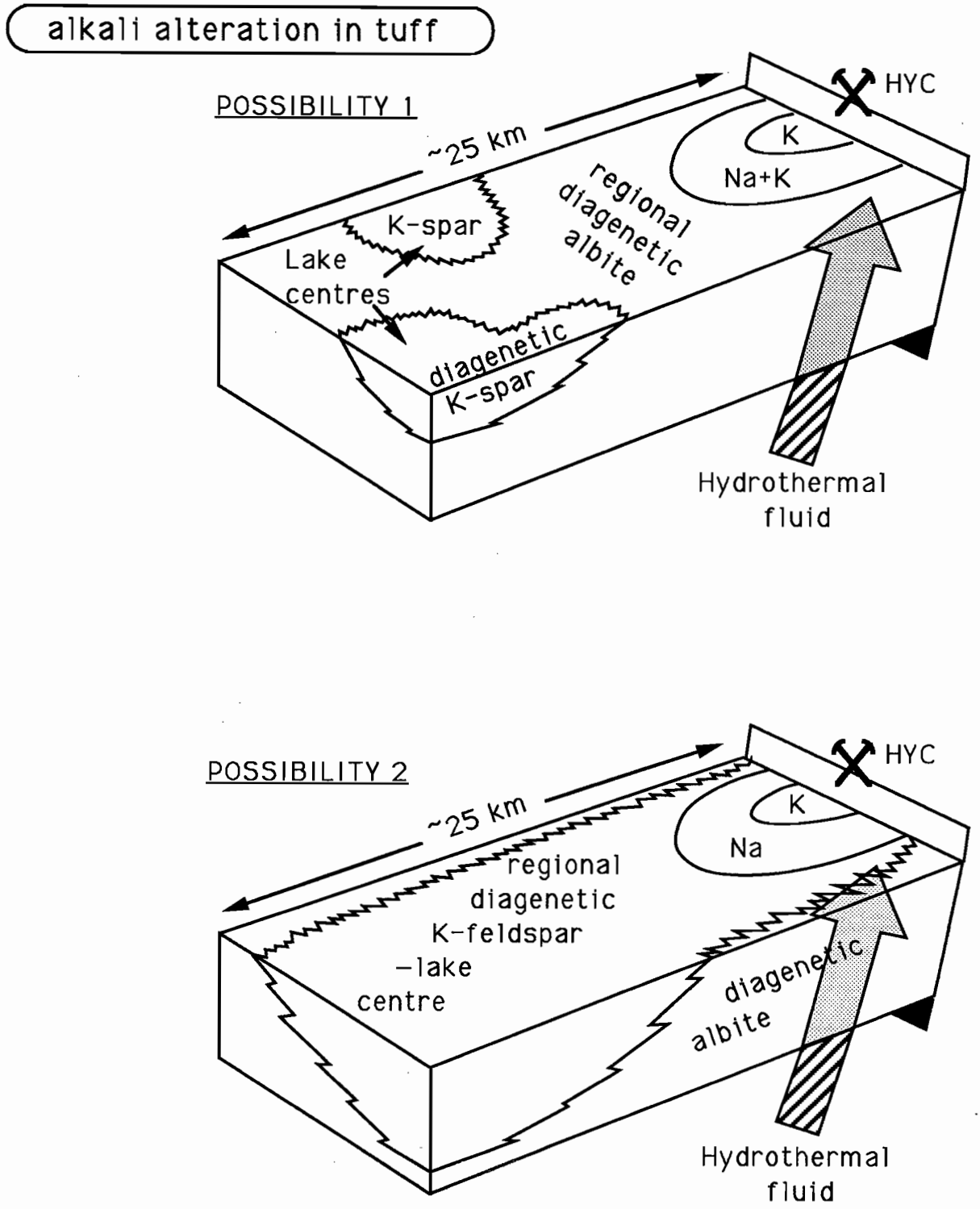

Figure 2. There are three possible means of explaining the known distribution of alkali elements in tuff in the Barney Creek Formation: (1) areas of both hydrothermal and diagenetic K-addition within a general background of albite (Na addition); (2) areas of K and Na hydrothermal addition into a diagenetic K-rich background; and (3) more extensive hydrothermal K-addition than has been previously realised, related to extensive areas of faulting and sub-basin development.

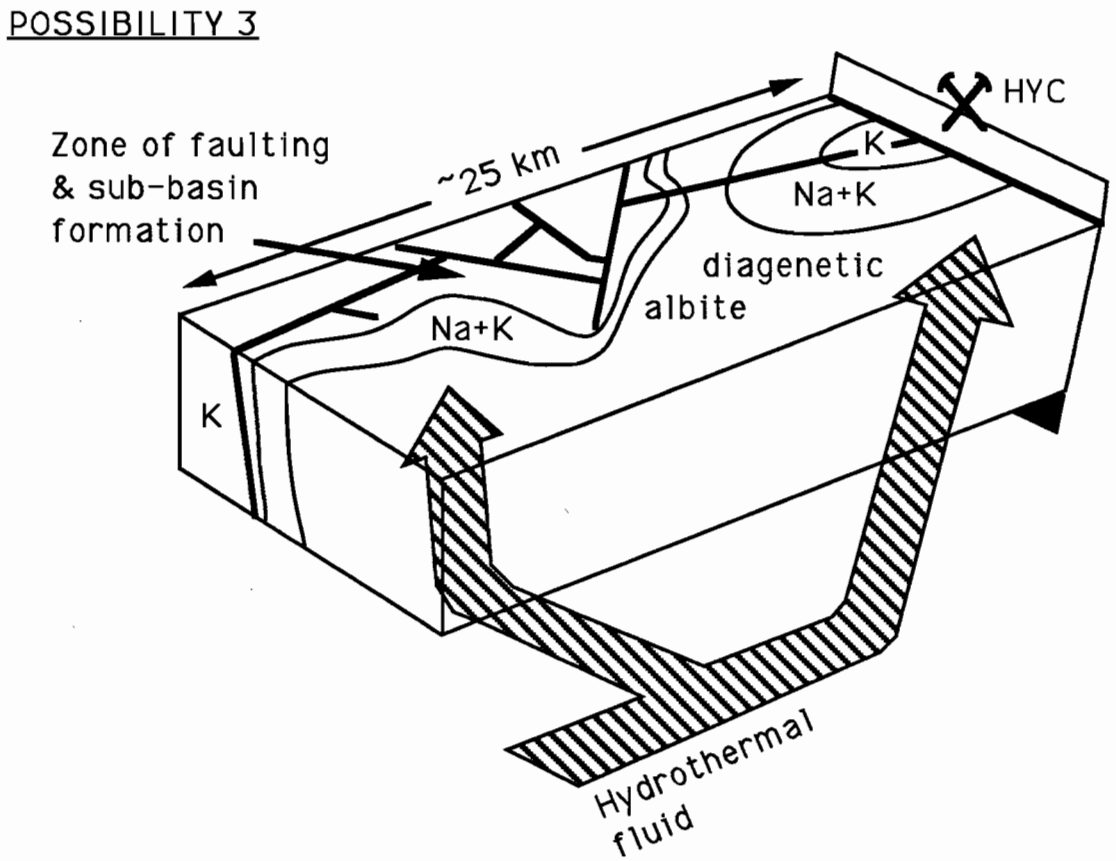

Figure 2 (cont.). See previous page for description.

Dolomite, and with distance above the ore horizon, within tuff. In addition, the percentage of feldspar altered to clay in tuff shows a systematic variation paralleling the feldspar mineralogical changes, with greater alteration found closer to the Cooley Dolomite. K-feldspar from the mineralised horizons was notably far coarser than that regionally developed in the Barney Creek Formation tuffs, commonly containing sulfide inclusions, and exhibiting intergrowths of adularia and sphalerite, suggesting that at least some K-feldspar was deposited as an intimate part of the ore paragenetic sequence. Logan(1979) interpreted the feldspar zonation as the product of a changing hydrothermal fluid moving outward from its source, and interpreted the clay alteration as a later lower temperature hydrothermal fluid overprint derived from the same source. High field strength element concentrations of tuff at HYC were determined by Dashlooty & Davidson (in press), who found Ti, Zr, Y and Nb to be immobile with increasing potassium and base-metal contents, considered to be indices of increasing alteration.

Davidson & Dashlooty (in press) have demonstrated a southerly source for volcaniclastics in the BCF at the HYC mine and at the Glyde sub-basin (80 km south of HYC). In the Glyde sub-basin, unaltered or sodically altered tuffs were documented, whereas Corbett et al. (1975) and Large & Finlow-Bates (1982) found only K-feldspar-bearing tuff over a wide area west of HYC, sampling surface samples. In the Emu Plains sub-basin (DDH Emu 9) west of HYC, Logan(1979) found that Barney Creek Formation tuffs coincident with low grade mineralisation were albitic, overlying mixed K-feldspar+albite tuff, and then K-feldspar-only tuff. He also found that tuff from six other drillholes within BCF, arrayed aproximately 20 km around HYC, consisted entirely of K-feldspar. In summary, tuffs associated with base metal mineralisation in the Barney Creek Formation contain microcline, adularia and albite arranged in complex but systematic patterns. Tuff in the Barney Creek Formation west of HYC, in areas where no nearby mineralisation is known, are K-feldspar dominated. Tuffs in the isolated barren Glyde sub-basin 80 km south are albitic or do not display alkali element alteration (Fig. 1).

Discussion of previous work

The available data indicates that volcaniclastic rocks in the McArthur Group inherited their anomalous alkali element contents post-depositionally, as the result of interaction with sub-surface fluid. Given the regional geological evidence of shallow saline sedimentary environments within parts of the Barney Creek Formation, it is reasonable to expect that the volcaniclastic rocks reacted initially with evaporitic brines in the near-surface environment, and that their chemistry and mineralogy *initially* reflected the degree of evaporitive concentration of near-surface waters. However, the K-feldspar-rich tuff observed by Corbett et al. (1975) and Logan (1979) in unmineralised Barney Creek Formation is very extensive, possibly more extensive than might be expected from simple crystallisation of the diagenetic end-products of a playa lake. Approximately 100x evaporation of normal seawater is required for deposition of K-phases by evaporation. An origin of regional alkali alteration by this means will be tested by determining the concentrations of elements that are normally concentrated by evaporation and then incorporated into minerals, including B, Br, Cl and I.

A second mechanism for regional alkali alteration is the circulation of deep hydrothermal fluids, fluids which may relate in some way to base metal mineralisation. Secondary K-feldspar replacement is favoured by high fluid aK^+ / aH^+, and is accomplished by exchange reactions such as

$$NaAlSi_3O_8 + K^+ = KAlSi_3O_8 + Na^+$$

Thermodynamic data for this reaction suggests that at low hydrothermal temperatures (<100° C) K-feldspar exchange is favoured even where fluid Na/K ratios are greater than 100:1, but this favourability is eroded above 200° C (Senderov, 1973; Agron & Bentor, 1981), where large increases in $[K^+]$ are required to maintain K-feldspar stability above 200° C. More detailed analysis of the thermodynamics of the Na-K-Al-Si-H_2O system will provide useful independent constraints on the development of alkali alteration by this means.

Logan (1979) documents the intimate intergrowth of microcline, adularia and base-metal sulfides in tuff at HYC, indicating that at least some K-feldspar grew in equilibrium with hydrothermal fluid, a feature which must be considered in hydrothermal modelling of the ore fluid. It is likely that this alteration was imposed on diagenetically altered tuff, which may be represented by the generally albitic alteration documented by Logan(1979) on the peripheries of the deposit. If this sodic alteration is indeed representative of the regional diagenetic background alteration, as would be supported by the chemistry of barren tuff in the Glyde Sub-basin, what is its relationship to barren K-feldspar-rich tuff identified by other workers as the regional tuff-type, west of HYC? This question needs to be addressed.

Possible scenarios considering differing combinations of diagenetic and hydrothermally-

derived feldspar-types are contained in figure 2. The detailed work of Logan (1979) at HYC indicates the importance of identifying overprinting relationships, which may alter the major element, trace element and isotopic geochemistry of volcaniclastic rocks, and act to camouflage the major precursor alteration events.

RESEARCH APPROACH AND PROGRESS

Are they really volcaniclastic rocks?

There is a prevailing skepticism that the resistant pink or buff siliceous or feldspathic beds in the McArthur Basin, commonly referred to as tuff or tuffite, are volcaniclastic rocks. In thin section, these rocks are very fine-grained and altered, so that petrographic texture is not always a useful criteria. However, they clearly represent something unusual within the host sediment. Other origins suggested are chemically precipitated "magadiitic" K-rich cherts, post-depositionally altered zones within the normal sediment package (with no original chemical differences), or feldspathic turbidites.

In some beds, numerous cuspate shapes have been observed that are morphologically similar to volcanic glass shards (Croxford & Jephcott 1972, Logan 1979, Davidson & Dashlooty in press). These are best preserved where they were enclosed early in the diagenetic history by biogenic pyrite or dolomite concretions. They are generally destroyed by albite, K-feldspar or carbonate replacement.

Three approaches will be used to evaluate the origin of these rocks.

(1) Macrotextures: many beds display internal structures such as grading, cross-bedding, etc which can be used as an indication of the origin of the bed.

(2) Relict crystals: many beds, although generally fine-grained, contain a suite of larger crystals which have not been replaced and can be used to indicate the origin of the bed, particularly by comparison with grains in adjacent beds. The important characters to measure are sphericity, size, presence/ absence of overgrowths, orientation, and identity, to assess the maturity of grains. Volcanic-derived crystals in airfall tuffs are euhedral or broken, or may display resorbed margins; grain-size will be graded through a bed, and a sub-bedding parallel orientation will prevail. Volcanic-derived crystals and shards deposited by mass flow processes will also be graded, but may not have a preferred orientation, depending on their position in the bed. Both types will have sharp bases and diffuse tops.

(3) Geochemistry: Davidson & Dashlooty (in press) have demonstrated that some volcaniclastic rocks in the Barney Creek Formation display regular geochemical trends and constant ratios of their high field strength elements. For instance, it has been possible to demonstrate a comagmatic source for tuffs in the HYC and Glyde Sub-basins, although these areas are 80 km apart. It remains to be determined if these trends and ratios differ to those of the enclosing sediments, but if they do, geochemistry may also be a valuable way of discriminating volcanic from non-volcanic products.

Geochemistry

A collection of volcaniclastic rocks from HYC (18 samples) supplied by Mount Isa Mines Ltd, and 10 samples from the Glyde sub-basin, has formed the starting material for geochemical research. This sample set represents (1) {HYC} material subjected to hydrothermal fluid interaction during base metal deposition, and (2) {Glyde River} possibly the least altered volcaniclastic material presently available from the McArthur Group. These rocks have been analysed for major elements, trace elements (Cu, Pb, Zn, Ba, Ni, Rb, Sr, Zr, Y, Nb, Sc, Cr, V, La, Ce, Nd, Tl, Br and As), REE (selected samples), and wholerock oxygen isotopes. Thin-sections have been prepared for all samples.

Core sampling of volcaniclastic rocks from drillholes BJ4, BB2, MY4, MY5, McA5 and McA20, all held at the NTGS core store, was aimed at obtaining "volcaniclastic" samples at varying distances from the HYC deposit. This sample set represents the background potassic alteration which is reportedly widespread west of HYC within the Barney Creek Formation. The sample set will be analysed for the element group indicated above (preparation has already commenced). Samples of the lithologies enclosing the volcaniclastic rocks will also be analysed, for comparison.

Once preparation is complete, all samples collected to date will be analysed commercially for Cl, B, and CO_2, which cannot be done at the University of Tasmania. The mineralogy of all samples will also be determined using XRD analysis.

Radiometric analysis

A four channel spectrometer borrowed from the NTGS in the 1993 season was used on core to locate areas of alkali alteration. The results of this analysis

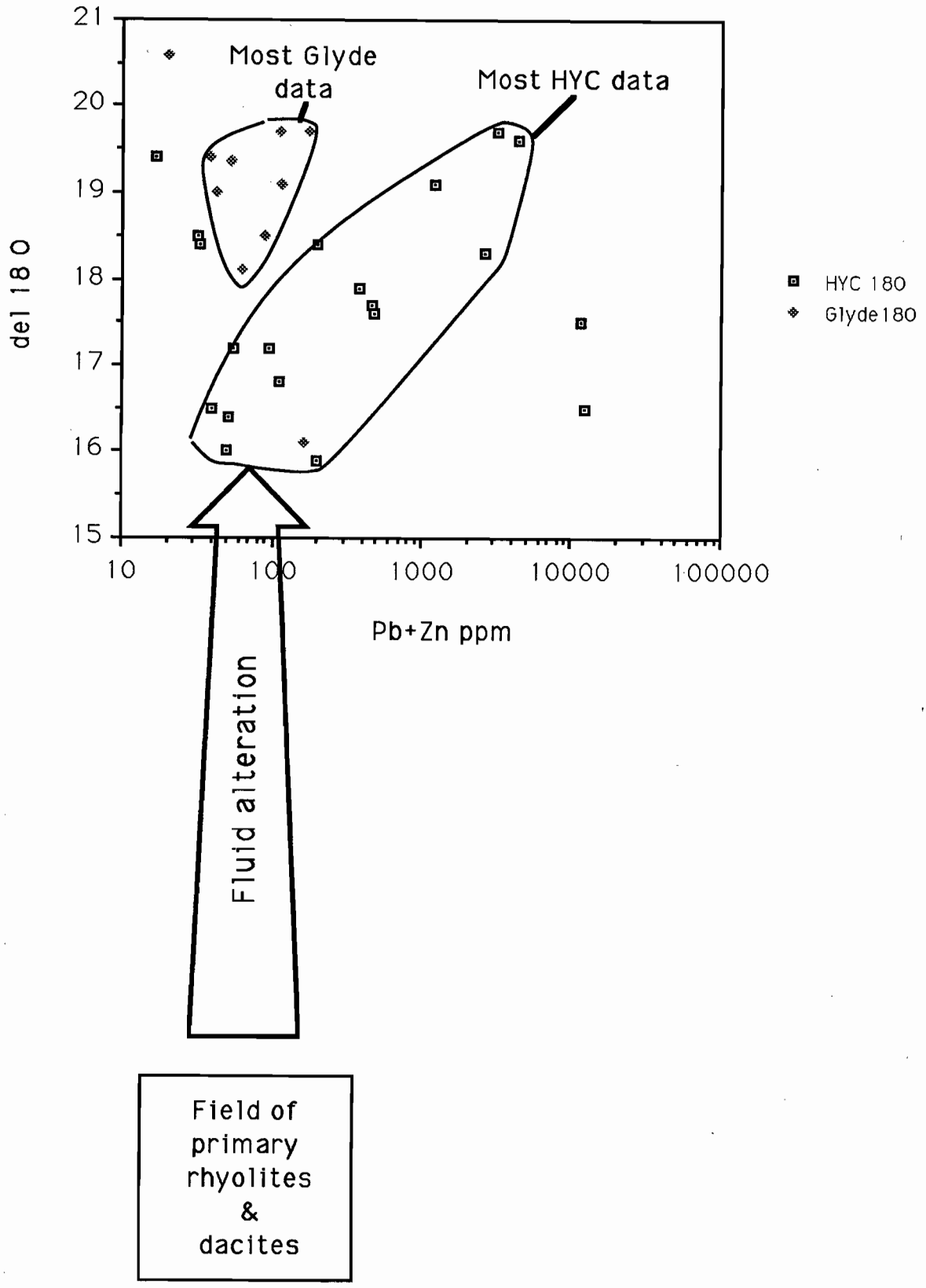

Figure 3. Wholerock oxygen isotope-(Pb+Zn) plot comparing Glyde sub-basin and HYC sub-basin volcaniclastic rocks. The two populations are notably separated at the same (Pb+Zn) value.

will be compared to geochemical data obtained from the same cores to check the validity of the radiometric method. If the results are favourable this may be the best quick method to identify potassic alteration in drillholes.

Caranbirini Prospect

A base-metal prospect geologically analogous to the HYC deposit, and occurring approximately 10km north of HYC, was investigated using NTGS open-file drill-core. The prospect is currently held by MIM Ltd. Investigation showed that two of four deep drillholes through the prospect are still available for inspection (82CA1 & 82CA4). Geological logging of these indicates substantial areas of dolomitic alteration, associated with base metal enrichment, affecting a breccia analogous to the Cooley Dolomite Member, adjacent to Barney Creek Formation, Reward Dolomite, and Lynott Formation. No tuffaceous or potentially tuufaceous beds were identified. Substantial total count gradients occur within the breccia and the overlying sediments, indicating that alkali element zonation may be a feature of the alteration. Future work will examine the nature and conditions of the alteration and veining. The prospect has many features in common with the upper portions of the HYC ore-system. The causes of the alkali element zonation will be determined using major element geochemistry and XRD analysis. The stratigraphically lower portions of this prospect are very deep and yet to be drilled.

Stable isotope geochemistry

Whole rock oxygen isotope analysis of volcaniclastic material can provide information on fluid oxygen isotope compositions (an indicator of fluid source), the amount of fluid involved in the alkali alteration process, the shape of mineralising systems, and temperatures (mineral pairs are required). This type of work has been carried out around VMS ores with some success, but has not yet been applied to shale-hosted Pb-Zn systems.

Whole rock oxygen isotope analysis identifies two separate populations for tuff in the HYC and the Glyde Sub-basins. Both populations have experienced significant oxygen isotope exchange, hence it is incorrect to consider the Glyde Sub-basin samples to be unaltered, although the major element compositions seem to be relatively primary.

The HYC data suggest a complex fluid interaction pattern. In the simplest systems, a rock in contact with the hottest fluid in an ore system will be the most isotopically depleted (have the lowest $\delta^{18}O$ values). If base metal contents correlate with the hottest part of any hydrothermal system, a negative correlation between base metals and $\delta^{18}O$ would be expected. Exactly the opposite occurs at HYC (Fig. 3), suggesting either that base metals were not deposited by cooling, or that samples containing the greatest Pb+Zn have been systematically enriched in $\delta^{18}O$ after their deposition. This might occur if a lower temperature, less extensive fluid overprinted higher temperature alteration close to the Emu Fault, as documented by Logan (1979). XRD mineralogic analysis will provide further insights into this problem, and interpretation is continuing.

RESEARCH OBJECTIVES IN 1994 (G.DAVIDSON, HALF-TIME ON THE PROJECT)

1. Complete the geochemical analysis of materials which were collected in 1993, as outlined above.

2. Attempt to determine the conditions of alkali alteration using fluid inclusions, stable isotopes, and geochemical modelling (in collaboration with David Cooke).

3. Airborne radiometrics will be used as the basis for fieldwork in 1994. In particular, units with a high or variable K-channel response will be examined with a spectrometer on the ground, and samples taken for geochemical analysis. The aim is to determine if airborne radiometrics can provide real information on the extent of alkali alteration in the McArthur Group, and hence constrain models of fluid circulation.

4. Petrographically and geochemically analyse samples from the Caranbirini prospect, to gain first-hand information on the development of an HYC-like system.

5. Complete a review of fluid circulation and geothermal activity in modern intracontinental rifts.

6. Formulate a model of alkali element enrichment for the McArthur Group which explains the observations made in this and other studies.

REFERENCES

Adshead, N. (1993) Geol. Soc. Aust. Abs. 35, 52–53.
Agron N. & Bentor Y.K. (1981) J. Geol. 89, 479–495.
Beardsmore, T. J. (1988) Geol. Soc. Abs. 21, 55–56.
Beeson R., Berg R.C. & Crase N.J. (1989) Mineral. Deposita 24, 299–307.
Boles J.R. & Surdam R.C. (1979) Amer. J. Sci. 279, 832–853.
Corbett J.A., Lambert I.B. & Scott K.M. (1975) CSIRO Tech. Comm. 57.

Crick I.H., Boreham C.J., Cook A.C. & Powell T.G. (1988) *American Association of Petroleum Geologists Bulletin* **72**, 1495–1514.

Croxford N.J.W. (1964) Trans. Inst. Min. Metall. 74, 34–43.

Croxford N.J.W. & Jephcott S. (1972) Proc. Australas. Inst. Min. Metall. 243, 1–26.

Davidson G.J. (1989) (Ph.D) Starra and Trough Tank: iron-formation-hosted gold-copper deposits of northwest Queensland, Australia. (Unpubl.), University of Tasmania, 380 p.

Davidson, G.J., Large, R.R., Kary, G.L. & Osborne, R. (1989) Econ. Geol. Mon. 5, 135–150.

Davidson G.J. & Dashlooty S., in press, Australian Journal of Earth Sciences.

Dashlooty & Davidson G.J. (1986) Geol. Soc. Aust. Publ. 15, (abs.), p.54.

Deike R.G. & Fones B.F. (1980) In Nissenbaum A. (ed.) Hypersaline brines and evaporitic environments; Developments in Sedimentology 28, 167–193.

Hay R.L., Lee M., Kolata D.R., Matthews J.C. & Morton J.P. (1988) Geology 16, 743–747.

Jackson M.J., Muir M.D. & Plumb K.A. (1987) BMR Bulletin 220.

Krebs W. (1981) In Wolf K.H. (ed.) Handbook of strata-bound and stratiform ore deposits, 9, 509–549.

Large D. & Finlow-Bates T. (1982) The geochemistry of tuffites and volcanic debris in the Proterozoic ore-bearing sedimentary rock sequences of Northern Australia. Billiton unpubl. Rpt.

Lindley I.J. & Chapin C.E. (1986) Intern. Volcanolog. Congress Proc. 5: volcanism, hydrothermal systems and related mineralisation (abs), p. 100.

Logan R.G. (1979) The geology and mineralogical zoning of the H.Y.C. Ag-Pb-Zn deposit, McArthur River, Northern Territory, Australia. M.Sc thesis (ANU).

Moine B., Sauvan P. & Jarousse J. (1981) Cont. Miner. Pet. 76, 401–412.

Muir M.D. (1983) In Sangster D.F. (1983) Sediment-hosted stratiform lead-zinc deposits, Mineralogical Ass. of Canada, 141–174.

Roddy M.S., Reynolds S.E., Smith B.M. & Ruiz J. (1988) Geol. Soc. Am. Bull. 100, 1627–1639.

Senderov E.E. (1973) Geochem. Intern. 12, 1831–1837.

Sheppard R., & Gude A. (1968) U.S. Geol. Surv. Prof. Paper 587, 38 p.

Stamatakis M.G. (1989) Econ. Geol. 84, 788–798.

Vogt J.H. & Stumpfl E.F. (1987) Econ. Geol. 82, 805–825.

Wallace M.W., Gostin V.A. & Keays R.R. (1990) Geology 18, 132–135.

Transport and deposition of base metals from high temperature (250°C) sedimentary brines

David R. Cooke
Centre for Ore Deposit and Exploration Studies

SUMMARY

Numerical simulations of transport and depositional processes for high temperature (250°C) moderate salinity (10 eq. wt. % NaCl) sedimentary brines have revealed that significant base metal transport can occur in acidic oxidised, alkaline oxidised, and acidic reduced brines. Moderate salinity alkaline, reduced brines are not capable of carrying sufficient quantities of base metals to be important in sediment-hosted base metal deposit formation. Hematitic sandstones provide excellent aquifers for oxidised metalliferous brines. In contrast, significant alteration to potassic and/or propylitic assemblages will occur when brines interact with mafic volcanics. High temperature mineralised brines can migrate significant distances along faults without dumping their base metal load, provided the fluids do not interact significantly with the surrounding wallrocks. Cooling and/or boiling of these metal-rich fluids during cross-stratal transport will produce barren quartz veins. In the trap environment, mixing of metalliferous brines with anoxic seawater is an excellent mechanism for producing Zn-Pb-rich massive sulfide mineralisation. Mixing of the same brines with oxidised seawater produces siliceous Cu-Ag-rich exhalites. Interaction of reduced, acidic brines with pyritic dolomitic sediments results in the precipitation of simple Zn-Pb-rich sulfide mineralisation. More complex silicates are produced together with the base metal sulfides when the replacement process involves oxidised brines.

INTRODUCTION

The solubility of base metals as chloride complexes is highly dependent on the temperature, salinity, oxygen fugacity and pH of the transporting fluid. As part of an on-going study into the metal-carrying capacities and likely depositional mechanisms for various hypothetical 'sedimentary' brines, this report documents base metal transport and deposition from moderately acid and alkaline, reduced and oxidised saline brines at 250°C. The next report in this series will discuss the metal-carrying capacity of lower temperature (150°C) brines.

METHOD

Hypothetical brine compositions are calculated by making initial assumptions about the fundamental intrinsic parameters of the fluid (T, salinity, pH, oxygen fugacity, ΣS, ΣC). Forced mineral equilibration calculations are undertaken using SOLVEQ (Reed, 1982; Spycher and Reed, 1990) to add additional chemical components to the brine. If a component is too soluble (eg. Ba^{+2} in reduced fluids), forced mineral equilibration calculations will fail, and the concentration of that component must be taken from a modern published brine composition (eg. the Salton Sea brines) or assumed (see discussion about base and precious metals in sedimentary brines).

The components included in all calculations are:

- H^+ H_2O Cl^-
- HCO_3^- SO_4^{-2} $SiO_{2\,(aq)}$
- Al^{+3} Ca^{+2} Mg^{+2}
- Fe^{+2} Na^+ K^+
- Zn^{+2} Cu^+ Pb^{+2}
- Ag^+ $AuCl_2^-$ Ba^{+2}
- HS^- (reduced fluid) or $O_{2\,(aq)}$ (oxidised fluid)

Numerical simulations of transport and depositional processes (cooling, boiling, fluid

Codes: AMIRA / ARC Project P.384 - Proterozoic sediment-hosted base metal deposits. November 1993

mixing, water-rock interaction) are undertaken using the CHILLER software package (Spycher and Reed, 1990).

Base and precious metals in sedimentary brines

Previous workers have suggested that to form an economic mineral deposit, hydrothermal fluids must be carrying at least 1 - 20 ppm Zn, Pb or Cu, or 1 - 10 ppb Au in solution (the 'ore-forming window'; Roedder, 1960; Cooke *et al.*, 1993; Fig. 1). If metal concentrations are below these levels, then either a vast (most likely geologically unreasonable) quantity of fluid is required to form economic mineralisation in a single-pass fluid model, or continual dissolution and repricipitation of ore minerals must occur in a multistage model, requiring a long-lived hydrothermal system with fluid conduits that remain open, for the sulfides to be upgraded to economic concentrations.

Fluids that can carry in excess of 20 ppm base metals or more than 10 ppb Au are excellent transporting solutions. Evidence for the existence of high metal solubilities in hydrothermal fluids includes analyses of fluid inclusions in sphalerite from Creede, Colorado (up to 1.1% Zn and 0.9% Cu) and analyses of the Salton Sea geothermal brines (up to 540 ppm Zn and 102 ppm Pb; Skinner, 1979). High solubilities can, however, lead to a source rock problem, where there is not enough metal available to be leached from the source rocks to allow saturation of the fluid. In these cases, the fluids are likely to remain undersaturated (even grossly undersaturated in some cases) until sufficient chemical changes occur to lower the solubilities of the metals in solution. If an efficient trap mechanism is not met, the fluids may gradual dump their base metal load, resulting in a large (even basin-wide?) geochemical anomaly but no economic mineralisation. Possible examples where this may have occurred are the metalliferous black shales from the Upper Pennsylvanian of Indiana, Kansas and Missouri (up to 0.34% Zn), and the Upper Devonian - Lower Mississipian New Albany Shale, which contain up to 0.92% Zn, 0.10% Pb and 0.02% Cu (Schultz, 1991).

In this study, Zn, Pb, Cu, Ag and Au concentrations are determined by forced mineral equilibration techniques for low metal solubility fluids. When fluids are capable of carrying more than 100 ppm Zn, Pb, or Cu, the base metal concentration is fixed at 100 ppm, allowing various depositional mechanisms to be tested for their effectiveness at extracting large quantities of base metals from solution. While concentrations of 100 ppm may seem excessive, this method allows us to assess whether a particular mechanism is capable of efficiently extracting base metals from solution. If the process cannot precipitate economic base metal mineralisation from a metal-rich solution, then it will not be able to produce economic mineralisation from less metalliferous brines. Using the same logic, an upper limit for Ag concentrations have been arbitrarily set at 1 ppm. In contrast, the upper limit for Au has been set at 0.01 ppb; lower than the 'ore-forming window' values of 1 - 10 ppb. This value was chosen because gold is not present in economic concentrations in sediment-hosted base metal deposits. Most likely, the fluids that form these deposits are either incapable of carrying ppb Au, or there is a source rock problem that prevents fluids from leaching enough Au to attain ppb levels.

Advantages and Disadvantages of this Technique

This unconventional approach to modelling hydrothermal systems has several advantages and disadvantages over more conventional approaches. By testing a large number of chemical and physical parameters, this technique allows us to predict what types of brines are capable of forming sediment-hosted base metal deposits, circumventing (to some extent) the problems caused by a dearth of fluid inclusion information. Testing a wide variety of depositional processes allows us to establish which mechanisms (cooling, replacement, fluid mixing) are likely to be most effective at extracting base metal mineralisation from solution and to predict likely mineral assemblages in the feeder systems. It also allows us to examine the perennial problem of depth of formation for these systems from a different perspective, by examining what mineral assemblages would be produced if the fluids did boil in the subsurface. By modelling water-rock interaction between the brines and known lithologies from sedimentary basins, it is possible to assess whether a given brine can be transported along an aquifer within the basin without undergoing significant modification. Where the brine compositions are modified, we can predict how the brine should evolve during prolonged interaction with that lithology. The approach has significant implications for exploration, because it is capable of predicting new types of exploration targets that have not previously been considered in sedimentary basins.

The major disadvantage of this technique is that the actual brine compositions responsible for the formation of deposits such as HYC and Mt. Isa may never actually be simulated, because of the vast array of possible fluid compositions. If one or more of the initial assumptions (eg. ΣS, ΣC, T, salinity, etc) is incorrect, then the mineral assemblages predicted during simulations of depositional processes may be totally unrealistic. Depending on basin lithologies, the hypothetical brine

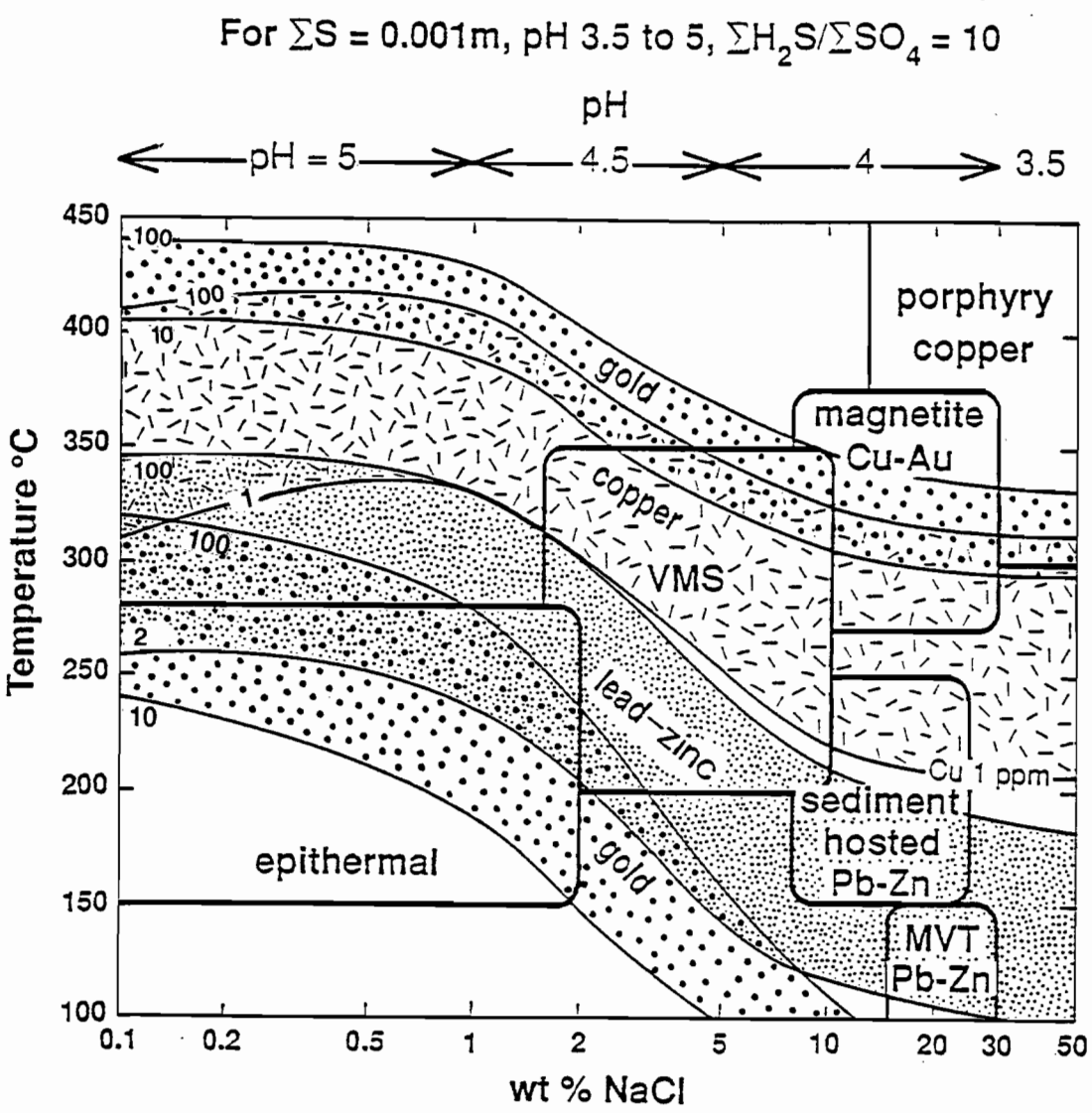

Figure 1. Temperature-salinity diagram demonstrating the relationship between fluid chemistry, metal-carrying capacity and ore deposit style. The zones of gold (1 - 100 pbb) and base metal deposition (1 - 100 ppm) are based on thermodynamic modelling of a solution with $\Sigma S = 0.001m$, $\Sigma H_2S / \Sigma SO_4^{-2} = 10$ and pH = 3.5 to 5. After Large (1992).

compositions may never have been able to form within that sedimentary basin (this could be tested by modelling brine-aquifer interaction). Equilibrium may never have been attained by the fluids (eg SO_4^{-2}/H_2S disequilibrium in low T fluids), possibly invalidating the simulations (there is currently no way to resolve the problem of disequilibrium in hydrothermal fluids). Other perennial problems that are not currently resolvable include the quality of thermodynamic data (ranges from good to poor to non-existent), our understanding of metal speciation in hydrothermal fluids (good to poor), precious metal substitution into sulfide lattices (eg. argentiferous galena and sphalerite), reaction kinetics (probably very important at low temperatures) and the currently-used methods of determining activity coefficients for aqueous species (calculations become increasingly dubious at higher salinities).

Even with all the problems outlined above, the technique still provides highly interesting (even provocative!) results. Although no simulation to date has produced a 'classic' sediment-hosted base metal deposit, the results provide invaluable insights into the processes that might control base metal transport and deposition. They also provide an insight into the behaviour of elements such as Fe, Mn and Ba that can form halos around mineralisation. An alternative technique that could be applied involves taking a brine of known composition (eg. the U.S. oil field brines) and try to evolve it into a mineralising solution. However, the oil field brines are renowned for their *incapacity* to transport base metals in solution. They are not

known to be associated with any significant base metal mineralisation, and any efforts to theoretically modify those brines to solution compositions that are capable of carrying base metals are probably just as artificial as trying to predict initial brine compositions from first principles.

INITIAL PARAMETERS

The starting parameters for the numerical simulations documented in this report are as follows:

- Temperature: 250°C
- Salinity: 10 eq. wt. % NaCl (8.16 wt % NaCl + 1 wt % KCl + 1 wt % $CaCl_2$)
- pH: 1 unit acid; 1 unit alkaline (relative to K-spar - muscovite)
- ΣS: 0.001 molal
- Redox state: reduced (pyrite field; $\Sigma H_2S/\Sigma SO_4^{-2} = 1000$); oxidised (hematite field; $\Sigma H_2S/\Sigma SO_4^{-2} = 0.01$)
- 'Dissolved CO_2: 1 molal

A total of four initial fluid compositions have been calculated (Table 1). They can be classified in general terms as (1) acid, oxidised; (2) acid, reduced; (3) alkaline, oxidised; (4) alkaline, reduced. Three of these brines are excellent transporting solutions for Zn, Pb and Ag (brines 1, 2 and 3). One is also an excellent transporting solution for Cu (brine 1), and two others are capable of carrying sufficient quantities of Cu to form economic mineralisation (brines 2 and 3), provided that Cu is at or close to saturation levels in the fluids. Brine 4 is incapable of carrying significant Zn, Pb or Cu - much higher salinities would be required at 250°C for a reduced, alkaline brine to be able to carry reasonable quantities of base metals in solution. It is worth noting, however, that significant Ag can be transported by brine 4, and there is some potential for this type of brine to form economic Ag or Ag-Au (epithermal?) mineralisation.

TRANSPORT AND DEPOSITIONAL PROCESSES

A series of numerical simulations have been conducted for each of the four brines listed in Table 1. These processes test the effects of various transport and depositional processes and can be subdivided into three categories:

Aquifer transport

To establish whether brines 1 - 4 could pass along a stratigraphic aquifer in a sedimentary basin without undergoing major chemical modifications, a series of water-rock interaction simulations have been undertaken at 250°C. The lithologies chosen for these calculations are (A) 'evaporite' (80% anhydrite, 10% quartz, 10% graphite); (B) hematitic sandstone (80% quartz, 10% muscovite, 10% hematite); and (C) mafic volcanic (50% anorthite, 10% albite, 35% pyroxene, 5% magnetite). Reactive components were deliberately exaggerated in some lithologies to ensure that they were potentially reactive (eg. 10% graphite in the 'evaporite'). Where possible, calculations continued to the point where the fluid had equilibrated with the aquifer. Other lithologies that remain to be tested by this technique include felsic volcanics, carbonates (dolomites and limestones) and red shales.

Cross-stratal transport

Chemical changes that may occur during cross-stratal brine migration along faults have been investigated by simulations of: (D) conductive cooling (250°C to 50°C) and (E) isoenthalpic boiling (250°C to 100°C). In these simulations, the fluids are assumed to be chemically isolated from the surrounding wallrocks. Such a situation could arise if the fluids rise rapidly along the fault, or if initial precipitation of quartz occurs along the walls of a fault. This *silica mantling* can effectively seal any later fluids from interaction with the wallrocks adjacent to the fault.

Depositional processes at the trap site

Simulations of potential base metal depositional mechanisms for sedimentary brines have been undertaken to test both syngenetic (fluid mixing, cooling) and diagenetic (replacement) depositional models. Individual scenarios are: (F) mixing with cold (5°C) oxidised seawater; (G) mixing with cold (5°C) anoxic seawater; (H) reaction with pyritic dolomitic siltstone (40% quartz, 40 % muscovite, 10 % dolomite, 10% pyrite); (I) interaction with pyritic dolomite (80 % dolomite, 10% pyrite, 10 % quartz); and (J) reaction with pyrite-rich carbonaceous dolostone (40% dolomite, 40% pyrite, 10% quartz, 10 % graphite). As for the aquifer transport simulations, some simulations involve abundant reactive components (eg. graphite, pyrite) to test their controls on base metal deposition.

	(1) - Acid, oxidised brine	(2) - Acid, reduced brine	(3) - Alkaline, oxidised brine	(4) - Alkaline, reduced brine
pH	4.13	4.13	6.13	6.13
Salinity	10.0 wt %	10.0 wt %	10.0 wt %	10.0 wt %
ΣS	0.001	0.001	0.001	0.001
log $f_{(O_2)}$	-31.50	-34.47	-33.50	-36.50
H^+	229.1	229.9	204.4	206.0
H_2O	1 kg	1 kg	1 kg	1 kg
Cl^-	60718.2	60733.4	60675.7	60689.3
SO_4^{-2}	85.53	2.190	85.47	
HCO_3^-	13861.5	13865.0	13851.8	13854.9
HS^-	-	29.28	-	29.26
$SiO_{2\ (aq)}$	*328.3*	*328.4*	*330.7*	*330.6*
Al^{+3}	*.047*	*0.049*	*0.041*	*0.042*
Ca^{+2}	3614.4	3615.4	*58.72*	*64.05*
Mg^{+2}	36.03	36.04	*0.390*	*0.422*
Fe^{+2}	*629.1*	*77.89*	*0.245*	*0.236*
K^+	5249.7	5251.0	5246.0	5247.1
Na^+	30298.3	30758.4	36680.2	36719.3
Mn^{+2}	1391.2	1391.5	*19.62*	*21.45*
Zn^{+2}	**100.1**	**100.1**	**100.0**	*0.092*
Cu^+	**100.1**	*1.788*	*6.484*	*0.008*
Pb^{+2}	**100.1**	**100.1**	**100.0**	*0.036*
Ag^+	**1.00**	**1.00**	**1.00**	*0.158*
$AuCl_2^-$	0.000014	0.000014	*2.46 E-07*	0.000014
Ba^{+2}	1.001	1.001	1.001	1.001
$O_{2\ (aq)}$ *	4.98 E-35	7.48 E-38	4.95 E-37	6.91 E-40

Table 1: Modelled brine compositions at 250°C. Component species concentrations are in ppm, except for $O_{2\ (aq)}$ and ΣS, which are given as molal units. Brines 1 and 3 are oxidised fluids (hematite stable: $a(H_2S) / a(SO_4^{-2}) = 0.01$). Brines 2 and 4 are reduced fluids (pyrite stable: $a(H_2S) / a(SO_4^{-2}) = 1000$). Brine compositions have been calculated based on the assumptions outlined above. **Bold type** indicates that although the fluids are undersaturated with a given metal, the concentration of that metal has been set at the upper limits of the ore-forming window (100 ppm for base metals, 1 ppm for Ag) - i.e the fluid is an **excellent** transporting solution for that metal. *Italics* indicates that total concentrations of component species have been calculated by forcing equilibration between the brines and the following minerals: $SiO_{2\ (aq)}$ - quartz; Al^{+3} - muscovite (brines 1 and 2) or K-feldspar (brines 3 and 4); Ca^{+2} - calcite (brines 3 and 4); Mg^{+2} - dolomite (brines 3 and 4); Fe^{+2} - hematite (brines 1 and 3) or pyrite (brines 2 and 4); Mn^{+2} - rhodochrosite (brines 3 and 4); Zn^{+2} - sphalerite (brine 4); Cu^+ - chalcopyrite (brines 2 and 4) or chalcocite (brine 3); Pb^{+2} - galena (brine 4); Ag^+ - acanthite (brine 4); $AuCl_2^-$ - gold (brine 3). Na^+ has been adjusted to maintain charge balance in the fluids, and Ba^{+2} concentrations are set at 1 ppm. For brines 1 and 2, Mn^{+2} and Mg^{+2} concentrations are set at 1390 ppm and 36 ppm respectively based on measured concentrations from the Salton Sea geothermal brines (listed in M^{c}Kibben and Williams, 1989).

In addition to its implications for cooling within a fault, the results of simulation (D) are also applicable to a brine pool depositional model, whereby high T brines discharge and disperse within a cool (50°C) high salinity brine pool. In this setting, the dominant control on ore deposition will be cooling due to heat conduction across the brine-seawater interface and into the underlying rock pile.

RESULTS

Due to the vast amount of information generated by CHILLER during a single numerical simulation, it is not possible to document in detail the behaviour of each of the individual 126 aqueous species, 20 component species, 8 gases and hundreds of mineral phases that are involved in each

Aquifer	Brine	Cu (%)	Pb (%)	Zn (%)	Ag (%)	Au (%)	Ba (%)	Mn (%)
Evaporite	acid, oxidised *	100	100	99	71	-	-	97
	acid, reduced *	84	100	99	73	-	-	85
	alkaline, oxidised*	100	100	100	88	4	-	-
	alkaline, reduced*	-	41	5	15	-	-	-
Hematitic sandstone	acid, oxidised	-	-	-	-	-	-	-
	acid, reduced	*65*	45	-	-	-	-	-
	alkaline, oxidised	-	-	-	-	-	-	-
	alkaline, reduced	33	-	-	-	-	-	-
Mafic volcanic	acid, oxidised *		-	-	86	100	-	71
	acid, reduced *	*63*	63	27	40	84	-	*0.3*
	alkaline, oxidised*	72	67	35	54	0.4	-	-
	alkaline, reduced*	33	-	-	-	-	-	-

Table 2: Percentage of total metal in solution extracted during water-rock interaction calculations. For each simulation, small increments of rock (0.1, 0.5, 1 and 5 grams) were progressively titrated into approximately one kilogram of brine until equilibrium was reached. * - indicates the reaction did not progress to completion. Numbers in **bold type** indicate efficient extraction of a metal over a small titration increment (i.e. the process is an efficient trap mechanism that could result in the deposition of economic concentrations of that metal). Numbers in *italics* indicate that the metal was extracted inefficiently (i.e. over a large number of titration increments) - the process is an inefficient trap mechanism that is unlikely to form an ore deposit. Numbers in plain type indicate that the metal was never present in sufficient quantities in the initial solution to be deposited in economic concentrations.

Process	Brine	Cu (%)	Pb (%)	Zn (%)	Ag (%)	Au (%)	Ba (%)	Mn (%)
Cooling (250° - 50°C)	acid, oxidised	*0.01*	-	-	-	100	-	-
	acid, reduced	*92*	*94*	-	100	100	-	-
	alkaline, oxidised	*0.3*	-	-	*10*	100	-	-
	alkaline, reduced	0.5	100	100	100	-	-	-
Boiling (250° - 100°C)	acid, oxidised	*1.9*	-	-	-	100	-	-
	acid, reduced	*88*	*27*	-	93	100	-	-
	alkaline, oxidised	*	*	*	*	*	*	*
	alkaline, reduced	100	100	100	100	-	100	98

Table 3: Percentage of total metal in solution extracted during cooling and boiling simulations for brines 1 to 4. Cooling increments of 5°C were used for each simulation. Numbers in **bold type** indicate efficient extraction of a metal over a small temperature interval (i.e. the process is an efficient trap mechanism that could result in economic concentrations of that metal). Numbers in *italics* indicate that the metal was extracted inefficiently (i.e. over a large temperature range) - the process is an inefficient trap mechanism that is unlikely to form an ore deposit. Numbers in plain type indicate that the metal was never present in sufficient quantities in the starting solution to deposit economic concentrations of metals. * - indicates that the simulation was unsuccessful.

calculation. Instead, this discussion is restricted to the *extraction efficiency* of various processes for the base metal (Zn, Pb, Cu), precious metal (Ag, Au), and two halo-forming components (Ba, Mn) in the initial hydrothermal solutions. The most efficient processes for extracting metals from a brine are most likely to be important depositional mechanisms. For the more favourable simulations, discussions of the solid phases that saturate during individual simulations are also provided, as this is a useful way of evaluating whether a given simulation is producing geologically realistic results.

Aquifer transport models

Table 2 lists the percentage of total metal extracted from solution during brine interaction with an evaporite (80% anhydrite, 10% quartz, 10% graphite), a hematitic sandstone (80% quartz, 10% hematite, 10% muscovite) and a mafic volcanic aquifer (50% anorthite, 10% albite, 35% pyroxene, 5% magnetite). Equilibrium was only achieved during calculations involving the hematitic sandstone. While the evaporite and the mafic volcanic proved too reactive for the fluids to fully equilibrate with, these simulations progressed far enough to allow comments to be made about the potential of the units as aquifers.

A: Evaporite

An anhydrite-rich carbonaceous evaporite bed is a poor aquifer for metalliferous brines; indeed, it would act as an excellent trap to fix base metals from solution. If a metal-rich brine similar in composition to brines 1 - 3 interacted with an anhydrite-rich evaporite for any significant period of time, the metal-carrying capacity of those brines would be effectively destroyed as the fluids came into equilibrium with the wall rock. Similarly, interaction of the evaporite with a metal-deficient reduced brine (eg. brine 4) will also fix metals out of solution, further lowering the metal-transporting ability of that fluid.

The 'evaporite' lithology chosen for these simulations is probably not representative of typical evaporites because it contains abundant graphite (10 wt. %), an organic matter analogue. Complex silicate (quartz ± muscovite), sulfide (pyrite, alabandite, sphalerite, galena, acanthite, Cu-sulfides), carbonate (calcite ± dolomite) and sulfate-bearing mineral assemblages were precipitated during reaction of the fluids with the evaporite. However, reactions of the acidic brines (1 and 2) with this lithology resulted in the deposition of large quantities of alabandite (MnS). Stratabound manganese sulfide deposits are not recognised in the geologic record, indicating that the predicted mineral assemblages are unrealistic. Future calculations will incorporate an improved evaporite mineralogy.

B: Hematitic sandstone

Hematitic sandstones can act as excellent aquifers for acid, oxidised metalliferous brines. Table 2 indicates that no metals precipitated during reaction of brine 1 with the sandstone. Figure 2*A* illustrates that the fluid and wallrocks equilibrated at the end of the first reaction increment (0.01 grams), and that no additional minerals were deposited (i.e. no wall rock alteration produced).

Oxidation of the pyrite-stable acidic, reduced brine occurred during interaction with the hematitic sandstone. A pyritic alteration zone developed as the reduced brine first came into contact with the sandstone (Figure 2*B*). Almost half of the Pb in solution precipitated as galena, and subeconomic chalcopyrite deposition also occurred (Table 2). At the end of the simulation, the resultant brine still contained 100 ppm Zn, > 50 ppm Pb and 1 ppm Ag, so it is still an excellent mineralising solution, although the Zn/Pb ratio of the brine changed significantly. This process could produce a sandstone-hosted Pb deposit as the brine migrates along the sandstone aquifer, if fluid flow is focussed enough.

Although a hematitic sandstone provides an excellent transporting medium for alkaline, oxidised metalliferous brines (Table 3), the presence of muscovite in the sandstone causes the pH of the solution to drop until the brine equilibrates with its surroundings. This results in a K-feldspar alteration zone developing at the expense of detrital muscovite (Figure 2C). An arkosic hematitic sandstone would provide a better aquifer for brines of this nature.

Brine 4 (alkaline, reduced) is significantly out of equilibrium with the hematitic sandstone, and reaction of the fluid with the wallrock produces an extensive K-feldspar-carbonate alteration zone (Figure 2*D*). Minor chalcopyrite deposition occurs during this simulation.

C: Mafic Volcanics

As for the evaporite, the mafic volcanics composition (anorthite, albite, diopside, magnetite) proved too reactive for full equilibrium to be calculated between the brines and the aquifer. Much of the copper and lead and significant quantities of zinc were extracted from brines 2 and 3 during the initial stages of the simulations (over 70 grams of rock added). No metals had been extracted from the acid, oxidised brine by the time

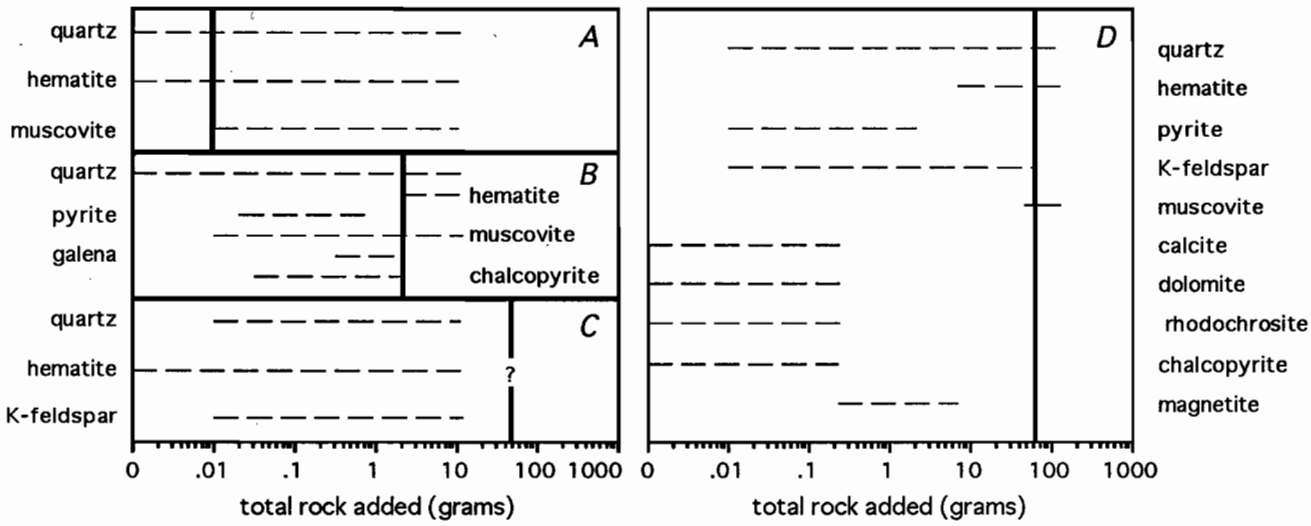

Figure 2: Mineral precipitation sequence calculated for interaction of brines 1 to 4 with a hematitic quartz sandstone. *A* - Brine 1 (acid, oxidised). *B* - Brine 2 (acid, reduced). *C* - Brine 3 (alkaline, oxidised). *D* - Brine 4 (alkaline, reduced). The bold vertical lines indicate the point at which equilibrium is attained between the fluids and the wallrock. Note that the reaction between brine 2 and the sandstone was not taken to completion, so muscovite did not stabilise.

the simulation ceased (after 421 grams of rock had been added). However, it is not possible to conclude that the mafic volcanics would pass a fluid of this composition without causing it to dump its metal load, because the metals may have been precipitated during later stages of water-rock interaction. Brine 4 (reduced, alkaline) precipitated minor copper mineralisation and abundant carbonates prior to failure of the simulation at 81 grams.

Biotite, talc, actinolite, epidote and carbonates were precipitated in conjunction with quartz, sulfides, feldspars and muscovite during the brine/mafic volcanic calculations. Actinolite, talc and biotite have most likely substituted for chlorite, which has poor quality thermodynamic data that prevents it from saturating during these simulations. Overall, the styles of alteration produced during interaction of the brines with mafic volcanics are K-silicate (K-feldspar and/or muscovite-dominated), and propylitic.

Cross-stratal transport models

The total metal precipitated during conductive cooling (250 - 50°C) and isoenthalpic boiling simulations (250 - 100°C) are listed in Table 3. Note that due to computational problems, it was not possible to simulate boiling of the alkaline, oxidised brine (Table 3).

D: Conductive cooling

Cooling of brine 1 (acid, oxidised) from 250° to 50°C did not remove any Zn, Pb or Ag from solution (Table 3). Furthermore, only 0.01% of the total Cu in solution was precipitated as chalcocite. Similarly, brine 3 (alkaline, oxidised) did not dump any Pb or Zn, and only 0.3 % total Cu (as chalcocite) and 10 % total Ag (as native silver) were precipitated during cooling (Table 3). These surprising results are due to the oxidised nature of the fluids, which were maintained throughout the cooling simulations. Oxidised, saline conditions favour high base metal solubilities even at low temperatures (eg. red-bed Cu deposits), and base metals would only be extracted from these fluids if they encountered a reductant or underwent significant dilution.

Conductive cooling of the acid, oxidised brine resulted in quartz deposition (99.7% of total material precipitated) with minor muscovite, chalcocite and gold. Similarly, brine 3 (alkaline, oxidised) precipitated quartz (99.8%) and minor K-feldspar, silver, chalcocite, hematite, muscovite and gold. Cooling of either brine type without any significant wallrock interaction would produce essentially barren quartz veins. The major implication from this results is that barren quartz veins in an oxidised basin (eg. the Tawallah Group sandstones) could have acted as feeders for hot (250C) metal-rich oxidised brines that dumped their loads in stratigraphically higher positions, when a suitable trap environment was encountered.

Cooling of the acid, reduced brine results in the precipitation of a quartz (70%) - galena (24%) - pyrite (5%) vein with traces of chalcopyrite, acanthite, graphite, bornite, muscovite, chalcocite and gold. Most of the Pb, Cu and Au in solution is inefficiently extracted (Table 3) over a wide

temperature interval, probably representing deposition over a 1 - 2 km vertical interval along faults through the upper crust. Ag was completely extracted over a 15°C cooling interval, and could form economic mineralisation by this process. Note that zinc again remained in solution throughout the cooling simulation. In this case, the acidic pH and high salinity of the brine, rather than the oxidation state of the fluid, allows high zinc solubilities at low temperatures.

Precipitation of a quartz vein (96.6 % quartz) with traces of graphite (2.9%), pyrite, K-feldspar, calcite, sphalerite, acanthite, galena, chalcopyrite, dolomite and muscovite occurred during 200°C of cooling of the reduced, alkaline brine. This process completely removed all Pb, Zn and Ag from solution (Table 3), but the low initial metal concentrations in the fluid only allow traces of base metals to be deposited. Ag was extracted as acanthite over a small temperature interval, suggesting that this process could produce economic epithermal-style Ag-rich quartz veins.

E: Isoenthalpic boiling

The boiling simulation for brine 1 (acid, oxidised) produced similar results to the equivalent cooling simulation. The only minerals precipitated over 150°C of boiling-induced cooling were quartz (96%), hematite (3%), and traces of chalcocite (0.8%), muscovite and gold. On mineralogical grounds, a vein precipitated from a boiling brine of this nature would be indistinguishable from a vein deposited by cooling of the same brine, although vein textures or fluid inclusions may provide some indication that boiling had occurred. Once again, no significant base metal deposition occurred (only 1.9 % total Cu, no Pb, Zn or Ag; Table 3), although gold was completely stripped from solution due to the strong temperature dependence of the gold chloride complex. These results indicate that 250°C acid, oxidised metalliferous brines can travel significant distances along structures, cooling and/or boiling along the way, without dumping their metal load provided that no reactive lithology or subsurface groundwater is encountered.

Deposition of Cu, Pb, Ag and Au occurred during boiling of the reduced, acid brine, but only Ag was deposited over a small enough temperature interval to possibly form economic vein-style mineralisation (Table 3). The simulation predicts a quartz (89%) - galena (9.4%) - chalcopyrite (1%) vein, with traces of muscovite, acanthite, bornite and gold. As for the equivalent cooling simulation, Zn remained in solution, causing the brine to evolve to higher Zn/Pb ratios by the end of the boiling process.

Boiling of the reduced, alkaline brine produced an argentiferous quartz-carbonate vein dominated by quartz (58.6%), calcite (31.3%), rhodochrosite (9.2%) with traces of pyrite, K-feldspar, talc, sphalerite, galena, acanthite, witherite, magnetite, chalcopyrite, dolomite, silver and biotite. Boiling effectively stripped out all metals and halo elements except for Au from the brine (Table 3), but only Ag was precipitated in potentially economic concentrations. Quartz-carbonate vein assemblages are common products of boiling in epithermal precious metal deposits, and the results of this simulation bear some similarities to the Ag-rich spectrum of epithermal deposits. However, there are some important differences, including the deposition of biotite, talc and witherite, which suggest that the fluid is not truly representative of epithermal conditions.

The appearance of witherite ($BaCO_3$) during the boiling simulation for a reduced, alkaline brine is worthy of some comment. This is one of the few simulations where Ba has been precipitated from solution, and it is the only simulation where barium is extracted as a carbonate phase. Barren barite ± witherite occurrences are scattered through the Selwyn Basin (Rhodes, pers. commun., 1993), and boiling of reduced, alkaline to near-neutral fluids may have played some part in the formation of these mineral occurrences.

Depositional models

Table 4 lists the percentage of total metal extracted from solution during simulations of mixing with oxidised seawater, mixing with reduced seawater, reaction with a pyritic dolomitic siltstone (10% pyrite, 10% dolomite, 40% quartz, 40 % muscovite), interaction with a pyritic dolomite (10% pyrite, 10% quartz, 80% dolomite) and reaction with a pyrite-rich carbonaceous dolostone (40% dolomite, 40% pyrite, 10% graphite, 10% quartz). Table 5 lists the seawater compositions used in the mixing simulations. The pyrite-rich carbonaceous dolostone has been deliberately made as reactive as possible, to establish whether abundant pyrite and/or graphite significantly enhances base metal deposition in comparison with the more 'typical' pyritic dolomite and dolomitic siltstone.

F: Mixing with oxidised seawater

For acidic brines, mixing with oxidised seawater proved to be highly effective at extracting copper and silver from solution (Table 4). Figures 3*A* and 4*A* illustrate that discharge of the acid, oxidised brine into an oxidised basin produces a zoned exhalative deposit with four distinct mineralogical zones extending out from the feeder: (1) proximal anhydrite - quartz - hematite - chalcocite; (2) quartz - hematite - barite - silver - kaolinite; (3) hematite -

Process	Brine	Cu (%)	Pb (%)	Zn (%)	Ag (%)	Au (%)	Ba (%)	Mn (%)
Mix with oxidised seawater	acid, oxidised	**41**	-	-	**96**	> 100	**70**	-
	acid, reduced	**73**	*6*	-	**72**	> 100	**70**	-
	alkaline, oxidised	*0.3*	-	-	*1*	> 100	**71**	-
	alkaline, reduced	> 100	> 100	> 100	**100**	-	**71**	-
Mix with reduced seawater	acid, oxidised	**100**	**99**	**64**	**100**	98	-	-
	acid, reduced	**96**	**100**	**100**	**100**	100	-	-
	alkaline, oxidised	**100**	**100**	**100**	**90**	98	-	-
	alkaline, reduced	54	92	87	**98**	-	-	-
Pyritic dolomitic siltstone	acid, oxidised	**100**	**88**	**77**	-	-	-	-
	acid, reduced	**83**	**86**	**72**	-	-	-	-
	alkaline, oxidised	**100**	**100**	**100**	**70**	6	-	-
	alkaline, reduced	0.3	-	-	-	-	-	-
Pyritic dolomite	acid, oxidised	**100**	**86**	**72**	-	-	-	-
	acid, reduced	**84**	**86**	**72**	-	-	-	-
	alkaline, oxidised	**100**	**100**	**100**	**75**	6	-	-
	alkaline, reduced	0.4	-	-	-	-	-	-
Py-rich carb. dolostone	acid, oxidised	**100**	**94**	**89**	-	-	-	-
	acid, reduced	**91**	**97**	**94**	-	-	-	-
	alkaline, oxidised	**100**	**100**	**100**	**86**	2	-	-
	alkaline, reduced	55	2.5	1	1	-	-	-

Table 4: Percentage of total metal in solution extracted during water-rock interaction calculations. For each simulation, small increments of fluid (≈ 0.05 and 0.5 grams) or rock (0.1, 0.5, 1 and 5 grams) were progressively titrated into approximately one kilogram of brine until equilibrium was reached. Numbers in **bold type** indicate efficient extraction of a metal over a small titration increment (i.e. the process is an efficient trap mechanism that could result in economic concentrations of that metal). Numbers in *italics* indicate that the metal was extracted inefficiently (i.e. over a large number of titration increments) - the process is an inefficient trap mechanism that is unlikely to form an ore deposit. Numbers in plain type indicate that the metal was never present in sufficient quantities in the starting solution to deposit economic concentrations of metals. > 100 indicates that the relevant metal was scavenged from seawater during the simulation.

silver - kaolinite ± muscovite; (4) distal hematite - silver - chalcocite - muscovite. The total proportions of minerals precipitated within the exhalite deposit would be 34% anhydrite, 31% quartz, 28% hematite, 6% chalcocite, 0.2% barite, 0.1% acanthite, and less than 0.1% muscovite, kaolinite, gibbsite and gold. No Zn or Pb minerals are precipitated during the mixing process. Instead, the high base metal concentrations within the brine are dispersed into seawater, where they would ultimately produce anomalous background base metal values in time-equivalent sediments.

Similar results were obtained during mixing of the acid, reduced brine with oxidised seawater, although some galena precipitated during this simulation (Table 4, Figures 3*B* and 4*B*). In this case, the exhalite is characterised by the following zones: (1) proximal anhydrite - quartz - pyrite - chalcopyrite; (2) quartz - galena - chalcocite - acanthite; (3) quartz - hematite - barite; (4) distal hematite (Figures 3*B* and 4*B*). The total mineral proportions are 43% anhydrite, 42% quartz, 10% pyrite, 3% hematite, 1% galena, 0.5% chalcopyrite, 0.2% barite, and less than 0.1% acanthite, muscovite, kaolinite, gibbsite, bornite, chalcocite and gold. Zn was dispersed into seawater.

Mixing of the alkaline oxidised brine with oxidised seawater produced a barren quartz - hematite - barite exhalite with traces of copper and silver (Table 3, Figure 3C). The base metal load of this brine was mostly dispersed into seawater.

An Ag-bearing siliceous pyritic exhalite with traces of muscovite, K-feldspar and base metals formed when the metal-poor alkaline, reduced

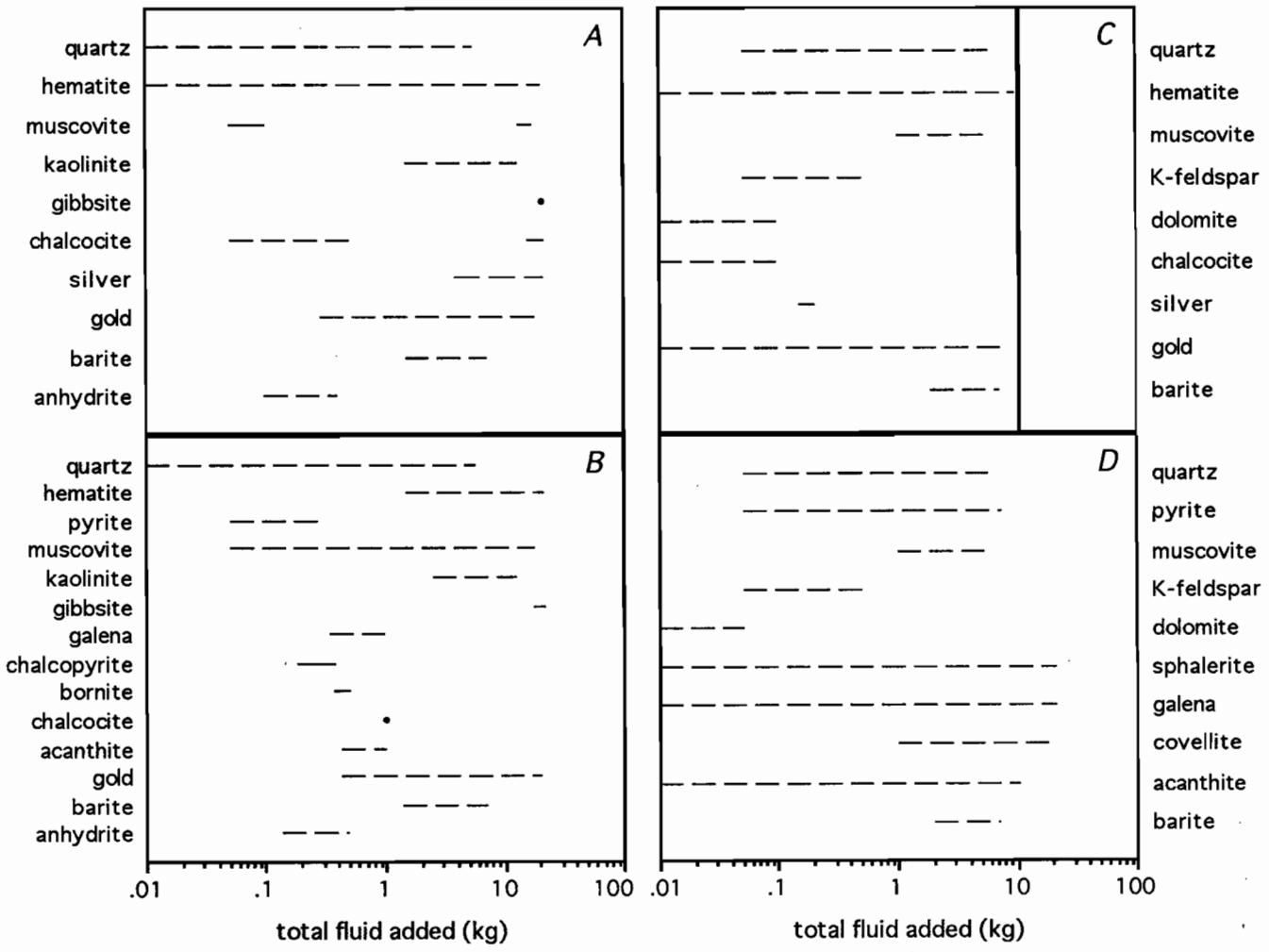

Figure 3: Mineral precipitation sequence calculated for mixing of≈ 1 kg of 250°C brines 1 to 4 with 5°C oxidised seawater. *A* - Brine 1 (acid, oxidised). *B* - Brine 2 (acid, reduced). *C* - Brine 3 (alkaline, oxidised). *D* - Brine 4 (alkaline, reduced). The bold vertical line indicate the point at which mineral precipitation ceased during mixing simulation C. Simulations A, B and D were stopped prior to the cessation of mineral deposition. However the bulk of the mineral load had been deposited by this time.

brine mixed with open seawater. While this type of exhalite mineralisation could be prospective for silver, the sulfide minerals would not be preserved within an oxidised ocean unless rapid burial occurred.

Barite precipitated in all four oxidised seawater mixing simulations, but not in any of the other simulations carried out for this report. It appears that barite is most effectively extracted from hydrothermal solutions where large quantities of aqueous sulfate become available, such as in oxidised marine basins.

G: Mixing with reduced seawater

Mixing of sedimentary brines with anoxic seawater is an excellent trap mechanism for base metal sulfides (Table 4), due to the combined effects of cooling, dilution, and the presence of reduced sulfur in the seawater. The process is highly efficient at extracting base metals over a small mixing increment, irrespective of the starting brine composition (Figure 5). The main differences between the four simulations are the minerals predicted to precipitate during the mixing process, and the amount of metals lost through dispersion into the overlying water column.

Three mineralogical zones are developed during mixing of the acid, oxidised brine with seawater (Figures 5A and 6A). Proximal to the feeder, a quartz - chalcocite - hematite zone develops. This gives way laterally to a galena - acanthite zone and finally to a distal pyrite - sphalerite ± galena zone (Figure 6A). The total proportions of minerals precipitated by this process are quartz (30%), pyrite (27%), chalcocite (16%), galena (14%), sphalerite (12%), hematite (0.7%), acanthite (0.1%), and less than 0.01% bornite, muscovite and gold. The high initial solubilities of Zn, Pb and Cu in the starting solution (Table 2) are what allow the formation of this high-grade polymetallic massive sulfide body. The extremely high Zn solubities (Zn is grossly

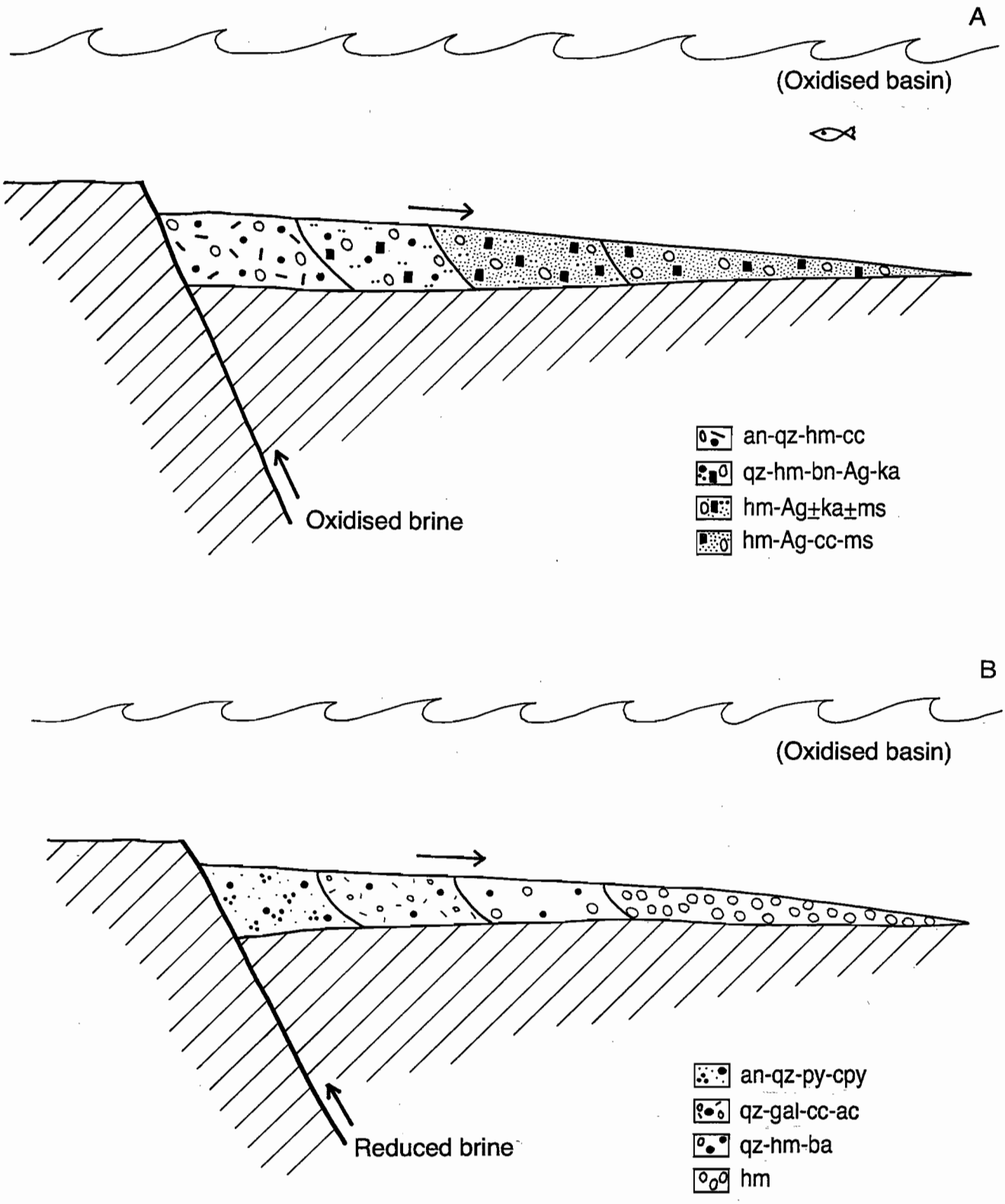

Figure 4. Mineral zonation and possible deposit morphology predicted for mixing of (A) 250°C oxidised brines with cool (5°C) oxidised seawater; and (B) 250°C reduced brines with oxidised seawater.

	Oxidised seawater	Anoxic seawater
pH	8.02	7.50
log $f_{(O_2)}$	-2.71	-76.40
H^+	0.001	0.101
H_2O	1 kg	1 kg
Cl^-	15205.8	21306.1
SO_4^{-2}	2726.2	80.8
HCO_3^-	142.8	27.9
HS^-	-	9.7
$SiO_{2\ (aq)}$	0.503	-
Al^{+3}	0.0009	-
Ca^{+2}	120.9	411.1
Mg^{+2}	11.9	1286.7
Fe^{+2}	4.22 E-08	4.23 E-11
K^+	401.1	379.1
Na^+	10821.9	10741.6
Mn^{+2}	0.0002	0.269
Zn^{+2}	0.002	0.000006
Cu^+	0.0005	0.003
Pb^{+2}	0.00003	5.63 E-14
Ag^+	0.00004	-
$AuCl_2^-$	0.000005	-
Ba^{+2}	0.002	1.50 E-07
$O_{2\ (aq)}$ *	0.101	-

Table 5: Modern-day oxidised and anoxic seawater compositions used in the mixing simulations (note the difference in oxygen fugacities for the two waters). All concentrations expressed as ppm, with the exception of H_2O (kg). The composition of oxidised seawater is taken from Drever (1984). Note that the seawater analysis as originally published is supersaturated with respect to muscovite, hematite, calcite and dolomite at 5°C. Consequently, the concentrations of K^+, Fe^{+2}, Ca^{+2} and Mg^{+2} have been reduced to 90% of saturation levels. Anoxic seawater composition compiled by D. Huston (pers. commun., 1993), mostly from data on the Black Sea.

undersaturated in brine 1) account for zinc's distal position in the precipitation sequence, and also for the loss of 36% of the zinc in solution through dispersal into seawater. A considerable degree of mixing is required to lower zinc solubilities sufficiently for zinc to saturate in the brine.

The predicted zonation for a massive sulfide body produced by mixing of the acid, reduced brine with anoxic seawater is a proximal siliceous Cu-rich core (quartz + pyrite + bornite), an intermediate quartz - galena - sphalerite - acanthite - chalcocite ± gold zone, and a distal Zn-rich massive sulfide zone (pyrite + sphalerite ± galena ± acanthite ± covellite; Figures 5*B* and 6*B*). This process is extremely efficient at extracting metals from the brine, with virtually all the Zn, Pb, Cu, Ag and Au dumped from solution (Table 4). The total proportion of minerals precipitated is 37% quartz, 23% sphalerite, 22% pyrite, 18% galena, 0.3% bornite, 0.2% acanthite, 0.03% chalcocite and less than 0.01% covellite and gold. The results of this simulation bears some similarities to the metal zonation observed in VHMS (volcanic-hosted massive sulfide) systems (eg. Eldridge et al., 1983), with a Cu-rich core passing out to a Zn-(Pb) rich zone. This resemblance is not surprising, since the fluids involved in VHMS mineralisation are known to be hot (200 - 350°C) reduced, moderately acid fluids (Pisutha-Arnond and Ohmoto, 1983; Ohmoto et al., 1983). The major difference between VHMS mineralogy and those predicted by this simulation are that bornite, chalcocite and covellite are predicted to precipitate instead of chalcopyrite. Choosing a higher total sulfur concentration in the initial brine would help stabilise chalcopyrite.

Mixing of an alkaline, oxidised brine with anoxic seawater is another highly efficient process for precipitating base metal sulfides (Table 4). However, the silicate minerals that are predicted to precipitate in conjunction with the sulfides are not generally recognised in SHMS (sediment-hosted massive sulfide) or VHMS deposits (eg. phlogopite, talc, magnesite; Figure 5C), suggesting that this scenario is not geologically realistic.

The metal-poor alkaline, reduced brine produces a talc (37%) + dolomite (29%) + magnesite (19%) + quartz (15%) + calcite (0.5%) + pyrite (0.1%) exhalite that contains reasonable quantities of silver but only traces of base metals when mixed with anoxic seawater (Table 4, Figure 5*D*). This appears to be another geologically unrealistic simulation, based on the esoteric mineralogy predicted for the exhalite body.

H: Reaction with pyritic dolomitic siltstone

Replacement reactions between oxidised brines (1 and 3) and a pyritic dolomitic siltstone at 250°C can effectively strip base metals from solution (Table 4). However, the sulfides will be intergrown with a variety of silicate, carbonate and oxide minerals (quartz, hematite, magnetite, dolomite, talc, muscovite, K-feldspar) that are more typical of distal skarns than SHMS deposits (Figures 7*A* and 7C). There is likely to be a temperature control on the development of the gangue phases, and lower temperature calculations may predict a more typical SHMS mineral assemblage via this type of replacement process.

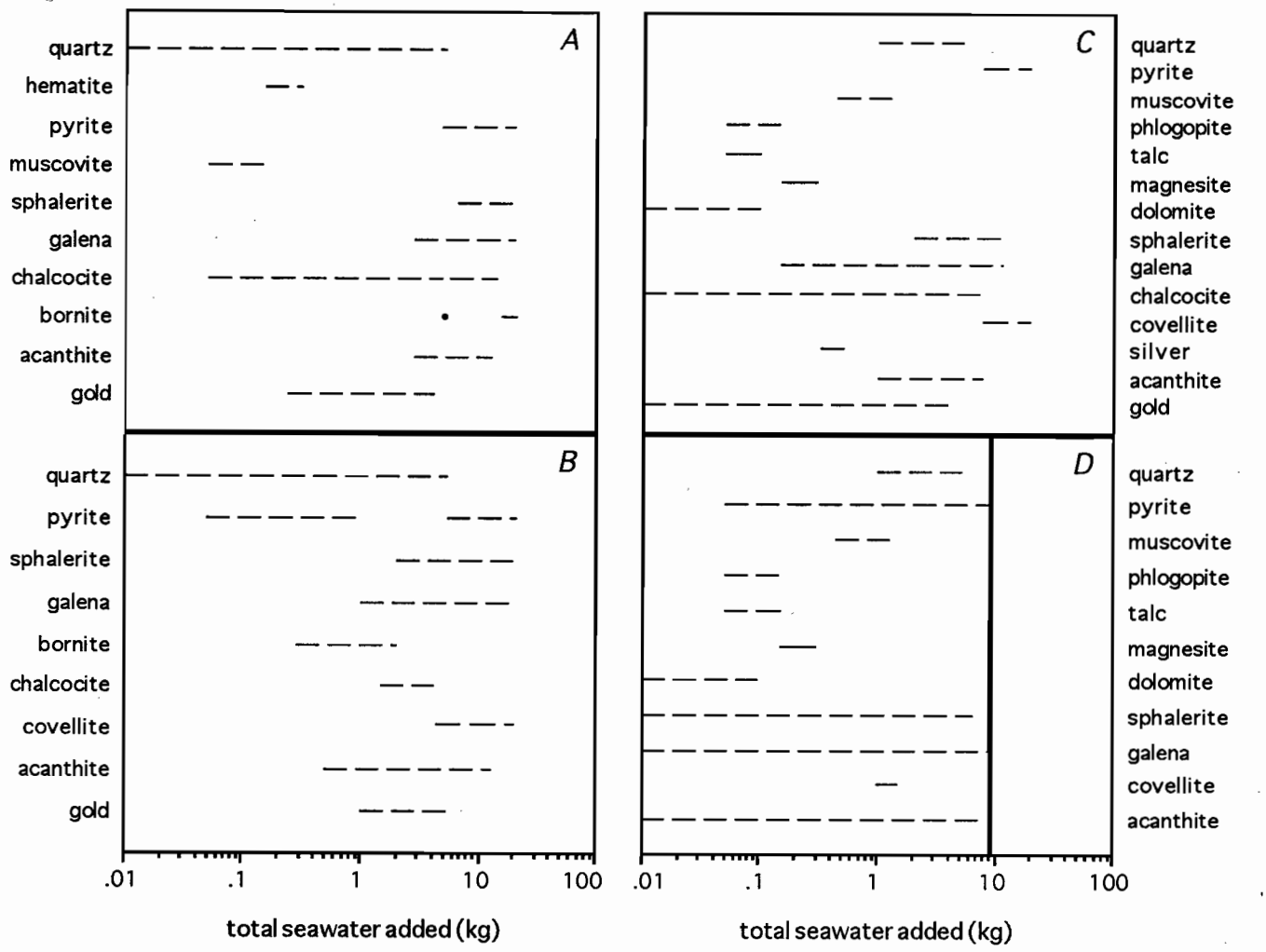

Figure 5: Mineral precipitation sequence calculated for mixing of ≈ 1 kg of 250°C brines with 5°C anoxic seawater. *A* - Brine 1 (acid, oxidised). *B* - Brine 2 (acid, reduced). *C* - Brine 3 (alkaline, oxidised). *D* - Brine 4 (alkaline, reduced). The bold vertical line indicate the point at which mineral precipitation ceased during simulation D. Simulations A, B and C were stopped prior to the cessation of mineral deposition. However the bulk of the mineral load had been deposited by this time.

Better results are predicted for the acid, reduced brine, which will precipitate a quartz - muscovite -pyrite - sphalerite - galena - chalcopyrite assemblage prior to final equilibration with the siltstone at 250°C (Figure 7*B*). This replacement process is highly effective at extracting base metals, dumping 72% of the total Zn, 86% Pb, and 83% Cu from solution (Table 4). In contrast, no Pb and Zn and only a small proportion of Cu were extracted when the metal-poor alkaline, reduced brine interacted with the siltstone (Table 4).

I: Reaction with pyritic dolomite

The results obtained for these four simulations are very similar to the pyritic dolomitic siltstone interactions (compare Figures 7 and 8). The main differences are caused by the lack of muscovite in the dolomite, which leads to the precipitation of only minor muscovite and/or K-feldspar (Figure 8). Base metals are efficiently stripped from the three metalliferous brines, while the metal-poor alkaline, reduced brine precipitates only minor Cu mineralisation (Table 4). The dolomite proved less reactive than the siltstone, equilibrating with the fluids after smaller amounts of water-rock interaction (compare Figures 7 and 8). Only the acid, reduced brine produced a simple, sulfide rich mineral assemblage (quartz-pyrite-sphalerite-galena-chalcopyrite-muscovite; Figure 8*B*). The oxidised brines produced more complicated mineral assemblages that are reminiscent of distal skarns (Figures 8*A* and 8*C*). The reduced, alkaline brine is close to equilibrium with the dolomite, requiring only 0.02 grams of rock to be reacted with it prior to attaining equilibrium (Figure 8D). A pyritic dolomite could therefore act as an aquifer for a reduced, alkaline brine of this nature.

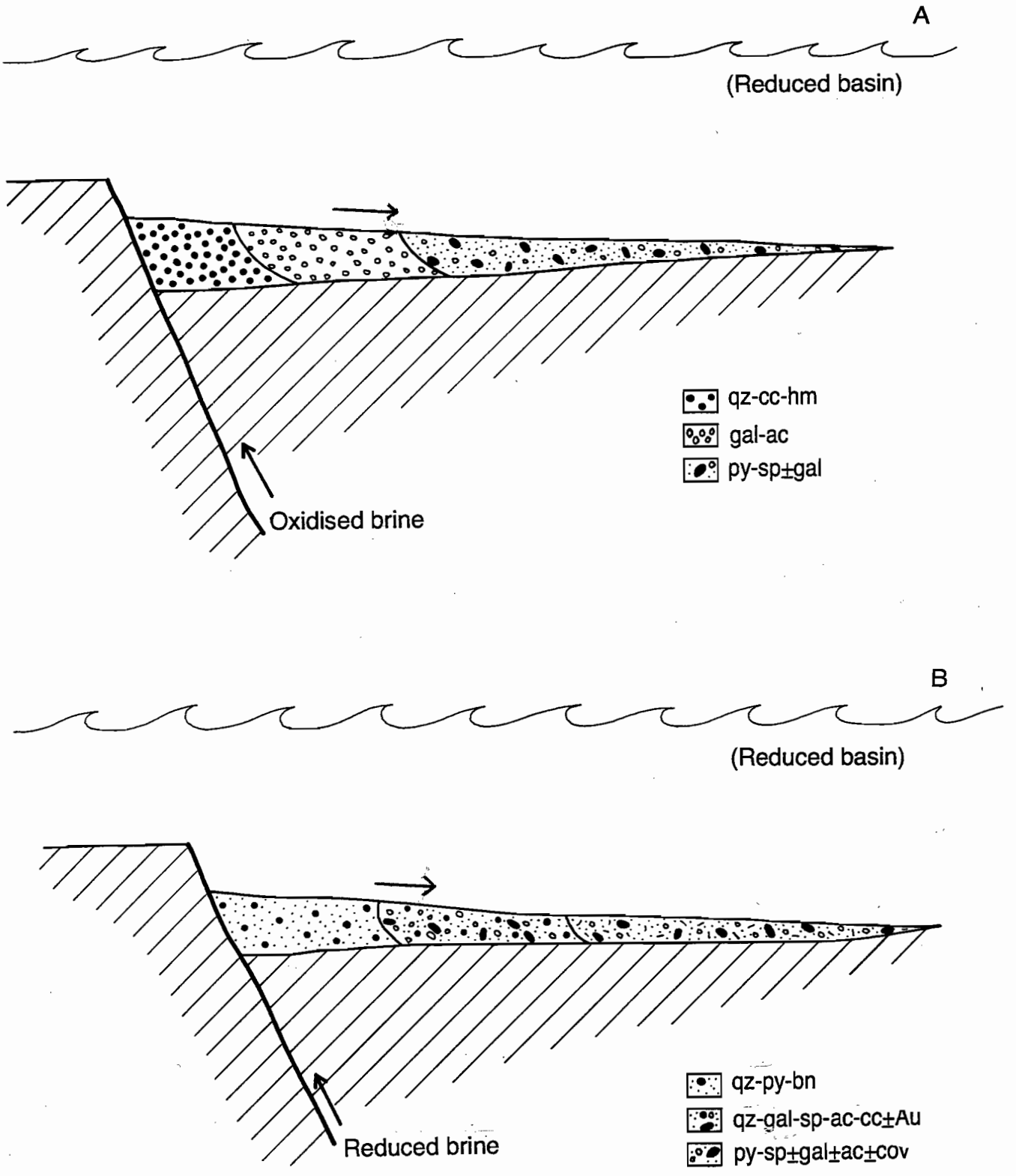

Figure 6. Mineral zonation and possible deposit morphology predicted for mixing of (A) 250°C oxidised brines with cool (5°C) reduced seawater; and (B) 250°C reduced brines with reduced seawater.

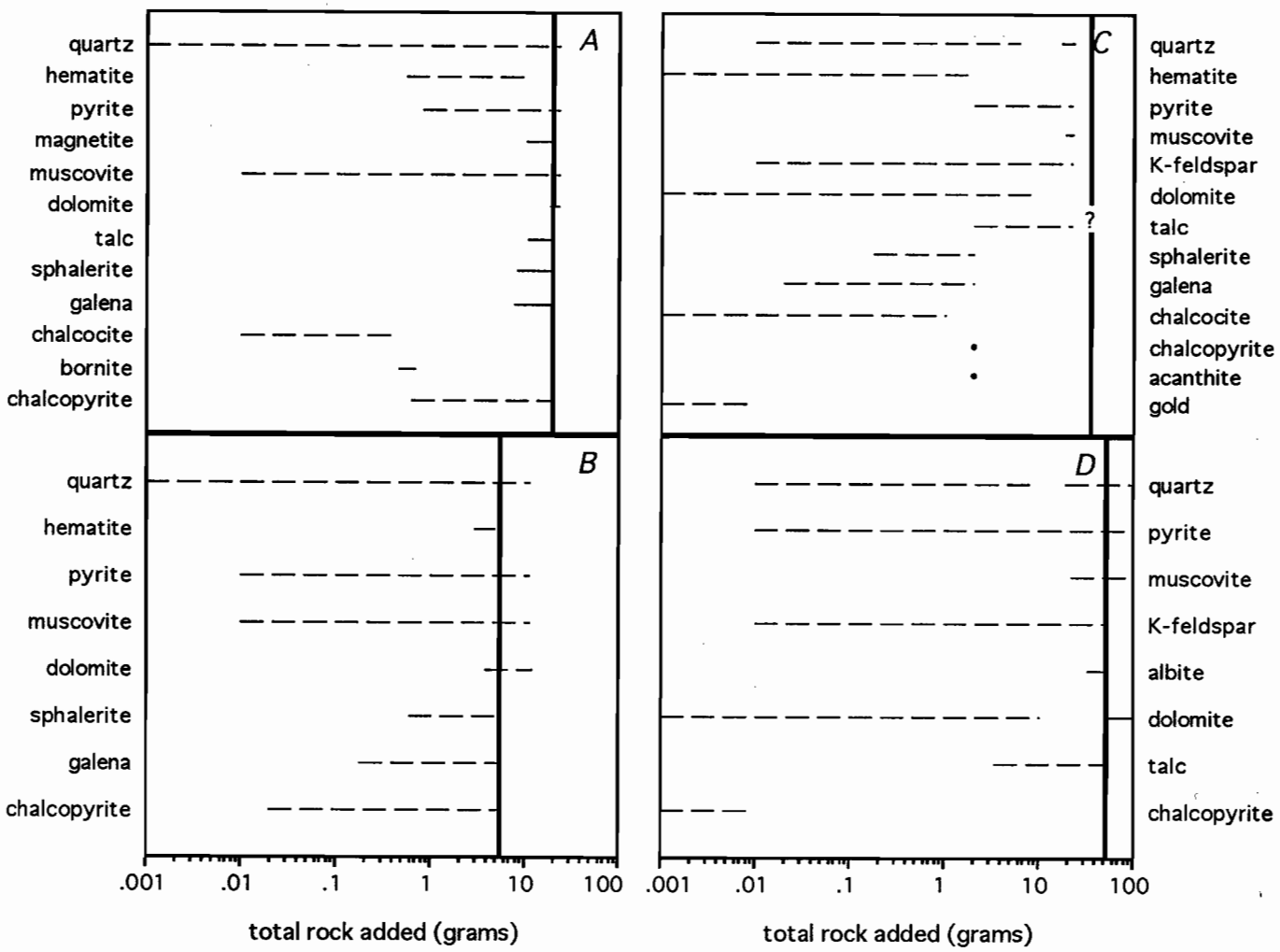

Figure 7: Mineral precipitation sequence calculated for interaction of ≈ 1 kg of 250°C brines with pyritic dolomitic siltstone. *A* - Brine 1 (acid, oxidised). *B* - Brine 2 (acid, reduced). *C* - Brine 3 (alkaline, oxidised). *D* - Brine 4 (alkaline, reduced). The bold vertical lines indicate the point at which the fluids have equilibrated with the wallrocks. Note - simulation C was not taken to completion.

J: Reaction with pyrite-rich carbonaceous dolostone

The presence of abundant pyrite and graphite in the dolostone only marginally improves the base metal extraction efficiency of this replacement process (Table 4). Improved base metal extraction is most likely a result of the presence of abundant reduced sulfur (within pyrite) in the wallrocks. Similar mineral assemblages are produced to the dolomite and siltstone interactions (compare Figure 9 with Figures 8 and 7), although one important difference is that abundant iron in the wall rock (as pyrite) leads to the development of secondary magnetite and Fe-rich biotite during interaction with the oxidised brines (Figures 9*A* and 9*C*). Primary graphite is recrystallised in the later stages of interaction between the oxidised brines with the wallrocks (Figures 9*A* and 9*C*). Surprisingly, the dolostone proved less reactive than the siltstone in all four simulations (compare Figures 7 and 9).

CONCLUSIONS

Although no simulation has produced what could be called 'classic' sediment-hosted base metal mineralisation, insights have been gained into a variety of processes that may occur in sedimentary basins. The major conclusions to be drawn from this study, and from Cooke (1992), are:

Brine compositions

- 250°C oxidised metalliferous brines are excellent transporting solutions that can potentially carry in excess of 100 ppm Cu, Zn, and Pb, and more than 1 ppm Ag as chloride complexes. Au will only be transported in large quantities as $AuCl_2^-$ if the brines are sufficiently acidic and/or oxidised.

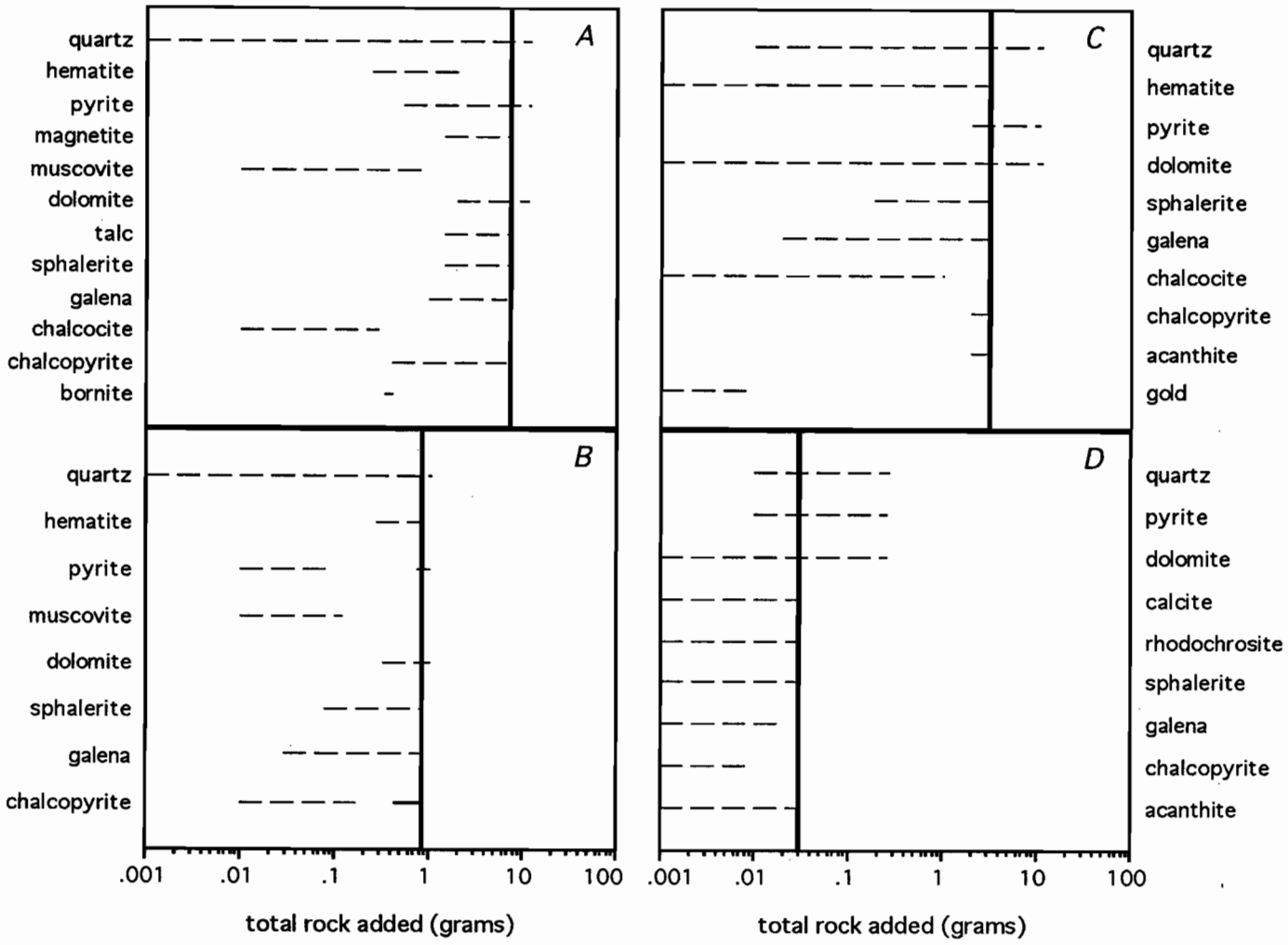

Figure 8: Mineral precipitation sequence calculated for interaction of ≈ 1 kg of 250°C brines with pyritic dolomite. *A* - Brine 1 (acid, oxidised). *B* - Brine 2 (acid, reduced). *C* - Brine 3 (alkaline, oxidised). *D* - Brine 4 (alkaline, reduced). The bold vertical lines indicate the point at which the fluids have equilibrated with the wallrocks.

- Reduced, acid brines can carry large amounts of Pb, Zn and Ag in solution at 250°C, but Cu can only be transported in large quantities under highly acidic conditions. Au transport as $Au(HS)_2^-$ is favoured under near-neutral pH conditions in reduced brines, so significant gold may be transported in weakly acidic, reduced sulfur-rich brines.

- Reduced, alkaline, moderately saline brines (10 wt. % eq. NaCl) cannot carry sufficient Cu, Pb or Zn at 250°C to precipitate economic base metal mineralisation. Higher salinity fluids will be capable of transporting greater quantities of base metals, but calcualtions have not been undertaken to ascertain whether this would bring base metal concnetrations in the fluid up to the 'ore-forming window'. Ag and/or Au may be transported in large quantities as bisulfide complexes by reduced, alkaline brines, provided the fluids are not too alkaline or too reduced (eg. pyrrhotite-stable).

Aquifer transport

- Hematitic sandstones can act as excellent aquifers for oxidised, metalliferous brines, allowing them to retain their full metal load during fluid migration (provided no significant cooling occurs). Detrital muscovite or K-feldspar will buffer the pH of the fluid, with alkaline, oxidised brines best transported by arkosic hematitic sandstones.

- Metal-poor, reduced, alkaline brines can exist within a dolomitic aquifer without undergoing significant chemical adjustments.

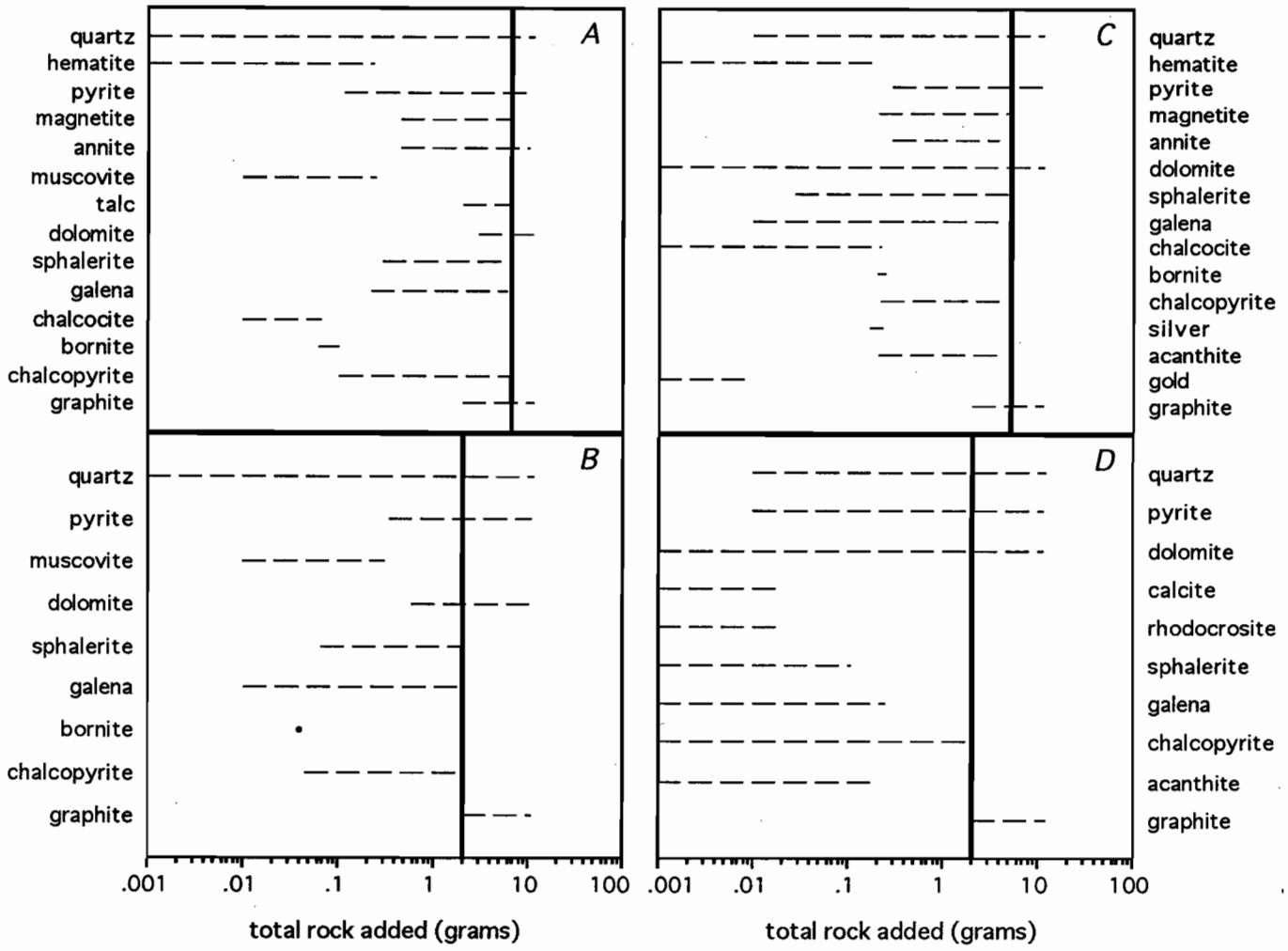

Figure 9: Mineral precipitation sequence calculated for interaction of ≈ 1 kg of 250°C brines with pyritic dolomitic carbonaceous siltstone. *A* - Brine 1 (acid, oxidised). *B* - Brine 2 (acid, reduced). *C* - Brine 3 (alkaline, oxidised). *D* - Brine 4 (alkaline, reduced). The bold vertical lines indicate the point at which the fluids have equilibrated with the wallrocks.

- Potassic and/or propylitic alteration is produced when 250°C sedimentary brines interact with mafic volcanics

Cross-stratal transport

- Conductive cooling of 250°C oxidised metalliferous brines in isolation will not cause significant base metal deposition. Base metals will only begin to precipitate if the redox state of the fluid is buffered by some external process (such as interaction with a reduced lithology). If the initial brine has a more reduced composition (eg. pyrite-stable), base metal deposition can occur during cooling, although the pH of the fluid becomes important in controlling the amount of base metals that remain in solution. Cooling metalliferous brines would be represented in the field by fault-hosted barren quartz veins (eg. faults in the Tawallah Group).
- Boiling of oxidised and reduced metalliferous brines would produce barren quartz veins that are mineralogically (but probably not texturally) indistinguishable from veins deposited from cooling fluids within a sedimentary basin. Depending on initial saturation levels, base metals may not be deposited from boiling oxidised brines. Boiling of a reduced, alkaline brine will produce quartz-carbonate veins reminiscent of Ag-rich epithermal deposits.

Depositional models

- Mixing of 250°C saline metalliferous brines with oxidised seawater can produce economic Cu-Ag-(Ba) mineralisation, possibly represented by some form of Fe- and sulfate-rich exhalite. Pb and Zn are dispersed into the overlying water column, producing anomalous background concentrations in the surrounding time-

equivalent sediments. These are the only simulations that predict barite deposition, probably due to the presence of abundant sulfate in oxidised seawater.

- Mixing of sedimentary brines with anoxic seawater is an excellent trap mechanism for base metal sulfides. A Zn-Pb rich massive sulfide with a Cu-rich core reminiscent of VHMS deposits will precipitate when a 250°C acid, reduced brine mixes with anoxic seawater. Oxidised brines will produce more Cu-rich mineralisation marked by the presence of abundant chalcocite or bornite.

- Interaction of acid, reduced sedimentary brines with various dolomitic and pyritic lithologies at 250°C produces relatively simple base metal sulfide-rich mineral assemblages. In contrast, oxidised metalliferous brines that interact with the same lithologies will precipitate more complex assemblages that are reminiscent of distal skarns. Overall, replacement reactions are efficient at extracting base metals from solution, and the best results are obtained when the brine is reduced and acidic.

REFERENCES

Cooke, D.R., 1992. Brine Chemistry: Sulfide solubilities and depositional processes in sedimentary brines: preliminary modelling results. AMIRA/ARC Project P.384, Report No. 1; 63-75.

Cooke, D.R., Huston, D.L., Large, R.R., and Gammons, C.H., 1993. Hydrothermal geochemistry. *In* CODES Masters of Economic Geology Course Work Manual 12, 2nd edition; 1-35.

Drever, J.I., 1984. The geochemistry of natural waters. Prentice-Hall, N.J.,p. 234.

Eldridge, C.S., Barton, P.B. Jr., and Ohmoto, H., 1983, Mineral textures and their bearing on formation of the Kuroko orebodies, *in* Ohmoto, H. and Skinner, B.J. eds., Kuroko and Related Volcanogenetic Massive Sulphide Deposits. Econ. Geol., Mon. 5: 241–281.

Large, R.R., 1992. Development of integrated ore deposit models for exploration. AUSIMM conference, Broken Hill, p. 175 - 179.

McKibben, M.A., and Williams, A.E., 1989. Metal speciation and solubility in saline hydrothermal fluids: an empirical approach based on geothermal brine data. Econ. Geol., 84: 1996-2007.

Ohmoto, H., Mizukami, M., Drummond, S.E., Eldridge, C.S. Pisutha-Arnold, V. and Lenagh, T.C., 1983, Chemical processes of Kuroko formation *in* Ohmoto, H. and Skinner, B.J. eds., Kuroko and Related Volcanogenetic Massive Sulphide Deposits. Econ. Geol., Mon. 5: 570–604.

Pisutha-Arnond, V. and Ohomoto, H., 1983, Thermal history, chemical and isotopic compositions of the ore-forming fluids responsible for the Kuroko massive sulfide deposits in the Hokuroko District of Japan, *in* Ohmoto, H. and Skinner, B.J. eds., Kuroko and Related Volcanogenetic Massive Sulphide Deposits. Econ. Geol., Mon. 5: 523–558.

Reed, M.H., 1982. Calculation of multicomponent chemical equilibria and reaction processes in systems involving minerals, gases and an aqueous phase. Geochim. Cosmochim. Acta, 46: 513-528.

Roedder, E., 1960. Fluid inclusions as samples of ore-forming fluids. 21st Inter. Geol. Cong., Copenhagen, Prag., pt. 16; 218-229.

Schultz, 1991. Metalliferous black shales: Accumulation of carbon and metals in cratonic basins. *In*: E.R. Force, J.J. Eidel and J.B. Maynard (Eds.) Sedimentary and diagenetic mineral deposits: a basin analysis approach to exploration. Rev. Econ. Geol., 5: 171-176.

Skinner, B.J., 1979. The many origins of hydrothermal mineral deposits. *In* Barnes, H.L. (ed.) Geochemistry of Hydrothermal Ore Deposits, 2nd edition. John Wiley and Sons, New York. 1 - 21.

Spycher, N.F., and Reed, M.H., 1990. Users Guide for CHILLER: A program for computing water-rock reactions, boiling, mixing and other reaction processes in aqueous-mineral-gas systems. University of Oregon (unpublished)

Progress Report: Transport and deposition of base metals from low temperature (150°C) sedimentary brines

David R. Cooke
Centre for Ore Deposit and Exploration Studies

SUMMARY

The depositional products predicted for 150°C brines during aquifer and cross-stratal transport, and in the trap environment are similar to those predicted for 250°C fluids (see Cooke, 1993). However, these moderate salinity (10 eq. wt. % NaCl) brines are mostly incapable of carrying sufficient base metals to form economic base metal mineralisation, unless the fluid is oxidised and/or acidic enough. High $CO_{2\ (aq)}$ contents (1 wt %) in the initial brines stabilises siderite as a depositional product in several low-T simulations, suggesting that sedimentary brines must be sufficiently overpressured to retain high CO_2 levels in solution. Reasonable water depths (at least several hundred metres) would be required to maintain such pressures.

INTRODUCTION

This report documents numerical simulations of transport and depositional processes for moderately saline (10 eq. wt. % NaCl) low temperature (150°C) sedimentary brines. During this study, it has become apparent that further simulations involving high salinity brines (20 eq. wt. % NaCl) are required to fully evaluate the metal-transporting and depositional capabilities of low temperature fluids. Consequently, the current report is a progress report only that contain preliminary results and data analysis. The concluding report in this series will discuss the final results of 150°C brine modelling.

METHOD AND INITIAL PARAMETERS

The methodology and assumptions applied here are identical to those discussed in Cooke (1993). The starting parameters for the numerical simulations documented in this report are as follows:

- Temperature: 150°C
- Salinity: 10 eq. wt. % NaCl (8.16 wt % NaCl + 1 wt % KCl + 1 wt % $CaCl_2$)
- pH: 1 unit acid; neutral; 1 unit alkaline (relative to K-spar - muscovite)
- ΣS: 0.001 molal
- Redox state: reduced (pyrite field; $\Sigma H_2S/\Sigma SO_4^{-2} = 1000$); oxidised (hematite or siderite field; $\Sigma H_2S/\Sigma SO_4^{-2} = 0.01$)
- Dissolved CO_2: 1 molal

A total of six initial fluid compositions have been calculated (Table 1). They can be classified in general terms as (1) acid, oxidised; (2) acid, reduced; (3) neutral, oxidised; (4) neutral, reduced; (5) alkaline, oxidised; (6) alkaline, reduced. Only one of these brines is an excellent transporting solutions for Zn and Pb (brine 1). Brine 3 is capable of carrying sufficient Zn and Pb at saturation levels to form economic base metal mineralisation. The other brines are only capable of producing subeconomic mineralisation at best. None of the brines can carry ore-forming quantities of Cu, while brines 1 - 4 are capable of carrying 10's - 100's ppb Ag. In the following discussion, only the acid, oxidised and neutral, oxidised brines will be referred to as 'metalliferous brines'.

Codes: AMIRA / ARC Project P.384 - Proterozoic sediment-hosted base metal deposits. November 1993

	1 - Acid, Oxidised	2 - Acid, Reduced	3- Neutral, Oxidised	4- Neutral, Reduced	5-Alkaline, Oxidised	6-Alkaline, Reduced
pH	4.29	4.29	5.29	5.29	6.29	6.29
Salinity	10.0 wt %	10.0 wt %	10.0 wt %	10.0 wt %	10.0 wt %	10.0 wt %
ΣS	0.001	0.001	0.001	0.001	0.001	0.001
log $f_{(O_2)}$	-42.90	-45.40	-43.90	-46.40	-44.90	-47.40
H^+	226.7	228.5	207.4	209.0	111.7	112.8
H_2O	1 kg	1 kg	1 kg	1 kg	1 kg	1 kg
Cl^-	60720.5	60749.1	60712.8	60716.7	60574.1	60577.5
SO_4^{-2}	85.02	85.06	85.01	85.01	84.82	84.82
HCO_3^-	13862.0	13868.6	13860.3	13861.2	13828.6	13829.4
HS^-	-	28.12	-	28.24	-	29.57
$SiO_{2\ (aq)}$	*102.3*	*102.4*	*102.4*	*102.4*	*103.0*	*103.0*
Al^{+3}	*0.0045*	*0.0045*	*0.0012*	*0.00126*	*0.0006*	*0.0006*
Ca^{+2}	3614.6	3616.2	*1535.3*	*1535.4*	*30.62*	*30.61*
Mg^{+2}	36.03	36.50	*9.623*	*9.594*	*0.223*	*0.222*
Fe^{+2}	*310.3*	*0.0044*	*3.822*	*0.0002*	*0.072*	*0.00003*
K^+	5249.9	5252.3	5249.2	5249.5	5237.2	5237.4
Na^+	30909.2	31016.6	34968.0	34979.3	38866.2	38868.6
Mn^{+2}	1391.3	1391.9	*70.48*	*70.48*	*1.480*	*1.479*
Zn^{+2}	**100.1**	*0.291*	*12.50*	*0.0070*	*0.146*	*0.0016*
Cu^+	*0.561*	*0.010*	*0.065*	*0.0087*	*0.0069*	*0.013*
Pb^{+2}	**100.1**	*0.074*	*3.944*	*0.0096*	*0.713*	*0.0042*
Ag^+	*0.691*	*0.024*	*0.074*	*0.014*	*0.0079*	*0.010*
$AuCl_2^-$	*3.69 E-08*	0.000014	*4.75 E-08*	0.000014	*2.35 E-07*	0.000014
Ba^{+2}	1.001	1.001	1.001	1.001	*0.182*	*0.182*
$O_{2\ (aq)}$ *	8.99 E-47	2.85 E-49	8.96 E-48	2.83 E-50	8.85 E-49	2.80 E-51

Table 1: Modelled brine compositions at 250°C. Component species concentrations are in ppm, except for $O_{2\ (aq)}$ and ΣS, which are given as molal units. Brines 1, 3 and 5 are oxidised fluids (hematite or siderite stable: $a(H_2S) / a(SO_4^{-2}) = 0.01$). Brines 2, 4 and 6 are reduced fluids (pyrite stable: $a(H_2S) / a(SO_4^{-2}) = 1000$). Brine compositions have been calculated based on the assumptions outlined in Cooke (1993). **Bold type** indicates that although the fluids are undersaturated with a given metal, the concentration of that metal has been set at the upper limits of the ore-forming window (100 ppm for base metals, 1 ppm for Ag) - i.e the fluid is an **excellent** transporting solution for that metal. ***Italics*** indicates that total concentrations of component species have been calculated by forcing equilibration between the brines and the following minerals: $SiO_{2\ (aq)}$ - quartz; Al^{+3} - muscovite (brines 1 and 2) or K-feldspar (brines 3, 4, 5 and 6); Ca^{+2} - calcite (brines 3, 4, 5, 6); Mg^{+2} - dolomite (brines 3, 4, 5, 6); Fe^{+2} - hematite (brine 1), pyrite (brines 2, 4, 6) or siderite (brines 3 and 5); Mn^{+2} - rhodochrosite (brines 3, 4, 5, 6); Zn^{+2} - sphalerite (brines 2, 3, 4, 5, 6); Cu^+ - bornite (brines 1, 2, 3, 4, 5) or chalcopyrite (brine 6); Pb^{+2}- galena (brines 2, 3, 4, 5, 6); Ag^+ - acanthite (brines 1 , 2, 3, 4, 5; 6); $AuCl_2^-$ - gold (brines 1, 3, 5); Ba^{+2} - witherite (brines 5, 6); Na^+ has been adjusted to maintain charge balance in the fluids, and, where possible, Ba^{+2} concentrations are set at 1 ppm. For brines 1 and 2, Mn^{+2} and Mg^{+2} concentrations are set at 1390 ppm and 36 ppm respectively based on measured concentrations from the Salton Sea geothermal brines (McKibben and Williams, 1989).

TRANSPORT AND DEPOSITIONAL PROCESSES

Numerical simulations of various transport and depositional processes have been undertaken for each of the six brines outline in Table 1. They are subdivided as follows:

Aquifer transport

Simulations of water-rock interaction between 150°C brines and a variety of lithologies have been undertaken to test the potential of each lithology to act as an aquifer. The lithologies are: (A) carbonaceous evaporite (80% anhydrite, 10%

Aquifer	Brine	Cu (%)	Pb (%)	Zn (%)	Ag (%)	Au (%)	Ba (%)	Mn (%)
Evaporite + graph.	acid, oxidised *	*99*	100	100	97	-	-	86
	acid, reduced *	24	54	88	-	-	-	87
	neutral, oxidised*	96	100	100	89	-	-	-
	neutral, reduced*	-	-	-	-	-	-	-
	alkaline, oxidised*	100	100	100	66	-	-	-
	alkaline, reduced*	-	-	-	-	-	-	-
Evaporite (no graphite)	acid, oxidised	*64*	*2.1*	-	37	-	-	-
	acid, reduced	46	5	7	-	-	-	-
	neutral, oxidised	-	-	-	-	-	-	-
	neutral, reduced	-	-	-	-	-	-	-
	alkaline, oxidised	-	1.4	-	-	-	-	-
	alkaline, reduced	-	-	-	-	-	-	-
Hematitic sandstone	acid, oxidised	-	-	-	-	-	-	-
	acid, reduced	-	-	-	-	98	-	-
	neutral, oxidised	-	-	-	-	94	-	-
	neutral, reduced	86	30	-	42	100	-	*0.2*
	alkaline, oxidised	-	-	-	-	100	-	-
	alkaline, reduced	99	33	52	75	100	*1.1*	*1.2*
Mafic volcanic A (+ mt)	acid, oxidised *	*71*	83	31	97	99	-	83
	acid, reduced *	88	57	60	45	100	-	83
	neutral, oxidised*	37	48	45	26	94	-	-
	neutral, reduced*	86	31	-	43	23	-	-
	alkaline, oxidised*	18	34	22	14	100	*2.2*	-
	alkaline, reduced*	99	34	52	80	100	*23*	-
Mafic volcanic B (no mt)	acid, oxidised	*43*	35	-	87	97	-	82
	acid, reduced *	37	88	98	41	-	-	83
	neutral, oxidised*	-	*16*	*1.8*	53	97	-	-
	neutral, reduced*	-	26	53	6	-	-	-
	alkaline, oxidised*	-	16	-	58	100	-	-
	alkaline, reduced*	-	5.9	-	-	-	-	-
Felsic volcanic A (+ mt)	acid, oxidised	*74*	81	29	83	92	-	90
	acid, reduced *	91	31	55	87	100	-	97
	neutral, oxidised*	100	100	100	95	95	49	89
	neutral, reduced*	98	31	-	76	100	49	88
	alkaline, oxidised*	99	98	99	83	100	*74*	*64*
	alkaline, reduced	99	34	52	91	100	77	66
Felsic volcanic B (no mt)	acid, oxidised	*40*	30	-	55	87	-	85
	acid, reduced	36	83	96	34	-	-	86
	neutral, oxidised	-	-	-	-	-	-	-
	neutral, reduced	-	-	-	-	-	-	-
	alkaline, oxidised	-	-	-	-	-	-	-
	alkaline, reduced	-	-	-	-	-	-	-
Limestone	acid, oxidised	*40*	-	-	46	86	-	84
	acid, reduced	37	82	95	33	-	-	84
	neutral, oxidised	-	-	-	-	-	-	-
	neutral, reduced	-	-	-	-	-	-	-
	alkaline, oxidised	-	-	-	-	-	-	-
	alkaline, reduced	-	-	-	-	-	-	-

Table 2: Percentage of total metal extracted during water-rock interaction calculations. For each simulation, small increments of rock (0.1, 0.5, 1 and 5 grams) were progressively titrated into approximately one kilogram of brine until equilibrium was reached. * - indicates the reaction did not progress to completion. Refer to Table 3 for explanation.

Process	Brine	Cu (%)	Pb (%)	Zn (%)	Ag (%)	Au (%)	Ba (%)	Mn (%)
Cooling	acid, oxidised	-	-	-	***6.6***	-	***3.5***	-
(150° -	acid, reduced	79	100	100	100	-	-	-
20°C)	neutral, oxidised	23	***0.01***	***0.01***	36	100	**47**	-
	neutral, reduced	23	100	100	100	-	**40**	-
	alkaline, oxidised	99	13	0.04	99	100	**92**	-
	alkaline, reduced	100	100	100	100	-	**91**	-
Boiling	acid, oxidised	***88***	**28**	-	**90**	100	-	-
(150° -	acid, reduced	100	100	99	98	-	-	***4.0***
100°C)	neutral, oxidised	66	***1.8***	***3.9***	99	100	**33**	**63**
	neutral, reduced	99	100	98	100	-	**33**	**63**
	alkaline, oxidised	-	-	-	100	100	**100**	**81**
	alkaline, reduced	99	99	100	99	-	**100**	**81**
Cool	acid, oxidised	-	-	-	***0.1***	0.3	-	-
after	acid, reduced	0.8	0.4	0.8	1.8	48	-	-
boiling	neutral, oxidised	-	-	-	0.1	< 0.01	**51**	-
(100° -	neutral, reduced	0.2	0.2	0.8	2.2	-	**50**	-
20°C)	alkaline, oxidised	-	-	-	0.1	< 0.01	***0.3***	-
	alkaline, reduced	0.1	1.1	0.1	1.1	-	***0.3***	-

Table 3: Percentage of total metal in solution extracted during cooling and boiling simulations for brines 1 to 4. Cooling increments of 5°C were used for each simulation. Numbers in **bold type** indicate efficient extraction of a metal over a small temperature interval (i.e. the process is an efficient trap mechanism that could result in economic concentrations of that metal). Numbers in ***italics*** indicate that the metal was extracted inefficiently (i.e. over a large temperature range) - the process is an inefficient trap mechanism that is unlikely to form an ore deposit. Numbers in plain type indicate that the metal was never present in sufficient quantities in the starting solution to deposit economic concentrations of metals.

quartz, 10% graphite); (B) evaporite (90% anhydrite, 10% quartz); (C) hematitic sandstone (80% quartz, 10% muscovite, 10% hematite); (D) mafic volcanic A (50% anorthite, 10% albite, 35% pyroxene, 5% magnetite); (E) mafic volcanic B (70% anorthite, 10% albite, 20% pyroxene); (F) felsic volcanic A (65% K-feldspar, 10% albite, 20% quartz, 5% magnetite); (G) felsic volcanic B (75% K-feldspar, 25% quartz); and (H) limestone (95% calcite, 5% quartz). Reactive components of some lithologies were deliberately exaggerated to ensure that the rock types were potentially reactive (eg. 10% graphite in the 'carbonaceous evaporite'). Where possible, calculations are continued to the point where the fluid equilibrates with the aquifer.

Cross-stratal transport and brine pool deposition

The chemical effects of cooling and boiling on low temperature sedimentary brines have been investigated by simulations of: (I) conductive cooling (150°C to 20°C); (J) isoenthalpic boiling (150°C to 100°C); and (K) cooling after boiling (100°C to 20°C). Because these simulations involve no water-rock interaction or fluid mixing, they best represent cooling and or boiling in a chemically isolated environment (eg. a quartz-lined fault). The cooling simulation also has relevance for brine pool depositional models, whereby a sedimentary brine discharges into a brine pool without undergoing significant mixing with the overlying water column. The cooling after boiling simulation represents a boiling sedimentary brine that discharges into a cool brine pool. Boiling stops at 100°C, and the fluid then cools by conduction and/or mixing as it flows out from the vent. Gases would ascend buoyantly from the vent and would be lost from the brine pool; consequently, in this simulation all gases are fractionated out of the system at 100°C.

Depositional processes at the trap site

As for the simulations of 250°C brines (Cooke, 1993), the potential base metal depositional mechanisms simulated for 150°C brines are: (L) mixing with cold (5°C) oxidised seawater; (M) mixing with cold (5°C) anoxic seawater; (N) reaction with pyritic dolomitic siltstone (40% quartz, 40% muscovite, 10% dolomite, 10% pyrite); (O) interaction with pyritic dolomite (80% dolomite,

10% pyrite, 10% quartz); and (P) reaction with pyrite-rich carbonaceous dolostone (40% dolomite, 40% pyrite, 10% quartz, 10% graphite).

RESULTS

The large number of simulations undertaken for this report (95) precludes a detailed analysis of the results obtained from each simulation. Attention will be focussed on the two Zn-Pb-rich brines (acid, oxidised and neutral, oxidised), with some discussion of interesting results from other simulations. As for Cooke (1993), discussion is restricted to the *extraction efficiency* of various processes for the base metal (Zn, Pb, Cu), precious metal (Ag, Au), and two halo-forming components (Ba, Mn) in the initial brines. Consideration will also be given to the solid phases that saturate during individual simulations.

Aquifer transport models

Table 2 lists the percentage of total metal extracted from solution during brine interaction with the various aquifer lithologies listed above. Equilibrium was not achieved during calculations involving felsic volcanic A (with the exception of the alkaline, reduced fluid), mafic volcanic A, mafic volcanic B, and the carbonaceous 'evaporite' due to the presence of reactive magnetite or (in the latter case) graphite. Nevertheless, these simulations progressed far enough to allow comments to be made about the aquifer potential of each lithology.

Comparing the results for the two evaporite lithologies in Table 2 demonstrates that the presence of carbonaceous material makes an anhydrite-rich evaporite more reactive to most fluids and will cause dumping of base and precious metals. In contrast, the evaporite with no carbonaceous material can act as a reasonable aquifer for neutral and alkaline fluids. Minor calcite ± pyrite precipitates during interaction between reduced and alkaline brines and the evaporite.

As for the 250°C simulations (Cooke, 1993), the hematitic sandstone provides an excellent aquifer for oxidised metalliferous brines (Table 2). The reduced, acid brine also retains its base metal load during brine migration through the sandstone, although some pyrite is deposited as the brine is oxidised to hematite-stable conditions.

Both mafic volcanic lithologies prove highly reactive to all six brine compositions (Table 2) and could not act as aquifers for significant base metal transport. K-silicate (muscovite or K-feldspar), carbonate and chlorite are common alteration products of these simulations. Minor analcime precipitated in one of the simulations involving the alkaline, oxidised brine.

The presence of magnetite in felsic volcanic A makes it highly reactive to all brine compositions (Table 2) and precludes it as an aquifer for base metal-rich solutions. In contrast, a rock comprised only of K-feldspar and quartz (felsic volcanic B) can act as an excellent aquifer for most brine compositions (Table 2). The metalliferous neutral, oxidised brine maintains its Zn-Pb content during minor carbonate alteration of the felsic unit, and the metal-rich acid, oxidised brine loses only 30% of its Pb and no Zn during sericite-carbonate alteration of the volcanic.

Limestones that contain only minor detrital quartz can provide excellent aquifers for low temperature brines. Significant base metal deposition only occurs during interaction with the acid, reduced brine. Abundant siderite alteration is produced during interaction with the acid, oxidised brine; note, however, that no Pb or Zn is deposited during this simulation.

Cross-stratal transport and brine pool models

The total metal precipitated during conductive cooling (250 - 50°C), isoenthalpic boiling simulations (250 - 100°C) and cooling after boiling (100° - 20°C) are listed in Table 3. Cooling and boiling generally proved more effective at extracting base metals from these lower temperature brines than for those considered in Cooke (1993) due in part to the lower temperatures modelled (20°C rather than 50°C). Note that cooling of a brine to 20°C is unlikely to happen during cross-stratal transport, but may happen during dispersion within a brine pool.

Cooling did not extract any significant Pb or Zn from the oxidised metalliferous brines (acid and neutral; Table 3). However, all of the Pb, Zn and Ag and most of the Cu was extracted during cooling of the reduced brines (Table 3). Cooling of the oxidised brines and the reduced acid brine would produce barren quartz veins in the field (> 99.5% quartz, traces of base metal sulfides, acanthite, muscovite, K-feldspar and/or witherite). Cooling of reduced neutral and alkaline brines during cross-stratal transport would produce carbonaceous quartz veins (≈ 85% total quartz, 15% graphite, traces of base metal sulfides).

Cooling of 150°C fluids by conduction as they disperse within a brine pool would effectively strip out all of the base metals from reduced fluids (Table 3). However, the reduced fluids modelled here do not contain sufficient base metals to form economic mineralisation. Cooling of metalliferous oxidised brines in a brine pool would not extract base metals (Table 3). Fluid mixing may facilitate base metal

deposition, but there is also the possibility that the base metal load would be dispersed into seawater without precipitating.

Boiling of oxidised metalliferous 150°C brines leaves most of the base metal load in solution (Table 3). In contrast, boiling of the reduced brines effectively strips all of the base metals out of solution in the first 5°C boiling increment. The results for the acid, reduced fluid contrasts with the results of the 250°C simulations (Cooke, 1993), where the equivalent brine retained most of its base metal load. The 150°C boiling event is more effective at extracting metals from solution because the first increment of boiling is a major degassing event, due to the fluids being CO_2-rich. Table 4 lists the saturation pressures for each of the 6 modelled brines and for pure water, together with the minimum depth those 150°C fluids can attain under hydrostatic conditions prior to the commencement of phase separation. This table demonstrates that 150°C CO_2-rich sedimentary brines cannot travel along faults in the near-surface environment without boiling unless a substantial body of water overlies them.

The boiling simulations predicted the following vein assemblages - acid, oxidised: 49% hematite, 33% quartz, 17% galena, 0.4% bornite, 0.4% acanthite, < 0.1% muscovite, gold and chalcocite; acid, reduced: 56% rhodochrosite, 44% quartz, 0.2% sphalerite, < 0.1% muscovite, acanthite, bornite, galena, gold, pyrite and chalcocite; neutral, oxidised: 84% calcite, 8.8% rhodochrosite, 5.7% quartz, 1.4% dolomite, 0.5% hematite, < 0.1% K-feldspar, chalcocite, galena, gold, silver, sphalerite and witherite; neutral, reduced: 80% calcite, 10% rhodochrosite, 8.4% quartz, 1.3% dolomite, <0.1% K-feldspar, acanthite, bornite, chalcocite, galena, sphalerite, witherite, gold and pyrite; alkaline, oxidised: 71% calcite, 25% quartz, 2.4% rhodochrosite, 1.6% dolomite, 0.3% witherite, < 0.1% silver, K-feldspar, gold and hematite; alkaline, reduced: 54% quartz; 43% calcite; 1.6% dolomite; 1.5% rhodochrosite; 0.2% witherite; < 0.1% acanthite, bornite, galena, sphalerite and gold. Boiling proved effective at extracting Mn and Ba from neutral and alkaline solutions (as rhodochrosite and witherite respectively). While carbonates are the major products of most of the simulations, there is a high degree of variance between the individual simulations when comparing the proportions of minerals precipitated and the predicted accessory phases. It is concluded that boiling of 150°C sedimentary brines should result in carbonate -quartz (± hematite) veins, but the mineralogy of an individual vein will depend strongly on the initial fluid composition.

Fluid	Saturation Pressure	Minimum Water Depth
Pure water	4.8 bars	40 m
acid, oxidised	48.8 bars	497 m
acid, reduced	48.7 bars	496 m
neutral, oxidised	44.8 bars	457 m
neutral, reduced	44.8 bars	457 m
alkaline, oxidised	25.8 bars	263 m
alkaline, reduced	25.9 bars	264 m

Table 4: saturation pressures and corresponding minimum water depths required to prevent boiling for 150°C pure water (data from Henley et al., 1993) and for the sedimentary brines listed in Table 1. Calculated water depths are approximate only because brine densities are assumed to be unity. High CO_2 contents in the sedimentary brines (1 wt %) require an overlying water column of several hundred metres to prevent phase separation.

Simulations of cooling of the boiled brines from 100° to 20°C were conducted to investigate whether boiling brines discharging into a brine pool would deposit their metal load in the feeder system, or during dispersal into the pool. Quartz was essentially the only mineral precipitated (> 98%) during all of these simulations. Because boiling was so effective at removing metals from the reduced brines, these fluids were essentially spent by the time they had boiled to 100°C, and further cooling only extracted what little metal was left in solution. In contrast, the metalliferous oxidised brines (which retained most of their metal load during the boiling simulations) did not deposit any base metals during cooling, again raising the possibility that oxidised brines will disperse their metal load into the overlying water column unless some mixing process acts to extract the metals from solution. It is concluded that brine pool cooling is probably an effective method at extracting base metals from reduced solutions, but is much less effective under oxidising conditions.

Simulations of depositional processes

Table 5 lists the results of fluid mixing and fluid-dolomitic sediment interaction. The seawater compositions used in mixing simulations are given in Cooke (1993).

Process	Brine	Cu (%)	Pb (%)	Zn (%)	Ag (%)	Au (%)	Ba (%)	Mn (%)
Mix with oxidised seawater	acid, oxidised	-	-	-	96.3	> 100	78	-
	acid, reduced	-	100	> 100	99	-	78	-
	neutral, oxidised	-	-	-	10	> 100	79	-
	neutral, reduced	> 100	> 100	> 100	98	-	79	-
	alkaline, oxidised	52	-	2.0	57	> 100	*19*	-
	alkaline, reduced	52	> 100	> 100	97	-	*19*	-
Mix with reduced seawater	acid, oxidised	***> 100***	100	100	100	99	-	-
	acid, reduced	> 100	100	100	96	-	-	-
	neutral, oxidised	> 100	**> 100**	100	99	49	-	-
	neutral, reduced	-	99	80	93	-	-	-
	alkaline, oxidised	> 100	100	100	96	-	-	-
	alkaline, reduced	-	99	43	91	-	-	-
Pyritic dolomitic siltstone	acid, oxidised	***95***	95	77	86	-	-	52
	acid, reduced	36	76	89	27	-	-	58
	neutral, oxidised	90	**86**	**86**	62	-	-	-
	neutral, reduced	-	-	-	-	-	-	-
	alkaline, oxidised	95	92	91	61	-	-	-
	alkaline, reduced	-	-	-	-	-	-	-
Pyritic dolomite	acid, oxidised	***95***	95	77	86	-	-	52
	acid, reduced	36	76	89	27	-	-	58
	neutral, oxidised	91	**87**	**86**	62	-	-	-
	neutral, reduced	-	-	-	-	-	-	-
	alkaline, oxidised	*	*	*	*	*	*	*
	alkaline, reduced	-	-	-	-	-	*0.2*	*0.2*
Py-rich carb. dolostone	acid, oxidised	***95***	99	97	94	-	-	53
	acid, reduced	43	76	89	26	-	-	58
	neutral, oxidised	96	100	100	89	-	-	*1.3*
	neutral, reduced	-	-	-	-	-	-	*0.1*
	alkaline, oxidised	96	100	100	76	-	*0.7*	*1.2*
	alkaline, reduced	-	-	-	-	-	-	*0.2*

Table 5: Percentage of total metal in solution extracted during water-rock interaction calculations. For each simulation, small increments of fluid (≈ 0.05 and 0.5 grams) or rock (0.1, 0.5, 1 and 5 grams) were progressively titrated into approximately one kilogram of brine until equilibrium was reached. Numbers in **bold type** indicate efficient extraction of a metal over a small titration increment (i.e. the process is an efficient trap mechanism that could result in economic concentrations of that metal). Numbers in ***italics*** indicate that the metal was extracted inefficiently (i.e. over a large number of titration increments) - the process is an inefficient trap mechanism that is unlikely to form an ore deposit. Numbers in plain type indicate that the metal was never present in sufficient quantities in the starting solution to deposit economic concentrations of metals. > 100 indicates that the relevant metal was scavenged from seawater during the simulation. * - indicates that the simulation has not been conducted yet.

Mixing of the 150°C sedimentary brines with oxidised seawater produces barren siliceous exhalites. No Cu-rich mineralisation is produced during these simulations due to the low initial Cu contents of the brines (compare Table 5 with Cooke, 1993). There is some potential for a Ag-rich quartz-hematite rock to form when the acid, oxidised brine mixes with seawater, but no base metal sulfides are precipitated. As noted in Cooke (1993), only the simulations involving mixing with oxidised seawater predict barite precipitation. In this case, however, barite only precipitates during the acid and neutral mixing simulations. Witherite forms in place of barite in the simulations involving alkaline brines. Base metals are scavenged from seawater during mixing with the reduced brines (Table 5). The total proportions of minerals precipitated during each simulation are - acid, oxidised: 72%

quartz, 25% hematite, 1.8% barite, 0.9% silver, < 0.1% acanthite and gold; acid, reduced: 96.5% quartz, 2.4% barite, 0.8% sphalerite, 0.2% galena, < 0.1% muscovite, pyrite and acanthite; neutral, oxidised: 89% quartz, 9% hematite, 2.2% barite, < 0.1% gold, acanthite and muscovite; neutral, reduced: 97% quartz, 2.4% barite, < 0.1% sphalerite, pyrite, acanthite, galena, muscovite and covellite; alkaline, oxidised: 70% quartz, 30% dolomite, < 0.1% K-feldspar, acanthite, bornite, sphalerite, witherite, chalcocite, hematite and muscovite; alkaline, reduced: 70% quartz, 30% dolomite, < 0.1% acanthite, galena, K-feldspar, sphalerite, witherite, pyrite, muscovite and covellite.

Pyrite-rich massive sulfide mineralisation is produced during mixing of an acid, oxidised brine with anoxic seawater. In contrast, a barren siliceous exhalite is produced when mixing involves the acid, reduced brine. Overall, these simulations were the most effective for extracting base metals from the 150°C brines (Table 5), but mixing with the neutral and alkaline brines caused precipitation of large quantities of dolomite and magnesite respectively. The total proportions of minerals precipitated during each simulation are - acid, oxidised: 68% pyrite, 15% sphalerite; 12% galena, 5% quartz, < 0.1% covellite, chalcocite, bornite, acanthite and gold; acid, reduced: 99% quartz, 0.8% sphalerite, 0.2% galena, < 0.1% acanthite, covellite and pyrite; neutral, oxidised: 77% dolomite, 14% quartz, 5.0% sphalerite, 2.2% pyrite, 1.3% galena, < 0.1% acanthite, bornite, muscovite, gold and covellite; neutral, reduced: 85% dolomite, 15% quartz, < 0.1% sphalerite, pyrite, acanthite, galena, and muscovite; alkaline, oxidised: 56% dolomite, 42% magnesite, 2% quartz, < 0.1% K-feldspar, acanthite, chalcopyrite, sphalerite, galena, pyrite, bornite and muscovite; alkaline, reduced: 56% dolomite, 42% magnesite, 2% quartz, < 0.1% acanthite, galena, K-feldspar, sphalerite, pyrite and muscovite.

All three pyritic dolomitic sediments provide good trap environments for base metals transported in oxidised 150°C brines (Table 5). Siderite is a common alteration product produced during interaction of the oxidised, CO_2 rich brines with the dolomitic sediments. Base metals are effectively extracted from the acid, reduced brine (Table 5), although no siderite is formed during this process. In direct contrast, the pyritic dolomitic sediments have potential as aquifers for the reduced neutral and alkaline brines (Table 5). No sulfides or precious metals are deposited, and minimal brine-rock interaction is required (less than 0.05 grams rock added) before equilibrium is achieved. Table 6 summarises the alteration minerals produced during simulations of brine-sediment interaction.

Lithology	Brine	Alteration Minerals
Pyritic dolomitic siltstone	acid, oxidised	sid, rhc, sp, gal, bn, cpy, ac
	acid, reduced	rhc, sp, gal, bn, ac
	neutral, oxidised	sid, Kf, ac, bn, gal, sp, cpy
	neutral, reduced	Kf
	alkaline, oxidised	sid, Kf, ac, gal, sp, ms
	alkaline, reduced	Kf
Pyritic Dolomite	acid, oxidised	sid, ms, rhc, sp gal, bn, cpy, ac
	acid, reduced	rhc, sp, gal, bn, ac, ms
	neutral, oxidised	sid, sp, gal, bn, cpy, ac
	neutral, reduced	Kf, cal, rhc
	alkaline, oxidised	no results yet
	alkaline, reduced	Kf, rhc, wit
Pyrite-rich carb. dolostone	acid, oxidised	sid, ms, rhc, sp gal, cpy, ac, Ag
	acid, reduced	rhc, sp, gal, bn, ac, ms
	neutral, oxidised	sid, sp, gal, bn, cpy, ac, cal, Kf rhc
	neutral, reduced	Kf, cal, rhc
	alkaline, oxidised	Kf, cal, rhc, sp gal, wit, ac, cpy
	alkaline, reduced	cal, rhc

Table 6: Alteration minerals produced during interaction of 150°C sedimentary brines and pyritic dolomitic sediments. Abbreviations: sid - siderite, ms - muscovite, Kf - K-feldspar, rhc - rhodochrosite, cal - calcite, wit - witherite, sp - sphalerite, gal - galena, cpy - chalcopyrite, bn - bornite, ac - acanthite, Ag - silver.

CONCLUSIONS

The preliminary results of this study indicate that 10 wt. % sedimentary brines can only carry significant base metals at 150°C if the brine is sufficiently oxidised and/or acidic. Hematitic sandstones, felsic volcanics (without appreciable magnetite) and limestones could all act as aquifers

for metalliferous oxidised brines without causing significant adjustment to the chemistry of the brine.

Cross-stratal cooling or boiling will extract base metals from reduced solutions but not from oxidised solutions. Barren quartz-hematite veins will be produced during cooling; carbonate-quartz veins will precipitate during boiling. Brine pool deposition of base metal sulfides is more likely for reduced brines; oxidised brines may disperse their metal load into seawater.

Mixing of oxidised metalliferous sedimentary brines with reduced seawater will produce a pyrite-rich Pb-Zn massive sulfide body. Interaction of oxidised brines with pyritic dolomitic sediments produces extensive siderite alteration in conjunction with base metal deposition.

The high dissolved CO_2 contents of the initial brines (1 wt. %) stabilise siderite as an alteration phase in several of the simulations. These high CO_2 levels can only be maintained if the fluids do not undergo boiling in the subsurface. Water depths in excess of 250 metres and 400 m are required to prevent the alkaline fluids and the neutral and acidic brines from boiling respectively.

REFERENCES

Cooke, D.R., 1993. Transport and deposition of base metals from high temperature (250°C) sedimentary brines. AMIRA/ARC Project P.384, Report No. 4; 111-130.

Henley, R.W., Truesdell, A.H., and Barton, P.B., Jr., 1983. Fluid-mineral equilibria in hydrothermal systems. Rev. Econ. Geol. 5, 267p.

M^{c}Kibben, M.A., and Williams, A.E., 1989. Metal speciation and solubility in saline hydrothermal fluids: an empirical approach based on geothermal brine data. Econ. Geol., 84: 1996-2007.

SECTION D

Appendix: Structural data

Uniq No.	Field No	Rock Code	Magn Susc.	Easting	Northing	Bed Dip	Bed Az	Ft Strike	Ft Dip	FtDipDir	Pitch	Movt	QV-dip	QV-dip az
1	MD1/92	PML	0.085	586870	8121714	18	132							
2	MD2/92	PTG	0.06	587789	8121542	71	14							
3	MD3/92	PTO	0.505	588021	8121577									
4	MD4/92	PTG	13	588133	8121594									
5	MD5/92	PTE	22.18	588247	8121588									
6	MD6/92	PTE	0.58	588236	8121406									
7	MD7/92	PMS	0.07	588177	8121106	15	44							
8	MD8/92	PMS	0.048	588161	8120997	32	240	148	50	N				
								110	32	N	80	Nil		
9	MD9/92	PTN	0.035			15	82							
10	MD10/92	PTN		588082	8120883	17	263	168	60	E	17	DEXT		
								348	60	E	20	DEXT		
								330	90	E	67	WBU		
								325	82	S	67	EBU		
								335	65	E	72	WBU		
11	MD11/92	PTN	0.05	588905	8121487	13	295	175	55	E	80	EBU		
12	MD12/92	1	0.096	589210	8121718	41	287							
13	MD13/92	PMS	0.058	589281	8121852	38	20	286	57	S	37	SIN 1ST		
								353	82	E	15	DEXT 2ND		
								191	84	E	26	DEXT		
14	MD14/92	PMS	0.06	589464	8121855	27	21							
15	MD15/92	5	0.064	589659	8121637	26	66							
16	MD 16/92	4	4.13	589719	8121511									
17	MD17/92	PMS	0.02	589855	8121458	10	265	257	69	N	12	SIN		
						45	295	318	76	S	15	SIN		
								281	66	S	20	DEXT		
18	MD18/92		0.51	589167	8121344	12	286							
19	MD19/92	3	0.43	589167	8120771									
20	MD20/92	6	0.056			1	290	180	12	E	70	REV		
21	MD21/92	6	0.066			1	97	183	3	E	90	REV		
22	MD22/92	6	0.065			9	139	175	66	E	0	DEXT		
								236	81	S	2	SIN		
23	MD23/92	2	0.023			23	268	50	57	E	57	REV/DEXT		
								303	82	S	1	SIN		
								218	53	S	2	SIN		
								302	81	S	5	SIN		
								326	88	N	45	SIN/NOR		
24	MD24/92	6	0.044	589104	8120264			99	74	N	6	DEXT		
25	MD25/92	6	0.083			15	303							
26	MD26/92	PTN	0.03					304	31	S	70	REV		
27	MD27/92	PTN	0.062	589388	8120451			69	56	S	48	DEXT/REV		
								9	57	E				
								35	56	E	13	DEXT		
								52	52	S	43	DEXT/REV		
28	MD28/92	4	24.8	589542	8120386									
29	MD29/92	1	0.16	589640	8120415	20	34							
30	MD30/92	2	0.052			7	180	2	14	E	80	REV		
								40	51	W	15	DEXT		
								143	83	S	15	DEXT		
								306	88	S	90	NOR		
								285	85	S	10	SIN		
31	MD31/92	6	0.0675	588734	8119532	49	60	1	71	E	0	DEXT		
								205	7	E	80	REV		
								23	52	W	75	REV		
32	MD32/92	6	0.065	588851	8119482	6	19	198	71	W	14	SIN		
33	MD33/92	6	0.043	588966	8119451	12	105	60	48	S	3	SIN		
								195	12	E	90	REV		
34	MD34/92	6	0.073	589065	8119410	13	298	20	63	W	90	REV		
								295	89	N	73	NBU/DEXT		
								279	35	N	51	REV/DEXT		
35	MD35/92	7	0.217	588524	8118670	57	43							
36	MD36/92	PTN	0.043	588800	8118767	45	260	357	69	W	18	DEXT		
								349	43	W	90	REV		
								258	20	N	5	DEXT		
37	MD37/92	PTN	0.055	588906	8118746	13	234	202	84	E	90	REV		
38	MD38/92	PTN	0.127	589036	8118783	19	249	339	40	W	70	REV 1ST		
								355	35	W	47	REV 2ND		
39	MD39/92	PTN	0.05	589249	8118781	13	80	222	80	N	6	SIN		
								344	56	W	17	DEXT		
40	MD40/92	PMS	0.023	588097	8118885	7	264							
41	MD41/92	PMS	0.03	588240	8119589									
42	MD42/92	PMS	0.05	588360	8120091	4	254	150	84	W	13	SIN		
								134	49	E	0	SIN		
43	MD43/92	1	0.103	587110	8121767	4	331							
44	MD44/92	PMS		587195	8122245	19	281	260	70	S	20	SIN		
								216	21	W	47	REV/DEXT		
								291	84	S	50	DEXT/NOR		
45	MD45/92	3	0.15	587280	8122058									
46	MD46/92	PMS	0.053	587394	8121981	17	267	177	177	W	85	REV		
								122	66	N	70	REV		
47	MD47/92	PMS		587518	8121958	6	340	305	5	S	0	DEXT		
								182	15	W	74	REV		
								174	83	E	80	REV		
48	MD48/92	3	0.5											
49	MD49/92	2	0.036	587994	8122403	6	279							
50	MD50/92	PTO	0.23	588098	8122231	65	60							
51	MD51/92	7	0.23	588244	8122058	14	318							
52	MD52/92	PTN	0.045	588295	8121975	11	270	340	14	E	75	REV		
53	MD53/92	1	0.08	588245	8121877	37	200							
54	ABF54/92			580777	8143078									
55	MPF55/92					37	271	281	65	N	40	SIN		
						36	245	155	36	S	12	SIN		
						49	271	253	10	S	90	REV		
						15	342							

56	MD56/92	2		584814	8123720	72	28	172	57	E	40	DEXT/NOR
						37	346	204	82	W	5	SIN 1ST
								299	63	S	70	REV 2ND
57	MD57/92	7	0.4	588470	8121870	29	146					
58	MD58/92	3	0.36	588537	8122000	26	324					
59	MD59/92	3	0.74	588575	8122470							
60	MD60/92	PMS	0.044	588630	8122570	13	30					
61	MD61/92	3	0.46					208	76	E	6	SIN
62	MD62/92	7		588481	8122650	48	130					
63	MD63/92	PTN		588392	8122123			349	39	E	85	REV
64	MD64/92	PMS		585264	8123103	4	190	280	86	S	22	SIN
								315	89	S	55	SIN/SWBU
								240	87	N	0	DEXT
65	TF65/92	PMS						180	35	W	90	WBU
								141	19	E	80	REV
								358	61	E	0	SIN 1ST
								312	85	S	5	DEXT 2ND
66	TF66/92	PMS						270	85	S	45	SIN/REV
67	TF67/92	PTL						130	79	E	5	SIN
								280	85	N	40	DEXT
								141	78	N	15	SIN 1ST
								176	71	W	5	DEXT 2ND
68	T1/93			477790	538215686	31	205	330	5	S	90	REV
69	T2/93			477718	538215855	27	208					
70	T3/93			477733	538215955							
71	T4/93			477710	538216195	27	222	245	85	S	90	SEBU
72	T5/93			487558	538215416	21	228					
73	T6/93			488334	538215969	11	242					
74	T7/93			488411	538216023	10	270					
75	T8/93			488600	538216280	12	260					
76	T9/93			489079	538216595	15	262					
77	T10/93			489727	538217175	15	40					
78	NR11/93											
79	NR12/93					85	50	325	60	S	85	NOR
								238	40	S	15	SIN/REV
								160	75	E	50	REV/SIN?
80	NR13/93					21	46					
81	NR13A/93							187	40	E	10	SIN
82	NR14/93					38	49	290	9	S	90	REV 1ST
								110	20	N	80	REV 2ND
83	NR15/93					25	60					
84	NR16/93					80	220	215	78	E	10	SIN
								188	48	W	60	NOR
								230	80	W	12	SIN
								235	62	W	10	DEXT
								20	80	E	12	SIN
85	NR17/93							80	28	N	40	SIN/REV
86	NR18/93											
87	NR19/93					30	50	278	57	S	75	REV
88	NR20/93							85	41	S	77	REV
89	NR21/93					72	70	350	35	W	77	REV
90	NR22/93					83	67	240	72	N	12	DEXT
								320	23	S	90	REV
								280	87	N	15	DEXT
91	CM23/93					75	305	228	32	N	20	SIN
92	CM24/93					77	285	326	46	S	65	NOR/SIN
93	CM25/93					67	25					
						57	280					
						47	86					
94	CM26/93					71	246	316	45	S	30	DEXT
						76	227					
95	CM27/93					72	50					
						40	120					
96	CM28/93					80	20	350	76	E	15	SIN
								180	85	E	10	DEXT
97	CM29/93							333	75	W	40	DEXT
98	KD30/93					33	320					
99	KD31/93					46	298					
						23	315					
						33	330					
100	KD32/93					32	305	347	70	W		SIN
						35	270					
						35	250					
						30	280					
101	KD33/93					73	230					
102	KD34/93											
103	KD35/93					40	275					
104	KD36/93					22	305	307	83	N	5	SIN
						53	278	325	85	S	12	DEXT
								225	65	N	25	NOR/SIN
								290	51	N	20	DEXT
								245	80	S	50	REV/SIN
105	KD37/93					36	305					
						26	307					
106	KD38/93					17	335	195	27	W	0	SIN
						30	275					
107	KD39/93											
108	KD40/93											
109	KD41/93					43	260					
110	KD42/93					35	230					
111	KD43/93					10	260					
112	MD44/93	PMS				4	45	336	16	W	85	REV
						12	52	177	15	W	65	REV
								322	12	E	70	REV
								200	77	W	12	SIN

							288	9	S	55	NOR/TBS		
							135	17	S	60	REV 1ST		
							255	77	N	10	SIN 2ND		
							310	63	S	37	SIN/REV		
113	MD45A/93	PMS			12	320	175	27	W	75	NOR		
							320	14	S	85	NOR		
							150	66	W	85	NOR		
							160	30	W	60	REV		
114	KLG45B/93	PMA			25	268							
115	FF46/93	PTE			36	125	35	36	S	60	REV		
116	FF47/93						175	26	W	85	REV		
117	FF48/93				12	270							
					17	282							
118	FF49/93						160	24	W	90	REV 1ST		
							345	57	W	90	REV 2ND		
119	FF50/93				55	60							
120	FF51/93						155	72	E	40	SIN/REV		
							95	71	N	20	DEXT 1ST		
							242	77	N	0	SIN 2ND		
121	MR53/93	PCC5	798917	538040375	55	345							
122	MR54/93	PCC5	799098	538041137	28	110	190	32	E	75	REV		
							30	30	E				
							25	60	E	0	DEXT		
							345	37	W	60	REV		
123	MR55/93	PGR		538043314			16	77	E	2	DEXT		
124	MR56/93	Ptw	799929	538045549			136	60	E	2	SIN	86	315
							295	83	S	7	SIN	75	285
							355	77	E	0	SIN	90	270
												90	195
												74	60
125	MR57/93		811100	538037300								85	205
												70	175
												79	106
												80	275
												71	345
												63	220
126	MR58/93		810550	538037900			120	80	S	20	DEXT		
127	MR59/93				10	120	92	83	S	70	NIL		
128	CM61A/93		556819	538235748			280	32	S	7	SIN		
	CM61B/93						200	65	W	10	DEXT		
	CM61C/93						91	47	N	12	SIN		
129	CM62/93		556725	538235699			235	60	S	5	SIN		
130	CM63/93	PRI	536592	538235700	65	336	210	60	E	15	SIN		
							75	55	N	75	?		
							270	20	N	85	REV?		
							290	68	N	65	NOR		
							272	31	N	5	SIN 1ST		
							272	31	N	85	NOR 2ND		
131	CM64/93	PRI	558068	538236392	77	325							
132	CM65/93		559339	538237083	79	353	236	28	E	45	REV/SIN		
							132	20	S	77	REV		
							347	53	E	80	NOR 1ST		
							340	50	E	60	NOR 2ND		
							90	28	S	50	REV		
133	CM66/93	PMS	561432	538244705	85	215	346	60	W	40	REV		
					60	240							
134	CM67/93	PMS/PTN	561609	538244798	72	260	240	38	E	65	REV		
					20	190							
135	LF68A/93	PML	568582	538261650	14	290							
136	LF68B/93	PML	568710	538261731	25	300							
137	LF68C/93	PMS	568820	538261657	75	278	207	90				87	110
												81	112
												90	2
												83	115
												82	352
												85	348
												85	344
												81	342
												82	328
												42	325
												65	330
												73	177
												87	10
												72	105
												70	125
												85	82
												55	132
												70	112
												64	107
												90	333
												89	349
												68	103
												60	172
												87	341
138	LF68D/93	PTL			21	180	200	75	W	7	DEXT	55	206
							322	35	N	25	DEXT/REV?	49	235
												85	300
												62	200
139	LF68E/93	PTL			20	110							

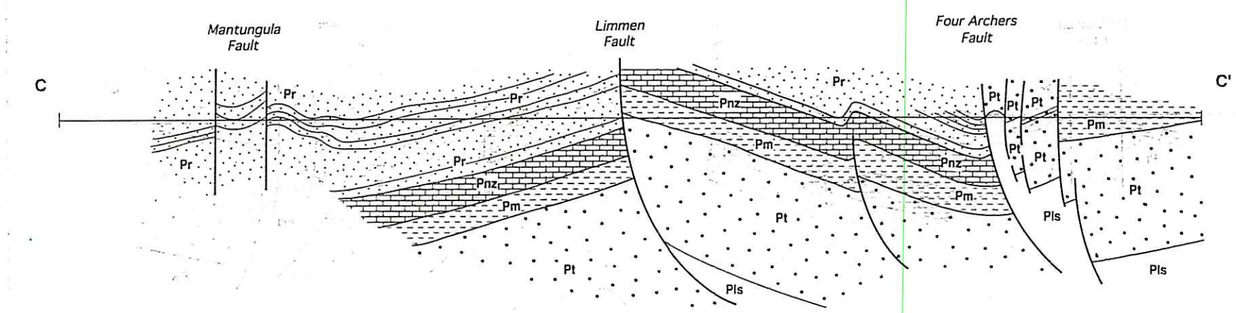

Fig. 2 Cross section C-C' through the Four Archers, Limmen and Mantungula Faults.

Fig. 1 Interpreted geological map of the northern part of the southern McArthur Basin. Data is from Rawlings et al. (1993) and other unpublished geological compilations of the NTGS and BMR (EC=Eastern Creek prospect, CM=Coppermine Creek prospect, AP= Apollo prospect).